UNIVERSITY OF CALIFORNIA
RIVERSIDE

Root-Knot Nematode-Triggered Defense Responses in *Arabidopsis thaliana* During Early Stages of Parasitism

A Dissertation submitted in partial satisfaction
of the requirements for the degree of

Doctor of Philosophy

in

Plant Pathology

by

Marcella Alves Teixeira

March 2017

Dissertation Committee:
Dr. Isgouhi Kaloshian, Chairperson
Dr. Phillip Roberts
Dr. Hailing Jin

The Dissertation of Marcella Alves Teixeira is approved:

_____

_____

_____

Committee Chairperson

University of California, Riverside

Acknowledgments

I am grateful for my supervisor Isgouhi Kaloshian for the support during the past years. Her trust extrapolated my specific research area and allowed me to explore themes I never considered I would be working on. I will forever remembeer her guidance during our research conduction and manuscripts writing, as well as all the suggestions she offered during these years. I am also deeply grateful to Barbara Jablonska, Gina Broitman-Maduro, James Peng, Ritu Chaudhary and Ming Wang for always being available during all the (several) times I needed help with my research.

I thank my committee members, Dr. Philip Roberts and Hailing Jin for tailoring my research through their questionings and suggestions and specially for being so enthusiastic during our meetings. I am grateful for the Nematology Department members Scott and Matthew for sharing their knowledge, experience and inoculum every time I asked. I specially thank Scott for the contribution with photography and nematology techniques.

I am grateful for having met Irma, Natalie, Hailey, Maggie, Jeanette and Jacob, inspiring colleagues who made some tougher moments somewhat easier. You are each very dear to me.

I acknowledge my funding agency, CAPES for the financial support during my PhD and my employer for allowing me to pursuit my PhD in the first place.

I was blessed to find close friends that became family and are always in my heart. I am thankful for having friends listening to all my theories and experimental plans, never showing how boring I was.

I specially thank my children, Daniella and Eduardo, for all their patience and support during these years. Most and foremost, I am forever grateful to my parents for showing me life's endless possibilities and teaching me to always question until I get a satisfactory answer.

Finally, I thank my dear husband, Jansen, who participated in every single step of my PhD, giving me suggestions, actually working at the bench with me, supporting me with our family. You made it possible.

To my family for their love and support

ABSTRACT OF THE DISSERTATION

Root-Knot Nematode-Triggered Defense Responses in *Arabidopsis thaliana* During Early Stages of Parasitism.

by

Marcella Alves Teixeira

Doctor of Philosophy, Graduate Program in Plant Pathology
University of California, Riverside, March, 2017
Dr. Isgouhi Kaloshian, Chairperson

Root-knot nematodes (*Meloidogyne* spp., RKN) are plant parasites responsible for great losses in agriculture worldwide. After penetrating host roots they establish feeding sites by modifying a few cells from the pericycle, which become multinucleated and enlarged, known as giant cells. Classical nematology research focuses on the characterization of nematode effectors and plant resistance genes. Therefore, little is known about basal immunity against plant parasitic nematodes. In Chapter One we use Arabidopsis thaliana and *M. incognita* interaction as a model system to investigate plant perception of parasitic nematodes. We show that RKNs can be perceived by plants irrespective of possible damage caused during migration and this perception relies on canonical immunity signaling partners. In addition, we show that RKN perception by Arabidopsis is mediated by BAK1-dependent and independent pathways. To best characterize the transcriptional responses induced by RKN in Arabidopsis roots we performed RNAseq analysis, which is described in Chapter Two. RNAseq analysis revealed induction of several genes 24h after inoculation with RKN in both wild type plants and *bak1-5* mutant

roots. To identify candidate nematode receptors, RNAseq data was searched for genes that were upregulated upon RKN inoculation and encoded proteins with predicted membrane localization and kinase domains. Screening Arabidopsis with mutations on a few of these mutants allowed identification of a negative regulator of immunity against RKN that has elevated basal levels of defense marker genes and respond to elicitor treatment with stronger and faster ROS burst. Interestingly, this negative regulator belongs to a family of proteins that has not been extensively characterized, the G-type lectin receptor kinases (G-LecRKs). The Chapter Three shows an update on the characterization of Arabidopsis G-LecRKs as well as the first characterization of tomato G-LecRKs by using a methodology well established for characterization of other lectin receptor kinases family. Our analysis shows an expansion of G-LecRKs family in tomato as compared to Arabidopsis and organization of genes in clusters throughout each species genome. Motif enrichment analysis shows conservation of motifs among members of G-LecRKS of Arabidopsis as well as among members of Arabidopsis, tomato and the previously characterized rice G-LecRKs.

Table of Contents

List of figures

List of tables

Introduction

Parasitic nematodes are threats to crop production, livestock and human health. Regarding human health, they present a major concern specially for developing countries where around 3 billion people are estimated to be infected with nematodes. Plant parasitic nematodes are soil dwelling animals that belong to a group of over 4,100 species (Decraemer & Hunt, 2006), are able to penetrate and parasitize plant roots and are responsible for $US157 billion in crop losses annually worldwide (Abad *et al.*, 2008).

To establish parasitism, nematodes first need to penetrate host tissues. This step requires overcoming physical and mechanical barriers, such as plant cell wall, animal skin and mucosal surfaces. While some parasites count on the help of insect vectors, such as filarial nematodes, others open their way inside host tissue with the aid of their stylets, such as the plant parasitic nematodes and animal hookworms (De Veer *et al.*, 2007).

The most specialized plant nematodes are the sedentary endoparasites, nematodes from the largely studied groups of root-knot nematode (RKN, *Meloidogyne* spp.) and cyst nematodes (CN, *Heterodera* spp. and *Globodera* spp.) (Jones *et al.*, 2013). Under proper environmental conditions, their infective stage, the second stage juveniles (J2), hatch from eggs, are attracted to and penetrate plant roots. Members of both groups migrate intercellularly (RKN) or intracellularly

(CN) towards the vascular cylinder, where they establish specialized feeding cells and become sedentary.

RKN induce the formation of giant cells, which are cells that undergo karyokinesis without cytokinesis, resulting in hypertrophied, enlarged, multinucleated structures. CN induce the formation of syncytia, which are also multinucleated enlarged cells, but not because of karyokinesis. Instead, they induce the degradation of cell walls, which ultimately leads to connection of adjacent cells, also resulting in multinucleated structures. Both feeding sites are nutrient sinks for the nematodes and tightly regulated by their effectors secreted into the plant apopolast as well as cells (Favery *et al.*, 2015; Rodiuc et al., 2014).

Also, aiming to acquire nutrients from their hosts, animal parasites migrate through and develop in several tissues and organs, such as gastrointestinal tract, blood, lymph ducts, muscle cells and eyes (Maule & Curtis, 2011). Therefore, despite their significant differences, animal and plant parasitic nematodes both need to migrate inside host tissue during early steps of interaction with their hosts. More specifically, they all intimately interact with their hosts through their body surface. As for filarial nematodes, besides the obvious interaction with their hosts, they also need to interact with, develop and migrate inside their vectors. Ultimately, nematodes complete their life cycles by producing progeny that initiate new rounds of infection.

Host immune defense responses

In the battle against pathogens, plants and animals are constantly monitoring for the presence of intruders to initiate defense responses. A first level of surveillance relies on perception of microbe-associated molecular patterns (MAMPs) by pattern-recognition receptors (PRRs). Characterized plant PRRs are receptor-like proteins (RLP) and receptor-like kinases (RLKs), while mammalian PRRs belong are Toll-like receptors (TLRs), C-type lectin receptors and nucleotide-binding oligomerization domain (NOD)-like receptors (NLRs) (Mittal *et al.*, 2014).

Perception of MAMPs by PRRs results in pattern-triggered immunity (PTI) and inflammatory response in plants and animals, respectively (Fraiture & Brunner, 2014). Early signaling events as activation of mitogen-activated protein (MAP) kinases, callose deposition, rapid ion fluxes across plasma membrane, generation of reactive oxygen species (ROS) and massive transcriptional reprograming are PTI hallmarks. Ultimately, PTI can lead to responses as plant stomatal closure and production of antimicrobial compounds such as phytoalexins and pathogenesis related (PR) proteins, reducing infection success and pathogen development (Zipfel, 2014; Cook *et al.*, 2015).

As with mammals, plants are exposed to a plethora of pathogens and need to be able to efficiently perceive and respond to them. A classic example of MAMPs commonly perceived by mammals and plants is the bacterial flagellin. Distinct epitopes are perceived by plant FLS2 (Flagellin sensitive 2) and mammal TLR5 (Toll-like receptor 5) and both perceptions require downstream signaling partners

specific for each organism, indicating that flagellin perception in both systems is based on converged evolution (Fraiture & Brunner, 2014).

As a counterattack, pathogens evolved to hamper or elude these responses through delivery of effectors, which act at various steps of immunity signaling and, consequently, disrupt defense responses. Therefore, effectors can confer some advantage during infection process, but unlike MAMPs, they are not essential for pathogen survival and vary largely between distinct species of a given pathogen. This constitutes a new task for plants and animals that is to evolve proteins able to perceive specific pathogen effectors or their activity. In plants, these presumably cytoplasmic proteins are known as resistance (R) proteins and mediate a much stronger level of defense response, the effector-triggered immunity (ETI), that frequently leads to a hypersensitive response (HR). The arms-race continues as hosts and pathogens continuously adapt and evolve new strategies to succeed on one side, in defense, and on the other side, on infection (Zipfel, 2014; Cook *et al.*, 2015).

In addition to the recognition of pathogens motifs, self-danger molecules, namely damage-associated molecular patterns (DAMPs), also trigger defense responses very similar to those induced by MAMPs (Mott *et al.*, 2014). DAMPs were originally described as a result of cell wall rupture, releasing fragments that are recognized by adjacent cells, such as oligogalacturonides (OGAs), produced by the activity of pathogen-encoded enzymes on plant cells (Vallarino & Osorio, 2012). Similarly, in mammals, a component of extracellular matrix, hyaluronan, is

broken into lower molecular weight fragments that serve as DAMPs and, therefore, activate immune defenses (Scheibner *et al.*, 2006). In addition, ATP, known to activate immunity in mammals (Gombault *et al.*, 2012) as well as in other animals (Heil & Land, 2014), was also characterized as a plant DAMP (Cao *et al.*, 2014b), and its receptor, DOES NOT RESPOND TO NUCLEOTIDES 1 (DORN1), was recently identified (Choi *et al.*, 2014).

A second type of DAMPs are transcriptionally regulated rather than being a degradation product. In plants, damage leads to transcription of long precursors proteins (PROPEPs), that are cleaved to generate small peptides Atpep1-8, recognized by PEP receptors 1 and 2 (PEPRs) (Krol *et al.*, 2010; Yamaguchi *et al.*, 2010; Bartels *et al.*, 2013; Mott *et al.*, 2014; Bartels & Boller, 2015). Like microbial pathogens, defense against nematode parasites, known to cause extensive damage while migrating, might count not only on perception of nematode-associated molecular patterns (NAMPs) but also on a strong DAMP perception. On the other hand, those nematodes known to migrate intercellularly cause very little damage and might therefore trigger a more specific response heavily relying on recognition of NAMPs.

While ETI depends on the recognition of specific effectors from nematodes in a species-specific manner, MAMPs are conserved across species, allowing researchers to aim for a broader protection and therapeutic options. Nevertheless, research on plant responses to nematodes has mainly focused on characterization of resistance genes (or ETI) and detailed description of nematode feeding sites.

However, several pieces of evidence have pointed to the existence of PTI against nematodes, such as production of ROS by plants and defense against it by nematodes (Zacheo *et al.*, 1982; Robertson *et al.*, 2000; Melillo *et al.*, 2006; Dubreuil *et al.*, 2011; Melillo *et al.*, 2011; Lin *et al.*, 2016; Teixeira *et al.*, 2016).

Pattern-triggered immunity

Host perception of conserved molecules from pathogens (MAMPs) is mediated by plasma membrane localized receptors, leading to pattern-triggered immunity (PTI). These conserved molecules are under both positive and negative selection pressure, to avoid recognition by hosts and to maintain function in the pathogen. In addition, these molecules are part of proteins that are abundantly produced by pathogens and essential for their fitness, making them excellent alert signals for hosts to perceive.

The best-characterized MAMP-PRR pair is the flagellin peptide flg22 and its receptor, the leucine rich repeat kinase FLS2. The peptide flg22 is composed of a stretch of 22 amino acids of the bacterial flagellin that is conserved across several bacterial species. Initially flg22 was identified based on the flagellin sequence of the pathogenic bacterium *Pseudomonas aeruginosa*, causing a strong alkalinization response in plant cells suspension-culture (Felix *et al.*, 1999). Treatment of Arabidopsis seedlings with flg22 was shown to induce defense responses such as transcriptional activation of defense marker genes and callose deposition, as well as inhibition of root growth suggesting a tradeoff between

defense and development (Gomez-Gomez *et al.*, 1999). Using flg22 to screen flagellin insensitivity mutants, its receptor FLS2 was discovered by a map-based cloning strategy. FLS2 was shown to be ubiquitously expressed in Arabidopsis leaves, stems and roots (Gomez-Gomez & Boller, 2000). More recently, FLS2 was also shown to be expressed in bacterial entry sites, both in roots or aboveground tissues (Beck *et al.*, 2014).

Since their initial description, flg22 perception by FLS2 has been intensively characterized, with extensive data on flg22-mediated plant defense responses, such as transcriptional regulation, callose deposition and ROS burst (Navarro *et al.*, 2004; Zipfel *et al.*, 2004). Additionally, other proteins involved in flg22 perception and downstream signaling have been identified and their molecular processes described. flg22 acts as a molecular glue that brings together FLS2 and the co-receptor BAK1, allowing FLS2 and BAK1 transphosphorylation and phosphorylation of the cytoplasmic protein Botrytis-induced kinase 1 (BIK1) (Chinchilla *et al.*, 2007; He *et al.*, 2007; Heese *et al.*, 2007; Lu *et al.*, 2010; Roux *et al.*, 2011; Sun *et al.*, 2013a; Sun *et al.*, 2013b). BIK1 then phosphorylates the respiratory burst oxidase homolog D (RBOHD), resulting in ROS burst and stomatal movement control regulating one of the bacterial entry sites (Li *et al.*, 2014). After flg22 perception, FLS2 is internalized and degraded as one of the PTI regulation mechanisms (Robatzek *et al.*, 2006; Salomon & Robatzek, 2006).

Further characterization of the different players of PTI signaling revealed interesting features of key proteins, such as diverse roles for BIK1 in defense,

being positive defense regulator against the biotrophic fungal pathogen *B. cinerea* and negative defense regulator against aphids and hemibiotrophic pathogenic bacterium *Pseudomonas syringae* pv. tomato (Veronese *et al.*, 2006; Lei *et al.*, 2014). Consistently, the BIK1 tomato ortholog, Tomato protein kinase 1 (TPK1b), is a positive regulator of defense against *B. cinerea* and the tobacco hornworm larvae, *Manduca sexta* (AbuQamar *et al.*, 2008).

Although flg22 treatment of *fls2* mutants could not trigger typical defense responses due to tack of flg22 recognition, treatment of the same mutants with crude bacterial extract could still affect disease development, suggesting existence of an additional molecule that can be recognized by an additional receptor (Kunze *et al.*, 2004). Investigation of additional elicitor molecules led to the identification of EF-Tu (Elongation factor thermo unstable), the most abundant protein found in bacterial cells, and subsequent identification of its Arabidopsis receptor the EFR (EF-Tu receptor) (Kunze *et al.*, 2004; Zipfel *et al.*, 2006).

The epitope recognized by EFR is elf18, a stretch of 18 amino acids localized on the highly conserved N-terminal region of the protein EF-Tu and, similar to flg22, triggers oxidative burst, transcriptional regulation of defense marker genes and callose deposition (Kunze *et al.*, 2004; Zipfel *et al.*, 2006). Unlike FLS2, which has been described in several plant species, such as tomato (*Solanum lycopersicum*), grapevine (*Vitis vinifera*), rice (*Oryza sativa*) and citrus (*Citrus paradisi*, *C. reticulata* and *Fortunella margarita*), EFR seems to be exclusively encoded by plants from the family Brassicaceae (Kunze *et al.*, 2004;

Zipfel *et al.*, 2006; Robatzek *et al.*, 2007; Takai *et al.*, 2008; Trda *et al.*, 2014; Shi *et al.*, 2016).

The absence of such receptor in other plants presents an opportunity for engineering resistance to bacterial pathogen by introducing the missing receptor into these plant species. A broad-spectrum bacterial resistance was shown by transforming different crops, such as rice, wheat (*Triticum aestivum*), tomato and *Nicotiana benthamiana* with the Arabidopsis EFR (Brutus & Yang He, 2010; Lacombe *et al.*, 2010; Lu *et al.*, 2015; Schoonbeek *et al.*, 2015; Schwessinger *et al.*, 2015). Interestingly, it has been recently shown that an alternative region of EF-Tu, termed EFa50, activates typical PTI responses in rice, suggesting the existence of additional receptors of this MAMP in species other than brassica plants (Furukawa *et al.*, 2013).

Research on these receptors has shown the great importance of plant immunity against pathogens and the remarkable negative impact their uncontrolled activation can have on plant growth and metabolism. These adverse effects are observed in certain mutants that can display extensive cell death and compromised development, such as the double mutant *bkk1 bak1* and the single mutant *bik1 (Veronese et al., 2006; He et al., 2007)*. Nevertheless, to ensure precise control of defense responses, plants have evolved negative regulators of defense. Interestingly, not all mutants of these negative regulators display altered development, as it is the case for the Arabidopsis *plb13* mutants (Lin *et al.*, 2015).

A good example of a negative regulator of defense is that mediated by the BAK1-interactin receptor-like kinase BIR2, a receptor-like kinase that interacts with BAK1 in the absence of MAMP perception preventing interaction between BAK1 and FLS2 and consequent trigger of PTI (Halter *et al.*, 2014). Interestingly, *bir2* mutants display enhanced resistance to bacterial pathogens and cell death but has no developmental defects (Halter *et al.*, 2014). Nevertheless, an increasing body of research shows induction of these negative regulators upon plant treatment with elicitors or inoculation with pathogens, suggesting an ongoing tight regulation of defense (Halter *et al.*, 2014; Lin *et al.*, 2015).

ROS burst and nematodes

ROS-mediated oxidative burst is one of immune responses hallmarks and occurs in early stages of interaction with pathogens. Despite their constitutive production, uncontrolled generation of ROS is lethal and can cause extensive damage to proteins, DNA and lipids, reason why ROS needs to be maintained at very low levels (Mittal *et al.*, 2014). The necessary balance is achieved by activity of distinct players, such as superoxide dismutase (SOD), catalase (CAT) and glutathione-S-transferases (GST) (Jones *et al.*, 2004; Das & Roychoudhury, 2014; Mittal *et al.*, 2014; Schieber & Chandel, 2014).

ROS have a role in mediating immune responses and as a signaling molecule in plants and animals, acting as a central regulator of immune responses (Mittal *et al.*, 2014). Investigation of peroxidases in defense against plant parasitic

nematodes dates from as early as 1971, when RKN infection of susceptible tomato was shown to lead to production of peroxidases 24 hours after inoculation (Huang *et al.*, 1971). RKN infection of tomato roots was shown to result in differential induction of peroxidases and superoxide dismutase (Zacheo *et al.*, 1982) and generation of hydrogen peroxide in apoplast and plasma membrane (Melillo *et al.*, 2006).

Consistently, the RKN infective-stage juveniles produce ROS scavenging proteins, peroxiredoxins (Molinari & Miacola, 1997), and their knockdown in the parasite results in 60% reduction of root galling (Dubreuil *et al.*, 2011). Detoxifying enzymes have been identified in other nematodes, such as the peroxiredoxin GrTpX (Robertson *et al.*, 2000) and the glutathione peroxidase gr-gpx-1(Jones *et al.*, 2004) from *G. rostochiensis*; the peroxiredoxin BxPrx, (Li *et al.*, 2011) and the catalases Bxy-ctl-1 and Bxy-ctl-2 (Vicente *et al.*, 2015) from the pinewood nematode (PWN, *Bursaphelenchus xylophilus*).

Interestingly, a recently characterized *M. javanica* effector, MjTTL5, interacts with *A. thaliana* ferredoxin:thioredoxin reductase catalytic subunit (AtFTRc), a key component of plant antioxidant system, leading to increased ROS-scavenging activity and suppression of basal defenses (Lin *et al.*, 2016). MjTTL5 shares a high degree of amino acid similarity with homologous proteins present in other RKN species including *M. incognita* (MiTTL5)*, M. enterolobii* (MeTTL5)*, M. hapla* (MhTTL5) and *M. chitwoodi* (McTTL5)(Lin et al., 2016). In addition, Arabidopsis plants compromised in ROS burst by *RBOHD* and *RBOHF* knockout

mutations (Teixeira *et al.*, 2016) or by MjTTL5 overexpression (Lin *et al.*, 2016) show enhanced susceptibility to RKN, in agreement with an important role for ROS burst affecting RKN parasitism. Considering MiTTL5 and MeTTL5 also interact with AtFRC (Lin *et al.*, 2016), it is reasonable to assume that this suppression of ROS might be a conserved RKN parasitism strategy. MjTTL5 has a domain of unknown function, DUF 290, that was shown to be necessary for interaction with AtFRC and a stretch of 48 amino acids is sufficient for this interaction and for MjTTL5 activity (Lin *et al.*, 2016). Further analysis of MjTTL5 amino acid composition revealed similarity to vertebrate nematode parasites such as *Brugia malayi*, *Toxocara canis*, *Loa loa*, *Haemonchus contortus* and *Dictyocaulus viviparus* (similarity ranging from 60 to 75%, E-values ≤1e-12), suggesting its homologs could also play a role in interfering with immune responses in animal parasitism.

Unlike RKN, CN cause marked damage while migrating intracellularly inside plant roots (Wyss *et al.*, 1992; Waetzig *et al.*, 1999). Interestingly, investigation to characterize the role of ROS during interaction between *H. schachtii* and Arabidopsis showed that plants compromised in ROS production were less susceptible to CN (Siddique *et al.*, 2014). However, *H. glycines*, a CN not as adapted to Arabidopsis as *H. schachtii*, induces significantly more necrosis and callose deposition during migration and cannot establish a properly functioning syncytium in Arabidopsis roots (Waetzig *et al.*, 1999), emphasizing the importance of ROS in plant defense and its fine tuning by plant parasitic nematodes. It is

noteworthy to mention that these two species of CNs have very distinct behaviors in Arabidopsis, most probably due to host adaptation.

Somewhat similarly, I observed differences in the infection rate of two *M. incognita* populations on Arabidopsis biotype Col-0 (unpublished data) likely due to PTI response. For highly adapted pathogens, disruption of PTI responses will likely not result in much benefit as any difference in infection might be very subtle to be detected. Inversely, not adapted pathogens are expected to extensively benefit from any disruption in PTI responses, allowing for otherwise subtle differences to be clearly detected.

Analysis of nematode-infected plant roots

Considering the remarkable phenotype caused by sedentary nematodes in plant roots, it is not surprising that the vast majority of studies on plant nematode interactions focus on transcriptome reprograming after establishment of the feeding sites by RKN and CN. The earliest investigation of transcriptomic changes pointed to 8 genes associated with defense responses in tomato roots at 12h post inoculation (hpi) with RKN (Lambert *et al.*, 1999). Using techniques ranging from differentially expressed cDNA library sequencing, microarray to RNAseq analysis, different groups have characterized transcriptomic changes in response to nematode infection, such as *H. glycines* and *M. incognita* in soybean (Alkharouf *et al.*, 2006; Ithal *et al.*, 2007; Klink *et al.*, 2007), *M. javanica* and *M. incognita* in tomato (Lambert *et al.*, 1999; Wang *et al.*, 2003; Bar-Or *et al.*, 2005; Schaff *et al.*,

2007; Bhattarai *et al.*, 2008), *M. javanica*, *M. incognita, H. glycines* and *H. schachtii* in Arabidopsis (Jammes *et al.*, 2005; Szakasits *et al.*, 2009; Barcala *et al.*, 2010; Kammerhofer *et al.*, 2015), *M. graminicola* and *H. oryzae* in rice (Kyndt *et al.*, 2012; Jia & Rock, 2013) (Table 1). The upregulation of transcript levels involved in basal defense during early time points and downregulation in later time points in compatible interactions support a model in which nematodes modulate plant responses to succeed (Goverse & Smant, 2014). Consistently, these transcriptome studies show significant upregulation of defense genes early during plant-nematode interactions and downregulation of these genes inside the feeding sites.

A few studies of transcriptome reprogramming induced by nematode parasitism allow inferences about basal defenses against nematodes (Lambert *et al.*, 1999; Alkharouf *et al.*, 2006; Schaff *et al.*, 2007; Bhattarai *et al.*, 2008; Kammerhofer *et al.*, 2015). Although limited by available techniques at the time these experiments were performed, the first investigation was an important step showing gene induction upon nematode infection during an early time point and by as low as 10 nematodes (Lambert *et al.*, 1999).

Consistently, early (12 hpi) CN penetration and migration resulted in induction of several transcripts, followed by marked downregulation of these transcripts at 24 hpi (Alkharouf *et al.*, 2006). Significant upregulation of genes was observed in tomato roots 24 hpi during both compatible and incompatible RKN interactions, suggesting the observed responses are mediated by basal immunity

(Bhattarai *et al.*, 2008). In addition, this investigation revealed the involvement of the defense hormone jasmonic acid (JA) in basal defense against RKN in tomato.

Recently a role for JA was also demonstrated in defense against CN in Arabidopsis (Kammerhofer *et al.*, 2015). A consistent observation that downregulation of defense-related genes upon successful feeding site establishment in investigations using various gene expression analyses, from single gene expression to high throughput sequencing, is supportive of the idea that nematodes control expression of defense-related genes in their feeding sites to successfully establish parasitism (Goverse & Smant, 2014).

Nematode effectors and pattern-triggered immunity

Effectors are secreted proteins essential for host manipulation and can be produced by and secreted through distinct organs, such as the oesophageal glands, the cuticle, the chemosensory amphids and the rectal glands (Davies & Curtis, 2011). There have been numerous investigations addressing plant parasitic nematode effectors, showing a variety of ways by which nematodes manipulate and interfere with the health of their hosts to their advantage (Jaubert *et al.*, 2002; Bellafiore *et al.*, 2008; Gheysen & Mitchum, 2011; Hewezi & Baum, 2013; Jaouannet *et al.*, 2013; Kandoth & Mitchum, 2013; Mitchum *et al.*, 2013; Goverse & Smant, 2014; Mantelin *et al.*, 2015) (Table 2).

Besides their role in feeding site establishment, characterization of nematode effectors has more recently shed light on the importance of PTI against

plant parasitic nematodes. The best-characterized nematode effector interfering with PTI responses is the *M. incognita* calreticulin (Mi-CRT), which is delivered into the plant apoplast (Jaubert *et al.*, 2005) and is able to suppress elf18-triggered PTI (Jaouannet *et al.*, 2013). Supporting a role in the cell membrane surface, Mi-CRT apoplast localization is essential for its activity, shown by the lack of activity after transformation of *A. thaliana* with Mi-CRT without its secretion signal peptide. Consistent with a role in PTI suppression, MiCRT silencing results in reduced infectivity of RKN (Dubreuil *et al.*, 2009; Jaouannet *et al.*, 2013) and plants overexpressing Mi-CRT are more susceptible and show repression of PTI marker genes after treatment with elf18 (Jaouannet *et al.*, 2013). Similarly, the recently characterized RKN effector MiMsp40 is also able to suppress both elf18-induced callose deposition and PTI marker genes expression (Niu *et al.*, 2016).

The *G. rostochiensis* effector GrUBCEP12 (ubiquitin carboxyl extension protein) is an example of CN effector involved in suppression of PTI. This effector is processed *in planta*, resulting in a 12-amino acid peptide, GrCEP12, able to suppress flg22-triggered production of ROS and PTI marker gene induction in *Nicotiana benthamiana* (Chen *et al.*, 2013; Chronis *et al.*, 2013). Additional CN effectors able to suppress PTI responses have also been identified including, Hs10A06 from *H. schachtii* (Hewezi *et al.*, 2010), GrVAP1 from *G. rostochiensis* (Lozano-Torres *et al.*, 2014) and Ha-annexin from *H. avenae* (Chen *et al.*, 2015).

While some effectors have not been clearly shown to specifically suppress PTI responses, such as Hg30C02 from *H. glycines* (Hamamouch *et al.*, 2012) and

Hs4F01 from *H. schachtii* (Patel *et al.*, 2010), they are good candidates for suppressors of plant basal immunity since they interact with Arabidopsis PR proteins.

Nematode-associated molecular patterns (NAMPs) and PRRs

As mentioned earlier, the first level of pathogen perception relies on the recognition of MAMPs. These molecules are abundantly produced during the pathogen life cycle and are under both negative and positive selection pressure (McCann *et al.*, 2012; Newman *et al.*, 2013). Several MAMPs and their PRRs have been described from microbial pathogens including flg22 and FLS2, flgII-28 and FLS3, LPS and LORE, elf18 and EFR, chitin and LYK5 (Felix *et al.*, 1999; Gomez-Gomez & Boller, 2000; Kunze *et al.*, 2004; Zipfel *et al.*, 2006; Cao *et al.*, 2014a; Ranf *et al.*, 2015; Hind *et al.*, 2016).

The first NAMP was just recently described and consists of a molecule necessary for nematode development and communication with other nematodes, the ascarosides. Ascarosides are molecules that act as dauer pheromones and aggregation and repulsion signals between nematodes (Ludewig and Schroeder, 2012). They were first characterized as a type of lipid that accounted for 25% of the total lipid content of *Ascaris lumbricoides*, a human parasite (Flury, 1912), are present in a wide range of nematode species including free living and parasitic (mammal, insect and plants) nematodes (Choe et al., 2012). Using selective Mass Spectrometry, ascaroside 18 was shown to be the most abundant ascaroside in

infective juveniles of five plant parasitic nematode species (Manosalva *et al.*, 2015). Their relevance in nematode biology, abundant synthesis and conservation across the kingdom make ascarosides a good candidate for a nematode-associated molecular pattern (NAMP). Consistently, ascarosides elicit defense responses in plants, increasing resistance to plant parasitic nematodes and other pathogens (Manosalva *et al.*, 2015).

Interestingly, although an ascaroside receptor has not yet been described, the hormone perception is mediated by BAK1 and BKK1 (Choi & Klessig, 2016). Consistent with the requirement for BAK1, the yet to be identified ascaroside receptor is likely conserved among distinct plant species, as the elicitation of defense responses was conserved in Arabidopsis, tomato, potato and barley plants (Manosalva *et al.*, 2015).

Potential NAMPS

Despite the increase in reports of new molecular patterns from different classes of pathogens observed in the past decade, only one plant parasitic nematode-associated molecular pattern (NAMP) has been described, the ascaroside 18 (Manosalva *et al.*, 2015). Nevertheless, NAMPs from animal parasites have been described earlier and the best example are the excretory/secretory glycoproteins (De Veer *et al.*, 2007). Although damage caused by nematodes has been characterized for certain plant parasites, separating damage signaling and NAMP

perception can be challenging in those systems where there is extensive damage during infection (Sheridan *et al.*, 2004; De Veer *et al.*, 2007; Siddique *et al.*, 2014).

The nematode surface coat

The nematode cuticle is covered by a surface coat (SC), composed of proteins and glycoproteins that originate from the cuticle hypodermis, amphids and secretory/excretory system (De Veer *et al.*, 2007; Davies & Curtis, 2011). Interestingly, this SC is constitutively shed and replaced by a new surface (Davies & Curtis, 2011). It is possible that proteins present in SC can be recognized by hosts and shed by nematodes to evade defense responses (De Veer *et al.*, 2007). The SC has been shown to play a significant role in the interaction of nematodes with different hosts, from entomopathogenic nematodes to plant and gastrointestinal parasites (Artis, 2006; Li *et al.*, 2007; Schmid-Hempel, 2008; Patel *et al.*, 2009; Davies & Curtis, 2011). Consistently, proteins of plant-parasitic nematode SC involved in protection against plant defense responses have also been detected. These include peroxiredoxins and fatty acid-and retinol-binding protein (FAR-1), involved in hydrogen peroxide metabolism and jasmonic acid signaling pathway, respectively (Molinari & Miacola, 1997; Li *et al.*, 2011; Iberkleid *et al.*, 2013).

Consistent with the pivotal role ROS burst plays in the establishment of parasitism by PWN, investigation of PWN surface coat revealed abundance of regulators and scavengers of ROS. Additionally, secretion of proteins on the SC

during pine parasitism was increased as compared to *in vitro* growth of PWN (Shinya *et al.*, 2010).

Indirect recognition: wounding perception

Nematode parasitism relies on the penetration and migration of an animal inside host tissue. Animal parasitic nematodes typically cause damage during penetration and migration inside their hosts. These activities result in activation of the adaptive type 2 immune responses (Gause *et al.*, 2013). It is natural, then, to expect that these activities result in damage, initiating a wounding response, rather than a response based on recognition of NAMP. As it is the case for other pathosystems, distinct migration strategies might result in specific outcomes.

RKN-induced hydrogen peroxide generation in tomato was shown to be a response to RKN presence and not associated with cellular damage (Melillo *et al.*, 2006). In addition, the possibility of RKN-induced wounding responses has been considered and approached through distinct methodologies, showing consistent defense activation after inoculation of 10 nematodes (Lambert *et al.*, 1999) or even by treatment of roots with nematode crude extracts (Teixeira *et al.*, 2016). These results suggest the existence of RKNs recognition by the host independent from any possible cellular damage.

Similarly, comparing responses upon *G. rostochiensis* penetration and mechanical stimulation by blunt pipettes or insertion of electrodes into root epidermal cells showed that plants respond differently to nematode infection and

mechanical factors causing wounding (Sheridan *et al.*, 2004). Nevertheless, *H. glycines* migration and probably damage caused, leads to hydrogen peroxide production (Siddique *et al.*, 2014). Interestingly, hydrogen peroxide production continues even after the nematode establishes a feeding site (therefore, it is not migrating anymore), suggesting something other than damage alone is recognized to trigger this defense response (Waetzig *et al.*, 1999).

Considering the nature of migration of nematodes inside plant tissues, some damage should be caused leading to plant response. The availability of Arabidopsis DAMP receptor mutants is a tool to address the relevance of such responses in the defense against nematodes. This possibility was explored using RKN, but no effect on nematode infection rate was observed using *dorn1* or *pepr1 pepr2* single and double mutants, suggesting that DAMP recognition alone might not play a significant role in defense against RKN (Teixeira *et al.*, 2016).

Objectives of dissertation research

Plant parasitic nematodes are responsible for great losses in agriculture and the broad host range of RKNs makes it challenging for growers to effectively adopt crop rotation, one of the simplest pathogen/pest control methods. Consequently, growers largely rely on the use of pesticides and genetic resistance to control plant parasitic nematodes including RKNs.

As previously described, although R gene-mediated resistance exerts a strong selection pressure on pathogen/pest populations, leading to selection of

virulent populations. Notably, plant immunity relies on perception of motifs from pathogens that are essential for their overall fitness and, are therefore, confer a more durable resistance. Despite its potential, basal immunity against plant parasitic nematodes has not been extensively researched. Therefore, the first objective of my dissertation research, presented in Chapter 1, was to answer if plants can actively perceive and initiate defense responses against RKNs. To address this question, we challenged Arabidopsis PTI mutants with RKNs and analyzed the expression of defense marker genes using RT-PCR and GUS reporter lines. The presented data showed that plants could perceive and mount defense responses against RKN during early stages of parasitism.

The second objective of my dissertation, presented in Chapter 2, was to evaluate the global transcriptome changes in Arabidopsis roots at early stages of RKN infection and identify membrane localized proteins potentially with roles in RKN immunity. Our approach was to use RNAseq to characterize differential gene expression during an early time point of RKN infection, 24h after inoculation, and search this transcriptome for genes that were induced upon RKN parasitism that encoded proteins with transmembrane and kinase domains with putative receptor functions. Evaluation of Arabidopsis mutants for a few of these genes identified a negative regulator of RKN immunity that has constitutive elevated levels of defense marker genes and shows a faster and stronger ROS burst after flg22 treatments. This negative regulator belongs to G-type lectin receptor kinases (G-LecRKs), a family of proteins that has not been extensively characterized. Therefore, the last

objective of my research, presented in Chapter 3, was to identify and characterize G-LecRKs from both Arabidopsis and tomato.

References

Abad P, Gouzy J, Aury J-M, Castagnone-Sereno P, Danchin EGJ, Deleury E, Perfus-Barbeoch L, Anthouard V, Artiguenave F, Blok VC, et al. 2008. Genome sequence of the metazoan plant-parasitic nematode *Meloidogyne incognita*. *Nature Biotechnology* **26**: 909-915.

AbuQamar S, Chai M-F, Luo H, Song F, Mengiste T. 2008. Tomato protein kinase 1b mediates signaling of plant responses to necrotrophic fungi and insect herbivory. *The Plant Cell* **20**(7): 1964-1983.

Alkharouf NW, Klink VP, Chouikha IB, Beard HS, MacDonald MH, Meyer S, Knap HT, Khan R, Matthews BF. 2006. Timecourse microarray analyses reveal global changes in gene expression of susceptible *Glycine max* (soybean) roots during infection by *Heterodera glycines* (soybean cyst nematode). *Planta* **224**: 838-852.

Artis D. 2006. New weapons in the war on worms: Identification of putative mechanisms of immune-mediated expulsion of gastrointestinal nematodes. *International Journal for Parasitology* **36**(6): 723-733.

Bar-Or C, Kapulnik Y, Koltai H. 2005. A broad characterization of the transcriptional profile of the compatible tomato response to the plant parasitic root knot nematode *Meloidogyne javanica*. *European Journal of Plant Pathology* **111**(2): 181-192.

Barcala M, Garcia A, Cabrera J, Casson S, Lindsey K, Favery B, Garcia-Casado G, Solano R, Fenoll C, Escobar C. 2010. Early transcriptomic events in microdissected Arabidopsis nematode-induced giant cells. *Plant Journal* **61**(4): 698-712.

Bartels S, Boller T. 2015. Quo vadis, Pep? Plant elicitor peptides at the crossroads of immunity, stress, and development. *Journal of Experimental Botany* **66**(17): 5183-5193.

Bartels S, Lori M, Mbengue M, van Verk M, Klauser D, Hander T, Böni R, Robatzek S, Boller T. 2013. The family of Peps and their precursors in *Arabidopsis*: differential expression and localization but similar induction of pattern-triggered immune responses. *Journal of Experimental Botany* **64**(17): 5309-5321.

Beck M, Wyrsch I, Strutt J, Wimalasekera R, Webb A, Boller T, Robatzek S. 2014. Expression patterns of *FLAGELLIN SENSING 2* map to bacterial entry sites in plant shoots and roots. *Journal of Experimental Botany* **65**(22): 6487-6498.

Bellafiore S, Shen Z, Rosso MN, Abad P, Shih P, Briggs SP. 2008. Direct identification of the *Meloidogyne incognita* secretome reveals proteins with host cell reprogramming potential. *PLoS pathogens* **4**(10): e1000192.

Bhattarai KK, Xie QG, Mantelin S, Bishnoi U, Girke T, Navarre DA, Kaloshian I. 2008. Tomato susceptibility to root-knot nematodes requires an intact jasmonic acid signaling pathway. *Molecular Plant-Microbe Interactions* **21**(9): 1205-1214.

Brutus A, Yang He S. 2010. Broad-spectrum defense against plant pathogens. *Nature Biotechnology* **28**(4): 330-331.

Cao Y, Liang Y, Tanaka K, Nguyen CT, Jedrzejczak RP, Joachimiak A, Stacey G. 2014a. The kinase LYK5 is a major chitin receptor in Arabidopsis and forms a chitin-induced complex with related kinase CERK1. *eLife*: e03766.

Cao Y, Tanaka K, Nguyen CT, Stacey G. 2014b. Extracellular ATP is a central signaling molecule in plant stress responses. *Current Opinion in Plant Biology* **20**(0): 82-87.

Chen C, Liu S, Liu Q, Niu J, Liu P, Zhao J, Jian H. 2015. An ANNEXIN-like protein from the cereal cyst nematode *Heterodera avenae* suppresses plant defense. *PLoS One* **10**: e0122256.

Chen S, Chronis D, Wang X. 2013. The novel GrCEP12 peptide from the plant-parasitic nematode *Globodera rostochiensis* suppresses flg22-mediated PTI. *Plant Signaling & Behavior* **8**(9): e25359.

Chinchilla D, Zipfel C, Robatzek S, Kemmerling B, Nürnberger T, Jones JD, Felix G, Boller T. 2007. A flagellin-induced complex of the receptor FLS2 and BAK1 initiates plant defence. *Nature* **448**(26): 497-500.

Choi HW, Klessig DF. 2016. DAMPs, MAMPs, and NAMPs in plant innate immunity. *BMC Plant Biology* **16**(1): 232.

Choi J, Tanaka K, Cao Y, Qi Y, Qiu J, Liang Y, Lee SY, Stacey G. 2014. Identification of a Plant Receptor for Extracellular ATP. *Science* **343**: 290-294.

Chronis D, Chen S, Lu S, Hewezi T, Carpenter SC, Loria R, Baum TJ, Wang X. 2013. A ubiquitin carboxyl extension protein secreted from a plant-parasitic nematode *Globodera rostochiensis* is cleaved in planta to promote plant parasitism. *Plant Journal* **74**: 185-196.

Cook DE, Mesarich CH, Thomma BP. 2015. Understanding plant immunity as a surveillance system to detect invasion. *Annual Review of Phytopathology* **53**: 541-563.

Das K, Roychoudhury A. 2014. Reactive oxygen species (ROS) and response of antioxidants as ROS-scavengers during environmental stress in plants. *Frontiers in Environmental Science* **2**.

Davies KG, Curtis RH. 2011. Cuticle surface coat of plant-parasitic nematodes. *Annual Review of Phytopathology* **49**: 135-156.

De Veer MJ, Kemp JM, Meeusen NT. 2007. The innate host defence against nematode parasites. *Parasite Immunology* **29**: 1 - 9.

Decraemer W, Hunt DJ. 2006. *Structure and classification*. Wallingford, Oxfordshire: CAB International.

Dubreuil G, Deleury E, Magliano M, Jaouannet M, Abad P, Rosso M-N. 2011. Peroxiredoxins from the plant parasitic root-knot nematode, *Meloidogyne incognita*, are required for successful development within the host. *International Journal for Parasitology* **41**: 385-396.

Dubreuil G, Magliano M, Dubrana MP, Lozano J, Lecomte P, Favery B, Abad P, Rosso MN. 2009. Tobacco rattle virus mediates gene silencing in a plant parasitic root-knot nematode. *Journal of Experimental Botany*.

Favery B, Quentin M, Jaubert-Possamai S, Abad P. 2015. Gall-forming root-knot nematodes hijack key plant cellular functions to induce multinucleate and hypertrophied feeding cells. *Journal of Insect Physiology*.

Felix G, Duran JD, Volko S, Boller T. 1999. Plants have a sensitive perception system for the most conserved domain of bacterial flagellin. *Plant Journal* **18**: 265-276.

Fraiture M, Brunner F. 2014. Killing two birds with one stone: trans-kingdom suppression of PAMP/MAMP-induced immunity by T3E from enteropathogenic bacteria. *Frontiers in Microbiology* **5**: 320.

Furukawa T, Inagaki H, Takai R, Hirai H, Che F-S. 2013. Two distinct EF-Tu epitopes induce immune responses in rice and Arabidopsis. *Molecular Plant-Microbe Interactions* **27**(2): 113-124.

Gause WC, Wynn TA, Allen JE. 2013. Type 2 immunity and wound healing: evolutionary refinement of adaptive immunity by helminths. *Nature reviews. Immunology* **13**(8): 607-614.

Gheysen G, Mitchum MG. 2011. How nematodes manipulate plant development pathways for infection. *Current Opinion in Plant Biology* **14**(4): 415-421.

Gombault A, Baron L, Couillin I. 2012. ATP release and purinergic signaling in NLRP3 inflammasome activation. *Frontiers in Immunology* **3**: 414.

Gomez-Gomez L, Boller T. 2000. FLS2: an LRR receptor-like kinase involved in the perception of the bacterial elicitor flagellin in Arabidopsis. *Molecular cell* **5**: 1003-1011.

Gomez-Gomez L, Felix G, Boller T. 1999. A single locus determines sensitivity to bacterial flagellin in *Arabidopsis thaliana*. *Plant Journal* **18**(3): 277-284.

Goverse A, Smant G. 2014. The activation and suppression of plant innate immunity by parasitic nematodes. *Annual Review of Phytopathology* **52**: 243-265.

Halter T, Imkampe J, Mazzotta S, Wierzba M, Postel S, Bücherl C, Kiefer C, Stahl M, Chinchilla D, Wang X, et al. 2014. The leucine-rich repeat receptor kinase BIR2 is a negative regulator of BAK1 in plant immunity. *Current Biology* **24**(2): 134-143.

Hamamouch N, Li C, Hewezi T, Baum TJ, Mitchum MG, Hussey RS, Vodkin LO, Davis EL. 2012. The interaction of the novel 30C02 cyst nematode effector protein with a plant β-1,3-endoglucanase may suppress host defence to promote parasitism. *Journal of Experimental Botany* **63**(10): 3683-3695.

He K, Gou X, Yuan T, Lin H, Asami T, Yoshida S, Russell SD, Li J. 2007. BAK1 and BKK1 regulate brassinosteroid-dependent growth and brassinosteroid-independent cell-death pathways. *Current Biology* **17**(13): 1109-1115.

Heese A, Hann DR, Gimenez-Ibanez S, Jones AM, He K, Li J, Schroeder JI, Peck SC, Rathjen JP. 2007. The receptor-like kinase SERK3/BAK1 is a central regulator of innate immunity in plants. *Proceedings of the National*

Academy of Sciences of the United States of America **104**(29): 12217-12222.

Heil M, Land WG. 2014. Danger signals – damaged-self recognition across the tree of life. *Frontiers in Plant Science* **5**: 578.

Hewezi T, Baum TJ. 2013. Manipulation of plant cells by cyst and root-knot nematode effectors. *Molecular Plant-Microbe Interactions* **26**(1): 9-16.

Hewezi T, Howe PJ, Maier TR, Hussey RS, Mitchum MG, Davis EL, Baum TJ. 2010. Arabidopsis spermidine synthase is targeted by an effector protein of the cyst nematode *Heterodera schachtii*. *Plant Physiology* **152**(2): 968-984.

Hind SR, Strickler SR, Boyle PC, Dunham DM, Bao Z, O'Doherty IM, Baccile JA, Hoki JS, Viox EG, Clarke CR, et al. 2016. Tomato receptor FLAGELLIN-SENSING 3 binds flgII-28 and activates the plant immune system. *Nature Plants* **2**: 16128.

Huang CS, Lin LH, Huang SP. 1971. Changes in peroxidase isoenzymes in tomato galls induced by *Meloidogyne incognita*. *Nematologica* **17**: 460-466.

Iberkleid I, Vieira P, de Almeida Engler J, Firester K, Spiegel Y, Horowitz SB. 2013. Fatty acid-and retinol-binding protein, Mj-FAR-1 induces tomato host susceptibility to root-knot nematodes. *PLoS One* **8**(5): e64586.

Ithal N, Recknor J, Nettleton D, Hearne L, Maier T, Baum TJ, Mitchum MG. 2007. Parallel genome-wide expression profiling of host and pathogen during soybean cyst nematode infection of soybean. *Molecular Plant-Microbe Interactions* **20**(3): 293-305.

Jammes F, Lecomte P, de Almeida-Engler J, Bitton F, Martin-Magniette ML, Renou JP, Abad P, Favery B. 2005. Genome-wide expression profiling of the host response to root-knot nematode infection in Arabidopsis. *Plant Journal* **44**(3): 447-458.

Jaouannet M, Magliano M, Arguel MJ, Gourgues M, Evangelisti E, Abad P, Rosso MN. 2013. The root-knot nematode calreticulin Mi-CRT is a key effector in plant defense suppression. *Molecular Plant-Microbe Interactions* **26**(1): 97-105.

Jaubert S, Ledger TN, Laffaire JB, Piotte C, Abad P, Rosso MN. 2002. Direct identification of stylet secreted proteins from root-knot nematodes by a proteomic approach. *Molecular & Biochemical Parasitology* **121**(2): 205-211.

Jaubert S, Milac AL, Petrescu AJ, de Almeida-Engler J, Abad P, Rosso MN. 2005. In planta secretion of a calreticulin by migratory and sedentary stages of root-knot nematode. *Molecular Plant-Microbe Interactions* **18**(12): 1277-1284.

Jia F, Rock CD. 2013. Jacalin lectin *At5g28520* is regulated by ABA and miR846. *Plant Signaling & Behavior* **8**(6): e24563.

Jones JT, Haegeman A, Danchin EGJ, Gaur HS, Helder J, Jones MGK, Kikuchi T, Manzanilla-López R, Palomares-Rius JE, Wesemael WML, et al. 2013. Top 10 plant-parasitic nematodes in molecular plant pathology. *Molecular Plant Pathology* **14**(9): 946-961.

Jones JT, Reavy B, Smant G, Prior AE. 2004. Glutathione peroxidases of the potato cyst nematode *Globodera rostochiensis*. *Gene* **324**: 47-54.

Kammerhofer N, Radakovic Z, Regis JMA, Dobrev P, Vankova R, Grundler FMW, Siddique S, Hofmann J, Wieczorek K. 2015. Role of stress-related hormones in plant defence during early infection of the cyst nematode *Heterodera schachtii* in Arabidopsis. *New Phytologist* **207**: 778-789.

Kandoth PK, Mitchum MG. 2013. War of the worms: how plants fight underground attacks. *Current Opinion in Plant Biology* **16**(4): 457-463.

Klink VP, Overall CC, Alkharouf NW, MacDonald MH, Matthews BF. 2007. Laser capture microdissection (LCM) and comparative microarray expression analysis of syncytial cells isolated from incompatible and compatible soybean (*Glycine max*) roots infected by the soybean cyst nematode (*Heterodera glycines*). *Planta* **226**(6): 1389-1409.

Krol E, Mentzel T, Chinchilla D, Boller T, Felix G, Kemmerling B, Postel S, Arents M, Jeworutzki E, Al-Rasheid KAS, et al. 2010. Perception of the *Arabidopsis* danger signal peptide 1 involves the pattern recognition receptor AtPEPR1 and its close homologue AtPEPR2. *Journal of Biological Chemistry* **285**(18): 13471-13479.

Kunze G, Zipfel C, Robatzek S, Niehaus K, Boller T, Felix G. 2004. The N terminus of bacterial elongation factor Tu elicits innate immunity in Arabidopsis plants. *Plant Cell* **16**: 3496-3507.

Kyndt T, Denil S, Haegeman A, Trooskens G, Bauters L, Van Criekinge W, De Meyer T, Gheysen G. 2012. Transcriptional reprogramming by root knot and migratory nematode infection in rice. *New Phytologist* **196**: 887-900.

Lacombe S, Rougon-Cardoso A, Sherwood E, Peeters N, Dahlbeck D, van Esse HP, Smoker M, Rallapalli G, Thomma BPHJ, Staskawicz B, et al. 2010. Interfamily transfer of a plant pattern-recognition receptor confers broad-spectrum bacterial resistance. *Nature Biotechnology* **28**(4): 365-369.

Lambert KN, Ferrie BJ, Nombela G, Brenner ED, Williamson VM. 1999. Identification of genes whose transcripts accumulate rapidly in tomato after root-knot nematode infection. *Physiological and Molecular Plant Pathology* **55**: 341-348.

Lei J, A. Finlayson S, Salzman RA, Shan L, Zhu-Salzman K. 2014. BOTRYTIS-INDUCED KINASE1 modulates Arabidopsis resistance to green peach aphids via PHYTOALEXIN DEFICIENT4. *Plant Physiology* **165**: 1657-1670.

Li L, Li M, Yu L, Zhou Z, Liang X, Liu Z, Cai G, Gao L, Zhang X, Wang Y, et al. 2014. The FLS2-associated kinase BIK1 directly phosphorylates the NADPH oxidase RbohD to control plant immunity. *Cell Host & Microbe* **15**: 329-338.

Li XY, Cowles RS, Cowles EA, Gaugler R, Cox-Foster DL. 2007. Relationship between the successful infection by entomopathogenic nematodes and the host immune response. *International Journal for Parasitology* **37**(3–4): 365-374.

Li Z, Liu X, Chu Y, Wang Y, Zhang Q, Zhou X. 2011. Cloning and characterization of a 2-cys peroxiredoxin in the pine wood nematode, *Bursaphelenchus xylophilus*, a putative genetic factor facilitating the infestation. *International Journa of Biological Sciences* **7**(6): 823-836.

Lin B, Zhuo K, Chen S, Hu L, Sun L, Wang X, Zhang LH, Liao J. 2016. A novel nematode effector suppresses plant immunity by activating host reactive oxygen species-scavenging system. *New Phytologist* **209**(3): 1159-1173.

Lin ZJ, Liebrand TW, Yadeta KA, Coaker G. 2015. PBL13 Is a Serine/Threonine protein kinase that negatively regulates Arabidopsis immune responses. *Plant Physiology* **169**(4): 2950-2962.

Lozano-Torres JL, Wilbers RH, Warmerdam S, Finkers-Tomczak A, Diaz-Granados A, van Schaik CC, Helder J, Bakker J, Goverse A, Schots A, et al. 2014. Apoplastic venom allergen-like proteins of cyst nematodes modulate the activation of basal plant innate immunity by cell surface receptors. *PLoS pathogens* **10**(12): e1004569.

Lu DP, Wu SJ, Gao XQ, Zhang YL, Shan LB, He P. 2010. A receptor-like cytoplasmic kinase, *BIK1*, associates with a flagellin receptor complex to initiate plant innate immunity. *Proceedings of the National Academy of Sciences of the United States of America* **107**(1): 496-501.

Lu F, Wang H, Wang S, Jiang W, Shan C, Li B, Yang J, Zhang S, Sun W. 2015. Enhancement of innate immune system in monocot rice by transferring the dicotyledonous elongation factor Tu receptor EFR. *Journal of Integrative Plant Biology* **57**(7): 641-652.

Manosalva P, Manohar M, von Reuss SH, Chen S, Koch A, Kaplan F, Choe A, Micikas RJ, Wang X, Kogel K-H, et al. 2015. Conserved nematode signalling molecules elicit plant defenses and pathogen resistance. *Nature Communications* **6**: 7795.

Mantelin S, Thorpe P, Jones JT 2015. Suppression of plant defences by plant-parasitic nematodes. In: Escobar C, Fenoll C eds. *Advances in botanical research*. Oxford, UK: Elsevier Ltd., 325-337.

Maule AG, Curtis R 2011. Parallels between plant and animal parasitic nematodes. In: Jones J, Gheyse G, Fenoll C eds. *Genomics and molecular genetics of plant-nematode interactions*: Springer.

McCann HC, Nahal H, Thakur S, Guttman DS. 2012. Identification of innate immunity elicitors using molecular signatures of natural selection. *Proceedings of the National Academy of Sciences of the United States of America* **109**(11): 4215-4220.

Melillo MT, Leonetti P, Bongiovanni M, Castagnone-Sereno P, Bleve-Zacheo T. 2006. Modulation of reactive oxygen species activities and H2O2 accumulation during compatible and incompatible tomato-root-knot nematode interactions. *New Phytologist* **170**: 501-512.

Melillo MT, Leonetti P, Leone A, Veronico P, Bleve-Zacheo T. 2011. ROS and NO production in compatible and incompatible tomato-*Meloidogyne incognita* interactions. *European Journal of Plant Pathology* **130**: 489-502.

Mitchum MG, Hussey RS, Baum TJ, Wang X, Elling AA, Wubben M, Davis EL. 2013. Nematode effector proteins: an emerging paradigm of parasitism. *New Phytologist* **199**: 879-894.

Mittal M, Siddiqui MR, Tran K, Reddy SP, Malik AB. 2014. Reactive oxygen species in inflammation and tissue injury. *Antioxidants & Redox Signaling* **20**(7): 1126-1167.

Molinari S, Miacola C. 1997. Antioxidant enzymes in phytoparasitic nematodes. *Journal of Nematology* **29**: 153-159.

Mott GA, Middleton MA, Desveaux D, Guttman DS. 2014. Peptides and small molecules of the plant-pathogen apoplastic arena. *Frontiers in Plant Science* **5**.

Navarro L, Zipfel C, Rowland O, Keller I, Robatzek S, Boller T, Jones JD. 2004. The transcriptional innate immune response to flg22. Interplay and overlap with Avr gene-dependent defense responses and bacterial pathogenesis. *Plant Physiology* **135**(2): 1113-1128.

Newman M-A, Sundelin T, Nielsen JT, Erbs G. 2013. MAMP (microbe-associated molecular pattern) triggered immunity in plants. *Frontiers in Plant Science* **4**: 139.

Niu J, Liu P, Liu Q, Chen C, Guo Q, Yin J, Yang G, Jian H. 2016. Msp40 effector of root-knot nematode manipulates plant immunity to facilitate parasitism. *Scientific Reports* **6**: 19443.

Patel N, Hamamouch N, Li C, Hewezi T, Hussey RS, Baum TJ, Mitchum MG, Davis EL. 2010. A nematode effector protein similar to annexins in host plants. *Journal of Experimental Botany* **61**(1): 235-248.

Patel N, Kreider T, Urban Jr JF, Gause WC. 2009. Characterisation of effector mechanisms at the host:parasite interface during the immune response to tissue-dwelling intestinal nematode parasites. *International Journal for Parasitology* **39**(1): 13-21.

Ranf S, Gisch N, Schaffer M, Illig T, Westphal L, Knirel YA, Sanchez-Carballo PM, Zahringer U, Huckelhoven R, Lee J, et al. 2015. A lectin S-domain receptor kinase mediates lipopolysaccharide sensing in *Arabidopsis thaliana*. *Nature immunology* **16**(4): 426-433.

Robatzek S, Bittel P, Chinchilla D, Kochner P, Felix G, Shiu SH, Boller T. 2007. Molecular identification and characterization of the tomato flagellin receptor LeFLS2, an orthologue of *Arabidopsis* FLS2 exhibiting characteristically different perception specificities. *Plant Molecular Biology* **64**: 539-547.

Robatzek S, Chinchilla D, Boller T. 2006. Ligand-induced endocytosis of the pattern recognition receptor FLS2 in Arabidopsis. *Genes Dev* **20**(5): 537-542.

Robertson L, Robertson WM, Sobczak M, Helder J, Tetaud E, Ariyanayagam MR, Ferguson MAJ, Fairlamb A, Jones JT. 2000. Cloning, expression and functional characterisation of a peroxiredoxin from the potato cyst nematode *Globodera rostochiensis*. *Molecular and Biochemical Parasitology* **111**(1): 41-49.

Rodiuc N, Vieira P, Banora MY, de Almeida Engler J. 2014. On the track of transfer cell formation by specialized plant-parasitic nematodes. *Frontiers in Plant Science* **5**: 160.

Roux M, Schwessinger B, Albrecht C, Chinchilla D, Jones A, Holton N, Malinovsky FG, Tor M, de Vries S, Zipfel C. 2011. The Arabidopsis leucine-rich repeat receptor-like kinases BAK1/SERK3 and BKK1/SERK4 are required for innate immunity to hemibiotrophic and biotrophic pathogens. *Plant Cell* **23**: 2440-2455.

Salomon S, Robatzek S. 2006. Induced Endocytosis of the Receptor Kinase FLS2. *Plant Signaling & Behavior* **1**(6): 293-295.

Schaff JE, Nielsen DM, Smith CP, Scholl EH, Bird DM. 2007. Comprehensive transcriptome profiling in tomato reveals a role for glycosyltransferase in *Mi*-mediated nematode resistance. *Plant Physiology* **144**(2): 1079-1092.

Scheibner KA, Lutz MA, Boodoo S, Fenton MJ, Powell JD, Horton MR. 2006. Hyaluronan fragments act as an endogenous danger signal by engaging TLR2. *The Journal of Immunology* **177**(2): 1272-1281.

Schieber M, Chandel Navdeep S. 2014. ROS function in redox signaling and oxidative stress. *Current Biology* **24**(10): R453-R462.

Schmid-Hempel P. 2008. Parasite immune evasion: a momentous molecular war. *Trends in Ecology & Evolution* **23**(6): 318-326.

Schoonbeek H-j, Wang H-H, Stefanato FL, Craze M, Bowden S, Wallington E, Zipfel C, Ridout CJ. 2015. Arabidopsis EF-Tu receptor enhances bacterial disease resistance in transgenic wheat. *New Phytologist* **206**(2): 606-613.

Schwessinger B, Bahar O, Thomas N, Holton N, Nekrasov V, Ruan D, Canlas PE, Daudi A, Petzold CJ, Singan VR, et al. 2015. Transgenic expression of the dicotyledonous pattern recognition receptor EFR in rice leads to ligand-dependent activation of defense responses. *PLoS pathogens* **11**(3): e1004809.

Sheridan JP, Miller AJ, Perry RN. 2004. Early responses of resistant and susceptible potato roots during invasion by the potato cyst nematode *Globodera rostochiensis*. *Journal of Experimental Botany* **55**(397): 751-760.

Shi Q, Febres VJ, Jones JB, Moore GA. 2016. A survey of FLS2 genes from multiple citrus species identifies candidates for enhancing disease resistance to *Xanthomonas citri* ssp. *citri*. *Hortic Res* **3**: 16022.

Shinya R, Morisaka H, Takeuchi Y, Ueda M, Futai K. 2010. Comparison of the surface coat proteins of the pine wood nematode appeared during host pine infection and in vitro culture by a proteomic approach. *Phytopathology* **100**(12): 1289-1297.

Siddique S, Matera C, Radakovic ZS, Shamim Hasan M, Gutbrod P, Rozanska E, Sobczak M, Angel Torres M, Grundler FM. 2014. Parasitic worms stimulate host NADPH oxidases to produce reactive oxygen species that limit plant cell death and promote infection. *Science signaling* **7**(320): ra33.

Sun YD, Han ZF, Tang J, Hu ZH, Chai CL, Zhou B, Chai JJ. 2013a. Structure reveals that BAK1 as a co-receptor recognizes the BRI1-bound brassinolide. *Cell Research* **23**(11): 1326-1329.

Sun YD, Li L, Macho AP, Han ZF, Hu ZH, Zipfel C, Zhou JM, Chai JJ. 2013b. Structural basis for flg22-induced activation of the Arabidopsis FLS2-BAK1 immune complex. *Science* **342**: 624-628.

Szakasits D, Heinen P, Wieczorek K, Hofmann J, Wagner F, Kreil DP, Sykacek P, Grundler FM, Bohlmann H. 2009. The transcriptome of syncytia induced by the cyst nematode *Heterodera schachtii* in Arabidopsis roots. *Plant Journal* **57**(5): 771-784.

Takai R, Isogai A, Takayama S, Che FS. 2008. Analysis of flagellin perception mediated by flg22 receptor OsFLS2 in rice. *Molecular Plant-Microbe Interactions* **21**(12): 1635-1642.

Teixeira MA, Wei L, Kaloshian I. 2016. Root-knot nematodes induce pattern-triggered immunity in *Arabidopsis thaliana* roots. *New Phytologist* **211**: 279-287.

Trda L, Fernandez O, Boutrot F, Heloir MC, Kelloniemi J, Daire X, Adrian M, Clement C, Zipfel C, Dorey S, et al. 2014. The grapevine flagellin receptor VvFLS2 differentially recognizes flagellin-derived epitopes from the endophytic growth-promoting bacterium *Burkholderia phytofirmans* and plant pathogenic bacteria. *New Phytologist* **201**: 1371-1384.

Vallarino JG, Osorio S. 2012. Signaling role of oligogalacturonides derived during cell wall degradation. *Plant Signaling & Behavior* **7**(11): 1447-1449.

Veronese P, Nakagami H, Bluhm B, AbuQamar S, Chen X, Salmeron J, Dietrich RA, Hirt H, Mengiste T. 2006. The Membrane-Anchored BOTRYTIS-INDUCED KINASE1 Plays Distinct Roles in Arabidopsis Resistance to Necrotrophic and Biotrophic Pathogens. *Plant Cell* **18**: 257-273.

Vicente CSL, Ikuyo Y, Shinya R, Mota M, Hasegawa K. 2015. Catalases induction in high virulence pinewood nematode *Bursaphelenchus xylophilus* under hydrogen peroxide-induced stress. *PLoS One* **10**(4): e0123839.

Waetzig GH, Sobczak M, Grundler F. 1999. Localization of hydrogen peroxide during the defence response of *Arabidopsis thaliana* against the plant parasitic nematode *Heterodera glycines*. *Nematology* **1**: 681-686.

Wang Z, Potter RH, Jones MGK. 2003. Differential display analysis of gene expression in the cytoplasm of giant cells induced in tomato roots by *Meloidogyne javanica*. *Molecular Plant Pathology* **4**(5): 361-371.

Wyss U, Grundler FMW, Munch A. 1992. The parasitic behaviour of second-stage juveniles of *Meloidogyne incognita* in roots of *Arabidopsis thaliana*. *Nematologica* **38**: 98-111.

Yamaguchi Y, Huffaker A, Bryan AC, Tax FE, Ryan CA. 2010. PEPR2 is a second receptor for the Pep1 and Pep2 peptides and contributes to defense responses in *Arabidopsis*. *Plant Cell* **22**: 508-522.

Zacheo G, Bleve-Zacheo T, Lamberti F. 1982. Involvement of superoxide dismutases and superoxide radicals in the susceptibility and resistance of tomato plants to infestation by *Meloidogyne incognita*. *Nematologia Mediterranea* **10**: 75-80.

Zipfel C. 2014. Plant pattern-recognition receptors. *Trends in Immunology* **35**: 345-351.

Zipfel C, Kunze G, Chinchilla D, Caniard A, Jones JD, Boller T, Felix G. 2006. Perception of the bacterial PAMP EF-Tu by the receptor EFR restricts Agrobacterium-mediated transformation. *Cell* **125**(4): 749-760.

Zipfel C, Robatzek S, Navarro L, Oakeley EJ, Jones JD, Felix G, Boller T. 2004. Bacterial disease resistance in Arabidopsis through flagellin perception. *Nature* **428**(6984): 764-767.

Table 1. Gene expression studies on plant-nematode interactions during the first 48h post inoculation (hpi).

Host	Nematode	Methodology	Findings	Reference
Tomato	*M. javanica*, 12 hpi	cDNA library	8 genes were induced both in susceptible and resistant plants	(Lambert et al., 1999)
	M. incognita, 12, 36 hpi	Microarray	Substantial changes in root gene expression occurred 12 hpi	(Schaff et al., 2007)
	M. incognita, 24 hpi		JA signaling is involved in basal defense against RKN	(Bhattarai et al., 2008)
Arabidopsis	*H. schachtii*, 24, 48 hpi	Reporter lines	WRKY transcription factors, repressed in syncytium, are induced early in interaction	(Ali et al., 2014)
	H. schachtii, 10 hpi	qPCR	JA signaling is involved in basal defense against cyst nematodes	(Kammerhofer et al., 2015)
	M. incognita, 24 hpi	qPCR and reporter lines	Basal defense marker genes are induced by RKN migration and its crude extract	(Teixeira et al., 2016)
Soybean	*H. glycines*, 6, 12, 24 hpi	Microarray	Differential gene induction occurs during first 12h of interaction	(Alkharouf et al., 2006)

Table 2. Nematode effectors and their activities to suppress PTI.

Nematode	Effector	Activity
M. incognita	MiCRT (Jaouannet et al., 2013)	Suppression of elf18-triggered induction of defense marker genes and callose deposition.
	MiMsp40 (Niu et al., 2016)	
M. javanica	MjTTL5 (Lin et al., 2016)	Suppression of flg22- triggered induction of defense marker genes and ROS generation.
G. rostochiensis	Gr-VAP1(Lozano-Torres et al., 2014)	Suppression of flg22-mediated disruption of root elongation, loss of basal immunity against microbial pathogens.
	GrCEP12 (Chen et al., 2013)	Suppression of flg22-triggered induction of defense marker genes and ROS generation.
H. schachtii	Hs10A06 (Hewezi et al., 2010)	Increased mRNA abundance of antioxidant genes upon nematode infection.
	Hs4F01 (Patel et al., 2010)	Interaction with *A. thaliana* oxidoreductase, possibly to limit defense gene expression.
H. glycines	Hg30C02 (Hamamouch et al., 2012)	Interaction with *A. thaliana* β-1,3-endoglucanase, possibly to neutralize its activity.

CHAPTER ONE

Root-knot nematodes induce pattern-triggered immunity in *Arabidopsis thaliana* roots

Abstract

Root-knot nematodes (RKN; *Meloidogyne* spp.) are plant parasites with a broad host range causing great losses worldwide. To parasitize their hosts, RKN establish feeding sites in roots known as giant cells. The majority of work studying plant-RKN interactions in susceptible hosts addresses establishment of the giant cells and limited information exists on the early defense responses. Here we characterize early defense or pattern-triggered immunity (PTI) against RKN in *Arabidopsis thaliana*. To address PTI, we evaluated known canonical PTI signaling mutants with RKN and investigated the expression of PTI marker genes after RKN infection using both qPCR and GUS reporter transgenic lines. We show that PTI compromised plants have enhanced susceptibility to RKN, including the *bak1-5* mutant. BAK1 is a common partner of distinct receptors of microbe- and damage-associated molecular patterns. Furthermore, our data indicate that nematode recognition leading to PTI responses involves camalexin and glucosinolate biosynthesis. While the RKN-induced glucosinolate biosynthetic pathway was *BAK1*-dependent, the camalexin biosynthetic pathway was only partially dependent on *BAK1*. Combined, our results indicate the presence of *BAK1*-dependent and -independent PTI against RKN in *A. thaliana*, suggesting the existence of diverse nematode recognition mechanisms.

Introduction

Plant parasitic nematodes are mostly soil dwelling microscopic worms responsible for over $US157 billion annual crop losses worldwide (Abad *et al.*, 2008). Among these nematodes, the most economically important group are the sedentary endoparasites that include root-knot nematodes (RKNs, *Meloidogyne* spp.) and cyst nematodes (*Heterodera* spp. and *Globodera* spp.) that are able to establish elaborate feeding sites near the plant vasculature (Jones *et al.*, 2013). Some RKNs have a wide host range, infecting thousands of plant species (Moens *et al.*, 2009). The infective stage is the second-stage juvenile (J2) which hatches from eggs, migrates towards plant root tips and penetrates behind the root tip in the root elongation zone. After successful penetration and migration inside the roots, the J2 induces the development of a feeding site that is comprised of a few enlarged cells, known as giant cells. These specialized cells are multinucleated due to nematode-induced karyokinesis without cytokinesis (Rodiuc *et al.*, 2014). Giant cells act as a nutrient sink providing the nematode with the nourishment it needs to develop and reproduce. Cortical cells surrounding the giant cells enlarge and form root galls, the typical disease symptom associated with RKN infection (Rodiuc *et al.*, 2014).

Plant immunity includes the perception of microbe-associated molecular patterns (MAMPs) by cell surface localized pattern recognition receptors (PRRs) (Zipfel, 2014). This perception leads to induction of pattern-triggered immunity

(PTI), which includes activation of mitogen-activated protein (MAP) kinases, rapid ion fluxes across the plasma membrane, callose deposition, reactive oxygen species (ROS) production and rapid changes in gene expression (Jones & Dangl, 2006; Zipfel, 2008). To overcome these defenses, pathogens and pests have evolved effectors to suppress PTI (Jones & Dangl, 2006). In turn, plants evolved resistance genes to recognize specific effectors and trigger effector-triggered immunity (ETI).

During the past decade, a number of MAMPs were identified such as fungal chitin, bacterial lipopolysaccharides, flagellin and elongation factor TU (EF-Tu). The flagellin-derived peptide flg22 is the best-studied MAMP and in *Arabidopsis thaliana* is recognized by the PRR FLAGELLIN-SENSING 2 (FLS2) (Gomez-Gomez & Boller, 2000). *FLS2* orthologs have been identified in several plant species including tomato (*Solanum lycopersicum*) (Robatzek *et al.*, 2007), *Nicotiana benthamiana* (Hann & Rathjen, 2007) grapevine (*Vitis vinifera*) (Trda *et al.*, 2014) and rice (*Oryza sativa*) (Takai *et al.*, 2008). EF-TU is an abundant bacterial protein recognized by the PRR EF-TU RECEPTOR (EFR), which seems to be exclusive to Brassicaceae (Kunze *et al.*, 2004). Both FLS2 and EFR encode membrane localized receptor kinases (RK) with extracellular leucine-rich repeats (LRR) and intracellular kinase domains and rely on the BRASSINOSTEROID INSENSITIVE-ASSOCIATED KINASE 1 (BAK1) for MAMP perception (Roux *et al.*, 2011; Sun *et al.*, 2013). BAK1 is a member of the somatic embryogenesis receptor kinases (SERKs) which also encode membrane localized LRR-kinases

(Chinchilla *et al.*, 2009). BAK1 is also required for the function of additional PRRs (Böhm *et al.*, 2014). This BAK1-dependent signaling is conserved among the distinct PRRs which involves BAK1-PRR transphosphorylation (Han *et al.*, 2014) and phosphorylation of the cytoplasmic BOTRYTIS-INDUCED KINASE 1 (BIK1) by BAK1 (Lu *et al.*, 2010). BIK1 in turn phosphorylates the RESPIRATORY BURST NADPH OXIDASE D (RBOHD) (Lu *et al.*, 2010; Kadota *et al.*, 2014; Li *et al.*, 2014) which leads to downstream signaling activation including mitogen-activated protein (MAP) kinase cascade and differential gene expression (Asai *et al.*, 2002).

Besides MAMPs, plants also recognize self-danger molecules or danger-associated molecular patterns (DAMPs) originating from cellular damage (Boller & Flury, 2012). Several DAMPs were recently identified in *A. thaliana* as endogenous peptide elicitors (*At*Peps) and are induced by wounding, pathogen infection and PAMP or hormone treatments (Huffaker *et al.*, 2006; Huffaker & Ryan, 2007). The small peptides *At*peps1-8 are examples of DAMPs recognized by the PEP RECEPTORs (PEPR) 1 and PEPR2 (Krol *et al.*, 2010; Yamaguchi *et al.*, 2010; Bartels *et al.*, 2013). Both receptors encode membrane localized LRR-RKs. Similar to FLS2 and EFR, these PEPRs also require BAK1 as a recognition partner and share downstream defense signaling (Schulze *et al.*, 2010; Flury *et al.*, 2013). Extracellular ATP (eATP), known for its role in extracellular signaling in mammals is an additional example of DAMP. In plants, eATP acts also as a DAMP and accumulates in the plant apoplast in response to chitin or wounding (Tanaka *et al.*,

2014). The plant eATP receptor, DOES NOT RESPOND TO NUCLEOTIDES 1 (*DORN1*), was recently identified (Choi *et al.*, 2014). *DORN1* encodes an extracellular legume-type lectin domain, a transmembrane domain and an intracellular kinase domain.

Currently, the study of plant defense to nematodes is mostly restricted to disease resistance proteins and ETI combined with nematode effectors and their roles in parasitism (Kaloshian *et al.*, 2011; Mitchum *et al.*, 2013; Goverse & Smant, 2014; Mantelin *et al.*, 2015). Similar to microbial pathogens, several nematode effectors have been shown to target and suppress plant immunity. These include GrCEP12 and GrVAP1, peptides from *Globodera rostochiensis* (Chen *et al.*, 2013; Lozano-Torres *et al.*, 2014), *Ha-annexin* from *Heterodera avenae* (Chen *et al.*, 2015), and the Mi-CRT from *Meloidogyne incognita* (Jaouannet *et al.*, 2013). The identification of nematode effectors that suppress immunity supports the notion that overcoming plant immunity is important for successful nematode parasitism.

Orthologs of *BAK1* have been identified in a number of plant species including *N. benthamiana* and tomato (Hann & Rathjen, 2007; Chaparro-Garcia *et al.*, 2011; Mantelin *et al.*, 2011). Earlier, we characterized three tomato SERK members, and two of them, *SlSERK3A* and *SlSERK3B*, share high sequence similarity with the *A. thaliana SERK3*/*BAK1* (Mantelin *et al.*, 2011). Using virus-induced gene silencing (VIGS) we showed enhanced susceptibility to RKN in *SlSERK3A*- or *SlSERK3B*-silenced tomato plants suggesting the presence of PTI against RKN (Peng & Kaloshian, 2014). In this work, we characterize PTI

responses in *A. thaliana* against *M. incognita* and describe the presence of *BAK1*-dependent and independent PTI against this species.

Materials and Methods

M. incognita culture and inoculum preparation

Meloidogyne incognita (Kofoid and White) Chitwood, isolate P77R3, maintained on tomato cultivar UC82, grown in UC mix and sand (1:9, vol/vol), was used. Plants were fertilized once a week with MiracleGro ® (Scotts Miracle-Gro Co) water soluble all-purpose plant food and kept in a glasshouse at 24˚ to 30˚C.

Nematode eggs were extracted from roots using 10% bleach and sieving (Hussey & Barker, 1973). Eggs and plant debris collected on a 500-mesh sieve were fractionated three times on 35% sucrose and rinsed several times with sterile water. The collected eggs were surface sterilized by shaking in 5% bleach for 5 minutes and rinsed with sterile water. This procedure was repeated three times. Surface sterilized eggs were hatched under sterile conditions in a modified Baermann funnel (Martinez de Ilarduya *et al.*, 2001). Two days later, J2s were collected, counted and suspended in a 0.5% carboximethylcellulose solution.

Arabidopsis thaliana growth and nematode inoculations

Seeds of *Arabidopsis thaliana* (L.) Heynh wild-type Col-0 and mutants, all in Col-0 background, were surface sterilized and kept at 4˚C for 5 days before plating. For RKN infection assays, seeds were plated on Gamborg media (Sigma-Aldrich) (pH 6.0) supplemented with 3% sucrose and 0.6% daishin agar (Bioworld) and maintained in plant growth rooms with 12 h light photoperiod at 24˚C. For galling

assays, two-week-old seedlings, with six seedlings per plate, were inoculated with 100 J2s per seedling and maintained as described above. Five plates were used per treatment. At two-week stage, except for oxDORN1 and the *dorn1-3* mutant, root growth of the tested mutants was similar to wild type Col-0 (Appendix A). Four weeks after inoculation, plants were evaluated for number of galls. The number of galls on Col-0 roots was defined as 100 percent and number of galls on mutant roots was reported relative to number of galls on Col-0 roots.

For RKN attraction assays, eight-day-old seedlings (Appendix A) plated as described above, were removed from agar plates and placed in PF-127 medium (23% wt/vol; Sigma-Aldrich) containing J2s as described by Fudali et al. (2013). Briefly, the nematode concentration in PF-127 was adjusted to 200 J2s ml^{-1} and 1 ml of this solution was added to each well of a 12-well tissue culture plate (Corning Inc.) followed by placement of one *A. thaliana* seedling into each well. The number of nematodes touching the terminal 7 mm of the root tip was counted at the indicated times. The number of J2s touching wilt-type Col-0 roots was defined as 100 percent and the number of J2s touching mutant roots was reported relative to the wild-type reference.

For RKN penetration assays, 20 seeds were plated per plate on Gamborg media as described above. Eight-day-old seedlings (Appendix A) were inoculated with 100 J2s per seedlings and maintained as described above. Seedlings were gently removed from plates for staining at the desired time points.

For acid fuchsin staining, seedlings were treated with 10% bleach for one minute, washed well with water and boiled for 10 seconds in acid fuchsin solution (3.5% acid fuchsin in 25% acetic acid). After the solution cooled to room temperature, seedlings were transferred to a destaining solution (1:1:1 acetic acid:glycerol:H_2O) and the number of nematodes inside the roots was evaluated using a stereoscope.

For double staining of the GUS reporter lines, seedlings were processed as described by Millet *et al.* (2010) with modifications. Briefly, plates were flooded with PBS and roots were gently removed from the agar media and transferred to GUS substrate solution (50mM sodium phosphate, pH7, 10mM EDTA, 0.5mM$K_4[Fe(CN)_6]$, 0.5mM $K_3[Fe(CN)_6]$, 0.5mM X-Guc, and 0.01% Silwet L-77). Seedlings were vacuum infiltrated for 5 min and incubated at 37˚C for 4 h. Seedlings were treated with 1% bleach solution for 3 min, washed in water, stained with acid fuchsin and destained as described above. Seedlings were viewed and imaged on a Leica DMR compound microscope using differential interference contrast (DIC) optics.

Nematode extract and treatment

For treatment of *A. thaliana* seedlings with nematode extracts, seeds were grown in liquid Murashige & Skoog Basal Salt media (Phytotechnology Laboratories) and maintained in a plant growth room with 12 h light photoperiod at 24˚C.

J2s were spun down to a volume of about 500 μl in a 1.5 ml tube and frozen in liquid N_2. The frozen J2 pellet was ground in a mortar and pestle and the powder was suspended in PBS (pH 7.0) and frozen at -20˚C overnight. After centrifugation at 9500 g for 15 min at 4˚C, the supernatant was used to treat 8-day-old *A. thaliana* GUS reporter lines overnight. Seedlings were washed in PBS, stained for GUS activity and fixed in 3:1 ethanol:acetic acid (Byrd *et al.*, 1983). The fixative was replaced with 95% ethanol, seedlings were cleared in lactic acid, mounted in 50% glycerol and viewed with DIC optics.

Pretreatment with flg22

Eight-day-old *A. thaliana* seedlings grown on Gamborg media were flooded with 6 ml of liquid MS for 48 h as described by Millet *et al.* (2010). The solution was then replaced with 1 μM flg22 (Bio-synthesis Inc, Lewisville, TX) or water as control for 3 h. Water or flg22 solution was removed and seedlings inoculated with 100 J2 per seedling. After 24 h, roots were stained using acid fuchsin and evaluated for nematode penetration.

Gene expression analysis

RNA was isolated from *A. thaliana* roots using GeneJET Plant RNA purification kit (Life Technologies). Three μg of RNA was DNase treated and used for cDNA synthesis using Superscript III reverse transcriptase enzyme (Invitrogen) and oligo-dT primers according to the manufacturer's recommendations.

Quantitative PCR was performed using gene-specific primers (Table 1), iQ SYBR Green Supermix (Biorad) in iCycler5 IQ (Biorad) in 15 μl using the following program: 94°C for 5 min, followed by 35 cycles of 94°C for 30 sec, 58°C for 30 sec, 72°C for 30 sec and a final cycle of 72°C for 3 min. Three biological replicates, with three technical replicates each, were performed and the generated threshold cycle (C_T) was used to calculate transcript abundance relative to the ribosomal gene 18S.

Statistical analysis

Pairwise comparisons of nematode penetration, root galling and gene expression analysis of mutants and treatments with wild-type Col-0 was performed using Student *t*-test.

Results

The *bak1-5* mutant displays enhanced susceptibility to RKN

Our previous work suggested a role for *SlSERK3A and SlSERK3B* in tomato defense against RKN (Peng & Kaloshian, 2014). To further characterize *SERK3/BAK1* role in basal immunity against this nematode, we tested whether the enhanced susceptibility seen in *SlSERK3A* or *SlSERK3B* silenced tomato can be seen in the *A. thaliana bak1* mutant. For this purpose, we used the *A. thaliana bak1-5* mutant in RKN infection assays. The *bak1-5* mutant has a single amino acid substitution in the kinase domain that allows wild-type level protein accumulation but is impaired in PTI signaling (Schwessinger *et al.*, 2011). *A. thaliana bak1-5* seedlings infected with RKN J2s supported significantly higher number of galls compared to the wild type (Figure 1.1A), confirming the results obtained with RKN infection of *SlSERK3A* and *SlSERK3B* silenced tomato (Peng & Kaloshian, 2014).

The observed increase in root galling of *bak1-5* could be due to enhanced attraction of nematode to *bak1-5* roots compared to wild type. To address this possibility, a test for nematode attraction to roots was performed (Wang *et al.*, 2009). PF-127, a copolymer that is liquid at 15°C but forms a transparent gel at room temperature, was used for this assay (Ko & Van Gundy, 1988). J2 attraction to *bak1-5* and wild-type roots was tested in PF-127 and roots were evaluated at 2, 4, 6, 9, 12 and 24 h after initiation of the assay. No difference in nematode

attraction to the roots of these two genotypes was observed (Appendix B). The enhanced root galling combined with lack of difference in attraction to roots suggest the existence of an impediment in nematode penetration. To evaluate the rate of root penetration of J2s, *bak1-5* and wild-type roots were infected with RKN and the number of nematodes inside the roots were evaluated at 9, 18, and 24 h after inoculation. This time course was chosen to include all early steps of RKN penetration and migration inside the roots before reaching the vascular cylinder where they establish a feeding site (Wyss *et al.*, 1992). No difference in the number of J2s was observed at 9 h, however, at both 18 h and 24 h the number of J2s was significantly higher in *bak1-5* than in wild-type roots (Figure 1.1B) consistent with the enhanced galling phenotype observed in this mutant.

PTI treatment enhances resistance to RKN

The enhanced susceptibility to RKN in *bak1-5* suggests PTI is involved in RKN resistance. To confirm a role for PTI in RKN defense, *A. thaliana* wild-type seedlings were treated with flg22 peptide, the potent elicitor of immunity, prior to inoculation with RKN. Significantly lower numbers of J2s were present inside the roots of seedlings pretreated with flg22 indicating flg22 treatment enhanced the resistance to RKN (Figure 1.2).

RKN recognition requires the canonical PTI signaling partners

Following MAMP recognition, BAK1 phosphorylates the receptor-like cytoplasmic kinase *BIK1* to modulate downstream signaling (Kadota *et al.*, 2014; Li *et al.*, 2014). To assess a role for *BIK1* in RKN defense, *bik1* mutant was evaluated for RKN infection. Significantly higher numbers of galls were observed on *bik1* mutant roots compared to wild type (Figure 1.3) indicating BIK1 is a positive regulator of RKN defense.

BIK1 phosphorylates the respiratory burst NADPH oxidase D (RBOHD) to enhance ROS burst (Kadota *et al.*, 2014; Li *et al.*, 2014). *RBOHD* and *RBOHF* are known to have a partially redundant function in defense (Torres *et al.*, 2002; Kwak *et al.*, 2003; Siddique *et al.*, 2014). To assess a role for RBOH in RKN defense, the *rbohD rbohF* double mutant was used in the RKN assay. Significantly higher numbers of galls were observed on the *rbohD rbohF* double mutant compared to wild type (Figure 1.3) indicating a positive role for RBOH in RKN defense.

Canonical PTI responses are induced by RKN in *A. thaliana* roots

Treatment of *A. thaliana* roots with flg22 induces expression of cytochrome P450 *CYP71A12* involved in the phytoalexin camalexin biosynthesis, transcription factor (TF) *MYB51* that regulates glucosinolate biosynthesis as well as TF *WRKY11* involved in basal defense (Millet *et al.*, 2010). To determine whether RKN infection activates expression of these genes in roots, *CYP71A12*, *MYB51* and *WRKY11* promoter::GUS *A. thaliana* transgenic lines were inoculated with RKN and

evaluated for GUS activity. RKN infection elicited GUS activity in *CYP71A12* and *WRKY11* reporter lines at both the root elongation zone and tips, while GUS activity in the *MYB51* reporter line was restricted to the elongation zone (Figure 1.4A). The observed GUS activity in the three reporter lines overlapped with the presence of nematodes in these root zones.

Unlike cyst nematodes, RKNs cause minimum damage during root penetration (Wyss *et al.*, 1992). However, RKN penetration and intercellular migration could induce DAMP and activate expression of defense-related genes. To evaluate whether the observed GUS activity could be detected without any root damage in the absence of nematode penetration, we used J2 crude extracts to treat the GUS reporter lines. GUS activity was observed in the roots of all three reporter lines mainly in the root elongation zone (Figure 1.4A), where RKN penetrate roots, but not in the root maturation zone (Appendix C). To further confirm the induction of *CYP71A2, MYB51* and *WRKY11* by RKN infection, expression of these genes was evaluated in *A. thaliana* roots 24 h after RKN inoculation. We also evaluated expression of *BAK1* by RKN infection. All four genes, including *BAK1*, were induced in wild-type roots by RKN (Figure 1.4B).

Although recognition of the well characterized MAMPs flagellin and EF-Tu are *BAK1*-dependent, other MAMPs such as chitin activate PTI responses in a *BAK1* independent manner (Gimenez-Ibanez *et al.*, 2009; Zipfel, 2014). To confirm *BAK1*-dependency of nematode induced PTI responses, we evaluated expression of *CYP71A2, MYB51* and *WRKY11* in nematode-inoculated *bak1-5* roots.

Surprisingly, even though *BAK1, MYB51* and *WRKY11* induction were completely abolished in this mutant, induction of *CYP71A12* was only partially attenuated (Figure 1.4C) indicating distinct regulations of these PTI responses.

Camalexin, glucosinolate and basal defense are involved in resistance against RKN

RKN infection of roots triggered upregulation of genes involved in the biosynthesis of camalexin and glucosinolate, well-known antimicrobial compounds (Beekwilder *et al.*, 2008; Schlaeppi *et al.*, 2010; Stotz *et al.*, 2011; Kettles *et al.*, 2013; Wang *et al.*, 2013). Both *cyp71A12* mutant and *cyp71A13* mutant are only partially compromised in camalexin production (Nafisi *et al.,* 2007; Millet *et al.,* 2010). Therefore, to evaluate the role of camalexin in RKN defense, a *pad3* mutant impaired in camalexin biosynthesis was used (Glazebrook & Ausubel, 1994). The *pad3* mutant displayed significantly higher number of galls compared to wild type (Figure 1.5) indicating a positive role for camalexin in nematode defense.

Similarly, the *myb34* and *myb51* single mutants are only partially compromised in glucosinolate production (Frerigmann & Gigolashvili, 2014). However, the double mutant *myb34 myb51* is completely impaired in glucosinolate production (Frerigmann & Gigolashvili, 2014) and was therefore used to investigate the role of glucosinolate in defense against RKN. The *myb34 myb51* double mutant infected with RKN displayed significantly higher numbers of galls

compared to wild type indicating a positive role for glucosinolate in RKN defense (Figure 1.5).

The peptide flg22 induces *WRKY11* in *A. thaliana* roots. *WRKY11* can function in partial redundancy with *WRKY17* (Journot-Catalino *et al.*, 2006). Therefore, both single and double mutants of these WRKYs were used in RKN assays. The *wrky11* and *wrky17* single mutants as well as the *wrky11 wrky17* double mutant displayed significantly higher numbers of galls compared to wild type (Figure 1.5), indicating that both TFs are positive regulators of RKN defense. The number of galls on the single and double mutants were not significantly different suggesting *WRKY11* and *WRKY17* do not function redundantly in this pathosystem.

RKN infection is not perceived by the MAMP receptor FLS2 and the DAMP receptors PEPR1, PEPR2 and DORN1

Nematodes are soil dwelling animals and are exposed to soil inhabiting microbes. It is therefore likely that the bacteria associated with the J2s are perceived by the flagellin receptor FLS2, which requires BAK1 as a co-receptor, and trigger PTI *(*Chinchilla *et al., 2007;* Sun *et al., 2013)*. To address this possibility, we inoculated two *fls2* mutant lines with RKN and evaluated for galling. The number of root galls (Figure 1.6A) of both *fls2* mutants was not significantly different than the wild type, suggesting that RKN recognition does not involve perception of bacteria attached to the nematode surface.

Nematode penetration into roots can cause damage that varies depending on the nematode species (Sijmons *et al.*, 1991; Wyss *et al.*, 1992; Grundler *et al.*, 1997). To evaluate whether possible damage caused by RKN penetration could lead to RKN perception by *A. thaliana*, double mutants of the well characterized, and functionally redundant DAMP receptors *PEPR1* and *PEPR2* (Krol *et al.*, 2010) were evaluated with RKN. PEPR1 and PEPR2 also require BAK1 for their function (Schulze *et al.*, 2010). Similar to *fls2* mutants, the number of root galls (Figure 1.6B) of the *pepr1 pepr2* double mutant was not significantly different than the wild type, indicating that these receptors are not involved in the RKN-elicited PTI responses. Herbivore attack or pathogen-induced cell lysis can result in leakage of ATP to extracellular space (Choi *et al.*, 2014; Tanaka *et al.*, 2014). To evaluate the role of a broader DAMP receptor, a mutant and an overexpression line of the recently characterized ATP receptor DORN1 were evaluated with RKN (Choi *et al.*, 2014). Similar to the phenotypes of the *pepr1 pepr2* double mutant, the number of root galls (Figure 1.6B) of *dorn1-3* mutant and the oxDORN1 line were not significantly different from the wild type.

At the time of nematode inoculation for the galling assays, at 2- to 3-week-old seedling stage, both *dorn1-3* and oxDORN1 had compromised root growth pattern and were affected in gravitropism (Appendix A). The root growth of 8-day-old *dorn1-3* and oxDORN1 seedlings, with mainly a taproot, was similar to wild type and both genotypes displayed only limited gravitropism (Appendix A). To confirm the RKN galling phenotype of *dorn1-3* and oxDORN1, 8-day-old seedlings

were used in RKN penetration assays. In addition to the wild-type Col-0, mutants of the other plant receptors used in our experiments, *fls2* and *pepr1 pepr2,* were also included in this assay. Consistent with the galling phenotype, the number of J2s inside the roots of the *fls2* mutant and the *pepr1 pepr2* double mutant was not significantly different from the wild type (Figure 1.7). Similarly, the number of J2s inside the roots of *dorn1-3* and oxDORN1 was not significantly different from the wild type (Figure 1.7) suggesting no role for DORN1 in RKN perception.

Discussion

While extensive research has focused on MAMP perception in plant leaves, little is known about MAMP perception in roots (Millet *et al.*, 2010). Similarly, research on plant-nematode interactions is mostly limited to the study of disease resistance genes and ETI responses, in addition to understanding the processes involved in the establishment of feeding sites by sedentary endoparasitic nematodes (Jones *et al.*, 2011). Existing information suggests that nematodes also induce PTI responses (Lambert *et al.*, 1999; Alkharouf *et al.*, 2006; Melillo *et al.*, 2006; Bhattarai *et al.*, 2008; Ali *et al.*, 2014; Siddique *et al.*, 2014; Kammerhofer *et al.*, 2015). However, canonical PTI responses against plant parasitic nematodes have not been well characterized. Our work shows that PTI responses are activated by RKN infection and the existence of BAK1-dependent and -independent immune signaling against this pest.

In an earlier work our lab showed that the tomato *SlSERK3A* and *SlSERK3B* are required for RKN defense (Peng & Kaloshian, 2014). In this study, using RKN infection of the *A. thaliana bak1-5* mutant, we show that *BAK1,* the *SlSERK3* orthologous gene in *A. thaliana*, is also required for RKN defense in *A. thaliana* indicating a conserved role for *BAK1* in tomato and *A. thaliana*.

To successfully infect plant roots, RKN infection is characterized by three phases; attraction to the root tips, root penetration and migration, and establishment of a feeding site (Goverse & Smant, 2014). To characterize the role

of *BAK1* we evaluated these three steps during RKN infection in *bak1-5* and wild type. Based on our results, RKN attraction to roots was eliminated as the cause for the enhanced susceptibility seen in the *bak1-5* mutant. The enhanced RKN penetration of *bak1-5 roots*, within 24 h while nematodes are migrating and have not established a feeding site, is in agreement with the role of *BAK1* in early steps of pathogen recognition. This observed enhanced penetration during the first 24h was positively correlated with enhanced root galling observed 4 weeks after inoculation, illustrating the relevance of *BAK1*-induced defenses against RKN.

Consistent with a *BAK1*-dependent recognition of RKN, single mutant *bik1* and double mutant *rbohD rbohF*, both impaired in BAK1 signaling, also displayed enhanced susceptibility to RKN. Unlike the role of BIK1 as a negative regulator of aphid defense (Lei *et al.*, 2014), BIK1 is a positive regulator of RKN defense similar to its role in defense against microbial pathogens (Veronese *et al.*, 2006; Lu *et al.*, 2010; Zhang *et al.*, 2010). Recently, it has been shown that BIK1 directly phosphorylates RBOHD to enhance ROS production (Kadota *et al.*, 2014; Li *et al.*, 2014). The NADPH oxidases RBOHD and RBOHF have been shown to affect resistance against a number of pathogens including cyst nematodes (Torres *et al.*, 2002; Mersmann *et al.*, 2010; Marino *et al.*, 2012; Siddique *et al.*, 2014).

RKN penetration and migration were previously shown to cause production of H_2O_2 in susceptible and resistant tomato roots (Melillo *et al.*, 2006). The H_2O_2 was localized in the apoplast and at the plasma membrane. In addition, treating the roots with NADPH oxidase inhibitor resulted in decrease of H_2O_2 accumulation

after RKN infection, indicating that membrane localized RBOHs are responsible for the production of ROS. Interestingly, the presence of H_2O_2 was not associated with cellular destruction suggesting that H_2O_2 is produced as a reaction to RKN perception (Melillo *et al.*, 2006).

To overcome adverse effects of the ROS burst, RKNs have acquired ROS scavenging enzymes such as peroxiredoxins (Molinari & Miacola, 1997; Dubreuil *et al.*, 2011). Peroxiredoxins were localized in tissues surrounding the J2 cuticle and in the hypodermis, tissues in close contact with plant cells suggesting a direct role for these peroxiredoxins in ROS scavenging. Consistent with their role in protecting RKN against ROS burst, RNAi-mediated knockdown in *M. incognita* resulted in 60% reduction in root galling (Dubreuil *et al.*, 2011). Taken together, these previous findings combined with our results indicate the importance of ROS burst in early steps of host-RKN interactions.

While the ROS burst negatively affects RKN infection, cyst nematodes require proper functioning *RBOH* activity for successful establishment in *A. thaliana* roots (Siddique *et al.*, 2014). Lower numbers of the cyst nematode *Heterodera schachtii* developed on *rbohD rbohF* mutant roots and extensive cell death was observed in this mutant as early as 6 h after *H. schachtii* inoculation. Unlike RKN, cyst nematodes cause extensive damage during root migration (Wyss *et al.*, 1992; Waetzig *et al.*, 1999). To modulate cell death, RBOHD- and RBOHF–dependent ROS production is known to suppress cell death in neighboring cells

(Torres *et al.*, 2005). It is speculated that *H. schachtii* manipulates this NADPH oxidase regulation of ROS for its advantage (Siddique *et al.*, 2014).

Our results indicate that treatment of *A. thaliana* roots with flg22 was effective in restricting RKN penetration of wild-type roots similar to flg22 treatment of leaves restricting microbial pathogen infection (Newman *et al.*, 2002; Kunze *et al.*, 2004; Mishina & Zeier, 2007; Nguyen *et al.*, 2010; Lloyd *et al.*, 2014). Recently, treatment of *A. thaliana* roots with the nematode ascaroside 18 (ascr#18) was shown to also protect against RKN and cyst nematode establishment (Manosalva *et al.*, 2015). Ascarosides are nematode-specific glycosides of the dideoxysugar ascarylose with a fatty acid derived lipophilic side chain (Ludewig & Schroeder, 2013). Interestingly, ascr#18 activates the canonical PTI defense responses and induces enhanced resistance against a broad-spectrum of pathogens similar to MAMP and DAMP treatments (Manosalva *et al.*, 2015). Therefore, ascr#18 is likely a nematode-associated molecular pattern. It is unknown whether ascr#18 recognition involves PRR and requires BAK1.

Consistent with the effectiveness of flg22 treatment against RKN infection, it has been shown that nematodes have evolved effectors to suppress PTI. The RKN *M. incognita* effector Mi-CRT, encoding a calreticulin, suppresses elf18-induced PTI (Jaouannet *et al.*, 2013), while the cyst nematode *Globodera rostochiensis* effector GrCEP12, encoding a ubiquitin carboxyl extension protein, suppresses flg22-induced PTI (Chen *et al.*, 2013; Chronis *et al.*, 2013).

Suppression of PTI by nematodes effectors indicates the importance to overcome PTI by these parasites.

RKN infection induced expression of genes involved in camalexin biosynthesis (*CYP71A12*), glucosinolate biosynthesis (*MYB51)* and basal defense activation (*WRKY11)*. Earlier it was shown that both flg22 and chitin treatments induce expression of these genes in *A. thaliana* roots albeit at different developmental zones (Millet *et al.*, 2010). In the present work the GUS reporter lines showed that the pattern of expression of these genes by RKN infection, in the root elongation zone, is similar to flg22 treatment but not to chitin treatment. RKN penetrate roots in the elongation zone in a similar region as bacteria (Wyss *et al.*, 1992; Millet *et al.*, 2010). It is intriguing to speculate that PTI is induced in restricted tissue zones critical for entry of pathogens and parasite (Millet *et al.*, 2010).

The induction of *CYP71A12* expression and enhanced susceptibility of *pad3* mutant indicate a role for camalexin in RKN defense similar to its role in *A. thaliana* against *H. schachtii* (Ali *et al.*, 2014). Phytoalexins have been shown to be involved in nematode resistance in several crops (Kaplan *et al.*, 1980; Baldridge *et al.*, 1998; Hölscher *et al.*, 2014). *CYP71A12* expression was only partially attenuated in the *bak1-5* mutant suggesting that *CYP71A12*-regulated camalexin biosynthesis is only partly dependent on *BAK1.* In addition, these results suggest the existence of at least two distinct nematode recognition pathways, BAK1-dependent and -independent.

A. thaliana myb34 myb51 double mutant, completely compromised in glucosinolate production, showed higher susceptibility to RKN indicating a role for glucosinolate in RKN defense. Nematodes are known to suppress defense-related genes in their feeding sites (Kyndt *et al.*, 2012). Indeed, analysis of *A. thaliana* transcriptome changes upon RKN infection showed that *MYB34* is significantly downregulated in giant cells suggesting that RKN have the ability to suppress glucosinolate production in feeding sites (Portillo *et al.*, 2013).

The TF *WRKY11* was initially characterized in *A. thaliana* as a negative regulator of bacterial defense (Journot-Catalino *et al.*, 2006). Interestingly, *WRKY11* is induced in *A. thaliana* seedlings and roots in response to flg22 treatment (Millet *et al.*, 2010). Our data showed that *WRKY11* is also induced by RKN infection and is a positive regulator of RKN defense. An investigation on the role of WRKY TFs in defense against cyst nematodes also identified *WRKY11* and *WRKY17* as positive regulators of nematode defense and demonstrated their downregulation in syncytia, the cyst nematode feeding site (Ali *et al.*, 2014).

The role of *BAK1* in RKN defense indicates that RKN are perceived by cell surface localized receptor(s). The few DAMP receptor mutants we tested did not have enhanced susceptibility phenotype. In addition, the PTI marker gene induction was observed in GUS reporter lines by treatment with RKN extracts. Taken together these results indicate that *A. thaliana* perceives the nematode. However, we cannot exclude the possibility that damage caused by nematode infection is also perceived as not all known DAMP receptors were evaluated in the

present work and additional yet unidentified DAMP receptors probably exist. Similar to microbial pathogens, it is likely that more than one RKN molecular pattern is perceived by *A. thaliana* in a *BAK1*-dependent manner. Additionally, the existence of *BAK1*-independent defense suggests additional nematode patterns that do not require *BAK1* could be perceived by the plant host.

In *A. thaliana*, fungal chitin elicitor perception is independent of BAK1 and involves the CHITIN ELICITOR RECEPTOR KINASE 1 (CERK1) and LYSIN MOTIF RECEPTOR KINASE 5 (LYK5) (Gimenez-Ibanez *et al.*, 2009; Cao *et al.*, 2014). A chitin elicitor could be a nematode-associated molecular pattern recognized by plants (Millet *et al.*, 2010). Chitin is present in plant parasitic and free-living nematode eggshells and in the pharyngeal lumen walls of the free-living nematode *Caenorhabditis elegans* (Veronico *et al.*, 2001; Fanelli *et al.*, 2005; Zhang *et al.*, 2005). Since our assays were performed with J2s and not eggs, the *BAK1*-independent *CYP71A12* expression was not induced by egg chitin perception. It is not clear whether the pharyngeal lumen of the plant parasitic J2s also contain chitin (Veronico *et al.*, 2001; Fanelli *et al.*, 2005). Further studies are needed to elucidate the role of chitin in nematode defense.

References

Abad P, Gouzy J, Aury J-M, Castagnone-Sereno P, Danchin EGJ, Deleury E, Perfus-Barbeoch L, Anthouard V, Artiguenave F, Blok VC, et al. 2008. Genome sequence of the metazoan plant-parasitic nematode *Meloidogyne incognita*. *Nature Biotechnology* **26**: 909-915.

Ali MA, Wieczorek K, Kreil DP, Bohlmann H. 2014. The beet cyst nematode *Heterodera schachtii* modulates the expression of WRKY transcription factors in syncytia to favour its development in *Arabidopsis* roots. *PLoS One* **9**: e102360.

Alkharouf NW, Klink VP, Chouikha IB, Beard HS, MacDonald MH, Meyer S, Knap HT, Khan R, Matthews BF. 2006. Timecourse microarray analyses reveal global changes in gene expression of susceptible *Glycine max* (soybean) roots during infection by *Heterodera glycines* (soybean cyst nematode). *Planta* **224**: 838-852.

Asai T, Tena G, Plotnikova J, Willmann MR, Chiu WL, Gomez-Gomez L, Boller T, Ausubel FM, Sheen J. 2002. MAP kinase signalling cascade in Arabidopsis innate immunity. *Nature* **415**: 977-983.

Baldridge GD, O'Neill NR, Samac DA. 1998. Alfalfa (*Medicago sativa* L.) resistance to the root-lesion nematode, *Pratylenchus penetrans*: defense-response gene mRNA and isoflavonoid phytoalexin levels in roots. *Plant Molecular Biology* **38**: 999-1010.

Bartels S, Lori M, Mbengue M, van Verk M, Klauser D, Hander T, Böni R, Robatzek S, Boller T. 2013. The family of Peps and their precursors in *Arabidopsis*: differential expression and localization but similar induction of pattern-triggered immune responses. *Journal of Experimental Botany* **64**: 5309-5321.

Beekwilder J, van Leeuwen W, van Dam NM, Bertossi M, Grandi V, Mizzi L, Soloviev M, Szabados L, Molthoff JW, Schipper B, et al. 2008. The impact of the absence of aliphatic glucosinolates on insect herbivory in Arabidopsis. *PLoS One* **3**: e2068.

Bhattarai KK, Xie QG, Mantelin S, Bishnoi U, Girke T, Navarre DA, Kaloshian I. 2008. Tomato susceptibility to root-knot nematodes requires an intact jasmonic acid signaling pathway. *Molecular Plant-Microbe Interactions* **21**: 1205-1214.

Böhm H, Albert I, Fan L, Reinhard A, Nürnberger T. 2014. Immune receptor complexes at the plant cell surface. *Current Opinion in Plant Biology* **20**: 47-54.

Boller T, Flury P 2012. Peptides as danger signals: MAMPs and DAMPs. In: Irving HR, Gehring C eds. *Plant signalling peptides, signaling and communication in plants*. Berlin: Springer, 163-181.

Byrd DW, Kirkpatrick T, Barker KR. 1983. An improved technique for clearing and staining plant tissue for detection of nematodes. *Journal of Nematology* **14**: 142-143.

Cao Y, Liang Y, Tanaka K, Nguyen CT, Jedrzejczak RP, Joachimiak A, Stacey G. 2014. The kinase LYK5 is a major chitin receptor in Arabidopsis and forms a chitin-induced complex with related kinase CERK1. *eLife*: e03766.

Chaparro-Garcia A, Wilkinson RC, Gimenez-Ibanez S, Findlay K, Coffey MD, Zipfel C, Rathjen JP, Kamoun S, Schornack S. 2011. The receptor-like kinase SERK3/BAK1 is required for basal resistance against the late blight pathogen *Phytophthora infestans* in *Nicotiana benthamiana*. *PLoS One* **6**: e16608.

Chen C, Liu S, Liu Q, Niu J, Liu P, Zhao J, Jian H. 2015. An ANNEXIN-like protein from the cereal cyst nematode *Heterodera avenae* suppresses plant defense. *PLoS One* **10**: e0122256.

Chen S, Chronis D, Wang X. 2013. The novel GrCEP12 peptide from the plant-parasitic nematode *Globodera rostochiensis* suppresses flg22-mediated PTI. *Plant Signaling & Behavior* **8**: e25359.

Chinchilla D, Shan L, He P, de Vries S, Kemmerling B. 2009. One for all: the receptor-associated kinase BAK1. *Trends in Plant Science* **14**: 535-541.

Chinchilla D, Zipfel C, Robatzek S, Kemmerling B, Nürnberger T, Jones JD, Felix G, Boller T. 2007. A flagellin-induced complex of the receptor FLS2 and BAK1 initiates plant defence. *Nature* **448**: 497-500.

Choi J, Tanaka K, Cao Y, Qi Y, Qiu J, Liang Y, Lee SY, Stacey G. 2014. Identification of a Plant Receptor for Extracellular ATP. *Science* **343**: 290-294.

Chronis D, Chen S, Lu S, Hewezi T, Carpenter SC, Loria R, Baum TJ, Wang X. 2013. A ubiquitin carboxyl extension protein secreted from a plant-

parasitic nematode *Globodera rostochiensis* is cleaved in planta to promote plant parasitism. *Plant Journal* **74**: 185-196.

Dubreuil G, Deleury E, Magliano M, Jaouannet M, Abad P, Rosso M-N. 2011. Peroxiredoxins from the plant parasitic root-knot nematode, *Meloidogyne incognita*, are required for successful development within the host. *International Journal for Parasitology* **41**: 385-396.

Fanelli E, Di Vito M, Jones JT, De Giorgi C. 2005. Analysis of chitin synthase function in a plant parasitic nematode, *Meloidogyne artiellia*, using RNAi. *Gene* **349**: 87-95.

Flury P, Klauser D, Schulze B, Boller T, Bartels S. 2013. The anticipation of danger: microbe-associated molecular pattern perception enhances AtPep-triggered oxidative burst. *Plant Physiology* **161**: 2023-2035.

Frerigmann H, Gigolashvili T. 2014. MYB34, MYB51, and MYB122 distinctly regulate indolic glucosinolate biosynthesis in *Arabidopsis thaliana*. *Molecular Plant* **7**: 814-828.

Frerigmann H, Glawischnig E, Gigolashvili T. 2015. The role of MYB34, MYB51 and MYB122 in the regulation of camalexin biosynthesis in *Arabidopsis thaliana*. *Frontiers in Plant Science* **6**: 654.

Fudali SL, Wang C, Williamson VM. 2013. Ethylene signaling pathway modulates attractiveness of host roots to the root-knot nematode *Meloidogyne hapla*. *Molecular Plant-Microbe Interactions* **26**: 75-86.

Gimenez-Ibanez S, Hann DR, Ntoukakis V, Petutschnig E, Lipka V, Rathjen JP. 2009. AvrPtoB targets the LysM receptor kinase CERK1 to promote bacterial virulence on plants. *Current Biology* **19**: 423-429.

Glazebrook J, Ausubel FM. 1994. Isolation of phytoalexin-deficient mutants of *Arabidopsis thaliana* and characterization of their interactions with bacterial pathogens. *Proceedings of the National Academy of Sciences, USA* **91**: 8955-8959.

Gomez-Gomez L, Boller T. 2000. FLS2: an LRR receptor-like kinase involved in the perception of the bacterial elicitor flagellin in Arabidopsis. *Molecular cell* **5**: 1003-1011.

Goverse A, Smant G. 2014. The activation and suppression of plant innate immunity by parasitic nematodes. *Annual Review of Phytopathology* **52**: 243-265.

Grundler FMW, Sobczak M, Lange S. 1997. Defence responses of *Arabidopsis thaliana* during invasion and feeding site induction by the plant–parasitic nematode *Heterodera glycines*. *Physiological and Molecular Plant Pathology* **50**: 419-429.

Han Z, Sun Y, Chai J. 2014. Structural insight into the activation of plant receptor kinases. *Current Opinion in Plant Biology* **20**: 55-63.

Hann DR, Rathjen JP. 2007. Early events in the pathogenicity of *Pseudomonas syringae* on *Nicotiana benthamiana*. *Plant Journal* **49**: 607-618.

Hölscher D, Dhakshinamoorthy S, Alexandrov T, Becker M, Bretschneider T, Buerkert A, Crecelius AC, De Waele D, Elsen A, Heckel DG, et al. 2014. Phenalenone-type phytoalexins mediate resistance of banana plants (*Musa* spp.) to the burrowing nematode *Radopholus similis*. *Proceedings of the National Academy of Sciences, USA* **111**: 105-110.

Huffaker A, Pearce G, Ryan CA. 2006. An endogenous peptide signal in *Arabidopsis* activates components of the innate immune response. *Proceedings of the National Academy of Sciences, USA* **103**: 10098-10103.

Huffaker A, Ryan CA. 2007. Endogenous peptide defense signals in *Arabidopsis* differentially amplify signaling for the innate immune response. *Proceedings of the National Academy of Sciences, USA* **104**: 10732-10736.

Hussey R, Barker KR. 1973. A comparison of methods of collecting inocula of *Meloidogyne* species including a new technique. *Plant Disease Report* **57**: 1025-1028.

Jaouannet M, Magliano M, Arguel MJ, Gourgues M, Evangelisti E, Abad P, Rosso MN. 2013. The root-knot nematode calreticulin Mi-CRT is a key effector in plant defense suppression. *Molecular Plant-Microbe Interactions* **26**: 97-105.

Jones J, Gheysen G, Fenoll C. 2011. *Genomics and molecular genetics of plant-nematode interactions*. Dordrecht, The Netherlands: Springer.

Jones JD, Dangl JL. 2006. The plant immune system. *Nature* **444**: 323-329.

Jones JT, Haegeman A, Danchin EGJ, Gaur HS, Helder J, Jones MGK, Kikuchi T, Manzanilla-López R, Palomares-Rius JE, Wesemael WML, et al. 2013. Top 10 plant-parasitic nematodes in molecular plant pathology. *Molecular Plant Pathology* **14**: 946-961.

Journot-Catalino N, Somssich IE, Roby D, Kroj T. 2006. The transcription factors WRKY11 and WRKY17 act as negative regulators of basal resistance in *Arabidopsis thaliana*. *Plant Cell* **18**: 3289-3302.

Kadota Y, Sklenar J, Derbyshire P, Stransfeld L, Asai S, Ntoukakis V, Jones JD, Shirasu K, Menke F, Jones A, et al. 2014. Direct regulation of the NADPH oxidase RBOHD by the PRR-associated kinase BIK1 during plant immunity. *Molecular cell* **54**: 43-55.

Kaloshian I, Desmond OJ, Atamian HS 2011. Disease resistance-genes and defense responses during incompatible interactions. In: Jones J, Gheysen G, Fenoll C eds. *Genomics and molecular genetics of plant-nematode interactions*. Netherlands: Springer, 309-324.

Kammerhofer N, Radakovic Z, Regis JMA, Dobrev P, Vankova R, Grundler FMW, Siddique S, Hofmann J, Wieczorek K. 2015. Role of stress-related hormones in plant defence during early infection of the cyst nematode *Heterodera schachtii* in Arabidopsis. *New Phytologist* **207**: 778-789.

Kaplan DT, Keen NT, Thomason IJ. 1980. Association of glyceollin with the incompatible response of soybean roots to *Meloidogyne incognita*. *Physiological Plant Pathology* **16**: 309-318.

Kettles GJ, Drurey C, Schoonbeek HJ, Maule AJ, Hogenhout SA. 2013. Resistance of *Arabidopsis thaliana* to the green peach aphid, *Myzus persicae*, involves camalexin and is regulated by microRNAs. *New Phytologist* **198**: 1178-1190.

Ko MP, Van Gundy SD. 1988. An alternative gelling agent for culture and studies of nematodes, bacteria, fungi, and plant tissues. *Journal of Nematology* **20**: 478-485.

Krol E, Mentzel T, Chinchilla D, Boller T, Felix G, Kemmerling B, Postel S, Arents M, Jeworutzki E, Al-Rasheid KAS, et al. 2010. Perception of the *Arabidopsis* danger signal peptide 1 involves the pattern recognition receptor AtPEPR1 and its close homologue AtPEPR2. *Journal of Biological Chemistry* **285**: 13471-13479.

Kunze G, Zipfel C, Robatzek S, Niehaus K, Boller T, Felix G. 2004. The N terminus of bacterial elongation factor Tu elicits innate immunity in Arabidopsis plants. *Plant Cell* **16**: 3496-3507.

Kwak JM, Mori IC, Pei ZM, Leonhardt N, Torres MA, Dangl JL, Bloom RE, Bodde S, Jones JD, Schroeder JI. 2003. NADPH oxidase *AtrbohD* and *AtrbohF* genes function in ROS-dependent ABA signaling in Arabidopsis. *EMBO Journal* **22**: 2623-2633.

Kyndt T, Denil S, Haegeman A, Trooskens G, Bauters L, Van Criekinge W, De Meyer T, Gheysen G. 2012. Transcriptional reprogramming by root knot and migratory nematode infection in rice. *New Phytologist* **196**: 887-900.

Lambert KN, Ferrie BJ, Nombela G, Brenner ED, Williamson VM. 1999. Identification of genes whose transcripts accumulate rapidly in tomato after root-knot nematode infection. *Physiological and Molecular Plant Pathology* **55**: 341-348.

Lei J, A. Finlayson S, Salzman RA, Shan L, Zhu-Salzman K. 2014. BOTRYTIS-INDUCED KINASE1 Modulates Arabidopsis Resistance to Green Peach Aphids via PHYTOALEXIN DEFICIENT4. *Plant Physiology* **165**: 1657-1670.

Li L, Li M, Yu L, Zhou Z, Liang X, Liu Z, Cai G, Gao L, Zhang X, Wang Y, et al. 2014. The FLS2-associated kinase BIK1 directly phosphorylates the NADPH oxidase RbohD to control plant immunity. *Cell Host & Microbe* **15**: 329-338.

Lloyd SR, Schoonbeek HJ, Trick M, Zipfel C, Ridout CJ. 2014. Methods to study PAMP-triggered immunity in Brassica species. *Molecular Plant-Microbe Interactions* **27**: 286-295.

Lozano-Torres JL, Wilbers RH, Warmerdam S, Finkers-Tomczak A, Diaz-Granados A, van Schaik CC, Helder J, Bakker J, Goverse A, Schots A, et al. 2014. Apoplastic venom allergen-like proteins of cyst nematodes modulate the activation of basal plant innate immunity by cell surface receptors. *PLoS pathogens* **10**: e1004569.

Lu DP, Wu SJ, Gao XQ, Zhang YL, Shan LB, He P. 2010. A receptor-like cytoplasmic kinase, *BIK1*, associates with a flagellin receptor complex to initiate plant innate immunity. *Proceedings of the National Academy of Sciences, USA* **107**: 496-501.

Ludewig AH, Schroeder FC 2013. Ascaroside signaling in *C. elegans*.In WormBook. http://www.wormbook.org: The *C. elegans* Research Community, WormBook. [accessed 11 October 2015].

Manosalva P, Manohar M, von Reuss SH, Chen S, Koch A, Kaplan F, Choe A, Micikas RJ, Wang X, Kogel K-H, et al. 2015. Conserved nematode signalling molecules elicit plant defenses and pathogen resistance. *Nature Communications* **6**: 7795.

Mantelin S, Peng HC, Li B, Atamian HS, Takken FL, Kaloshian I. 2011. The receptor-like kinase SlSERK1 is required for *Mi-1*-mediated resistance to potato aphids in tomato. *Plant Journal* **67**: 459-471.

Mantelin S, Thorpe P, Jones JT 2015. Suppression of plant defences by plant-parasitic nematodes. In: Escobar C, Fenoll C eds. *Advances in botanical research*. Oxford, UK: Elsevier Ltd., 325-337.

Marino D, Dunand C, Puppo A, Pauly N. 2012. A burst of plant NADPH oxidases. *Trends in Plant Science* **17**: 9-15.

Martinez de Ilarduya O, Moore AE, Kaloshian I. 2001. The tomato *Rme1* locus is required for *Mi-1*-mediated resistance to root-knot nematodes and the potato aphid. *Plant Journal* **27**: 417-425.

Melillo MT, Leonetti P, Bongiovanni M, Castagnone-Sereno P, Bleve-Zacheo T. 2006. Modulation of reactive oxygen species activities and H2O2 accumulation during compatible and incompatible tomato-root-knot nematode interactions. *New Phytologist* **170**: 501-512.

Mersmann S, Bourdais G, Rietz S, Robatzek S. 2010. Ethylene signaling regulates accumulation of the FLS2 receptor and is required for the oxidative burst contributing to plant immunity. *Plant Physiology* **154**: 391-400.

Millet YA, Danna CH, Clay NK, Songnuan W, Simon MD, Werck-Reichhart D, Ausubel FM. 2010. Innate immune responses activated in *Arabidopsis* roots by microbe-associated molecular patterns. *Plant Cell* **22**: 973-990.

Mishina TE, Zeier J. 2007. Pathogen-associated molecular pattern recognition rather than development of tissue necrosis contributes to bacterial induction of systemic acquired resistance in Arabidopsis. *Plant Journal* **50**: 500-513.

Mitchum MG, Hussey RS, Baum TJ, Wang X, Elling AA, Wubben M, Davis EL. 2013. Nematode effector proteins: an emerging paradigm of parasitism. *New Phytologist* **199**: 879-894.

Moens M, Perry RN, Starr JL 2009. Meloidoyne species - a diverse group of novel and important plant parasites. In: Perry RN, Moens M, Starr JL eds. *Root-knot nematodes*. London: CAB International, 1-13.

Molinari S, Miacola C. 1997. Antioxidant enzymes in phytoparasitic nematodes. *Journal of Nematology* **29**: 153-159.

Nafisi M, Goregaoker S, Botanga CJ, Glawischnig E, Olsen CE, Halkier BA, Glazebrook J. 2007. Arabidopsis cytochrome P450 monooxygenase 71A13 catalyzes the conversion of indole-3-acetaldoxime in camalexin synthesis. *Plant Cell* **19**: 2039-2052.

Newman M-A, Von Roepenack-Lahaye E, Parr A, Daniels MJ, Dow JM. 2002. Prior exposure to lipopolysaccharide potentiates expression of plant defenses in response to bacteria. *Plant Journal* **29**: 487-495.

Nguyen HP, Chakravarthy S, Velasquez AC, McLane HL, Zeng L, Nakayashiki H, Park DH, Collmer A, Martin GB. 2010. Methods to study PAMP-triggered immunity using tomato and *Nicotiana benthamiana*. *Molecular Plant-Microbe Interactions* **23**: 991-999.

Peng HC, Kaloshian I. 2014. The tomato leucine-rich repeat receptor-like kinases *SlSERK3A* and *SlSERK3B* have overlapping functions in bacterial and nematode innate immunity. *PLoS One* **9**: e93302.

Portillo M, Cabrera J, Lindsey K, Topping J, Andres MF, Emiliozzi M, Oliveros JC, Garcia-Casado G, Solano R, Koltai H, et al. 2013. Distinct and conserved transcriptomic changes during nematode-induced giant cell development in tomato compared with Arabidopsis: a functional role for gene repression. *New Phytologist* **197**: 1276-1290.

Robatzek S, Bittel P, Chinchilla D, Kochner P, Felix G, Shiu SH, Boller T. 2007. Molecular identification and characterization of the tomato flagellin receptor LeFLS2, an orthologue of *Arabidopsis* FLS2 exhibiting characteristically different perception specificities. *Plant Molecular Biology* **64**: 539-547.

Rodiuc N, Vieira P, Banora MY, de Almeida Engler J. 2014. On the track of transfer cell formation by specialized plant-parasitic nematodes. *Frontiers in Plant Science* **5**: 160.

Roux M, Schwessinger B, Albrecht C, Chinchilla D, Jones A, Holton N, Malinovsky FG, Tor M, de Vries S, Zipfel C. 2011. The Arabidopsis leucine-rich repeat receptor-like kinases BAK1/SERK3 and BKK1/SERK4

are required for innate immunity to hemibiotrophic and biotrophic pathogens. *Plant Cell* **23**: 2440-2455.

Schlaeppi K, Abou-Mansour E, Buchala A, Mauch F. 2010. Disease resistance of Arabidopsis to *Phytophthora brassicae* is established by the sequential action of indole glucosinolates and camalexin. *Plant Journal* **62**: 840-851.

Schulze B, Mentzel T, Jehle AK, Mueller K, Beeler S, Boller T, Felix G, Chinchilla D. 2010. Rapid heteromerization and phosphorylation of ligand-activated plant transmembrane receptors and their associated kinase BAK1. *Journal of Biological Chemistry* **285**: 9444-9451.

Schwessinger B, Roux M, Kadota Y, Ntoukakis V, Sklenar J, Jones A, Zipfel C. 2011. Phosphorylation-dependent differential regulation of plant growth, cell death, and innate immunity by the regulatory receptor-like kinase BAK1. *PLoS Genet* **7**: e1002046.

Siddique S, Matera C, Radakovic ZS, Shamim Hasan M, Gutbrod P, Rozanska E, Sobczak M, Angel Torres M, Grundler FM. 2014. Parasitic worms stimulate host NADPH oxidases to produce reactive oxygen species that limit plant cell death and promote infection. *Science signaling* **7**: ra33.

Sijmons PC, Grundler FMW, Von Mende N, Burrows PR, Wyss U. 1991. *Arabidopsis thaliana* as a new model host for plant-parasitic nematodes. *Plant Journal* **1**: 245-254.

Stotz HU, Sawada Y, Shimada Y, Hirai MY, Sasaki E, Krischke M, Brown PD, Saito K, Kamiya Y. 2011. Role of camalexin, indole glucosinolates, and side chain modification of glucosinolate-derived isothiocyanates in defense of Arabidopsis against *Sclerotinia sclerotiorum*. *Plant Journal* **67**: 81-93.

Sun YD, Li L, Macho AP, Han ZF, Hu ZH, Zipfel C, Zhou JM, Chai JJ. 2013. Structural basis for flg22-induced activation of the Arabidopsis FLS2-BAK1 immune complex. *Science* **342**: 624-628.

Takai R, Isogai A, Takayama S, Che FS. 2008. Analysis of flagellin perception mediated by flg22 receptor OsFLS2 in rice. *Molecular Plant-Microbe Interactions* **21**: 1635-1642.

Tanaka K, Choi J, Cao Y, Stacey G. 2014. Extracellular ATP acts as a damage associated molecular pattern (DAMP) signal in plants. *Frontiers in Plant Science* **5**: 446.

Torres MA, Dangl JL, Jones JD. 2002. Arabidopsis gp91phox homologues *AtrbohD* and *AtrbohF* are required for accumulation of reactive oxygen intermediates in the plant defense response. *Proceedings of the National Academy of Sciences, USA* **99**: 517-522.

Torres MA, Jones JD, Dangl JL. 2005. Pathogen-induced, NADPH oxidase-derived reactive oxygen intermediates suppress spread of cell death in *Arabidopsis thaliana*. *Nature Genetics* **37**: 1130-1134.

Trda L, Fernandez O, Boutrot F, Heloir MC, Kelloniemi J, Daire X, Adrian M, Clement C, Zipfel C, Dorey S, et al. 2014. The grapevine flagellin receptor VvFLS2 differentially recognizes flagellin-derived epitopes from the endophytic growth-promoting bacterium *Burkholderia phytofirmans* and plant pathogenic bacteria. *New Phytologist* **201**: 1371-1384.

Veronese P, Nakagami H, Bluhm B, AbuQamar S, Chen X, Salmeron J, Dietrich RA, Hirt H, Mengiste T. 2006. The Membrane-Anchored BOTRYTIS-INDUCED KINASE1 Plays Distinct Roles in Arabidopsis Resistance to Necrotrophic and Biotrophic Pathogens. *Plant Cell* **18**: 257-273.

Veronico P, Gray LJ, Jones JT, Bazzicalupo P, Arbucci S, Cortese MR, Di Vito M, De Giorgi C. 2001. Nematode chitin synthases: gene structure, expression and function in *Caenorhabditis elegans* and the plant parasitic nematode *Meloidogyne artiellia*. *Molecular Genetics and Genomics* **266**: 28-34.

Waetzig GH, Sobczak M, Grundler F. 1999. Localization of hydrogen peroxide during the defence response of *Arabidopsis thaliana* against the plant parasitic nematode *Heterodera glycines*. *Nematology* **1**: 681-686.

Wang C, Lower S, Williamson VM. 2009. Application of pluronic gel to the study of root-knot nematode behaviour. *Nematology* **11**: 453-464.

Wang Y, Bouwmeester K, van de Mortel JE, Shan W, Govers F. 2013. A novel Arabidopsis-oomycete pathosystem: differential interactions with *Phytophthora capsici* reveal a role for camalexin, indole glucosinolates and salicylic acid in defence. *Plant Cell & Environment* **36**: 1192-1203.

Wyss U, Grundler FMW, Munch A. 1992. The parasitic behaviour of second-stage juveniles of *Meloidogyne incognita* in roots of *Arabidopsis thaliana*. *Nematologica* **38**: 98-111.

Yamaguchi Y, Huffaker A, Bryan AC, Tax FE, Ryan CA. 2010. PEPR2 is a second receptor for the Pep1 and Pep2 peptides and contributes to defense responses in *Arabidopsis*. *Plant Cell* **22**: 508-522.

Zhang J, Li W, Xiang T, Liu Z, Laluk K, Ding X, Zou Y, Gao M, Zhang X, Chen S, et al. 2010. Receptor-like cytoplasmic kinases integrate signaling from multiple plant immune receptors and are targeted by a *Pseudomonas syringae* effector. *Cell Host & Microbe* **7**: 290-301.

Zhang Y, Foster JM, Nelson LS, Ma D, Carlow CKS. 2005. The chitin synthase genes *chs-1* and *chs-2* are essential for *C. elegans* development and responsible for chitin deposition in the eggshell and pharynx, respectively. *Developmental Biology* **285**: 330-339.

Zipfel C. 2008. Pattern-recognition receptors in plant innate immunity. *Current Opinion in Immunology* **20**: 10-16.

Zipfel C. 2014. Plant pattern-recognition receptors. *Trends in Immunology* **35**: 345-351.

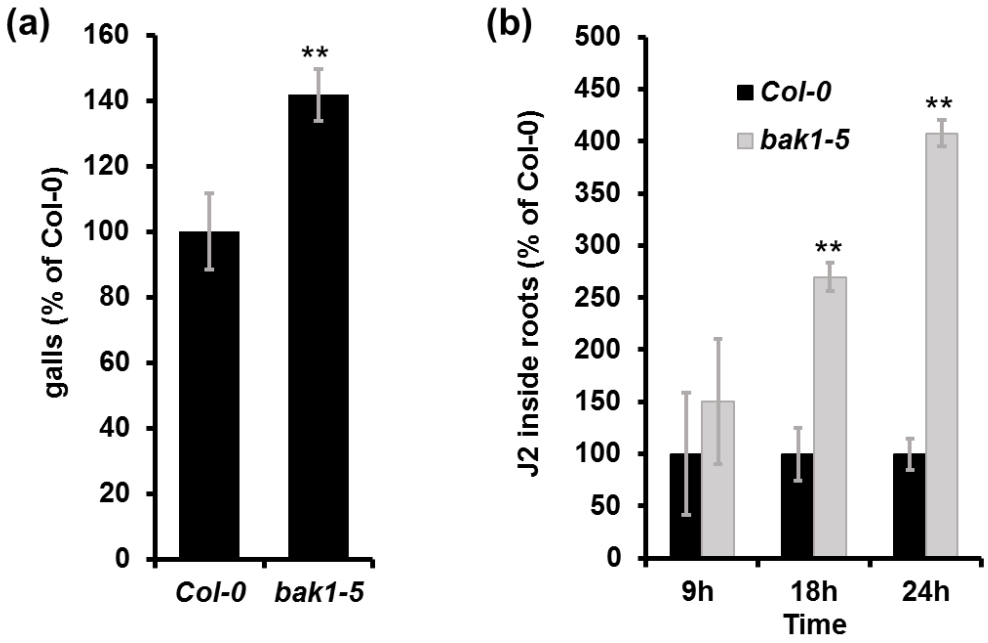

Figure 1.1. *BAK1* is involved in nematode resistance. (a) Percentage of root galls on *bak1-5* mutant relative to wild type Col-0 at 4 weeks after root-knot nematode (RKN) inoculation ± SE, n=30. This experiment was performed seven times with similar results. (b) Percentage of nematodes inside the root tips of 8-day-old *A. thaliana bak1-5* mutant seedlings relative to Col-0 ± SE, n=12, at the indicated time after inoculation. This experiment was performed twice with similar results. **p<0.01. In both experiments, seedlings were inoculated with 100 J2s each.

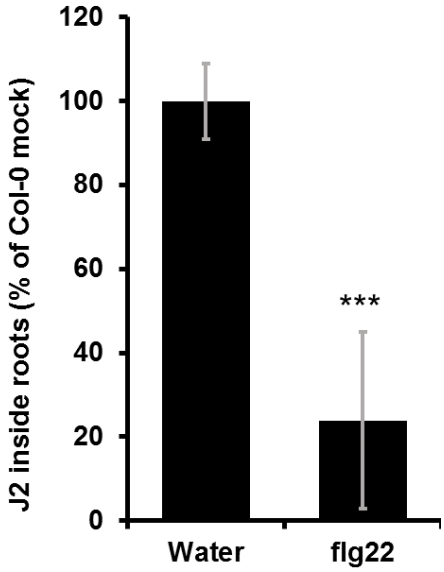

Figure 1.2 Pretreatment with the defense inducer flg22 enhances resistance to RKN. Percentage of J2 inside the root tips of 8-day-old *A. thaliana* Col-0 seedlings treated with 1 µM flg22 relative to mock-treated control ± SE, n=10. Seedlings were inoculated with 100 J2s each and experiment was performed three times with similar results. ***p<0.001.

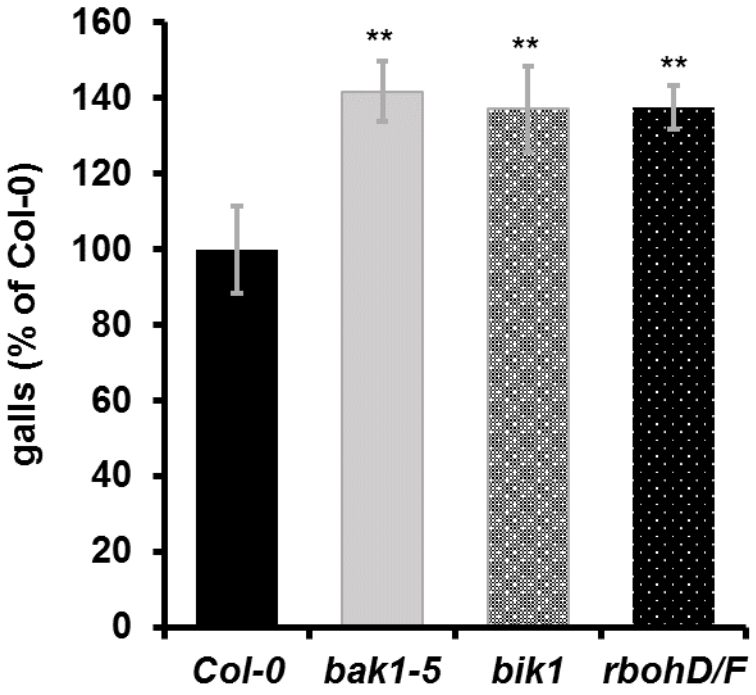

Figure 1.3 Nematode recognition depends on canonical PTI signaling partners. Percentage of root galls on *A. thaliana* mutants relative to wild type Col-0 4 weeks after RKN inoculation ± SE, n=30. Seedlings were inoculated with 100 J2s each and experiments were performed three times with similar results. **p<0.01.

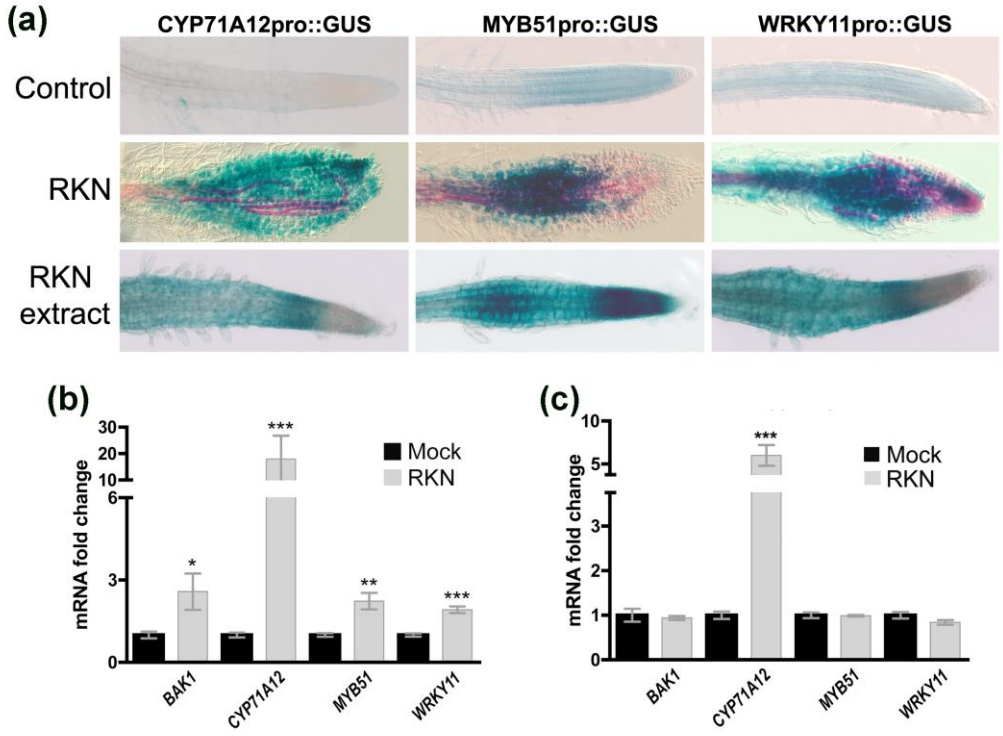

Figure 1.4. Nematodes trigger expression of PTI marker genes *CYP71A12, MYB51* and *WRKY11* involved in camalexin biosynthesis, glucosinolate biosynthesis and basal defense, respectively. (a) Elicitation of GUS activity 24 h post inoculation with RKN or treatment with crude RKN extracts in *A. thaliana* transgenic lines expressing GUS. These experiments were performed six times with similar results. RT-qPCR analysis of gene transcript levels in eight days-old seedling roots of Col-0 (b) or *bak1-5* mutant (c) mock treated or 24 h post inoculation with RKN. 18S was used as internal control. Bars show the means ± SE, n=3. *p<0.05, **p<0.01 and ***p<0.001.

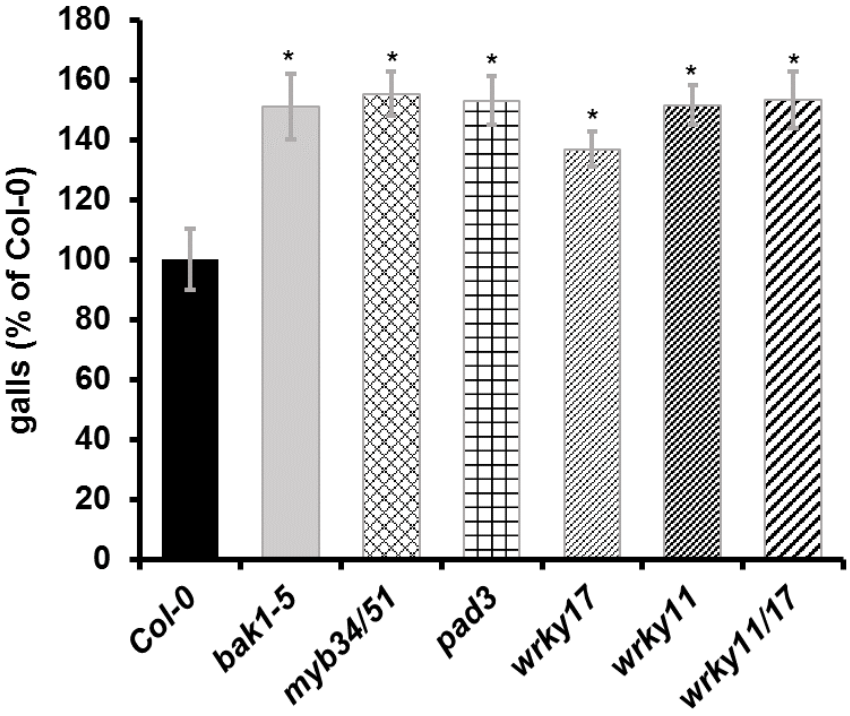

Figure 1.5. Basal defense, glucosinolate and camalexin participate in nematode resistance. Percentage of root galls on *A. thaliana* mutants relative to wild type Col-0 4 weeks after RKN inoculation ± SE, n=30. Seedlings were inoculated with 100 J2s each and experiments were performed three times with similar results. *p<0.05.

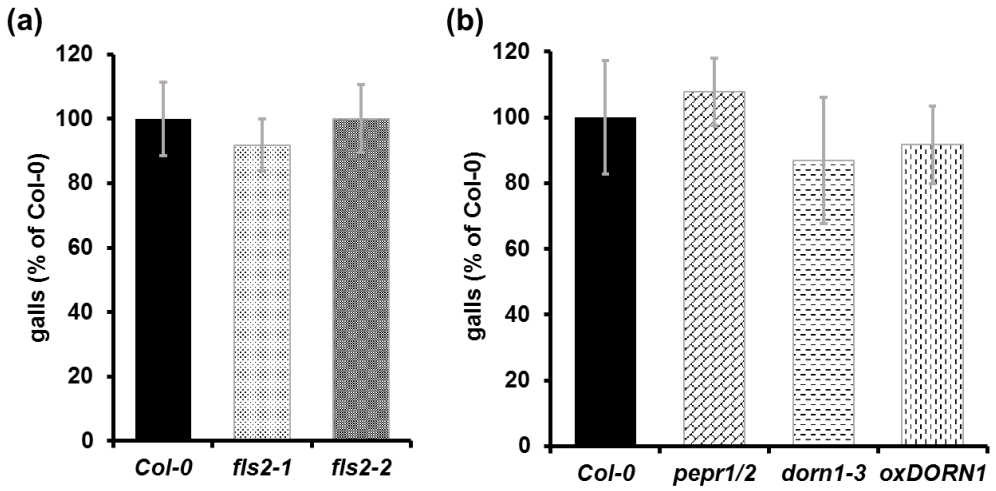

Figure 1.6. RKNs are not perceived by the tested MAMP (a) or DAMP (b) receptors. Percentage of root galls on *A. thaliana* mutants relative to wild type Col-0 4 weeks after RKN inoculation ± SE, n=30. Seedlings were inoculated with 100 J2s each and experiments were performed three times with similar results. No significant difference was observed between Col-0 and the tested genotypes.

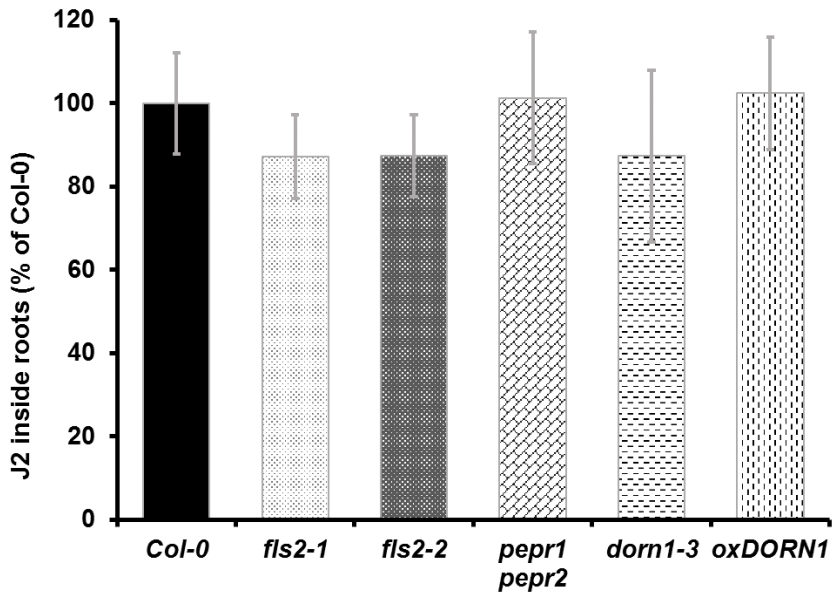

Figure 1.7. RKNs penetrate equally roots of *A. thaliana* wild type Col-0 and the tested MAMP and DAMP receptor mutants. Percentage of J2s inside the mutant root tips of 8-day-old *A. thaliana* relative to wild-type Col-0 seedlings ± SE, n=30. Seedlings of wild-type Col-0 and MAMP receptor mutants *fls2-1* and *fls2-2,* DAMP receptors double and single mutants *pepr1 pepr2* and *dorn1-3,* respectively, and oxDORN1 line were inoculated with 100 J2 each. Experiments were performed three times with similar results. No significant difference was observed between Col-0 and the tested genotypes.

Table 1.1. Primers used in quantitative real-time PCR.

Gene Accession number	Primers	Reference
AtCYP71A12 AT2G30750	F-GATTATCACCTCGGTTCCT R-CCACTAATACTTCCCAGATTA	Millet *et al.* (2010)
AtBAK1 AT4G33430	F-GACCTTGGGAATGCAAATCTATC R-AAAACTGATTGGAGTGAAAAGTGAAA	Korner *et al.* (2013)
AtMYB51 AT1G18570	F-ACAAATGGTCTGCTATAGCT R-CTTGTGTGTAACTGGATCAA-	Millet *et al.* (2010)
AtWRKY11 AT4G31550	F-CCACCGTCTAGTGTAACACTCGAT R-TGCAACGGAGCAGAAGCAAGGAA	Journot-Catalino *et al.* (2006)
At18S At2G01010	F-GGTGGTAACGGGTGACGGAGAAT R-CGCCGACCGAAGGGACAAGCCGA	Ali *et al.* (2014)

CHAPTER TWO

G-LecRK-VI.13 acts as a negative regulator of defense against root-knot nematodes

Abstract

Plant parasitic nematodes are responsible for extensive crop losses worldwide. One of such nematodes is the root-knot nematode (*Meloidogyne* spp., RKN), which penetrate plant roots and, after migrating between plant cells, establishes a feeding site known as giant cells in the root pericycle. Although detailed description has been made on giant cells formation and differential gene regulation, there is limited characterization of plant transcriptional responses to RKN penetration and migration inside plant roots and characterization of players in this process. To investigate transcriptome responses to early stage of parasitism by RKN, we performed RNAseq analysis using Arabidopsis root tissue 24h after inoculation with RKN. Data revealed the existence of transcriptional reprogramming 24h after inoculation with RKN in both in wild type (WT) Col-0 and *bak1-5* mutant roots. RNAseq data were searched for genes that showed upregulation upon Col-0 RKN inoculation that encoded proteins with predicted membrane localization and kinase domains. Screening Arabidopsis mutants for a few of these genes allowed identification of a pair of allelic mutants with increased resistance to RKN, suggesting the gene to be a negative regulator of immunity against RKN. Further characterization showed that these mutants displayed elevated basal levels of defense marker genes and increased and faster ROS burst upon flg22 treatment. This gene belongs to a underexplored protein family, the G-type lectin receptor kinases (G-LecRKs) that is present in all plant species searched, revealing a

possible application for crop protection. Therefore, tomato genome was searched for homologs and candidates are suggested.

Introduction

Plant parasitic nematodes (PPN) are in majority soil dwelling parasites that penetrate root tissue and establish intimate relationship with their hosts. Plant-nematode signaling starts even before nematode actual penetration, during attraction of nematodes to the roots by soil dispersion of root diffusates (Goverse & Smant, 2014). Although the precise molecules responsible for nematode attraction have not been described, the plant hormone ethylene was shown to play a role in the signaling involved in nematode attraction to plant roots, with ET overproducing plants showing decreased attraction (Fudali *et al.*, 2013).

After finding their host, different species of PPN deploy specific strategies to actively penetrate plant tissue. Root-knot nematodes (*Meloidogyne* spp., RKN) are sedentary endoparasites highly adapted to their hosts. These nematodes use their stylets to penetrate plant roots and migrate between cortical cells until they reach the vascular cylinder, where they establish their feeding site (Wyss *et al.*, 1992; Goverse & Smant, 2014; Rodiuc et al., 2014). RKNs induce formation of enlarged, multinucleated cells termed giant cells. Each feeding site is comprised of six to eight giant cells, which are surrounded by neighboring cells, forming galls. The giant cells are a result of mitosis without cytokinesis and, as a result of multiple mitoses and DNA replication cycles, are hypertrophied and multinucleated (de Almeida Engler et al, 2010; Rodiuc, 2014). These feeding sites act as nutrient sinks, nourishing RKN during their entire life cycle, which culminates with the

female development and massive production of eggs laid in a gelatinous matrix protruded from the adult female on the surface of plant roots (Jones *et al.*, 2013). The symptoms observed on susceptible root systems are the galls or knots, and those in aboveground tissue include impaired growth and wilting (Jones *et al.*, 2013).

Unlike RKNs, cyst nematodes (*Heterodera* spp. and *Globodera* spp., CN) can penetrate any region of plant roots and cause extensive damage during migration inside plant tissues (Sijmons *et al.*, 1991). Members of this group are also highly specialized parasites that become sedentary after establishment of their feeding site, the syncytium, formed by degeneration of the cell wall of a few plant cells (Jones *et al.*, 2013; Rodiuc et al., 2014). Once again, these parasites infection results in affected root morphology and nutrients and water absorption, resulting in aboveground symptoms such as wilting and retarded development (Jones *et al.*, 2013).

Successful establishment and maintenance of feeding site by PPNs ultimately defines the outcome of plant-nematode interaction. Therefore, scientists studying plant-nematode interactions have intensively characterized giant cell formation and the cells inside the galls surrounding the parasites (Wang *et al.*, 2003; Bar-Or *et al.*, 2005; Jammes *et al.*, 2005; Schaff *et al.*, 2007; Bhattarai *et al.*, 2008; Barcala *et al.*, 2010; Ibrahim *et al.*, 2011; Portillo *et al.*, 2013; Goverse & Smant, 2014). This focus has overlooked the initial perception of nematode during early stages of parasitism, their penetration and migration phases.

Early pathogen perception is described to be performed by plasma membrane localized proteins that mount a surveillance system based on variable ectodomain specificity (Zipfel, 2014). These pattern recognition receptor (PRR) proteins perceive molecular motifs that are conserved across a range of different species of a certain pathogen class, such as the flagellin of bacteria or chitin from fungi and are activate an immune response known as pattern-triggered immunity (PTI) (Jones & Dangl, 2006; Zipfel, 2014).

The classical PTI model is based on flagellin perception by the receptor FLS2 (FLAGELLIN SENSITIVE 2). The highly conserved stretch of 22 amino acids, flg22, present on the N terminus of bacterial flagellin acts as a molecular glue that brings together FLS2 and the co-receptor BAK1 (BRI 1-associated kinase 1), eliciting downstream signaling that culminates in transcriptional changes, callose deposition and ROS burst (Felix *et al.*, 1999; Gomez-Gomez *et al.*, 1999; Zipfel *et al.*, 2004; Chinchilla *et al.*, 2007). Notably, flg22-mediated defense elicitation is followed by transcriptional induction of FLS2 and BAK1, but also, induction of negative regulators of immunity, such as PBL13 (AvrPphB SUSCEPTIBLE1-LIKE13) (Lin *et al.*, 2015). Additionally, as a regulatory mechanism, after elicitation of defense responses FLS2 is internalized from the plasma membrane to internal vesicles, likely to degrade this receptor once it becomes activated by flg22 (Salomon & Robatzek, 2006; Ben Khaled *et al.*, 2015).

Despite the great potential of the broad and lasting defense mediated by PTI responses, nematode-related immunity research has largely focused on

characterization of resistance (R) gene-mediated defense and nematode effectors (Gheysen & Mitchum, 2011; Goto *et al.*, 2013; Goverse & Smant, 2014). Nevertheless, a few investigations have characterized transcript changes in response to nematode infection at early time points. One of the first descriptions of expression changes describes eight genes to be differentially expressed in response to RKN both in susceptible and resistant tomato (*Solanum lycopersicum*) plants only 12h after inoculation, while nematodes were still migrating inside plant tissues (Lambert *et al.*, 1999). The fact that the genes were differentially expressed in susceptible and resistant plants suggest that the response observed is involved in basal defense against RKN and does not require activity of the resistance gene (Lambert *et al.*, 1999).

Interestingly, transcriptome of tomato roots, collected 24h after RKN inoculation, still showed consistently more upregulation than downregulation of differentially expressed genes, although at this ti

me point small sized galls were already observed on the roots and that time point likely did not represent plant response to nematode migration (Bhattarai *et al.*, 2008). Differential gene expression was also observed using GUS reporter lines, which allowed to observe activation of specific transcripts at the beginning of plant-nematode interactions, followed by downregulation of transcripts inside the feeding sites (Ali *et al.*, 2014). This likely reflects nematode manipulation of transcription inside the feeding sites and may represent the described observation

that once PPNs establish feeding sites they reprogram cell machinery in their favor (Goverse & Smant, 2014).

The most recent description of differential gene expression early during interaction was performed for cyst nematode-inoculated Arabidopsis roots. The authors described induction of defense hormone-related transcripts and characterize the participation of jasmonic acid at early interaction between cyst nematodes and Arabidopsis (Kammerhofer *et al.*, 2015).

In the current chapter, we characterize Arabidopsis responses to RKN early during their interaction with the host. Because a role for BAK1 in this early interaction has been previously described (Teixeira et al., 2016), we also characterize the transcriptome changes in the roots of the *bak1-5* mutant, shown to have increased susceptibility to RKN. Furthermore, analysis of differentially expressed genes encoding proteins with plasma membrane localization and kinase domains was used to identify proteins with roles in immunity against RKN.

Material and methods

M. incognita culture and inoculum preparation

Meloidogyne incognita isolate P77R3 was maintained on tomato cultivar UC82. Plants were grown in UC mix and sand (1:9, vol/vol), fertilized with MiracleGro ® (Scotts Miracle-Gro Co) water soluble all-purpose plant food and kept in a glasshouse at 24˚ to 30˚C.

M. incognita eggs were extracted from roots using 10% bleach and sieving (Hussey & Barker, 1973). Eggs and plant debris collected on 500 mesh sieve were fractionated three times on 35% sucrose and rinsed several times with sterile water. The collected eggs were surface sterilized by shaking in 5% bleach for 5 minutes and rinsed with sterile water. This procedure was repeated three times. Surface sterilized eggs were hatched under sterile conditions in a modified Baermann funnel (Martinez de Ilarduya *et al.*, 2001). Two days later, infective-stage juveniles (J2s) were collected, counted and suspended in a 0.5% carboximethylcellulose solution.

Plant material and growth conditions

Arabidopsis seeds were surface sterilized and cold treated for all subsequent use. For RKN infection assays, seeds were plated on Gamborg media (Sigma-Aldrich) (pH 6.0) supplemented with 3% sucrose and 0.6% daishin agar (Bioworld) and maintained in plant growth rooms with 12 h light photoperiod at 24˚C. Two-week-

seedlings; with six seedlings per plate, and 8-day-old seedlings, with 20 seedlings per plate, were used for galling assay and RKN-induced gene expression analysis, respectively. Seedlings were inoculated with 100 J2s per seedling and maintained as described above. For galling assay, plants were evaluated four weeks after inoculation for number of galls. For gene expression analysis, samples were collected 24 hours after inoculation and frozen until further processing.

Library preparation and Illumina sequencing

RNA was isolated from Arabidopsis roots using GeneJET Plant RNA purification kit (Life Technologies). Approximately three µg of total RNA of each sample was used for mRNA-Seq library construction using NEBNext Ultra RNA Library Prep Kit for Illumina (New England BioLabs) following manufacturer's instructions. Libraries were diluted to a final concentration of 10nM and four libraries were multiplexed per read flow cell. Multiplexed libraries were sequenced on Illumina HiSeq2500 DNA Sequencer.

The high-quality reads were aligned to the *Arabidopsis thaliana* genome (Tair 10), available at "The Arabidopsis Information Resource" (TAIR), using Tophat2/Bowtie2 (Berardini et al., 2015; Kim et al., 2013; Langmead and Salzberg, 2012). Read overlapping with annotation range of interest were counted for each sample using summarizeOverlaps function (Lawrence et al., 2013). The read counting was performed for exonic gene regions in a non-strand specific manner.

The analysis of differentially expressed genes was performed by edgeR package from Bioconductor (Robinson et al., 2010).

RNAseq data analysis

Complete list of detected differentially expressed genes (DEG) was filtered considering a false discovery rate (FDR) of 0.01 and fold change (FC) of 1.0. DEG lists were submitted to enrichment analysis using Mapman and agriGO (Thimm *et al.*, 2004; Du *et al.*, 2010). Mapman was used for overview and biotic stress classification of DEG, considering a statistical significance of $p<0.05$ considering the Wilcoxon Rank Sum test. For gene set enrichment analysis in cellular compartment and biological process, the online tool agriGO was used to detect significantly enriched GO terms compared with the genome-wide background.

Database searches, protein domain organization and genome organization

To identify G-LecRK-VI.13 homologs, the entire protein sequence was used to perform a search in The Arabidopsis Information Resource (TAIR) (http://arabidopsis.org) website (Berardini et al., 2015).

Candidate sequences were manually annotated regarding the presence of conserved domains using InterPro (http://ebi.ac.uk/interpro) (Mitchell *et al.*, 2014), which combines analysis from a number of distinct databases (CATH-3D, CDD, HAMAP, PANTHER, Pfam, PIRSF, PRINTS, ProDom, PROSITE, SFLD, SMART, SUPERFAMILY, TIGRFAM, TMHMM).

Similarity among amino acid and DNA sequences was evaluated using Clustal Omega (http://www.ebi.ac.uk/Tools/msa/clustalo/) (Sievers et al., 2011) and genes with over 50% similarity at nucleotide or amino acid levels were grouped together in the same Clades.

Phylogenetic analysis

Full-length sequences were aligned using the default settings of ClustaW and phylogenetic tree construction was performed using MEGA 7 (Kumar *et al.*, 2016). The neighbor joining method (Saitou & Nei, 1987), with bootstrap analysis using 1000 replicates was employed to generate the phylogenetic trees.

Protein localization prediction

Gene identifiers and protein sequences were used to query "The SUBcellular localization database for Arabidopsis proteins", SUBA3 (http://suba3.plantenergy.uwa.edu.au/) (Tanz *et al.*, 2013; Hooper *et al.*, 2014), TargetP 1.1 Server (http://www.cbs.dtu.dk/services/TargetP/) (Emanuelsson *et al.*, 2007) and "subCELlular LOcalization predictor" CELLO v.2.5 (http://cello.life.nctu.edu.tw/) (Yu *et al.*, 2006).

Gene expression analysis

RNA was isolated from Arabidopsis roots and leaves using GeneJET Plant RNA purification kit (Life Technologies) and Trizol (Life Technologies), respectively.

Three μg of RNA was DNase treated and used for cDNA synthesis using Superscript III reverse transcriptase enzyme (Invitrogen) and oligo-dT primers according to the manufacturer's recommendations.

Quantitative RT-PCR analysis was performed using gene-specific primers (Table 1), iQ SYBR Green Supermix (Biorad) in iCycler5 IQ (Biorad) in 15 μl using the following program: 94°C for 5 min, followed by 35 cycles of 94°C for 30 sec, 58°C for 30 sec, 72°C for 30 sec and a final cycle of 72°C for 3 min. Three biological replicates, with three technical replicates each, were performed and the generated threshold cycle (C_T) was used to calculate transcript abundance relative to the ribosomal gene 18S.

Flagellin-induced seedling root growth inhibition

Seeds were surface sterilized as mentioned above and plated on one-half-strength MS plates supplemented with 1μM flg22. Root growth was measured 14 days later. Results were evaluated using ANOVA and Tukey HSD test, with n = 12. Experiment was repeated twice with similar results.

ROS burst assay

ROS burst was evaluated using 3-week-old Arabidopsis plants. Leaves were excised into 2 mm pieces using a blade and floated overnight on sterile water in a petri dish. Similar size leaves were transferred to a white 96-welll plate (Corning Costar) with 170 μl sterile water supplemented with 100nM flg22, 20 μM luminol

(Sigma) and 5 µg ml^{-1} horseradish peroxidase (Sigma). Luminescence was measured with a Tecan Infinite F200 plate reader. Experiments were repeated 4 times.

Transfer DNA insertion localization

Genomic DNA was extracted from At1g61550 mutant lines SALK_128729 and SAIL_63_G02 and used to perform PCR using left and right border primers (LBb1.3 and RBb; LB3, QR1) with gene specific primers in various combinations. Amplicons were sequenced and obtained sequences were aligned to At1g61550 sequence and to the Transfer DNAs (T-DNA) pROK2 and pCSA110 to precisely determine the insertion localizations.

***Pseudomonas syringae* pv. *tomato* (*Pst*) DC3000 and *Pst* DC3000 *hrcC* assays**

Inoculation with *Pst* DC3000 was performed as described by Ishiga et al. 2012 (Ishiga *et al.*, 2011). Arabidopsis WT Col-0 and both At1g61550 mutant lines were grown on one-half strength MS medium with Gamborg Vitamins and 0.3% Daishin agar. Before plating the seeds, plates were dried overnight in the hood with closed lids. A suspension of *Pst* DC3000 at 5 x 10^6 colony forming units (CFU)/ml was used to flood plates with 2-week-old Arabidopsis for 3 min at room temperature. The bacterial suspension was removed, plates sealed and incubated in a plant

growth room with 12 h light photoperiod at 24˚C. 2 plates with 8 seedlings were used for each genotype.

Symptoms were evaluated at 3 days after inoculation. Four seedlings were pooled together to constitute one technical replicate and had their weigh measured. Seedlings were then surface-sterilized using 5% H_2O_2 for 3 min, followed by 3 washes with sterile water. Each sample was then homogenized in sterile water, diluted and plated on LB medium overnight. Colonies were counted and normalized to CFU/mg fresh weight.

Inoculation with *Pst* DC3000 *hrcC* was performed by hand infiltrating using a needless syringe, a suspension of 5 x 10^4 CFU/ml of *Pst* DC3000 *hrcC* into the abaxial side of 3-week-old Arabidopsis seedlings. Plants were kept in the same conditions as described for the *Pst* DC3000 assay and samples collected 3 days later. Infiltrated leaves were sampled into 1-cm^2 pieces and surface-sterilized as described for *Pst* DC3000. Three leaf discs were pooled together to make one sample, homogenized in sterile water, diluted and plated on LB medium and incubated overnight at 28°C. Colonies were counted and normalized to CFU/cm^2 fresh weight.

Results

RNAseq analysis

The induction of defense marker genes in response to RKN was previously shown in Arabidopsis roots 24h after inoculation, a time when the nematodes are in the migratory phase and before initiating a feeding site (Teixeira et al, 2016). Therefore, a transcriptome profiling using RNAseq analysis of root tips infected with RKN at the same time point was performed. RNA was extracted from X-Y cm of Arabidopsis roots infected with RKN. Control samples were collected from mock-inoculated plants collected from similar regions of roots as the inoculated samples. BAK1 was previously shown to contribute to defense responses against RKN. Therefore, the mutant *bak1-5* was also included in the RNAseq analysis to characterize the BAK1-dependent transcriptional changes.

We initially characterized the transcriptome difference between naive Col-0 and *bak1-5* mutant in the absence of RKN inoculation. Using as parameters a false discovery rate (FDR) of 1% and fold change of 1.0, 190 genes were differentially expressed in the *bak1-5* roots as compared to Col-0 roots (Appendix D). Of these, 87 and 103 genes were constitutively upregulated and downregulated, respectively, in *bak1-5* roots as compared to Col-0 roots (Figure 2.1A). An agriGO gene enrichment analysis for cellular compartment shows enrichment of transcripts for extracellular region (Figure 2.1B).

Mapman analysis of DEGs in the *bak1-5* roots showed enrichment for genes involved in transport, RNA and secondary metabolisms (Figure 2.2A). Consistent with the overview of DEGs using Mapman, an enrichment analysis in biotic stress responses showed enrichment for genes involved in regulation of transcription (a subset of RNA pathway revealed in the overview) and secondary metabolism (Figure 2.2B).

Interestingly, gene ontology analysis for biological process showed that naïve *bak1-5* roots displayed significant abundance of GO terms involved in response to stimulus (adjusted p-value = 3.77e-07), signaling (adjusted p-value = 0.00147) and lipid metabolic process (adjusted p value = 0.000842) (Figures 2.3 and 2.4). Dissection of genes involved in response to stimulus and signaling showed convergence of these responses to the cellular response to phosphate starvation (adjusted p value = 3.77e-07) (Figure 2.3). Interestingly, a specific branching of response to stimulus showed enrichment for GO terms involved in response to chitin (adjusted p value = 2.81e-06) (Figure 2.3). Further investigation of GO terms enriched for lipid metabolic process revealed ultimate abundance of genes involved in galactolipid biosynthetic process (adjusted p-value = 3.77e-07) (Figure 2.4).

A total of 19,305 and 19,282 transcripts were detected as responsive to RKN-inoculated Col-0 and *bak1-5* roots, respectively, using a false discovery rate (FDR) of 0.01 and fold change cutoff set at 1.0 (Figure 2.5, Appendices E and F). Overall, more genes were upregulated than downregulated following RKN

inoculation of both WT Col-0 and *bak1-5* roots (Figure 2.5A). Analysis of differentially expressed genes (DEG) in each genotype showed that approximately 30% of the DEG was commonly upregulated in roots of both genotypes in response to RKN, while 16% were commonly downregulated (Figure 2.5B and 2.5C). These results confirm those previously observed that RKN penetration/migration perception can occur independent from BAK1 (Teixeira et al. 2016).

Using Mapman to perform gene enrichment analysis on relative expression levels of the transcripts in Col-0 infected roots compared to noninfected roots revealed enrichment for genes involved in signaling, cell wall and hormone metabolism (Figure 2.6A). Interestingly, *bak1-5* roots have an enrichment for genes involved in signaling, cell and photosynthesis in response to RKN (Figure 2.6A).

Consistent with the existence of a BAK1-independent RKN perception pathway, RNAseq analysis of *bak1-5* mutant roots inoculated with RKN still reveled substantial induction of genes involved in biotic stress (Figure 2.6B), such as peroxidases and signaling proteins. Nevertheless, genes encoding cell wall proteins, Pathogenesis Related (PR) proteins and glutathione S transferases were enriched in Col-0 roots (Figure 2.6B) with such enrichment not observed for the *bak1-5* mutant roots.

Consistent with an early response to RKN migration inside plant tissues, both genotypes had significant enrichment for transcripts related to the extracellular region (Figure 2.7).

Gene enrichment analysis of biological processes showed significant abundance of genes involved in defense responses in both WT Col-0 and mutant *bak1-5* roots (Figure 2.8A and 2.8B). Interestingly, genes enriched for death, localization and secondary metabolic process were not observed in *bak1-5* roots, but a new category consisting of small molecule biosynthetic process, is specifically enriched in the *bak1-5* roots, (Figure 2.8B).

Evaluation of gene enrichment in biological processes also revealed a different pattern among the two genotypes concerning enrichment for hormone-related transcripts (Figures 2.9 and 2.10). Col-0 roots responded to RKN with a stronger enrichment for genes involved in perception in jasmonic acid, besides an enrichment for both jasmonic and salicylic acid biosynthesis-related transcripts (Figure 2.9). On the other hand, *bak1-5* roots responded to RKN with a weaker enrichment for jasmonic acid, but also, enrichment for ethylene biosynthesis-related transcripts, with no enrichment for hormones perception-related transcripts (Figure 2.10).

To validate the RNAseq data, genes that upregulated, downregulated or not detected in Col-0 roots in response to RKN inoculation were investigated with gene-specific primers (Table 2.2) using qPCR (Figure 2.11A). Similarly, genes that

were not detected or upregulated in *bak1-5* mutant roots in response to RKN were investigated using qPCR (Figure 2.11B).

Validation using qPCR showed overall similar pattern as observed with RNAseq, except for detection of few transcripts that were not detected using RNAseq, such as At1g29740, At5g41290, At2g19210 and At4g21210 in Col-0 and At1g05700, At5g59660 and At3g19320 in the *bak1-5* mutant. In addition, RNAseq data showed that transcripts of the gene At1g21210 were upregulated in roots of *bak1-5* mutant in response to RKN, but qPCR data showed repression of this gene's transcripts.

Using Mapman, the list of DEGs was queried for genes encoding receptor like proteins, with putative plasma membrane localization with a kinase domain. This search resulted in 14 RLKs (Table 2.1), with three also induced in the *bak1-5* roots in response to RKN infection. Interestingly, two of these RLKs, At1g51830 and At1g51840, are localized in tandem and have opposing behavior in Col-0 and *bak1-5*.

FLS2 was among the 14 RLKs identified and the *fls2-1* mutant of this gene has been shown not to exhibit altered resistance phenotype to RKN (Teixeira et al 2016). Therefore, our analysis focused on the remaining 13 genes. The Salk Institute Genomic Analysis Laboratory (SIGnAL) website was used to identify lines with mutation in each of these genes for further characterization of their roles in RKN resistance (Alonso, 2003). For each of these genes, two mutant lines were

obtained, except for two genes, AT3G59750, for which only one mutant was available, and At1g51840, for which no mutant lines were available.

All the mutant lines were insertion mutants in Col-0 background, namely SALK, SAIL and GK lines. They were genotyped using both antibiotic selection and PCR amplification with gene specific primers (Table 2.3) and T-DNA border primers (LB3, LBb1.3 and o8474) indicating all obtained lines were heterozygous. Homozygous lines were obtained from self-fertilization of heterozygous plants and their homozygosity was confirmed with PCR.

Once two independent mutant lines were obtained from each gene, they were challenged with RKN to characterize their susceptibility by evaluating root galling. Two mutant lines from each of the genes At2g19190, At1g55200, At1g61550 and At4g08850 were evaluated with RKN. At2g19190, At1g55200 and At4g08850 mutant lines were as susceptible to RKN as WT Col-0, while both At1g61550 mutants [SALK_128729 (line #12) and SAIL_63_G02 (line #16)] showed significantly less number of galls indicating enhanced resistance to RKN (Figure 2.12).

At1g61550 and mutant lines characterization

The At1g61550 genomic sequence is 3,629 nucleotides long, with 8 exons, and a cDNA of 2,982 nucleotides (Figure 2.13A). Protein domain characterization using Interpro revealed that At1g61550 encodes a protein that belongs to the G-lectin receptor kinase family with G-type lectin domain, a transmembrane domain and a

serine/threonine kinase domain (Figure 2.14) (Mitchell *et al.*, 2014). In addition to these domains, it contains a S-locus glycoprotein, epidermal growth factor-like (EGF), and the plasminogen-apple-nematode motifs (PAN) (Figure 2.14) and it is hereafter, referred to as G-LecRK-VI.13. Analysis of the kinase domains reveals this G-LecRK-VI.13 encodes a protein with a putative active kinase domain that has all 11 known conserved kinase subdomains of active kinases (FIG) (Hanks & Hunter, 1995).

The T-DNA insertion in the genome of the SALK_128729 (line #12) mutant was predicted to be in the first exon, while the insertion in the genome of the SAIL_63_G02 (line #16) mutant was predicted to be in the seventh exon (Berardini et al., 2015). To confirm the locations of the T-DNA insertions in both mutants, their genomic DNA was used in PCR. The predicted region of the T-DNA insertion of the mutant line SALK_128729 was amplified using the T-DNA left border primer LB1.3 and the gene-specific genotyping reverse primer, SALK_128729R (Table 2.3). Sequencing this amplified product revealed that the insertion is localized 49 bp upstream of G-LecRK-VI.13 start codon. The same approach was used to localize the mutation in the SAIL_63_G02 mutant line. Sequencing this product revealed a 61bp deletion and introduction of a premature stop codon in the kinase domain by the T-DNA insertion (Figure 2.13B). Interestingly, sequencing of the SAIL-63_G02 T-DNA right border flanking region was only possible using the primer LB3 (left border primer) and the gene-specific genotyping forward primer,

revealing that this line results from at least two T-DNA insertions in tandem, with the first one being inverted.

To confirm the prediction of the existence and nature of transcripts in these 2 mutants, G-LecRK-VI.13 gene expression was evaluated using two primer sets in semi-quantitative RT-PCR (Figure 2.13B). The first set of primers annealed to a region located between exon 6 to exon 7 and no transcript could be amplified from the cDNA prepared from either G-LecRK-VI.13 mutant lines (Figure 2.13). The second set of primers annealed to a region located between exon 7 and exon 8, right before the predicted insertion site in mutant line SAIL_63_G02. This primer pair amplified transcripts from the SAIL_63_G02 mutant line but no product could be amplified from the SALK_128729 mutant line (Figure 2.13). These results revealed that while line SALK_128729 (line # 12) is a knockout line and no G-LecRK-VI.13 transcripts were detected with both primer sets used, the mutant line SAIL_63_G02 (line #16) is transcribed producing a truncated version of G-LecRK-VI.13 transcript.

G-LecRK-VI.13 mutant has elevated basal expression of defense marker genes

Because of the observed enhanced resistance in At1g61550 mutant lines, we hypothesized that this gene might act as a negative regulator of defense responses. To address this possibility, 4-week-old naïve Arabidopsis seedlings were used to investigate the expression of salicylic acid (*PR1*), jasmonic acid

and/or ethylene (*PDF1.2*) defense hormone regulated marker genes as well as a camalexin–related gene (*PAD3*) required for RKN defense (Figure 2.15). Our results showed that *PR1* expression is repressed while *PDF1.2* and *PAD3* are induced in the roots of the SALK_128729 mutant line (#12) (Figure 2.15), indicating a role for jasmonic acid or ethylene in the observed phenotype. To further identify which one of these two hormones is involved in the observed response, the expression of additional genes was investigated, namely *JAR1* (Jasmonate resistant 1, jasmonate-isoleucine synthase), *OPR3* (12-oxophytodieoate reductase 3, jasmonate biosynthesis) and *EIN2* (Ethylene insensitive 2, ET signaling). Although no difference was observed in *EIN2* expression in SALK_128729 roots as compared to Col-0 roots, both *OPR3* and *JAR1* were constitutively up-regulated in the mutant roots, showing constitutive activation of defense responses involving Jasmonic acid pathway (Figure 2.15).

At1g61550 was induced upon nematode inoculation at 24h after inoculation. Therefore, it was hypothesized that this gene is involved in early defense responses, or PTI responses. The flg22 peptide is a potent elicitor of PTI responses and its effect on plants can be evaluated indirectly by the root growth upon treatment of seedlings with flg22. Hence, to evaluate if these mutants would respond to flg22 with a stronger root development inhibition, seedling root inhibition assay was performed, treating the WT Col-0, both At1g61550 mutant lines (number 12 and 16) and the *fls2-1* mutant (negative control) with 1µM flg22. There

was no difference on root length between At1g61550 mutants and the WT (Figure 2.16), suggesting these mutants do not display increased sensitivity to flg22.

G-LecRK-VI.13 mutants have increased resistance to *Pst* DC3000 *hrcC*

To assess a role for G-LecRK-VI.13 in resistance against bacterial pathogens, Arabidopsis G-LecRK-VI.13 mutant lines were evaluated for resistance against the pathogenic *Pst* DC3000 and the non-pathogenic *Pst* DC3000 *hrcC*. Inoculation of WT Col-0 Arabidopsis and G-LecRK-VI.13 seedlings with *Pst* DC3000 resulted in similar levels of bacterial titers indicating no difference in susceptibility among these genotypes (Figure 2.17A). In contrast, inoculation of Arabidopsis seedlings with *Pst* DC3000 *hrcC* revealed that the G-LecRK-VI.13 mutants showed significantly lower levels of bacterial titer compared to Col-0, indicating enhanced resistance to this non-pathogenic bacterial strain (Figure 2.17B).

G-LecRK-VI.13 mutant lines have stronger and faster induction of reactive oxygen species (ROS) burst

One of the PTI hallmarks is the reactive oxygen species (ROS) burst, which is known to be strongly activated by flg22. To characterize At1g61550 mutant lines regarding flg22-triggered ROS burst, they were evaluated in a ROS assay. Both lines showed a significantly more rapid and robust ROS burst as compared to WT Col-0 (Figure 2.18).

Constitutive activation of defense responses can lead to an effect on plant development, with plants showing reduced growth, such as that observed for *bkk1 bak1* double mutant (Heese et al., 2007). Remarkably, neither mutant lines of At1g61550 show any observable growth defects (Figure 2.19).

Identification of tomato **putative homologs of G-LecRK-VI.13**

To identify putative homologs of G-LecRK-VI.13 in tomato, G-LecRK-VI.13 protein sequence was used to perform alignment with the tomato G-LecRKs. To infer on the relationship between the protein encoded by G-LecRK-VI.13 and tomato proteins, the obtained alignment was used to construct a phylogenetic tree using the Neighbor Joining method (Saitou & Nei, 1987). This analysis showed that G-LecRK-VI.13 grouped with a cluster of 14 tomato genes (Figure 2.20). Characterization of the tomato protein sequences and domains revealed that the Solyc03g006720, Solyc03g006730.A and Solyc03g006730.B have higher amino acid identity to G-LecRK-VI.13 (46, 48, 48% identity, respectively) (Table 2.4), but lack one of the domains encoded by this protein, the EGF domain. Therefore, a search was performed among the 14 tomato genes to identify putative homologs with the EGF domain, which resulted in the identification of only 2 genes encoding this domain, Solyc04g008400.A and Solyc04g58110, with 44 and 43% identity to G-LecRK-VI.13, respectively. As expected, the three genes that do not encode proteins with EGF have higher amino acid identity among them, ranging from 78 to 83%. Similarly, the two genes encoding proteins with EGF have higher identity

between them (83% amino acid identity) (Table 2.4). Thus, 5 genes were considered as putative G-LecRK-VI.13 tomato homologs, based on amino acid percent identity and encoded domains (Figure 2.20, Table 2.4).

Discussion

Transcriptome analyses performed in root galls or giant cells after inoculation with RKN show an overall downregulation of transcripts in response to RKN (Schaff *et al.*, 2007; Caillaud *et al.*, 2008; Barcala *et al.*, 2010; Portillo *et al.*, 2013). This downregulation is believed to be mediated by nematode effectors, which would actively modulate plant responses to successfully complete their life cycle (Goverse & Smant, 2014; Mantelin *et al.*, 2015). Interestingly, transcriptome investigation of plant responses at earlier time points reveal an opposite trend of upregulation of differentially expressed genes suggesting reduced levels of interference of RKN on plant responses (Lambert *et al.*, 1999; Bhattarai *et al.*, 2008; Ali *et al.*, 2014).

In the current RNAseq analysis we observed overall induction of DEG in two Arabidopsis genotypes, the wild-type Col-0 and the mutant *bak1-5*. Consistent with the predicted existence of BAK1-dependent and independent plant responses to RKN, this mutant still responded to RKN penetration/migration, although with a different pattern from that observed in WT plants, with decreased representation of genes encoding for PR proteins and glutathione S transferases, for example. Interestingly, glutathione S transferases are involved in regulation of oxidative burst and the decrease of these protein responses in *bak1-5* mutant might suggest that this response is compromised in this mutant. Indeed, reduction in ROS burst

in *bak1* mutants has been previously demonstrated after treatment with flg22 and elf18 (Chinchilla *et al.*, 2007; Roux *et al.*, 2011).

Consistent with perception of nematodes during early stage of parasitism, penetration and migration, there is a significant enrichment of gene ontology terms for the extracellular region in transcriptomes of both genotypes. Early pathogen perception in plants is mediated by plasma membrane localized receptor-like proteins and our search of the RNAseq data revealed 14 genes with membrane predicted localization to be induced in Col-0 roots in response to RKN. Initial characterization of the role of these genes in defense against RKN allowed identification of a negative regulator of RKN immunity from a family of largely unexplored proteins.

Although research on receptor like proteins has frequently resulted in identification of positive regulators of immunity, there has been recently an increase in number of publications describing negative regulators of plant immunity (Gou *et al.*, 2009; Wang *et al.*, 2009; Shi *et al.*, 2013; Wang *et al.*, 2013; Lin *et al.*, 2015). Because of the high energy cost of defense responses, it is natural to expect plants to deploy a tightly control system to keep defense responses in a neutral stage in the absence of elicitation (Lozano-Duran *et al.*, 2013; Belkhadir *et al.*, 2014; Lin *et al.*, 2015). As a result of a multi player control, mutations in a single negative regulator often does not result in plant developmental defects, although mutations of multiple players might result in strong defects (Heese *et al.*, 2007; Halter *et al.*, 2014; Lin *et al.*, 2015).

Our root growth inhibition assay result is similar to that observed for the mutant of the cytoplasmic kinase PBL13, in which no increased sensitivity was observed to flg22 treatment. This is in contrast to the phenotype observed for the negative immune regulator BAK1-INTERACTING RECEPTOR-LIKE KINASE 2 (*bir2)* mutants, which displayed a strong increase in root growth inhibition upon treatment with both flg22 and elf18 elicitors (Halter *et al.*, 2014; Lin *et al.*, 2015). Nevertheless, defense marker genes were constitutively upregulated in plants with mutations of negative regulators, revealing an ultimate impact in transcriptional regulation of plant defense responses (Halter *et al.*, 2014; Lin *et al.*, 2015).

Notably, both PBL13 and G-LecRK-VI.13 transcripts are induced after Arabidopsis challenge with flg22 and RKN, respectively (Lin *et al.*, 2015). It is interesting that identification of BIR2 was the result of the characterization of proteins present in the BAK1 complex at the plasma membrane (Halter *et al.*, 2014). Similarly, future analysis of proteins present in the same complex as G-LecRK-VI.13 constitutively or after RKN perception will allow further characterization of its role as a negative regulator of immunity.

Previous investigations have shown the importance or jasmonic acid signaling pathway at early stages of parasitism against cyst nematodes (Kammerhofer *et al.*, 2015). Our data indicates that jasmonic acid signaling participates in resistance to RKN in Arabidopsis. Although Arabidopsis jasmonic acid mutants have not been characterized for RKN susceptibility, accumulation of transcripts of genes involved in JA biosynthesis or signaling pathways have been

previously correlated with enhanced resistance to RKN (Fujimoto *et al.*, 2011; Nahar *et al.*, 2013). Screening jasmonic acid mutants with RKN is necessary to better characterize the contribution of this defense hormone to RKN resistance.

The identification of tomato candidate homologs will allow the use of this negative regulator as a tool for developing RKN resistant varieties as well as provide a possible broad-spectrum pathogen control. This could be achieved by creating null mutations in G-LecRK-VI.13 using the emergent RNA-guided genome-editing technology CRISPR-Cas9 (clustered regularly interspaced short palindromic repeat-associated nuclease 9). This technology has proven efficient in different plant species, including tomato, rice (*Oryza sativa*), and soybean (*Glycine max*) (Miao et al., 2013; Shan et al., 2013; Brooks et al., 2014; Zhang et al., 2014; Jacobs et al., 2015; Ma et al., 2015; Sun et al., 2015; Ding et al., 2016; Pan et al., 2016).

Future analysis of proteins present in the same complex as G-LecRK-VI.13 will allow further characterization of its role as a negative regulator of immunity. It will be also interesting to investigate the function for each of the G-LecRK-VI.13 domains, other than the G-lectin, transmembrane and kinase, for which no clear functional roles have been documented.

References

Ali MA, Wieczorek K, Kreil DP, Bohlmann H. 2014. The beet cyst nematode *Heterodera schachtii* modulates the expression of WRKY transcription factors in syncytia to favour its development in *Arabidopsis* roots. *PLoS One* **9**(7): e102360.

Bar-Or C, Kapulnik Y, Koltai H. 2005. A broad characterization of the transcriptional profile of the compatible tomato response to the plant parasitic root knot nematode *Meloidogyne javanica*. *European Journal of Plant Pathology* **111**(2): 181-192.

Barcala M, Garcia A, Cabrera J, Casson S, Lindsey K, Favery B, Garcia-Casado G, Solano R, Fenoll C, Escobar C. 2010. Early transcriptomic events in microdissected Arabidopsis nematode-induced giant cells. *Plant Journal* **61**(4): 698-712.

Belkhadir Y, Yang L, Hetzel J, Dangl JL, Chory J. 2014. The growth-defense pivot: crisis management in plants mediated by LRR-RK surface receptors. *Trends in Biochemical Sciences* **39**(10): 447-456.

Ben Khaled S, Postma J, Robatzek S. 2015. A moving view: Subcellular trafficking processes in pattern recognition receptor–triggered plant immunity. *Annual Review of Phytopathology* **53**(1): 379-402.

Berardini TZ, Reiser L, Li D, Mezheritsky Y, Muller R, Strait E, Huala E. 2015. The Arabidopsis information resource: making and mining the "gold standard" annotated reference plant genome. *Genesis* **53**(8): 474-485.

Bhattarai KK, Xie QG, Mantelin S, Bishnoi U, Girke T, Navarre DA, Kaloshian I. 2008. Tomato susceptibility to root-knot nematodes requires an intact jasmonic acid signaling pathway. *Molecular Plant-Microbe Interactions* **21**(9): 1205-1214.

Brooks C, Nekrasov V, Lippman ZB, Van Eck J. 2014. Efficient gene editing in tomato in the first generation using the clustered regularly interspaced short palindromic repeats/CRISPR-associated9 system. *Plant Physiology* **166**(3): 1292-1297.

Caillaud MC, Dubreuil G, Quentin M, Perfus-Barbeoch L, Lecomte P, de Almeida Engler J, Abad P, Rosso MN, Favery B. 2008. Root-knot nematodes manipulate plant cell functions during a compatible interaction. *Journal of Plant Physiology* **165**(1): 104-113.

Chinchilla D, Zipfel C, Robatzek S, Kemmerling B, Nürnberger T, Jones JD, Felix G, Boller T. 2007. A flagellin-induced complex of the receptor FLS2 and BAK1 initiates plant defence. *Nature* **448**(26): 497-500.

de Almeida Engler J, Rodiuc N, Smertenko A, Abad P. 2010. Plant actin cytoskeleton remodeling by plant parasitic nematodes. *Plant Signaling & Behavior* **5**(3): 213-217.

Ding Y, Li H, Chen LL, Xie K. 2016. Recent advances in genome editing using CRISPR/Cas9. *Frontiers in Plant Science* **7**: 703.

Du Z, Zhou X, Ling Y, Zhang Z, Su Z. 2010. agriGO: a GO analysis toolkit for the agricultural community. *Nucleic Acids Research* **38**(Web Server issue): W64-70.

Felix G, Duran JD, Volko S, Boller T. 1999. Plants have a sensitive perception system for the most conserved domain of bacterial flagellin. *Plant Journal* **18**: 265-276.

Fudali SL, Wang C, Williamson VM. 2013. Ethylene signaling pathway modulates attractiveness of host roots to the root-knot nematode *Meloidogyne hapla*. *Molecular Plant-Microbe Interactions* **26**: 75-86.

Fujimoto T, Tomitaka Y, Abe H, Tsuda S, Futai K, Mizukubo T. 2011. Expression profile of jasmonic acid-induced genes and the induced resistance against the root-knot nematode (*Meloidogyne incognita*) in tomato plants (*Solanum lycopersicum*) after foliar treatment with methyl jasmonate. *Journal of Plant Physiology* **168**(10): 1084-1097.

Gheysen G, Mitchum MG. 2011. How nematodes manipulate plant development pathways for infection. *Current Opinion in Plant Biology* **14**(4): 415-421.

Gomez-Gomez L, Felix G, Boller T. 1999. A single locus determines sensitivity to bacterial flagellin in *Arabidopsis thaliana*. *Plant Journal* **18**(3): 277-284.

Goto DB, Miyazawa H, Mar JC, Sato M. 2013. Not to be suppressed? Rethinking the host response at a root-parasite interface. *Plant Science* **213**: 9-17.

Gou M, Su N, Zheng J, Huai J, Wu G, Zhao J, He J, Tang D, Yang S, Wang G. 2009. An F-box gene, CPR30, functions as a negative regulator of the defense response in Arabidopsis. *Plant Journal* **60**(5): 757-770.

Goverse A, Smant G. 2014. The activation and suppression of plant innate immunity by parasitic nematodes. *Annual Review of Phytopathology* **52**: 243-265.

Halter T, Imkampe J, Mazzotta S, Wierzba M, Postel S, Bücherl C, Kiefer C, Stahl M, Chinchilla D, Wang X, et al. 2014. The leucine-rich repeat receptor kinase BIR2 is a negative regulator of BAK1 in plant immunity. *Current Biology* **24**(2): 134-143.

Hanks SK, Hunter T. 1995. Protein kinases 6. The eukaryotic protein kinase superfamily: kinase (catalytic) domain structure and classification. *Journal of the Federation of American Socities for Experimental Biology* **9**(8): 576-596.

Heese A, Hann DR, Gimenez-Ibanez S, Jones AM, He K, Li J, Schroeder JI, Peck SC, Rathjen JP. 2007. The receptor-like kinase SERK3/BAK1 is a central regulator of innate immunity in plants. *Proceedings of the National Academy of Sciences of the United States of America* **104**(29): 12217-12222.

Hussey R, Barker KR. 1973. A comparison of methods of collecting inocula of *Meloidogyne* species including a new technique. *Plant Disease Report* **57**: 1025-1028.

Ibrahim HM, Hosseini P, Alkharouf NW, Hussein EH, Gamal El-Din Ael K, Aly MA, Matthews BF. 2011. Analysis of gene expression in soybean (*Glycine max*) roots in response to the root knot nematode *Meloidogyne incognita* using microarrays and KEGG pathways. *BMC Genomics* **12**: 220.

Ishiga Y, Ishiga T, Uppalapati SR, Mysore KS. 2011. Arabidopsis seedling flood-inoculation technique: a rapid and reliable assay for studying plant-bacterial interactions. *Plant Methods* **7**: 32-32.

Jacobs TB, LaFayette PR, Schmitz RJ, Parrott WA. 2015. Targeted genome modifications in soybean with CRISPR/Cas9. *BMC Biotechnology* **15**: 16.

Jammes F, Lecomte P, de Almeida-Engler J, Bitton F, Martin-Magniette ML, Renou JP, Abad P, Favery B. 2005. Genome-wide expression profiling of the host response to root-knot nematode infection in Arabidopsis. *Plant Journal* **44**(3): 447-458.

Jones JD, Dangl JL. 2006. The plant immune system. *Nature* **444**(16): 323-329.

Jones JT, Haegeman A, Danchin EGJ, Gaur HS, Helder J, Jones MGK, Kikuchi T, Manzanilla-López R, Palomares-Rius JE, Wesemael WML, et al. 2013. Top 10 plant-parasitic nematodes in molecular plant pathology. *Molecular Plant Pathology* **14**(9): 946-961.

Kammerhofer N, Radakovic Z, Regis JMA, Dobrev P, Vankova R, Grundler FMW, Siddique S, Hofmann J, Wieczorek K. 2015. Role of stress-related hormones in plant defence during early infection of the cyst nematode *Heterodera schachtii* in Arabidopsis. *New Phytologist* **207**: 778-789.

Kim D, Pertea G, Trapnell C, Pimentel H, Kelley R, Salzberg SL. 2013. TopHat2: accurate alignment of transcriptomes in the presence of insertions, deletions and gene fusions. *Genome Biology* **14**(4): R36.

Kettles GJ, Kaloshian I. 2016. The potato aphid salivary effector Me47 is a glutathione-S-transferase involved in modifying plant responses to aphid infestation. *Frontiers in Plant Science* **7**(1142).

Lambert KN, Ferrie BJ, Nombela G, Brenner ED, Williamson VM. 1999. Identification of genes whose transcripts accumulate rapidly in tomato after root-knot nematode infection. *Physiological and Molecular Plant Pathology* **55**: 341-348.

Langmead B, Salzberg SL. 2012. Fast gapped-read alignment with Bowtie 2. *Nature Methods* **9**(4): 357-359.

Lawrence M, Huber W, Pagès H, Aboyoun P, Carlson M, Gentleman R, Morgan MT, Carey VJ. 2013. Software for computing and annotating genomic ranges. *PLoS Computational Biology* **9**(8): e1003118.

Lin ZJ, Liebrand TW, Yadeta KA, Coaker G. 2015. PBL13 Is a Serine/Threonine protein kinase that negatively regulates Arabidopsis immune responses. *Plant Physiology* **169**(4): 2950-2962.

Lozano-Duran R, Macho AP, Boutrot F, Segonzac C, Somssich IE, Zipfel C. 2013. The transcriptional regulator BZR1 mediates trade-off between plant innate immunity and growth. *eLife* **2**: e00983.

Ma X, Zhang Q, Zhu Q, Liu W, Chen Y, Qiu R, Wang B, Yang Z, Li H, Lin Y, et al. 2015. A Robust CRISPR/Cas9 System for Convenient, High-Efficiency Multiplex Genome Editing in Monocot and Dicot Plants. *Molecular Plant* **8**(8): 1274-1284.

Mantelin S, Thorpe P, Jones JT 2015. Suppression of plant defences by plant-parasitic nematodes. In: Escobar C, Fenoll C eds. *Advances in botanical research*. Oxford, UK: Elsevier Ltd., 325-337.

Martinez de Ilarduya O, Moore AE, Kaloshian I. 2001. The tomato *Rme1* locus is required for *Mi-1*-mediated resistance to root-knot nematodes and the potato aphid. *Plant Journal* **27**(5): 417-425.

Miao J, Guo D, Zhang J, Huang Q, Qin G, Zhang X, Wan J, Gu H, Qu LJ. 2013. Targeted mutagenesis in rice using CRISPR-Cas system. *Cell Research* **23**(10): 1233-1236.

Nahar K, Kyndt T, Hause B, Hofte M, Gheysen G. 2013. Brassinosteroids suppress rice defense against root-knot nematodes through antagonism with the jasmonate pathway. *Molecular Plant-Microbe Interactions* **26**(1): 106-115.

Pan C, Ye L, Qin L, Liu X, He Y, Wang J, Chen L, Lu G. 2016. CRISPR/Cas9-mediated efficient and heritable targeted mutagenesis in tomato plants in the first and later generations. *Scientific Reports* **6**: 24765.

Portillo M, Cabrera J, Lindsey K, Topping J, Andres MF, Emiliozzi M, Oliveros JC, Garcia-Casado G, Solano R, Koltai H, et al. 2013. Distinct and conserved transcriptomic changes during nematode-induced giant cell development in tomato compared with Arabidopsis: a functional role for gene repression. *New Phytologist* **197**: 1276-1290.

Robinson MD, McCarthy DJ, Smyth GK. 2010. edgeR: a Bioconductor package for differential expression analysis of digital gene expression data. *Bioinformatics* **26**(1): 139-140.

Rodiuc N, Vieira P, Banora MY, de Almeida Engler J. 2014. On the track of transfer cell formation by specialized plant-parasitic nematodes. *Frontiers in Plant Science* **5**: 160.

Roux M, Schwessinger B, Albrecht C, Chinchilla D, Jones A, Holton N, Malinovsky FG, Tor M, de Vries S, Zipfel C. 2011. The Arabidopsis leucine-rich repeat receptor-like kinases BAK1/SERK3 and BKK1/SERK4 are required for innate immunity to hemibiotrophic and biotrophic pathogens. *Plant Cell* **23**: 2440-2455.

Saitou N, Nei M. 1987. The neighbor-joining method: a new method for reconstructing phylogenetic trees. *Molecular Biology and Evolution* **4**(4): 406-425.

Salomon S, Robatzek S. 2006. Induced Endocytosis of the Receptor Kinase FLS2. *Plant Signaling & Behavior* **1**(6): 293-295.

Schaff JE, Nielsen DM, Smith CP, Scholl EH, Bird DM. 2007. Comprehensive transcriptome profiling in tomato reveals a role for glycosyltransferase in *Mi*-mediated nematode resistance. *Plant Physiology* **144**(2): 1079-1092.

Shan Q, Wang Y, Li J, Zhang Y, Chen K, Liang Z, Zhang K, Liu J, Xi JJ, Qiu JL, et al. 2013. Targeted genome modification of crop plants using a CRISPR-Cas system. *Nature Biotechnology* **31**(8): 686-688.

Shi Z, Maximova S, Liu Y, Verica J, Guiltinan MJ. 2013. The salicylic acid receptor NPR3 is a negative regulator of the transcriptional defense response during early flower development in Arabidopsis. *Molecular Plant* **6**(3): 802-186.

Sijmons PC, Grundler FMW, Von Mende N, Burrows PR, Wyss U. 1991. *Arabidopsis thaliana* as a new model host for plant-parasitic nematodes. *Plant Journal* **1**: 245-254.

Sun X, Hu Z, Chen R, Jiang Q, Song G, Zhang H, Xi Y. 2015. Targeted mutagenesis in soybean using the CRISPR-Cas9 system. *Scientific Reports* **5**: 10342.

Teixeira MA, Wei L, Kaloshian I. 2016. Root-knot nematodes induce pattern-triggered immunity in *Arabidopsis thaliana* roots. *New Phytologist* **211**: 279-287.

Thimm O, Blasing O, Gibon Y, Nagel A, Meyer S, Kruger P, Selbig J, Muller LA, Rhee SY, Stitt M. 2004. MAPMAN: a user-driven tool to display genomics data sets onto diagrams of metabolic pathways and other biological processes. *Plant Journal* **37**(6): 914-939.

Wang X, Basnayake BM, Zhang H, Li G, Li W, Virk N, Mengiste T, Song F. 2009. The Arabidopsis ATAF1, a NAC transcription factor, is a negative regulator of defense responses against necrotrophic fungal and bacterial pathogens. *Molecular Plant-Microbe Interactions* **22**(10): 1227-1238.

Wang Y, Dang F, Liu Z, Wang X, Eulgem T, Lai Y, Yu L, She J, Shi Y, Lin J, et al. 2013. CaWRKY58, encoding a group I WRKY transcription factor of *Capsicum annuum*, negatively regulates resistance to *Ralstonia solanacearum* infection. *Molecular Plant Pathology* **14**(2): 131-144.

Wang Z, Potter RH, Jones MGK. 2003. Differential display analysis of gene expression in the cytoplasm of giant cells induced in tomato roots by *Meloidogyne javanica*. *Molecular Plant Pathology* **4**(5): 361-371.

Wyss U, Grundler FMW, Munch A. 1992. The parasitic behaviour of second-stage juveniles of *Meloidogyne incognita* in roots of *Arabidopsis thaliana*. *Nematologica* **38**: 98-111.

Zhang H, Zhang J, Wei P, Zhang B, Gou F, Feng Z, Mao Y, Yang L, Zhang H, Xu N, et al. 2014. The CRISPR/Cas9 system produces specific and homozygous targeted gene editing in rice in one generation. *Plant Biotechnol J* **12**(6): 797-807.

Zipfel C. 2014. Plant pattern-recognition receptors. *Trends in Immunology* **35**: 345-351.

Zipfel C, Robatzek S, Navarro L, Oakeley EJ, Jones JD, Felix G, Boller T. 2004. Bacterial disease resistance in Arabidopsis through flagellin perception. *Nature* **428**(6984): 764-767.

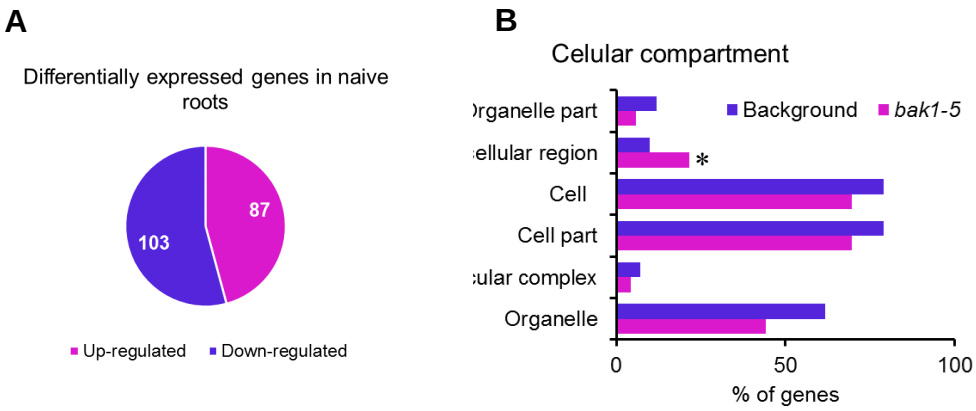

Figure 2.1. Overview of the constitutive differentially expressed genes and the cellular localization of their encoded proteins in naïve roots of the Arabidopsis mutant *bak1-5* as compared to the WT Col-0 (false discovery rate < 0.01, fold change = 1.0). (A) Number of differentially expressed genes (DEG). (B) Percentage of DEG classified into specific cellular compartments using Agrigo (* FDR = 0.00035).

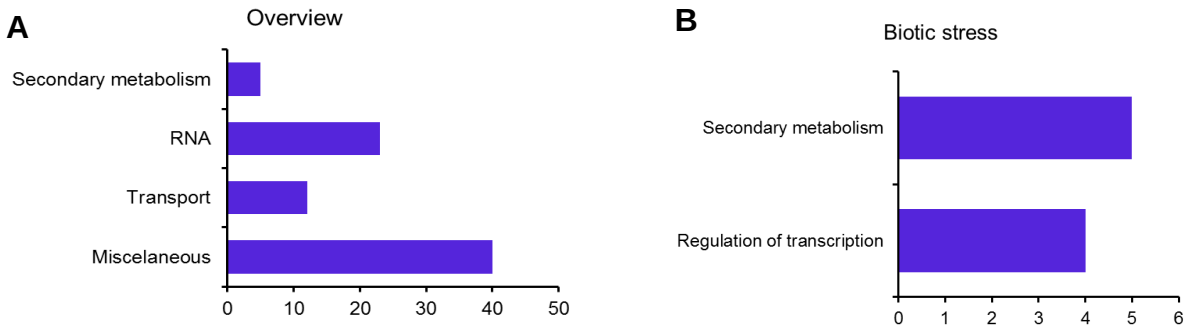

Figure 2.2. Overview of differentially expressed genes in RKN-infected Arabidopsis Col-0 (a) and *bak1-5* mutant (b) classified into functional categories (Mapman) over-represented with a statistical significance ($p<0.05$) using the Wilcoxon Rank Sum test.


GO:0008150
biological_process
GO:0023052 (0.00147)
signaling
33/185 | 2376/28397
GO:0009987
cellular process
GO:0050896 (3.77e-07)
response to stimulus
77/185 | 6292/28397
GO:0007154 (5.66e-05)
cell communication
19/185 | 758/28397
GO:0051716 (0.000261)
cellular response
to stimulus
35/185 | 2355/28397
GO:0009605 (1.49e-08)
response to
external stimulus
30/185 | 1087/28397
GO:0006950 (2.81e-06)
response to stress
56/185 | 4089/28397
GO:0042221 (3.74e-05)
response to
chemical stimulus
52/185 | 3978/28397
GO:0071496 (1.49e-08)
cellular response
to external stimulus
19/185 | 389/28397
GO:0009991 (1.55e-08)
response to
extracellular stimulus
19/185 | 406/28397
GO:0033554 (0.00176)
cellular response
to stress
24/185 | 1473/28397
GO:0010033 (0.00196)
response to
organic substance
36/185 | 2754/28397
GO:0031668 (1.49e-08)
cellular response
to extracellular stimulus
19/185 | 388/28397
GO:0031667 (2.07e-08)
response to
nutrient levels
18/185 | 367/28397
GO:0009743 (0.00147)
response to
carbohydrate stimulus
17/185 | 812/28397
GO:0031669 (1.49e-08)
cellular response
to nutrient levels
18/185 | 350/28397
GO:0042594 (4.78e-08)
response to
starvation
17/185 | 344/28397
GO:0010200 (2.81e-06)
response to chitin
16/185 | 421/28397
GO:0009267 (3.87e-08)
cellular response
to starvation
17/185 | 336/28397
GO:0016036 (3.77e-07)
cellular response
to phosphate starvation
12/185 | 169/28397

Figure 2.3. Biological process classification of differentially expressed genes (DEGs) involved in signaling and response to stimuli using singular enrichment analysis (SEA) from agriGO. DEGs (false discovery rate<0.01 and Fold change = 1.0) were analyzed for biological process enrichment and significance levels are presented in a color scale, in which white shows no significant enrichment and red indicates strong enrichment. Ratios at the bottom of the boxes inform number of genes in the input list that match the specific gene ontology (GO) term informed in the box relative to total number of genes in the input list and total genes in the background genome that match that GO term relative to total genes in the background set. The adjusted p-value for each enriched GO term is shown at the top of each box.

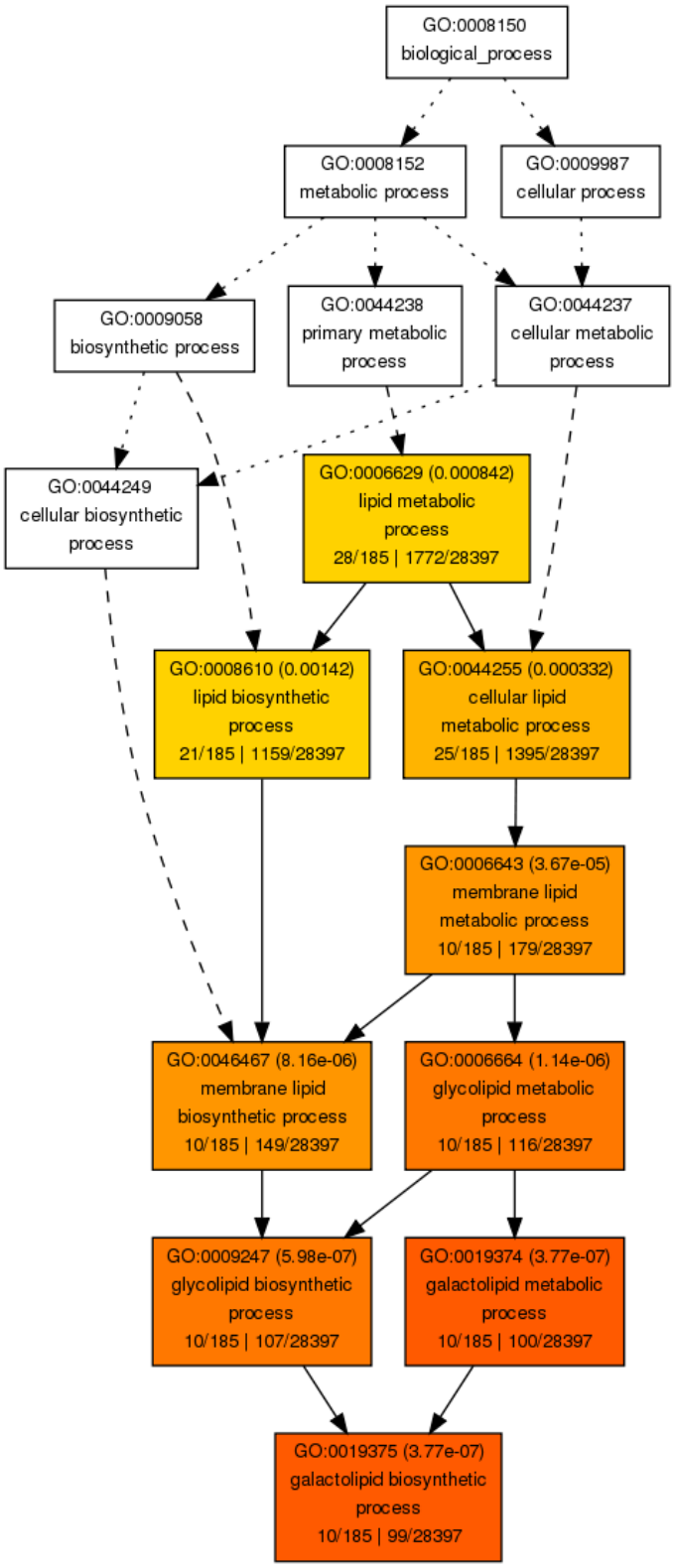
GO:0008150
biological_process
GO:0008152
metabolic process
GO:0009987
cellular process
GO:0009058
biosynthetic process
GO:0044238
primary metabolic process
GO:0044237
cellular metabolic process
GO:0044249
cellular biosynthetic process
GO:0006629 (0.000842)
lipid metabolic process
28/185 | 1772/28397
GO:0008610 (0.00142)
lipid biosynthetic process
21/185 | 1159/28397
GO:0044255 (0.000332)
cellular lipid metabolic process
25/185 | 1395/28397
GO:0006643 (3.67e-05)
membrane lipid metabolic process
10/185 | 179/28397
GO:0046467 (8.16e-06)
membrane lipid biosynthetic process
10/185 | 149/28397
GO:0006664 (1.14e-06)
glycolipid metabolic process
10/185 | 116/28397
GO:0009247 (5.98e-07)
glycolipid biosynthetic process
10/185 | 107/28397
GO:0019374 (3.77e-07)
galactolipid metabolic process
10/185 | 100/28397
GO:0019375 (3.77e-07)
galactolipid biosynthetic process
10/185 | 99/28397

Figure 2.4. Biological process classification of differentially expressed genes (DEGs) involved in lipid metabolic process using singular enrichment analysis (SEA) from agriGO. DEGs (false discovery rate<0.01 and Fold change = 1.0) were analyzed for biological process enrichment and significance levels are presented in a color scale, in which white shows no significant enrichment and red indicates strong enrichment. Ratios at the bottom of the boxes inform number of genes in the input list that match the specific gene ontology (GO) term informed in the box relative to total number of genes in the input list and total genes in the background genome that match that GO term relative to total genes in the background set. The adjusted p-value for each enriched GO term is shown at the top of each box.

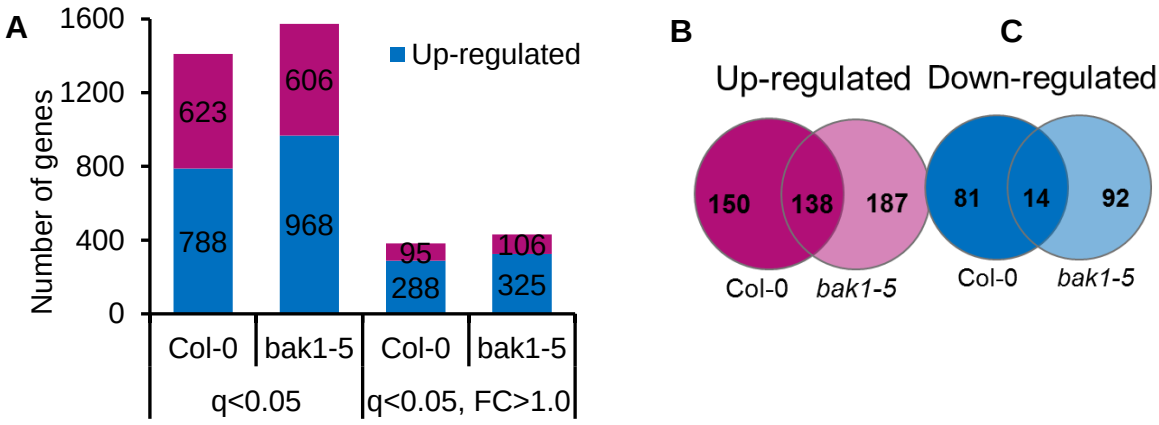

Figure 2.5. Changes in DEG during RKN infection of Arabidopsis roots. (A) Number of DEGs 24h after inoculation of Col-0 and *bak1-5* mutant with RKN. (B) Venn diagrams showing changes in DEGs in Col-0 and *bak1-5* roots 24h after RKN inoculation. Intersection of the diagrams represent genes commonly up-regulated in both genotypes. (C) Venn diagram showing changes in DEGs in Col-0 and *bak1-5* roots 24h after RKN inoculation. Intersection of the diagrams represent genes commonly down-regulated in both genotypes. q<0.05, fold change >1.

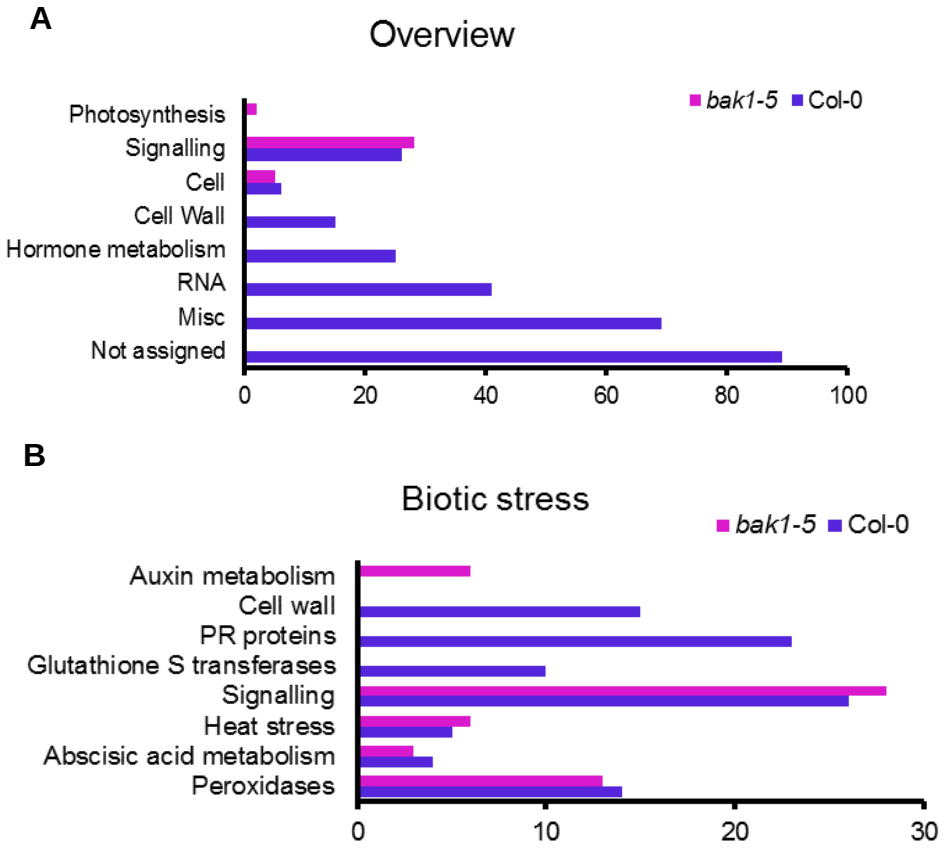

Figure 2.6. Overview of differentially expressed genes in RKN-infected Arabidopsis Col-0 and *bak1-5* mutant classified into overview (A) and biotic stress (B) functional categories (Mapman) over-represented with a statistical significance ($p<0.05$) using the Wilcoxon Rank Sum test.

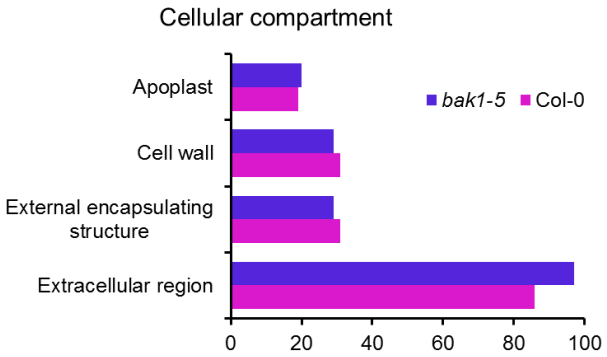

Figure 2.7. Overview of differentially expressed genes in RKN-infected Arabidopsis Col-0 and *bak1-5* mutant classified into different cellular compartments with a statistical significance ($p<0.01$). Only significant statistically cellular compartments were informed.

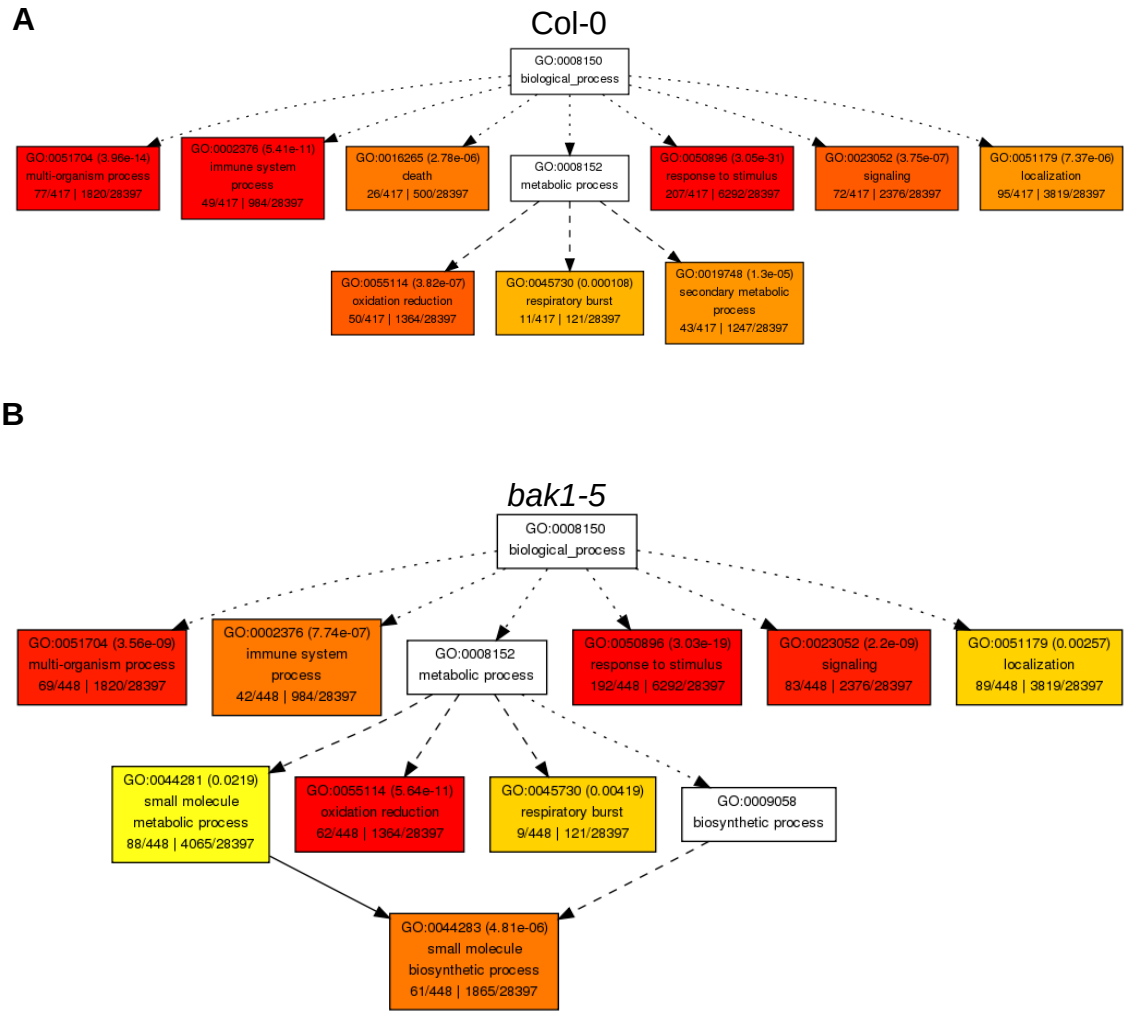

Figure 2.8. Biological process classification of differentially expressed genes (DEGs) in WT Col-0 and mutant *bak1-5* roots in response to RKN using singular enrichment analysis (SEA) from agriGO. DEGs (false discovery rate<0.01 and Fold change = 1.0) were analyzed for biological process enrichment and significance level is presented in a color scale, in which white shows no significant enrichment and red indicates strong enrichment. Ratios at the bottom of the boxes inform number of genes in the input list that match the specific gene ontology (GO) term informed in the box relative to total number of genes in the input list and total genes in the background genome that match that GO term relative to total genes in the background set. The adjusted p-value for each enriched GO term is shown at the top of each box.

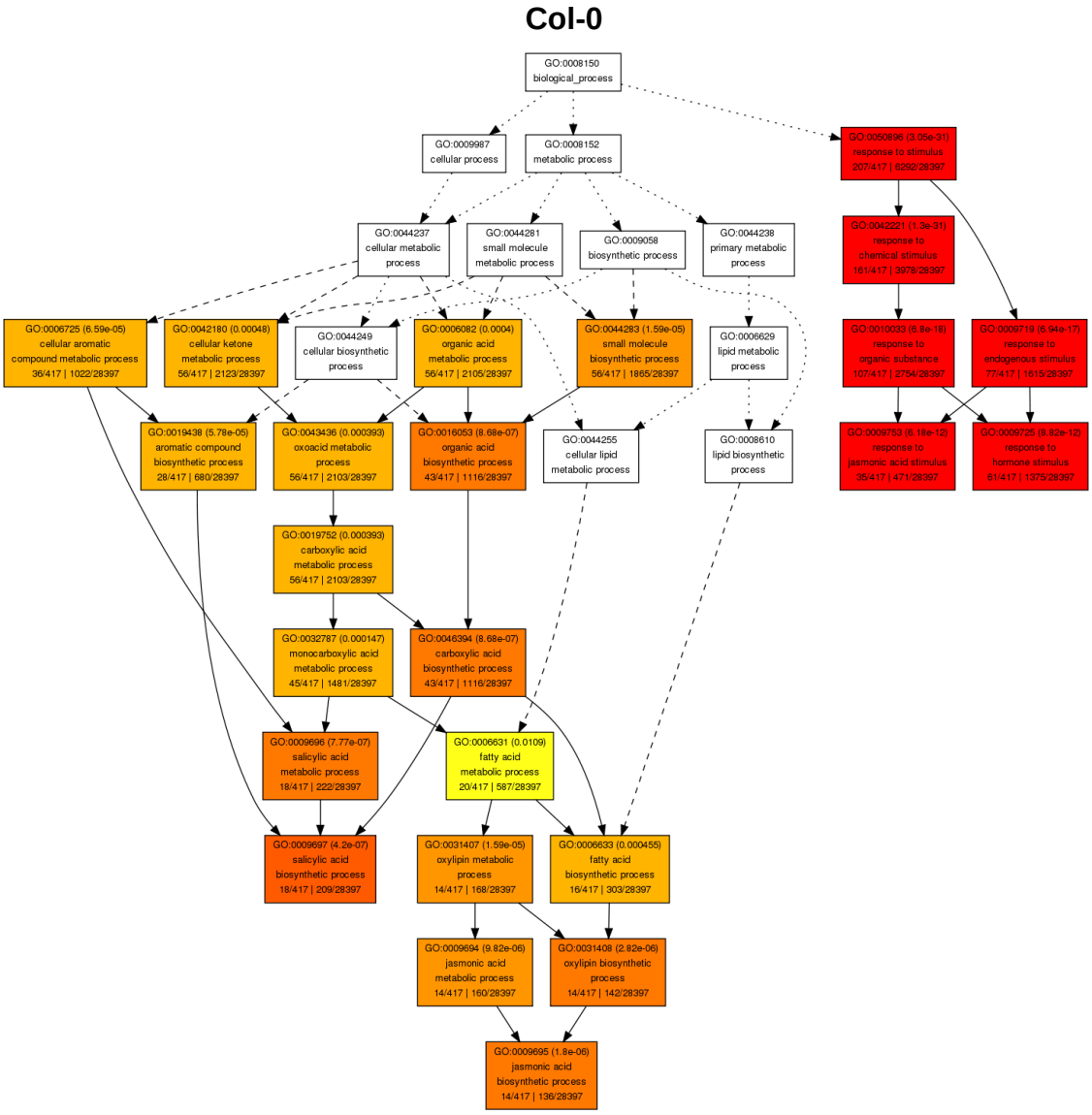

Figure 2.9. Biological process classification of differentially expressed genes (DEGs) in WT Col-0 roots in response to RKN using singular enrichment analysis (SEA) from agriGO. DEGs (false discovery rate<0.01 and Fold change = 1.0) were analyzed for hormone-related biological process enrichment and significance level is presented in a color scale, in which white shows no significant enrichment and red indicates strong enrichment. Ratios at the bottom of the boxes inform number of genes in the input list that match the specific gene ontology (GO) term informed in the box relative to total number of genes in the input list and total genes in the background genome that match that GO term relative to total genes in the background set. The adjusted p-value for each enriched GO term is shown at the top of each box.

bak1-5

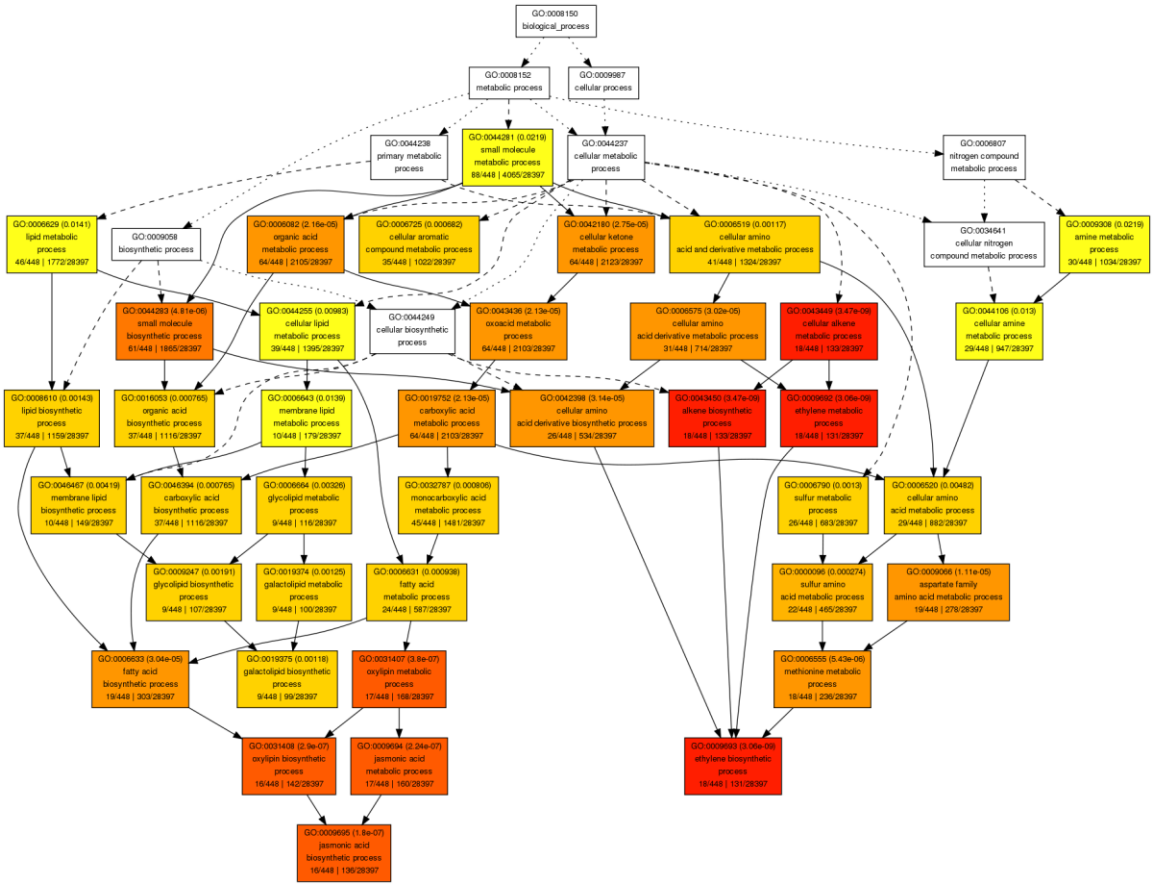

Figure 2.10. Biological process classification of differentially expressed genes (DEGs) in mutant *bak1-5* roots in response to RKN using singular enrichment analysis (SEA) from agriGO. DEGs (false discovery rate<0.01 and Fold change = 1.0) were analyzed for hormone-related biological process enrichment and significance level is presented in a color scale, in which white shows no significant enrichment and red indicates strong enrichment. Ratios at the bottom of the boxes inform number of genes in the input list that match the specific gene ontology (GO) term informed in the box relative to total number of genes in the input list and total genes in the background genome that match that GO term relative to total genes in the background set. The adjusted p-value for each enriched GO term is shown at the top of each box.

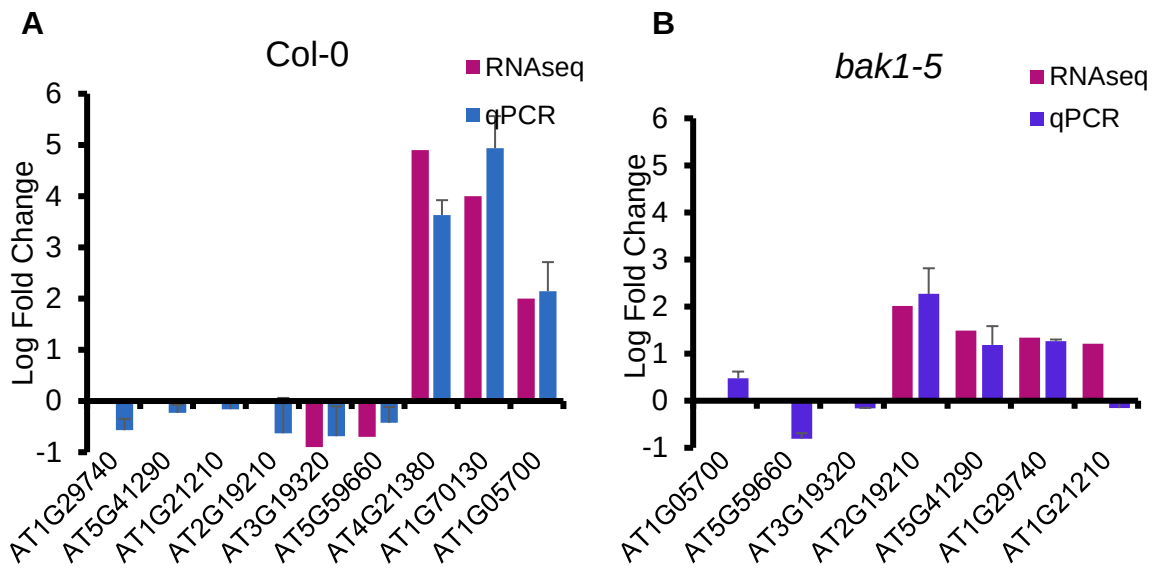

Figure 2.11. Quantitative reverse transcription PCR analysis of gene transcript abundance in 8-day-old seedling roots of Col-0 (A) or *bak1-5* mutant (B) 24 h after inoculation with RKN. The 18S gene was used as an internal control. Bars show the means SE± (n=3).

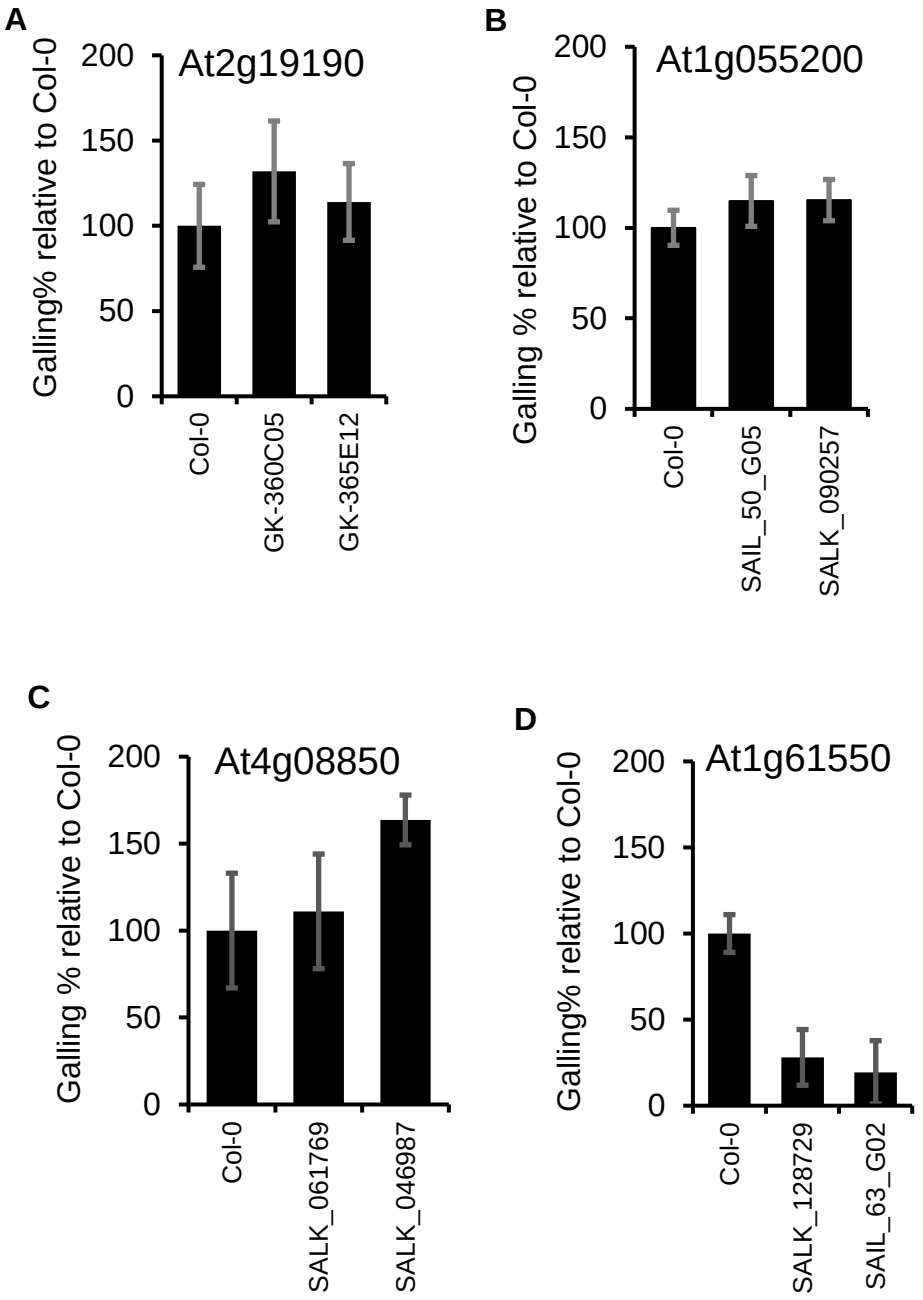

Figure 2.12. Root galling assay with Arabidopsis mutants. Percentage of root galls on the mutants relative to wild-type Col-0 at 4 weeks after RKN inoculation (±SE, n=30). Each experiment was performed three (A), (B), (D) or two (C) times with similar results.

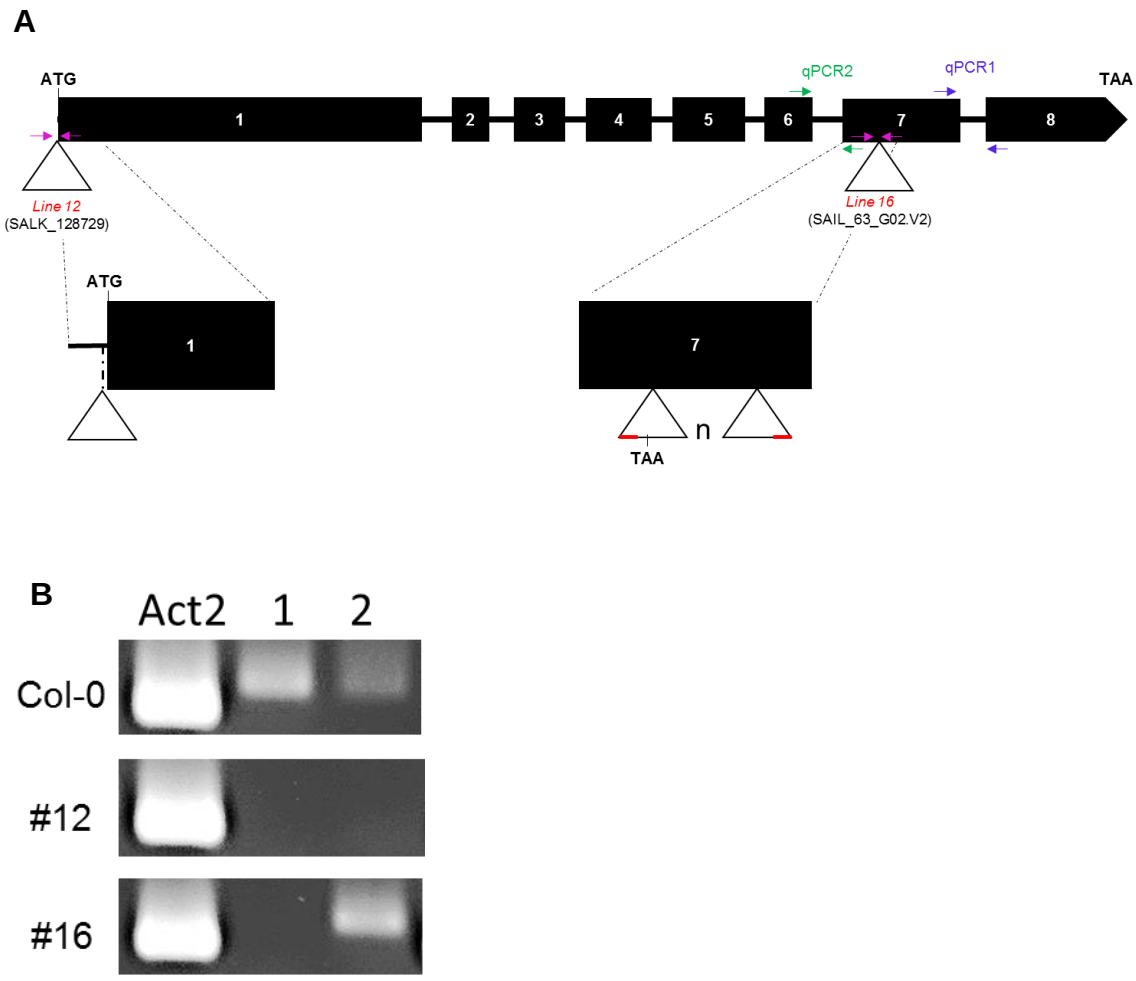

Figure 2.13. G-LecRK-VI.13 gene structure, locations of the T-DNA insertions and expression in mutant lines. (A) Line 12 (SALK_128729) has an insertion located in the promoter region of the gene and Line 16 (SAIL_63_G02) has an insertion in the seventh exon of the gene. Primer sets binding sites used for qPCR are indicated in green and blue arrows. Genotyping primers are indicated in purple arrows. Bottom shows insertions in detail, indicating SALK_128729 (#12) insertion in the promoter region and at least 2 insertions on SAIL_63_G02 line (#16), with indication of T-DNA left border (LB3) binding site as a red line. (B) Detection of transcript in Col-0 and mutant lines SALK_128729 (#12) and SAIL_63_G02(#16). At18S was used as amplification control. Numbers on the gel indicate primer sets qPCR1 (1) and qPCR2 (2), as indicated in diagram (A).

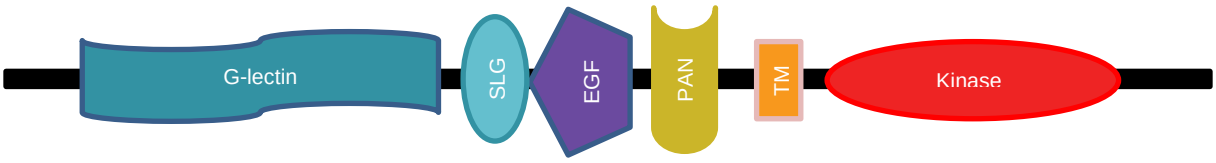

Figure 2.14. G-LecRK-VI.13 domains and organization. G-lectin, SLG, S-Locus glycoprotein; EGF, epidermal growth factor-like; PAN, plasminogen-apple-nematode; TM, transmembrane.

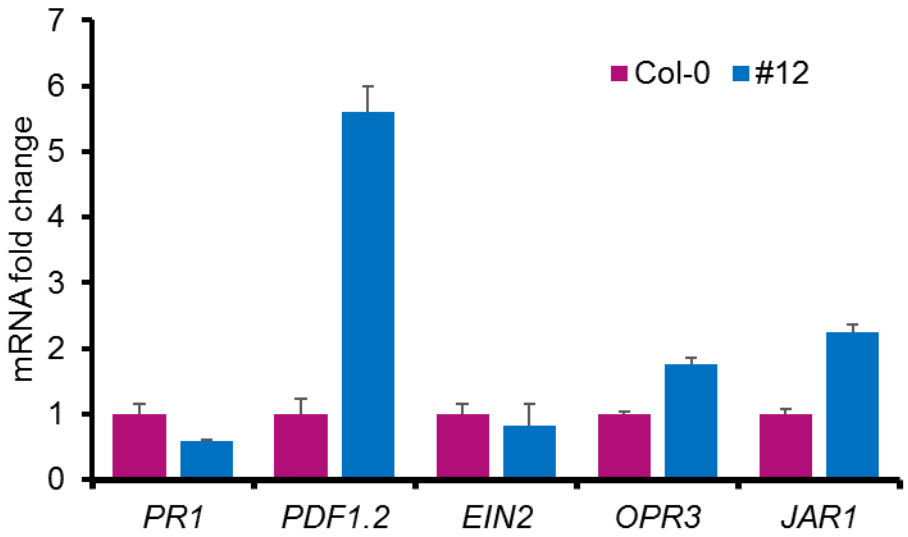

Figure 2.15. Quantitative reverse transcription PCR analysis of gene transcript abundance in 14 days old naïve seedling roots of Col-0 or G-LecRK-VI,13 mutant (SALK_ 128729, line 12). The 18S gene was used as an internal control. Bars show the means SE± (n=3).

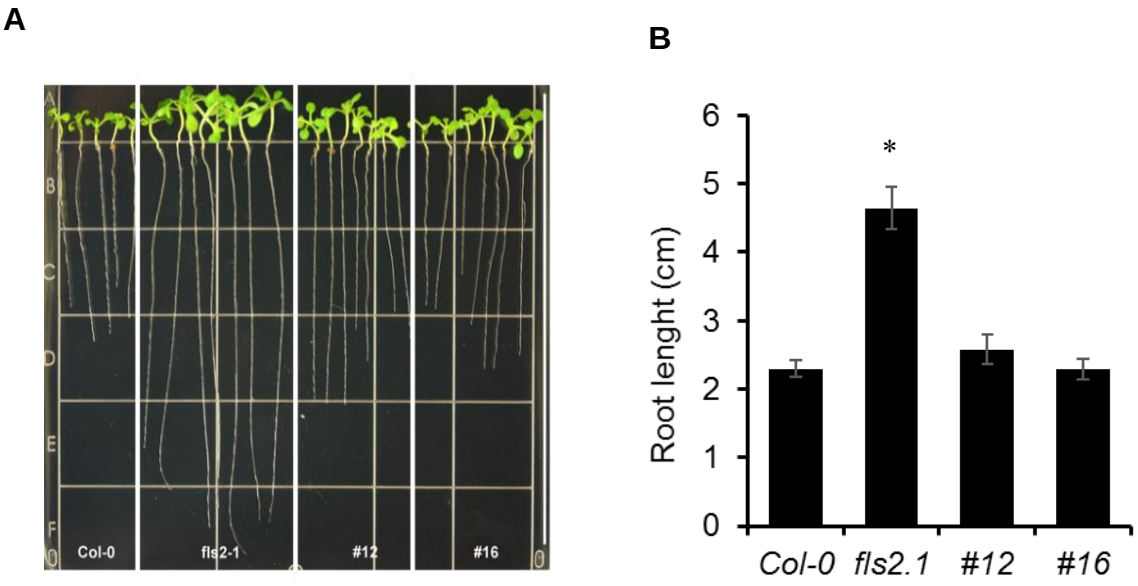

Figure 2.16. Arabidopsis G-LecRK-VI.13 mutant lines SALK_128729 (line 12) and SAIL_63_G02 (line 16) have WT flagellin-induced seedling root length inhibition. Seedlings were grown on one-half strength MS supplemented with 1µM flg22. Root length was measured 12 days after plating. ANOVA $p<0.05$, Tukey HSD Test, *$p<0.05$.

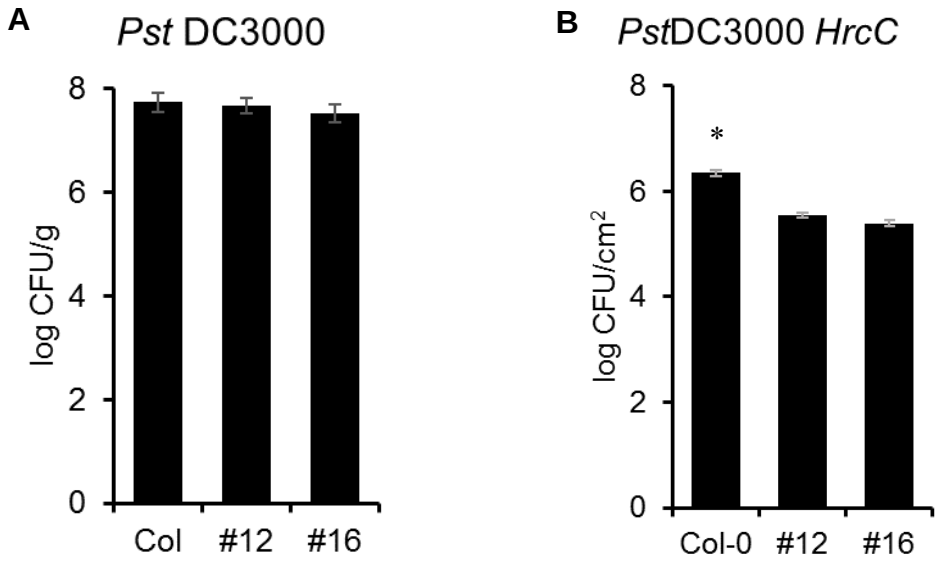

Figure 2.17. Arabidopsis G-LecRK-VI.13 mutant lines SALK_128729 (line 12) and SAIL_63_G02 (line 16) display increased resistance to *Pst* DC3000 *hrcC*. (A) Seedlings were grown on one-half strength MS medium with Gamborg Vitamins and 0.3% Daishin agar and flood inoculated with a *Pst* DC3000 suspension of 5 x 10^6 CFU/ml. (B) Seedlings were grown on soil and syringe infiltrated with *Pst* DC3000 *hrcC* in a suspension of 5 x 10^4 CFU/ml. ANOVA $p<0.001$, Tukey HSD Test, *$p<0.01$. Experiments were repeated twice.

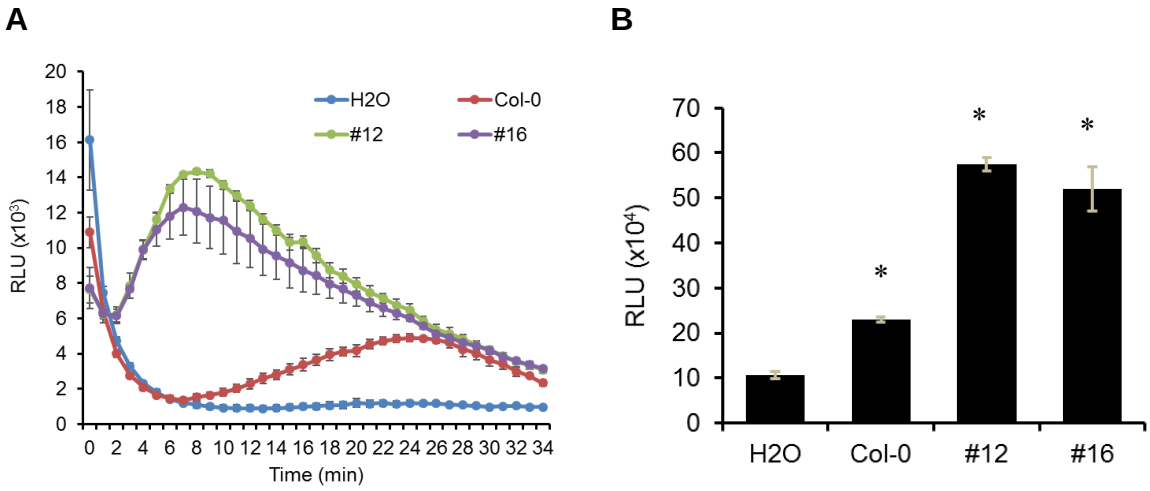

Figure 2.18. G-LecRK-VI.13 mutants SALK_128729 (line 12) and SAIL_63_G02 (line 16) show enhanced flg22-triggered ROS production. 3-week old plants were treated with 100µM flg22 and a luminol-based assay was used to quantify extracellular ROS. Charts show (A) relative light units (RLUs) detected after flg22 treatment and total RLU (B) detected over a 30 min period after flg22 treatment. ANOVA $p<0.0001$, Tukey HSD Test, *$p<0.05$ and **$p<0.01$.

Figure 2.19. G-LecRK-VI.13 mutant plants do not display compromised development. 2-week-old plants grown on MS media, with plates vertically positioned.

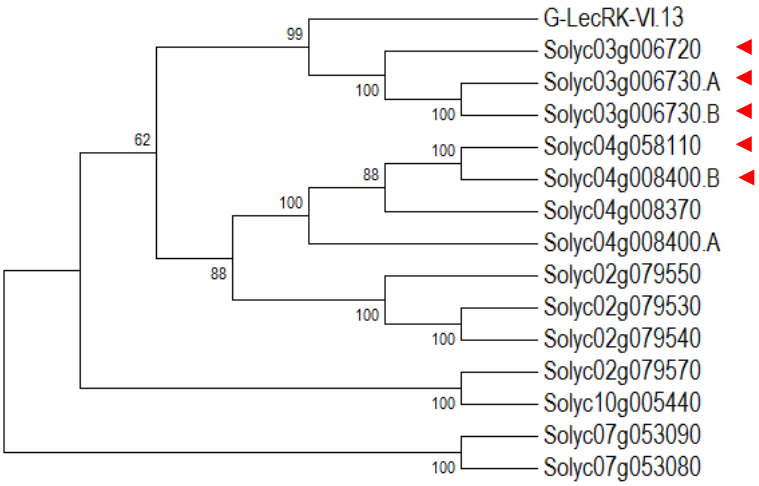

Figure 2.20. Phylogenetic analysis of similarity between G-LecRK-VI.13 and tomato closest homologs. The evolutionary history was inferred using the Neighbor-Joining method (Saitou & Nei, 1987). The evolutionary distances were computed using the Poisson correction method (Zuckerkandl & Pauling, 1965) and are in the units of the number of amino acid substitutions per site. Evolutionary analyses were conducted in MEGA7 (Kumar et al., 2015). Red arrows point to tomato candidate homologs for At1g61550.

Table 2.1. List of receptor-like kinases upregulated in WT Col-0 roots 24h after inoculation with RKN.

Accession number	Description	Fold changes	
		Col-0	*bak1-5*
AT4G21380	Receptor kinase 3/ARK3	4.9	Nd
AT1G70130	L-type lectin receptor kinase V.2/LECRK-V.2	4.0	Nd
AT1G05700	LRR Transmembrane kinase	2.0	Nd
AT1G51830	Transmembrane kinase	1.8	-2.3
AT1G51840	Transmembrane kinase	1.6	-2.24
AT5G46330	Flagellin sensitive 2/FLS2	1.5	Nd
AT3G59750	L-type lectin receptor kinase V.8/LECRK-V.8	1.5	Nd
AT1G55200	Transmembrane kinase	1.4	1.92
AT2G19190	flg22-induced receptor-like kinase 1/FRK1	1.2	Nd
AT1G61550	Transmembrane kinase	1.2	Nd
AT4G18250	Transmembrane kinase	1.1	1.77
AT5G25930	Transmembrane kinase	1.0	Nd
AT1G67000	Transmembrane kinase	1.0	2.17
AT4G08850	Transmembrane kinase	1.0	Nd

Table 2.2. Primers used in quantitative real-time PCR.

Primers	F	R	Reference
18S	GGTGGTAACGGGTGACGGAGAAT	CGCCGACCGAAGGGACAAGCCGA	Ali et al., 2014
PR1	TTATACTCAAGTAGTCTGGCGCA	TTGCAAGAAATGAACCACCA	Kettles and Kaloshian, 2016
PDF1.2	CCATCATCACCCTTATCTTCGC	TTGCAAGAAATGAACCACCA	Kettles and Kaloshian, 2016
EIN2	CCTTGTCACTAATGGAGCAGG	CACGATGAAGCCAAGCG	Kammerhofer et al., 2015
OPR3	TCCTCATCACTCCCTTGCCT	GCTCGCTTACCTTCACGTTACAC	Ozalvo et al., 2014
JAR1	GCTACATTTGCTGTGATTCCG	GGTATCGATACAACCCTGCG	Kammerhofer et al., 2015
At1g61550-qPCR1	CACAGCATCAAACCACTCAAC	GTGGGATGCGTCTGTGTATTA	This chapter
At1g61550-qPCR2	CGTCTTCCATCCTGTTGCCA	AATGGTCTTCTTGCGCTGGT	This chapter
At1g29740	CTCGGCATAGCAGCCTTAAT	CCTCAAACTGAAGGAACCTCTT	This chapter
At5g41290	CTCCACTCTTAGCAACCAATCA	GTTGACGTCTCCTGTGCATAA	This chapter
At2g19210	GAGATGTGAAGCCGGCTAAT	CAGCGGTTGTATCCTGGTTAT	This chapter
At3g19320	GTCACCATCTTTCACGCAAAC	GGAACTCTCCAGAGAGCTTATTG	This chapter
At5g59660	ACCAACCATGTCTCAGGTAATC	CCACCGAAGTATCCAAGCTAAT	This chapter
At4g21380	GCAGAGGACAGACCAACTATG	AGACTTCTCTCCAGGCAATAAC	This chapter
At1g70130	GTTGGGACAGTGGAGACATA	GAGCAAAGCAATCCCAGTTTC	This chapter
At1g05700	GGAGAATCAGAAACCGGAGAAA	AATAACTTCGGTCAAGTCCTCG	This chapter

Table 2.3. Primers used for genotyping of Arabidopsis mutants.

		Genotyping primers	
Accession #	Mutation lines	F sequence	R sequence
AT4g21380	SALK_001986	TCAAAGACATCAGTTCAGGGG	TTCACTGTCCATGATTCATCG
	SAIL_860_D12	ACGAATGTACCGGAGTGGTC	CACCATTCTCACATTCTACCCC
AT1g70130	SALK_020262	CCCAAAGGAAGCCTTGATAAG	GGAGTTATGAGCTATGCGTGC
	SALK_136952	GACTTGCGAAGCTATGTGACC	GCACAGCTCAACAAATTAGGG
AT1g05700	SALK_048526	ATACATGCCGAGTCGTGATTC	CTTCTTTGGAAACAATGCTCG
	SALK_025603	ATATATGACCCGTTAACCCGC	CTTAGGTTTCTCGGGAACGAC
AT1g51830	SALK_093514	ACAATTCCAAACCCTCCTTTC	AATCAGTTGGCAAGGAGATCC
	GK-075E01	CCTACCAAATTCTTGTGATGAACT	ATGCATGGGCCATTACAT
AT3G59750	SALK_202952	TGATCTTGAAACGTTGTTCCC	AGCATACACAGTCCGGTTCAC
AT1g55200	SAIL_50_G05	CATCGCCACAATGTTACATTG	GCAAGCAGAGACATTTGAACC
	SALK_090257	TACTCGTTCGGGGTTGTATTG	TGATGCTTTTGTTGACTCACG
AT2g19190	GK-360C05	TATGCACCTTCTCTGTTTTTGAGC	GGAGAACAAGTTGCTGTCAAGGTA
	GK-365E12	TATGCACCTTCTCTGTTTTTGAGC	GGAGAACAAGTTGCTGTCAAGGTA
AT1g61550	SALK_128729	AAACACAGTGGTTTCTGGGTG	TGCACTAGACCCGTTAGATGC
	SAIL_63_G02	GAGATTTGGGGGAAAGTTGAG	CGCAGGATTGTAGGAACTCTG
AT4g18250	SALK_152321	GCTATGCTCCATCGACTCAAC	TCTCCATCTTTTGTGGACAGC
	SALK_001241	ATCGATGACGGACAAATCAAC	GAGATGTGGTTGCAATGAAGG
AT5g25930	SALK_091274	CTATCGGAATCTTAGCCGGAG	TGGTGCTTAACGGAGACTCTG
	GK-751D04	GATTCTGAATTCAACGCGAAGAT	TTCTTCGTCGCCTCAAGTCC
AT1g67000	GK-350G09	AATGTATCCTATTGTACCC	GGAGAACAAGTTGCTGTCAAGGTA
	GK-118A10	AATGTATCCTATTGTACCC	GGAGAACAAGTTGCTGTCAAGGTA
AT4g08850	SALK_061769	TCCCCAATCTCACTTTTGTTG	TTTGACTTTGTTCCCAGTTGG
	SALK_046987	CAAAGGGAATAGTTTCTCCGG	TTGGATCGAATTCTCCTGTTG

Table 2.4. Percent identity matrix among G-LecRK-VI.13 putative tomato homologs and G-LecRK-VI.13.

	G-LECRK-VI.13	SOLYC03G006720	SOLYC03G006730.A	SOLYC03G006730.B	SOLYC04G008400.A	SOLYC04G058110
G-LECRK-VI.13	100					
SOLYC03G006720	46.41	100				
SOLYC03G006730.A	47.93	78.19	100			
SOLYC03G006730.B	48.17	77.52	82.95	100		
SOLYC04G008400.A	44.14	46.34	43.82	42.95	100	
SOLYC04G058110	42.95	45.09	43	42.84	82.28	100

CHAPTER THREE

Classification and phylogenetic analyses of Arabidopsis and tomato G-type lectin receptor kinases

Abstract

Pathogen perception by plants is mediated by plasma membrane-localized immune receptors that have varied extracellular domains. Lectin receptor kinases (LecRKs) are among these receptors and are subdivided into 3 classes, C-type LecRKs (C-LecRKs), L-type LecRKs (L-LecRKs) and G-type LecRKs (G-LecRKs). While C-LecRKs are represented by one or two members in all plant species investigated and have unknown functions, L-LecRKs have been characterized in a few plant species and have been shown to play roles in plant defense against pathogens. While Arabidopsis G-LecRKs have been characterized, this family have not been studied in tomato. This chapter updates the current characterization of Arabidopsis G-LecRKs and characterizes the tomato G-LecRKs. Additionally, using parameters established for Arabidopsis L-LecRKs, G-LecRKs nomenclature is suggested for both Arabidopsis and tomato. Moreover, using phylogenetic analysis we show the relationship among the members of G-LecRKs in both plant species. Furthermore, investigating presence of motifs in G-LecRKs identified conserved motifs among members of G-LecRKs across these plant species.

Introduction

In the constant war against pathogens, plants are equipped with a surveillance system that relies on pattern-recognition receptors (PRRs), proteins localized at the plasma membrane with ectodomains that screen the environment for conserved microbial and damage-associated signals. In addition to the ectodomain, a subgroup of these PRRs has intracellular kinase domains and are, therefore, known as receptor kinases (RKs). Plant RKs have undergone a recent expansion, with the *Arabidopsis thaliana* (Arabidopsis) genome encoding more than 600 RKs (Lehti-Shiu & Shiu, 2012). According to their ectodomains, they can be further classified into specific subgroups, such as leucine-rich repeat RK (LRR-RK) and lectin RK (LecRKs). Receptor kinases are involved in several cellular processes, from adaptation to abiotic stresses to defense responses against pathogens and pests and interactions with microbial symbionts (Bouwmeester *et al.*, 2011; Gilardoni *et al.*, 2011; Arnaud *et al.*, 2012; Desclos-Theveniau *et al.*, 2012; Singh *et al.*, 2012; Armijo *et al.*, 2013; Cheng *et al.*, 2013; Singh *et al.*, 2013; Singh & Zimmerli, 2013; Lannoo & Van Damme, 2014; Zipfel, 2014; Bigeard *et al.*, 2015; Macedo *et al.*, 2015). Several RKs and elicitor pairs have been described to date and illustrate the recognition of bacteria and fungi by plants (Zipfel, 2014) (Figure 3.1).

The best-characterized PRR-elicitor pair is the Arabidopsis LRR-RK FLS2 (FLAGELLIN SENSITIVE2) and the peptide flg22, consisting of a stretch of 22

amino acids of the N-terminal bacterial flagellin (Felix *et al.*, 1999). In addition to Arabidopsis, FLS2 orthologs have been identified in several plant species including tomato (*Solanum lycopersicum*), grapevine (*Vitis vinifera*), rice (*Oryza sativa*) and citrus (*Citrus paradisi*, *C. reticulata* and *Fortunella margarita*) (Robatzek *et al.*, 2007; Takai *et al.*, 2008; Trda *et al.*, 2014; Shi *et al.*, 2016). Interestingly in tomato, a distinct peptide from that of flg22, flgII-28, is perceived by the LRR-RK FLS3, and similar to FLS2, its perception and downstream signaling requires a second LRR-RK, BAK1 (BRASSINOSTEROID INSENSITIVE 1-ASSOCIATED KINASE 1) (Chinchilla *et al.*, 2007; Heese *et al.*, 2007; Hind *et al.*, 2016). Other receptor-ligand pairs include chitin perception by LYSM-RKs and xylanase perception by the LRR-RK EIX2 (Figure 3.1) (Ron & Avni, 2004; Cao *et al.*, 2014a). Although a co-receptor has not been characterized for xylanase perception, chitin perception requires participation of the LYSM-RK CERK1 (CHITIN ELICITOR RECEPTOR KINASE 1) (Shinya *et al.*, 2012). Interestingly, chitin perception in rice is mediated by the LYSM-RK CEBiP (CHITIN ELICITOR BINDING PROTEIN), which lacks a kinase domain and relies on its co receptor CERK1 for kinase signaling of chitin perception (Shimizu *et al.*, 2010) (Figure 3.1).

The LecRKs are a second type of receptors known for their role in carbohydrate binding (Singh & Zimmerli, 2013). Based on their ectodomains, LecRKs can be classified into C-type, L-type or G-type (Figure 3.2). C-type (Calcium-dependent) LecRKs (C-lecRK) contain the C-type motif that is commonly found in several proteins from mammals and have been shown to have a role in

innate immunity (Vaid *et al.*, 2012; Vaid *et al.*, 2013; Lannoo & Van Damme, 2014). Interestingly, in plants, this LecRK is represented by one gene in Arabidopsis, rice and tomato and two genes in wheat (Vaid *et al.*, 2012; Wang *et al.*, 2015b; Shumayla *et al.*, 2016).

The L-type (legume-like) LecRKs (L-LecRKs) consist of members of a large family and have well-characterized roles in plant defense. Investigations in Arabidopsis, rice, tomato, *Nicotiana benthamiana* and wheat revealed 45, 72, 22, 37, 84 members of this family, respectively (Vaid *et al.*, 2012; Wang *et al.*, 2015b; Shumayla *et al.*, 2016). Several reports link genes of this family to defense against pathogens; for example, AtLecRK-I.9 against the bacterial pathogen *Pseudomonas syringae* (Balagué *et al.*, 2016), AtLecRK-IX.I and LecRK-IX.2 against the pathogenic oomycetes *Phytophthora brassicae* and *P. capsici* (Wang *et al.*, 2015a), AtLecRK-I.9 against *P. infestans* (Bouwmeester & Govers, 2009), and AtLecRK-VI.2 against the pathogenic bacteria *P. syringae* and *Pectobacterium carotovorum* (Singh *et al.*, 2013; Huang *et al.*, 2014). Additionally, L-type LecRKs have been implicated in perception of the danger molecule extracellular ATP, by the AtLecRK-I.9 (Cao *et al.*, 2014b; Choi *et al.*, 2014).

The G-type LecRKs (G-LecRKs), previously known as B-type LecRKs, are proteins with an ectodomain that resembles the *Galanthus nivalis* agglutinin (GNA) (Van Damme *et al.*, 2007; Lannoo & Van Damme, 2014). Previous investigations identified 32 members of this family in Arabidopsis, 100 in rice and 177 in wheat (Vaid *et al.*, 2012; Shumayla *et al.*, 2016). The best-known members of this group

are the S-locus receptor kinases, known for their role in self-incompatibility in flowering plants (Kusaba *et al.*, 2001; Sherman-Broyles *et al.*, 2007). Besides the G-type lectin and the kinase domains, G-LecRKs can have additional domains such as a cysteine-rich domain, known as the epidermal growth factor (EGF) domain, which is thought to play a role in disulfide bonds formation (Shiu, SH & Bleecker, AB, 2001). Additionally, family members may contain the plasminogen-apple-nematode (PAN) motif, which likely has a role in protein-protein or protein-carbohydrate interactions (Tordai *et al.*, 1999).

Typically, members of large families do not have consistent nomenclature as frequently not all members are identified at the same time. While the Arabidopsis L-LecRK family members have a clear systematic nomenclature based on chromosome location and amino acid and nucleotides identity (Bouwmeester & Govers, 2009), members of the G-LecRKs do not have such nomenclature. Similarly, although L-LecRKs have been characterized in different plant species (Vaid *et al.*, 2012; Wang *et al.*, 2015b; Shumayla *et al.*, 2016), tomato G-LecRKs have not been described to date.

In the present chapter, we searched the genomes of Arabidopsis and tomato to identify and characterize G-LecRKs. The analysis allowed identification of incorrect gene annotations in genome databases and to infer on gene expansion and sequence similarity between G-LecRKs in each plant species. As a result of this investigation, we were able to suggest a nomenclature for members of this

gene family from both Arabidopsis and tomato similar to the one used for Arabidopsis L-LecRKs (Bouwmeester & Govers, 2009).

Material and methods

Database searches, protein domain organization and genome organization

To identify Arabidopsis G-LecRKs a first search was performed using the G-lectin domain of At1g61550 as the query followed by the G-lectin domain of At1g61400, At2g19130, At4g21390 and At5g60900 for a second search in The Arabidopsis Information Resource (TAIR) (http://arabidopsis.org) website.

To identify tomato G-LecRKs, the At1g61550 G-lectin domain was used as the query at the Sol Genomics Network (SGN) (https://solgenomics.net) and at the National Center for Biotechnology Information (NCBI) (https://www.ncbi.nlm.nih.gov/) websites. Results with e-value < 0 were considered G-LecRKs candidates. After the tomato G-LecRKs initial search using At1g61550 lectin domain, a second search was performed at NCBI website and both searches were cross-analyzed to compile a list of all possible G-type LecRKs candidates.

Candidate sequences were manually annotated regarding the presence of conserved domains using InterPro (http://ebi.ac.uk/interpro) (Mitchell *et al.*, 2014), which combines analysis from a number of distinct databases (CATH-3D, CDD, HAMAP, PANTHER, Pfam, PIRSF, PRINTS, ProDom, PROSITE, SFLD, SMART, SUPERFAMILY, TIGRFAM, TMHMM) and is, therefore, a more inclusive search engine. Genes encoding both a G-type lectin and a kinase domain were considered G-LecRKs.

The localization of G-LecRKs on the Arabidopsis genome was visualized using the chromosomal map tool from TAIR (http://arabidopsis.org/jsp/ChromosomeMap/tool.jsp). The localization of G-LecRKs on the tomato genome was visualized using NCBI Map Viewer (https://www.ncbi.nlm.nih.gov/projects/mapview/).

Arabidopsis predicted kinase domain sequences were aligned using ClustaW and the alignment was manually checked to identify the kinase subdomains using *At*LecRK-VI.2 as a reference (Singh *et al.*, 2013; Wang *et al.*, 2015b). Similarly, tomato predicted kinase domain sequences were aligned with the kinase domain of Solyc03g006720 and the kinase subdomains were manually checked.

Similarity among amino acid and DNA sequences was evaluated using Clustal Omega (http://www.ebi.ac.uk/Tools/msa/clustalo/) and genes with over 50% similarity at nucleotide or amino acid levels were grouped together in the same Clades.

Phylogenetic analysis

Complete Arabidopsis and tomato nucleotide and amino acid sequences were retrieved from TAIR and The Sol Genomics Network (SGN) as described. Full-length sequences were aligned using the default settings of ClustaW and phylogenetic tree construction was performed using MEGA 7 (Kumar *et al.*, 2016). The neighbor joining method (Saitou & Nei, 1987), with bootstrap analysis using

1000 replicates was employed to generate the phylogenetic trees. The sequences of the proteins WAK1 (At1g21250), PERK1 (At3g24550), C-LecRK (At1g52310), LecRK-V.8 (At3g56750) and LecRK-I.5 (At3g45430) were used to root the Arabidopsis phylogenetic trees (Vaid *et al.*, 2012). The protein sequences of the L-LecRK Solyc07g065610 and C-LecRK Solyc02g068370 were used to root the tomato phylogenetic trees.

Motif identification

Investigation of conserved motifs in the ectodomains of Arabidopsis and tomato G-LecRKs was performed using the default settings at MEME Suite 4.11.2 (Multiple EM for Motif Elicitation) (http://meme-suite.org/tools/meme) (Bailey *et al.*, 2009).

Protein localization prediction

Multiple protein subcellular localization tools were used to localize the Arabidopsis and tomato G-LecRKs. Arabidopsis gene identifiers were used to query "The SUBcellular localization database for Arabidopsis proteins", SUBA3 (http://suba3.plantenergy.uwa.edu.au/) (Tanz *et al.*, 2013; Hooper *et al.*, 2014). Additionally, amino acid sequences of both Arabidopsis and tomato G-LecRKs were analyzed using TargetP 1.1 Server (http://www.cbs.dtu.dk/services/TargetP/) (Emanuelsson *et al.*, 2007) and "subCELlular LOcalization predictor" CELLO v.2.5 (http://cello.life.nctu.edu.tw/) (Yu *et al.*, 2006).

Results

Characterization of the Arabidopsis G-LecRKs and suggestion of a nomenclature

To characterize Arabidopsis G-LecRKs, a BLASTp analysis (Altschul *et al.*, 1997) was performed at the TAIR website using the region comprising the predicted G-type lectin domain (Marchler-Bauer *et al.*, 2015), amino acids 24-170 from At1g61550. The search resulted in 34 genes with scores ranging from 194 to 40 and E values ranging from 2e-50 to 8e-04. Hits with E-values higher than 0 were not considered for this analysis. From the obtained sequences, four (At1g61400, At2g19130, At4g21390 and At5g60900) were chosen for use as new queries to fish additional candidates. These analyses resulted in a total of 46 genes encoding proteins with lectin domains. Of these 46 sequences, 37 encoded proteins with kinase domains. The remaining nine sequences encoded proteins without kinase domains and therefore were not considered for further analyses (Table 3.1).

Unlike Arabidopsis L-LecRKs, for which most members are localized on chromosomes 5 and 3 (Vaid *et al.*, 2012; Wang *et al.*, 2015b), the vast majority of the Arabidopsis G-LecRKs are localized on chromosome 1 (29 members), followed by chromosome 4 (eight members), chromosome 5 (four members), chromosome 2 (three members) and chromosome 3 (two members) (Figure 3.3).

Previous characterization of Arabidopsis G-LecRKs includes 31 genes, all also identified in our search. A gene, At1g61460, was not detected in our search.

To confirm the identity of this gene, its protein was used in domain search using Interpro. Domain predictions showed that At1g61460 encodes a SLG, PAN, TM and kinase domains, but not a lectin domain. Because of the absence of the lectin domain, this gene was not considered as G-LecRKs and was not used in further analyses.

The presence of sites essential for catalytic activity (Hanks & Hunter, 1995) of the G-LecRKs was investigated by aligning the amino acid sequences of the kinase domains (KDs) to the LecRK-VI.2 KD (Singh *et al.*, 2013). The alignment revealed overall conservation of the ATP binding and the catalytic sites, with a few substitutions in the other kinase subdomains (Figure 3.4). One of the G-LecRK genes, At1g67520, revealed a truncated kinase domain, lacking 4 (VIII – XI) of the 11 kinase sub-domains. Additionally, At2g41890 lacked essential sites at the Subdomain I, where kinases have the consensus motif Gly-x-Gly-x-x-Gly-x-Val (G-x-G-x-x-G-x-V), and the subdomain XI (Figure 3.4). There was also one amino acid change on its catalytic loop at subdomain VI, where kinases have the motif His-Arg-Asp-Leu-Lys-x-x-Asn (H-R-D-L-K-x-x-N) (Hanks & Hunter, 1995). The essential arginine and aspartic acid residues were substituted for glycine and asparagine, respectively.

Alignment of the 37 Arabidopsis proteins was used to construct rooted phylogenetic trees with 1000 bootstrap replicates using Mega 7 (Kumar *et al.*, 2016). Phylogenetic analysis using the full-length protein sequences allowed to separate Arabidopsis G-LecRKs into 6 groups and two singletons (At4g11900 and

At4g03230) (Figure 3.5A). Besides analysis of the full-length proteins, phylogenetic analyses were performed using only the kinase domains or the lectin domains. Using the alignment of the kinase domains to construct phylogenetic trees resulted in separation of the G-LecRKs into 7 groups and one singleton (At4g11900). Although the tree topology using the kinase domains follows that of the full-length proteins, the group IV from the phylogenetic tree prepared with the full-length protein sequences was separated into two groups, IV and VII in the tree constructed using the kinase domain sequences (Figure 3.5B). Phylogenetic analysis based on the lectin domains (Figure 3.5C) separated the G-LecRKs into 9 groups and two singletons (At4g00340 and At4g03230). Two groups were the same as those originating from the analyses using either the full-length proteins or the kinase domains (Groups III and VI) showing the overall similarity of the proteins. The singleton groups formed using the kinase domains (Group I) was separated into 3 groups using the lectin domains, representing the diversity of this domain compared to the high conservation of the kinase domains.

Nomenclature for the Arabidopsis G-LecRKs

The L-LecRKs were previously classified and a nomenclature was established based on the amino acid and nucleotide sequences of the 45 members of the family (Bouwmeester & Govers, 2009). In that system, Clades were designated by Roman numerals and clusters by Arabic numerals followed by letters. The Clades are groups of genes with at least 50% nucleotides and amino acid identity between

homologs. Arabic numerals in a cluster refer to chromosome numbers, while letters refer to the physical proximity of genes on the chromosome with nine being the maximum number of genes in a cluster (Bouwmeester & Govers, 2009). Following a similar approach, we classified the 37 members of the Arabidopsis G-LecRK into five clusters and six Clades (Table 2). The largest Clade identified contains 13 members, followed by two smaller Clades with four members each and an additional three Clades with two members each (Figure 3.5; Table 3.2). Ten genes were not placed in any Clade, behaving as singletons. Interestingly, one of these singleton genes is located on Chromosome 1 where the vast majority of G-LecRKs are localized.

Prediction of Arabidopsis G-LecRKs localization

Arabidopsis G-LecRKs localization was predicted using "The SUBcellular localization database for Arabidopsis proteins", SUBA3 (http://suba3.plantenergy.uwa.edu.au/) (Tanz *et al.*, 2013; Hooper *et al.*, 2014). This tool predicted all Arabidopsis proteins to be localized at the plasma membrane, consistent with the existence of a transmembrane domain.

SUBA predictions were further investigated with TargetP 1.1 (http://www.cbs.dtu.dk/services/TargetP/) (Emanuelsson *et al.*, 2007). This tool predicts protein localization by analyzing cleavage sites predictions and, therefore, predicts localization to chloroplast, mitochondria or secretory pathways. As control, we used proteins (WAK1, LecRK-I.5 and LecRK-V.8) that have been shown to

localize at the plasma membrane and were used in our phylogenetic analysis. All these control proteins and most of the Arabidopsis G-LecRKs were predicted to have a signal peptide for secretion. Two genes, At1g61390 and At1g61400, encode proteins predicted to localize at the mitochondria membrane and one gene, At1g11280, encodes a protein for which localization was not predicted by Target P 1.1.

As an additional tool to validate localization predictions, the subCELlular LOcalization tool CELLO (Yu *et al.*, 2006) was also used. CELLO predictions mostly confirmed the predictions obtained by SUBA, but additionally revealed possible specific localization of a couple G-LecRKs (Table 3). These are At4g27290 and At5g60900 which encode proteins without a transmembrane domain, based on domain search performed using Interpro, although both proteins were predicted to localize at the plasma membrane by SUBA. Interestingly, CELLO prediction added the possibility that these proteins could also localize to the nucleus and cytoplasm (Table 3).

Characterization of tomato G-LecRKs

Using the same strategy used to retrieve the Arabidopsis G-LecRKs, tomato genome was queried for G-type lectin homologs using the lectin domain of At1g61550, hereafter referred to as G-LecRK-VI.13. Two databases, SGN (Sol Genomic Network) and NCBI, were searched. The search against SGN resulted in 21 hits with similarity to our query sequence. The search against NCBI resulted

in more numerous hits and the combined results from these two searches yielded 61 distinct sequences with a G-type lectin domain (Table 4). To assure a comprehensive search, three random tomato G-type lectins were chosen to query again the tomato genome using their predicted G-lectin domain, resulting in three additional candidates, Solyc07g053220, Solyc1g005290 and Solyc05g008310.

Three of the identified G-type lectin containing sequences were miss-annotated. For example, although SGN referred to Solyc03g006730 as a single gene our analysis demonstrated the existence of two G-LecRKs within this sequence. Therefore, this sequence was split into two genes that we refer to as Solyc03g006730.A and Solyc03g006730.B (with 86.2% amino acid identity). Similarly, Solyc04g008400 and Solyc07g055640 were also annotated as single proteins, but each encodes two G-LecRKs and were therefore separated into Solyc04g008400.A and Solyc04g008400.B (with 68.4% amino acid identity) and Solyc07g055640.A and Solyc07g055640.B (with 54.94% amino acid identity).

Thus, 80 tomato sequences were identified that encoded a G-type lectin domain. Similar to Arabidopsis, the great majority of the tomato proteins lack the EGF domain, with only seven tomato genes predicted to encode this domain (Table 4). Of the 80 tomato sequences, 72 encoded proteins with both G-type lectin and KDs and were considered as G-LecRKs for further analysis.

Unlike the L-LecRKs, for which there was a reduction in number of members in tomato (22 members) as compared to Arabidopsis (45 members) (Wang *et al.*,

2015b), the G-LecRK family underwent an expansion in tomato. While L-LecRKs are mostly localized on chromosomes 9 and 10 (with members located on 8 of the 12 tomato chromosomes) (Vaid *et al.*, 2012; Wang *et al.*, 2015b), G-LecRKs are distributed throughout the 12 tomato chromosomes, with over half (55%) localized on chromosomes 7, 2 and 3 (18, 11 and 11 members, respectively) (Figure 3.6).

Like Arabidopsis, the presence of sites essential for catalytic activities of the 11 kinase sub-domains (Hanks & Hunter, 1995) was investigated in the tomato G-LecRKs. The alignment of the tomato G-LecRKs KDs revealed overall conservation of the ATP-binding and catalytic sites, with a few substitutions in the other kinase subdomains (Figure 3.7). Nevertheless, the search revealed seven truncated kinases, those from genes Solyc04g008400.B, Solyc03g006780, Solyc04g008370, Solyc04g077300, Solyc07g055630, Solyc07g055640.A, Solyc07g063750 and Solyc05g079710 (Table 3.5, Figure 3.7). Additionally, Solyc07g063810 has conservation of subdomains VI to XI (which includes the motif HRDLKxxL), but displays several amino acid modifications in subdomains I to V (which include motif GxGxxGxV) suggesting it is likely an inactive kinase. Solyc03g063650 has a substitution of the aspartic acid to asparagine at the subdomain VI in the kinase activity site and lacks essential amino acids of subdomains I to IV suggesting it is also likely an inactive kinase (Figure 3.7).

Nomenclature for the tomato G-LecRKs

Following the same approach used to suggest a nomenclature for the Arabidopsis G-LecRKs, the 72 tomato G-LecRK members were evaluated regarding their identity at both amino acid and nucleotide levels and those members with 50% or higher identity were grouped in the same Clade. This methodology allowed the grouping of tomato G-LecRKs into 12 clusters, which are defined by proximity of the genes on the chromosome (Table 6). Additionally, these genes were grouped into 15 Clades, representing their amino acid sequence similarity (Table 6). The largest Clade contains 14 members, followed by two smaller Clades with four members, one Clade with three members and the remaining 11 with only 2 members. Surprisingly, despite the G-LecRK family expansion in tomato, 25 genes behaved as singletons and are not placed in any Clade. These singletons are spread on all but 3 chromosomes, 6, 10 and 12.

Similar to the phylogenetic analysis performed for Arabidopsis, tomato protein sequences were aligned and the obtained sequence alignments were subsequently used as input to construct neighbor-joining trees in MEGA7 (Figure 3.8). Phylogenetic analysis of the full-length protein sequences (Figure 3.8A) separates the G-LecRKs into 11 groups, with only two genes behaving as singletons (Solyc02g079710 and Solyc07g053080). Phylogenetic analysis of the KDs (Figure 3.8B) separates the G-LecRKs into 15 groups and 2 singletons (Solyc03g063650 and Solyc03g005130), while phylogenetic analysis of the lectin domains (Figure 3.8C) separates the G-LecRKs into 14 groups and 7 singletons.

Prediction of tomato G-LecRKs subcellular localization

Tomato G-LecRK sequences were used to predict protein localization with TargetP 1.1 (http://www.cbs.dtu.dk/services/TargetP/) (Emanuelsson *et al.*, 2007) (Table 7). The localization of tomato C-LecRKs and L-LecRKs has not been experimentally shown. However, L-LecRKs possess a transmembrane domain and are predicted to localize mostly at the plasma membrane with a few members predicted to localize to mitochondria or chloroplast (Vaid *et al.*, 2012). Nevertheless, we chose to investigate the localization predictions for the tomato C-LecRK Solyc02g068370 and L-LecRK Solyc07g065610 during our characterization of the tomato G-LecRK. Similar to the great majority of tomato G-LecRKs, targetP predicted that these two proteins also have secretion pathway signals (Table 7). Of the G-LecRKs, the protein encoded by Solyc02g079630 was predicted to have chloroplast localization. Four proteins (encoded by Solyc03g006730.B, Solyc07g055640.A, Solyc07g063810 and Solyc11g005630) were predicted to have mitochondrial localization. Six proteins (encoded by Solyc07g055640.B, Solyc08g076060, Solyc07g055650, Solyc07g055630, Solyc04g008400.B and Solyc02g030300) for which a signal peptide could not be predicted using this tool were not localized to a specific cell compartment (Table 3.7). Additionally, the subCELlular LOcalization tool, CELLO, was used to investigate the localization of the tomato G-LecRKs and showed an overlap of prediction of plasma membrane localization and presence of TargetP secretion pathway signal. Interestingly, this tool was able to predict subcellular localization

of proteins that TargetP could not predict localization for and was also able to predict membrane localization for proteins that did not have a predicted transmembrane domain, suggesting a different membrane activity for these proteins. Additionally, CELLO predictions also suggested multiple localizations for a few tomato G-LecRKs (such as Solyc01g006530 and Solyc07g055630) and contradicted a few predictions by TargetP (such as Solyc02g079630 and Solyc03g006730.B) (Table 7).

Comparison of Clade groupings between tomato and Arabidopsis G-LecRKs

To investigate the similarity between the Arabidopsis and tomato G-LecRKs, a phylogenetic analysis was performed using the full-length G-LecRKs protein sequences of both species (Figure 3.9). Consistently, members from the same Clade of each species grouped together, such as members of the Arabidopsis Clade II, At1g11340 and At1g11410 and members of tomato Clade VIII, Solyc02g079640 and Solyc03g006780. Interestingly, the construction of a phylogenetic tree with proteins from the two plant species allowed to infer proximity between Clades in both species, such as Arabidopsis Clade II and tomato Clades VI and VIII, which cluster together in this phylogenetic analysis (Figure 3.9). On the other hand, the current phylogenetic analysis allowed observation of higher identity between proteins of tomato Clade II and Arabidopsis Clade IV, At4g27290 and At4g27300, than the similarity among members of Arabidopsis Clade IV, which

partially, At4g21380, At1g65790, At1g65800, group with tomato Clades VI and VIII.

Comparison of conserved motifs in ectodomains of Arabidopsis and tomato

The predicted cytoplasmic localized regions of G-LecRKs consist of the extremely conserved KD. To investigate the presence of conserved motifs in the ectodomain of the Arabidopsis and tomato G-LecRKs, the amino acid sequences of the ectodomains were submitted to MEME Suite4.11.2 (Bailey *et al.*, 2009). Despite the high variability in the ectodomain, 6 motifs present in at least 29 of the 37 Arabidopsis sequences and in at least 45 of the 72 tomato sequences were identified.

The highest conserved ectodomain motif (Figure 3.10A) was present in all Arabidopsis and tomato G-LecRKs and it was previously shown to be present in 96% of the rice G-LecRKs (Vaid *et al.*, 2012). One of the motifs, a cysteine-rich region within the PAN domain (Figure 3.10B), is present in 34 and 66 of the Arabidopsis and tomato G-LecRKs, respectively. Interestingly, this motif is also conserved in 76 out of 100 rice G-LecRKs, and was previously identified in 27 Arabidopsis G-LecRKs (Vaid *et al.*, 2012). The conservation of the motifs in the ectodomain of both Arabidopsis and tomato G-LecRKs is remarkable considering that these extracellular domains harbor the lectin domain known to have low conservation among members of this family from a single plant species (Vaid *et al.*, 2012).

Discussion

Previous studies have reported Arabidopsis to have 32 (Shiu, S-H & Bleecker, AB, 2001; Vaid *et al.*, 2012) G-LecRKs members, different from the 37 members identified in the current analysis. One of the reasons for this discrepancy from Shiu and Bleecker (2001) might be the current improved annotation of the Arabidopsis genome. These authors also had the presence of a transmembrane domain as a criterion for their analysis, which was not used in the current analysis. As for the lower number identified by Vaid et al. (2012), it might be due to the fact that their analysis relied on sequence similarity to one gene sequence, At1g61610, while in our analysis, we used the candidates from our initial search to fish for additional candidates. Nevertheless, their overall criteria for candidates were the same as the ones used here, which are the presence of both a lectin and a kinase domain. Our search retrieved all genes identified by Vaid et al. (2012) and additional 15 sequences with a G-type lectin domain. Their gene list contained one gene different from the list presented here, At1g61460, which does not encode a G-type lectin domain and was never recovered in our Blastp searches. Of the 15 new sequences, nine do not encode a kinase domain and would not have been retrieved by Vaid et al. (2012) because their search strategy relied on the presence of a kinase domain. Therefore, our results added six genes to the previous list of Arabidopsis G-LecRKs. Of these six additional genes, At1g67520 encodes a protein with an atypical KD sequence, lacking subdomains VIII to XI, and

At2g41890 lacks essential amino acids at the ATP binding site (subdomain I) and the catalytic loop (Subdomain VI), suggesting a possible defect in the kinase activity (Bouwmeester & Govers, 2009).

Our data showed presence of G-LecRKs on all five chromosomes of Arabidopsis, different from the previous description where no members were identified on chromosome 5 (Vaid *et al.*, 2012). Interestingly, genes encoding proteins with EGF domains are present on chromosomes 1, 2 and 4, with a cluster of these genes that make up the clade VI (At1g61360, At1g61380, At1g61390, At1g61550) localized on chromosome 1. In addition, the two genes (At1g11340 and At1g11410), also encoding EGF domains, that comprise Clade I are likewise placed in the same cluster reflecting their similarity and physical proximity. Interestingly, although localized on different chromosomes, At1g61610 and At4g27290 both encode proteins with EGF domains and belong to the same Clade, V.

Consistent with a classification based on sequence identity, the groups observed in the phylogenetic analysis with the full-length protein sequences or specific domains (lectin or kinase) reflected those formed by the Clades suggested in Table 2, including overall grouping of the singletons in a specific Clade. Nevertheless, the phylogenetic tree constructed from alignment of the lectin domains separated members of one Clade into two, reflecting the higher variation present in this domain compared to the full-length sequences. This is not surprising

as this domain confers specificity to binding to different molecules and should, therefore, account for the highest variability within the protein sequence.

The same search methodology use for identifying Arabidopsis members of this family showed success with identification of the tomato members. These investigations of the tomato genome allowed the identification of 72 genes encoding proteins with both a kinase domain and a G-lectin domain and revealing expansion of genes of this family in tomato as compared to Arabidopsis. Similarly, analysis of amino acid and nucleotide identities allowed the separation of the tomato G-LecRKs into 15 clusters validated by the construction of phylogenetic trees with either the full-length protein sequences or the kinase and lectin domains.

In order to investigate the predicted localization of both Arabidopsis and tomato G-LecRKs, the amino acid sequences of these proteins were submitted to analysis with distinct prediction tools. SUBA is an Arabidopsis-specific tool that considers only the gene identifier rather than the amino acid sequence. However, one of the recently designated Arabidopsis identifiers, At1g11305, was not considered by this tool and therefore its localization was not predicted. At1g11305 was created when discovering miss-annotation of At1g11300 to contain two genes referred to as At1g11300 and At1g11305 (Trontin *et al.*, 2014). Nevertheless, the two additional tools used confirmed SUBA's prediction of plasma membrane localization of most of the Arabidopsis G-LecRKs. Interestingly, TargetP results suggested mitochondrial localization of two Arabidopsis G-LecRKs (At1g61390, At1g61400) grouped in the same cluster. Additionally, two genes (At4g27290 and

At5g60900) that were not predicted to encode transmembrane domains, but were predicted to localize at the plasma membrane by SUBA, were predicted to have multiple localizations at both the nucleus and the plasma membrane (At4g27290), or to the cytoplasm, nucleus and plasma membrane (At5g60900). It is possible that, since they do not possess a canonical transmembrane domain, these proteins might be involved specific activity within the G-LecRKs. Similarly, a couple of tomato G-LecRKs (Solyc07g063810 and Solyc07g063820) for which no transmembrane domains were predicted, were also predicted to localize at the plasma membrane by TargetP. Interestingly, three proteins that lack a transmembrane domain as predicted using Interpro (encoded by Solyc07g055630, Solyc07g055640.A and Solyc07g055640.B) were also predicted to localize in multiple subcellular compartments besides the plasma membrane, such as the mitochondria, cytoplasm and nucleus.

Similar to Arabidopsis, most of tomato G-LecRKs were also predicted to possess a secretion pathway signal by TargetP. Although most predictions by TargetP and CELLO show a correlation between secretion pathway and plasma membrane localization, there were a few contradictory predictions, such as two genes (Solyc01g006530 and Solyc01g014520) localized on chromosome 1 and one gene (Solyc04g008370) localized on chromosome 4 which are predicted by CELLO to have nuclear localization and by TargetP to have secretion signal. Interestingly, this tool predicted one protein (encoded by Solyc2g079630) to have chloroplast localization, while CELLO predict the same protein to have extracellular

and plasma membrane localization. Nevertheless, CELLO added localization prediction for proteins for which TargetP could not predict a localization.

Investigations of the relationship among members of the Arabidopsis and tomato G-LecRKs through the construction of a phylogenetic tree allowed the evaluation of the proximity between the Clades from both species. Surprisingly, this analysis also showed existence of higher similarity between Clades of tomato and Arabidopsis than similarity among few members of the same Arabidopsis Clade.

Although the analysis of the kinase domains showed overall conservation of subdomains and low variation among different members of G-LecRKs, the lectin domain presented a higher variability as observed by others previously (Vaid *et al.*, 2012; Wang *et al.*, 2015b). Interestingly, different members of G-LecRKs presented specific configurations of ectodomain, with the presence (or absence) of three domains, SLG, EGF and PAN. The importance of each of these domains as well as their contribution to G-LecRK activity have not been investigated so far. Nevertheless, it is to be expected that relevant regions at the ectodomain, outside of the region that confers binding specificity, would be conserved among different members of the same family. Consistent with this hypothesis, motif search among members of Arabidopsis and tomato revealed one motif (Figure 3.10A) to be present in all members of G-LecRKs from both plant species. This motif was also identified in a previous investigation in both Arabidopsis and rice (96% of rice G-LecRKs) (Vaid *et al.*, 2012). Interestingly, the second motif identified in our search

(Figure 3.10B), present in 34 Arabidopsis G-LecRKs and 66 tomato G-LecRKs was also identified by the same authors and is present in 76% of the rice G-LecRKs. The observation that lectin domain is the domain with low conservation in G-LecRKs and the presence of conserved motifs in the ectodomain shows that despite the lack of conservation of the lectin domain, specific motifs still hold conservation and might constitute essential sites for protein activity.

The present investigation added to the number of currently known Arabidopsis G-LecRKs and presented for the first time the characterization of tomato G-LecRKs. Using established parameters for Arabidopsis L-LecRKs, our investigation was able to suggest a nomenclature for both Arabidopsis and tomato and identified possible essential sites for G-LecRK activity for these plant species, with support from characterization of G-LecRKs in a monocot species, rice. Additionally, prediction of protein localization by different tools enriched the initial prediction of G-LecRKs plasma membrane localization and raised the possibility for specificity of modes of actions of a number of proteins depending on their specific subcellular localization patterns.

References

Altschul SF, Madden TL, Schäffer AA, Zhang J, Zhang Z, Miller W, Lipman DJ. 1997. Gapped BLAST and PSI-BLAST: a new generation of protein database search programs. *Nucleic Acids Research* **25**(17): 3389-3402.

Armijo G, Salinas P, Monteoliva MI, Seguel A, García C, Villarroel-Candia E, Song W, van der Krol AR, Álvarez ME, Holuigue L. 2013. A salicylic acid–induced lectin-like protein plays a positive role in the effector-triggered immunity response of *Arabidopsis thaliana* to *Pseudomonas syringae* Avr-Rpm1. *Molecular Plant-Microbe Interactions* **26**(12): 1395-1406.

Arnaud D, Desclos-Theveniau M, Zimmerli L. 2012. Disease resistance to *Pectobacterium carotovorum* is negatively modulated by the Arabidopsis Lectin Receptor Kinase LecRK-V.5. *Plant Signaling & Behavior* **7**(9): 1070-1072.

Bailey TL, Boden M, Buske FA, Frith M, Grant CE, Clementi L, Ren J, Li WW, Noble WS. 2009. MEME SUITE: tools for motif discovery and searching. *Nucleic Acids Research* **37**(Web Server issue): W202-208.

Balagué C, Gouget A, Bouchez O, Souriac C, Haget N, Boutet-Mercey S, Govers F, Roby D, Canut H. 2016. The *Arabidopsis thaliana* lectin receptor kinase LecRK-I.9 is required for full resistance to *Pseudomonas syringae* and affects jasmonate signalling. *Molecular Plant Pathology*: doi: 10.1111/mpp.12457.

Bigeard J, Colcombet J, Hirt H. 2015. Signaling mechanisms in pattern-triggered immunity (PTI). *Molecular Plant* **8**(4): 521-539.

Bouwmeester K, de Sain M, Weide R, Gouget A, Klamer S, Canut H, Govers F. 2011. The lectin receptor kinase LecRK-I.9 is a novel *Phytophthora* resistance component and a potential host target for a RXLR effector. *PLoS pathogens* **7**(3): e1001327.

Bouwmeester K, Govers F. 2009. Arabidopsis L-type lectin receptor kinases: phylogeny, classification, and expression profiles. *Journal of Experimental Botany* **60**(15): 4383-4396.

Cao Y, Liang Y, Tanaka K, Nguyen CT, Jedrzejczak RP, Joachimiak A, Stacey G. 2014a. The kinase LYK5 is a major chitin receptor in Arabidopsis and forms a chitin-induced complex with related kinase CERK1. *eLife*: e03766.

Cao Y, Tanaka K, Nguyen CT, Stacey G. 2014b. Extracellular ATP is a central signaling molecule in plant stress responses. *Current Opinion in Plant Biology* **20**(0): 82-87.

Cheng X, Wu Y, Guo J, Du B, Chen R, Zhu L, He G. 2013. A rice lectin receptor-like kinase that is involved in innate immune responses also contributes to seed germination. *Plant Journal* **76**(4): 687-698.

Chinchilla D, Zipfel C, Robatzek S, Kemmerling B, Nürnberger T, Jones JD, Felix G, Boller T. 2007. A flagellin-induced complex of the receptor FLS2 and BAK1 initiates plant defence. *Nature* **448**(26): 497-500.

Choi J, Tanaka K, Cao Y, Qi Y, Qiu J, Liang Y, Lee SY, Stacey G. 2014. Identification of a Plant Receptor for Extracellular ATP. *Science* **343**: 290-294.

Desclos-Theveniau M, Arnaud D, Huang T-Y, Lin GJ-C, Chen W-Y, Lin Y-C, Zimmerli L. 2012. The Arabidopsis Lectin Receptor Kinase LecRK-V.5 represses stomatal immunity induced by *Pseudomonas syringae* pv. *tomato* DC3000. *PLoS pathogens* **8**(2): e1002513.

Emanuelsson O, Brunak S, von Heijne G, Nielsen H. 2007. Locating proteins in the cell using TargetP, SignalP and related tools. *Nature Protocols* **2**(4): 953-971.

Felix G, Duran JD, Volko S, Boller T. 1999. Plants have a sensitive perception system for the most conserved domain of bacterial flagellin. *Plant Journal* **18**: 265-276.

Gilardoni PA, Hettenhausen C, Baldwin IT, Bonaventure G. 2011. *Nicotiana attenuata* lectin receptor kinase 1 suppresses the insect- Suppresses the Insect-mediated inhibition of induced defense responses during *Manduca sexta* herbivory. *Plant Cell* **23**(9): 3512-3532.

Hanks SK, Hunter T. 1995. Protein kinases 6. The eukaryotic protein kinase superfamily: kinase (catalytic) domain structure and classification. *Journal of the Federation of American Socities for Experimental Biology* **9**(8): 576-596.

Heese A, Hann DR, Gimenez-Ibanez S, Jones AM, He K, Li J, Schroeder JI, Peck SC, Rathjen JP. 2007. The receptor-like kinase SERK3/BAK1 is a central regulator of innate immunity in plants. *Proceedings of the National Academy of Sciences of the United States of America* **104**(29): 12217-12222.

Hind SR, Strickler SR, Boyle PC, Dunham DM, Bao Z, O'Doherty IM, Baccile JA, Hoki JS, Viox EG, Clarke CR, et al. 2016. Tomato receptor FLAGELLIN-SENSING 3 binds flgII-28 and activates the plant immune system. *Nature Plants* **2**: 16128.

Hooper CM, Tanz SK, Castleden IR, Vacher MA, Small ID, Millar AH. 2014. SUBAcon: a consensus algorithm for unifying the subcellular localization data of the Arabidopsis proteome. *Bioinformatics* **30**(23): 3356-3364.

Huang PY, Yeh YH, Liu AC, Cheng CP, Zimmerli L. 2014. The Arabidopsis LecRK-VI.2 associates with the pattern-recognition receptor FLS2 and primes *Nicotiana benthamiana* pattern-triggered immunity. *Plant Journal* **79**(2): 243-255.

Kumar S, Stecher G, Tamura K. 2016. MEGA7: Molecular Evolutionary Genetics Analysis version 7.0 for bigger datasets. *Molecular Biology and Evolution*.

Kusaba M, Dwyer K, Hendershot J, Vrebalov J, Nasrallah JB, Nasrallah ME. 2001. Self-incompatibility in the genus Arabidopsis: characterization of the S locus in the outcrossing *A. lyrata* and its autogamous relative *A. thaliana*. *Plant Cell* **13**(3): 627-643.

Lannoo N, Van Damme EJM. 2014. Lectin domains at the frontiers of plant defense. *Frontiers in Plant Science* **5**: 397.

Lehti-Shiu MD, Shiu S-H. 2012. Diversity, classification and function of the plant protein kinase superfamily. *Philosophical Transactions of the Royal Society B: Biological Sciences* **367**(1602): 2619-2639.

Macedo ML, Oliveira CF, Oliveira CT. 2015. Insecticidal activity of plant lectins and potential application in crop protection. *Molecules* **20**(2): 2014-2033.

Marchler-Bauer A, Derbyshire MK, Gonzales NR, Lu S, Chitsaz F, Geer LY, Geer RC, He J, Gwadz M, Hurwitz DI, et al. 2015. CDD: NCBI's conserved domain database. *Nucleic Acids Research* **43**(Database issue): D222-226.

Mitchell A, Chang H-Y, Daugherty L, Fraser M, Hunter S, Lopez R, McAnulla C, McMenamin C, Nuka G, Pesseat S, et al. 2014. The InterPro protein families database: the classification resource after 15 years. *Nucleic Acids Research*.

Robatzek S, Bittel P, Chinchilla D, Kochner P, Felix G, Shiu SH, Boller T. 2007. Molecular identification and characterization of the tomato flagellin receptor

LeFLS2, an orthologue of *Arabidopsis* FLS2 exhibiting characteristically different perception specificities. *Plant Molecular Biology* **64**: 539-547.

Ron M, Avni A. 2004. The receptor for the fungal elicitor ethylene-inducing xylanase is a member of a resistance-like gene family in tomato. *The Plant Cell* **16**(6): 1604-1615.

Saitou N, Nei M. 1987. The neighbor-joining method: a new method for reconstructing phylogenetic trees. *Molecular Biology and Evolution* **4**(4): 406-425.

Sherman-Broyles S, Boggs N, Farkas A, Liu P, Vrebalov J, Nasrallah ME, Nasrallah JB. 2007. S locus genes and the evolution of self-fertility in *Arabidopsis thaliana*. *Plant Cell* **19**(1): 94-106.

Shi Q, Febres VJ, Jones JB, Moore GA. 2016. A survey of FLS2 genes from multiple citrus species identifies candidates for enhancing disease resistance to *Xanthomonas citri* ssp. *citri*. *Horticulture Resarch* **3**: 16022.

Shimizu T, Nakano T, Takamizawa D, Desaki Y, Ishii-Minami N, Nishizawa Y, Minami E, Okada K, Yamane H, Kaku H, et al. 2010. Two LysM receptor molecules, CEBiP and OsCERK1, cooperatively regulate chitin elicitor signaling in rice. *The Plant Journal* **64**(2): 204-214.

Shinya T, Motoyama N, Ikeda A, Wada M, Kamiya K, Hayafune M, Kaku H, Shibuya N. 2012. Functional Characterization of CEBiP and CERK1 Homologs in Arabidopsis and Rice Reveals the Presence of Different Chitin Receptor Systems in Plants. *Plant and Cell Physiology* **53**(10): 1696-1706.

Shiu S-H, Bleecker AB. 2001. Receptor-like kinases from Arabidopsis form a monophyletic gene family related to animal receptor kinases. *Proceedings of the National Academy of Sciences of the United States of America* **98**(19): 10763-10768.

Shiu SH, Bleecker AB. 2001. Plant receptor-like kinase gene family: diversity, function, and signaling. *Science signaling* **2001**(113): re22.

Shumayla, Sharma S, Pandey AK, Singh K, Upadhyay SK. 2016. Molecular characterization and global expression analysis of Lectin Receptor Kinases in bread wheat *Triticum aestivum*. *PLoS One* **11**(4): e0153925.

Singh P, Chien C-C, Mishra S, Tsai C-H, Zimmerli L. 2013. The Arabidopsis lectin receptor kinase-VI.2 is a functional protein kinase and is dispensable

for basal resistance to *Botrytis cinerea*. *Plant Signaling & Behavior* **8**(1): e22611.

Singh P, Kuo Y-C, Mishra S, Tsai C-H, Chien C-C, Chen C-W, Desclos-Theveniau M, Chu P-W, Schulze B, Chinchilla D, et al. 2012. The lectin receptor kinase -VI.2 is required for priming and positively regulates Arabidopsis pattern-triggered immunity. *Plant Cell* **24**(3): 1256-1270.

Singh P, Zimmerli L. 2013. Lectin receptor kinases in plant innate immunity. *Frontiers in Plant Science* **4**.

Takai R, Isogai A, Takayama S, Che FS. 2008. Analysis of flagellin perception mediated by flg22 receptor OsFLS2 in rice. *Molecular Plant-Microbe Interactions* **21**(12): 1635-1642.

Tanz SK, Castleden I, Hooper CM, Vacher M, Small I, Millar HA. 2013. SUBA3: a database for integrating experimentation and prediction to define the SUBcellular location of proteins in Arabidopsis. *Nucleic Acids Research* **41**(Database issue): D1185-D1191.

Tordai H, Banyai L, Patthy L. 1999. The PAN module: the N-terminal domains of plasminogen and hepatocyte growth factor are homologous with the apple domains of the prekallikrein family and with a novel domain found in numerous nematode proteins. *FEBS Lett* **461**(1-2): 63-67.

Trda L, Fernandez O, Boutrot F, Heloir MC, Kelloniemi J, Daire X, Adrian M, Clement C, Zipfel C, Dorey S, et al. 2014. The grapevine flagellin receptor VvFLS2 differentially recognizes flagellin-derived epitopes from the endophytic growth-promoting bacterium *Burkholderia phytofirmans* and plant pathogenic bacteria. *New Phytologist* **201**: 1371-1384.

Trontin C, Kiani S, Corwin JA, Hématy K, Yansouni J, Kliebenstein DJ, Loudet O. 2014. A pair of receptor-like kinases is responsible for natural variation in shoot growth response to mannitol treatment in *Arabidopsis thaliana*. *The Plant Journal* **78**(1): 121-133.

Vaid N, Macovei A, Tuteja N. 2013. Knights in action: lectin receptor-like kinases in plant development and stress responses. *Molecular Plant* **6**(5): 1405-1418.

Vaid N, Pandey PK, Tuteja N. 2012. Genome-wide analysis of lectin receptor-like kinase family from Arabidopsis and rice. *Plant Molecular Biology* **80**(4-5): 365-388.

Van Damme EJ, Nakamura-Tsuruta S, Smith DF, Ongenaert M, Winter HC, Rouge P, Goldstein IJ, Mo H, Kominami J, Culerrier R, et al. 2007. Phylogenetic and specificity studies of two-domain GNA-related lectins: generation of multispecificity through domain duplication and divergent evolution. *Biochemical Journal* **404**(1): 51-61.

Wang Y, Cordewener JHG, America AHP, Shan W, Bouwmeester K, Govers F. 2015a. Arabidopsis Lectin Receptor Kinases LecRK-IX.1 and LecRK-IX.2 are functional analogs in regulating *Phytophthora* resistance and plant cell death. *Molecular Plant-Microbe Interactions* **28**(9): 1032-1048.

Wang Y, Weide R, Govers F, Bouwmeester K. 2015b. L-type lectin receptor kinases in *Nicotiana benthamiana* and tomato and their role in Phytophthora resistance. *Journal of Experimental Botany* **66**(21): 6731-6743.

Yu C-S, Chen Y-C, Lu C-H, Hwang J-K. 2006. Prediction of protein subcellular localization. *Proteins: Structure, Function, and Bioinformatics* **64**(3): 643-651.

Zipfel C. 2014. Plant pattern-recognition receptors. *Trends in Immunology* **35**: 345-351.

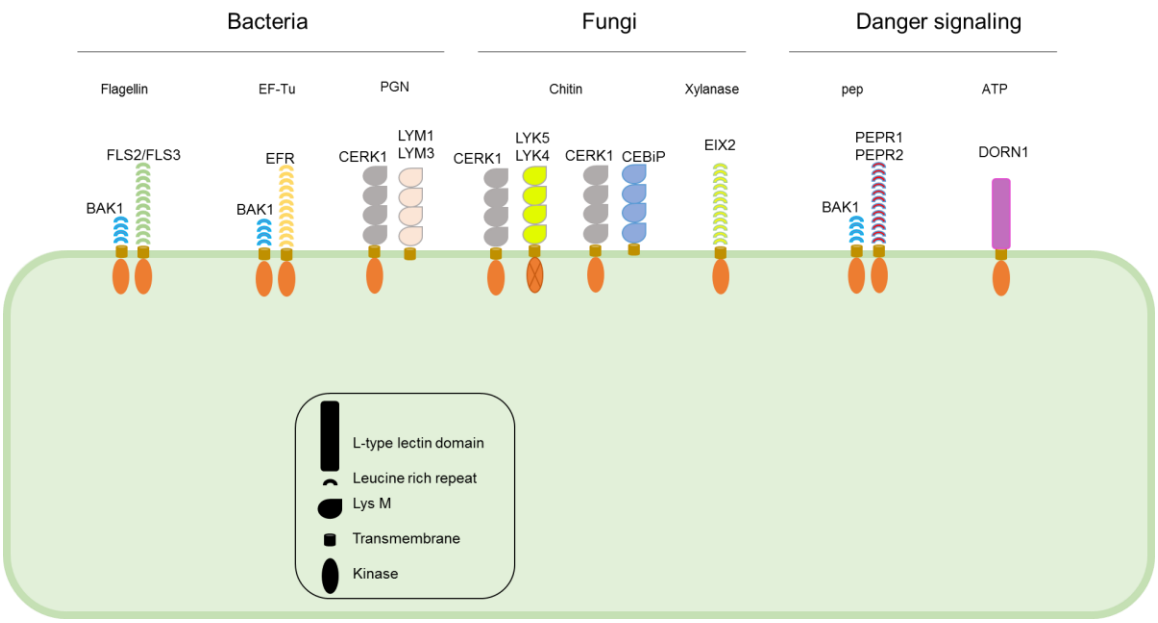

Figure 3.1. Plant receptor kinases that perceive pathogens and self danger molecules. The LRR-RKs FLS2 and FLS3 require the LRR-RK BAK1 and recognize the peptides flg22 and flgII-28, respectively (Zipfel *et al.*, 2004; Hind *et al.*, 2016), derived from bacteria flagellin. The Brassicacea specific LRR-RK EFR recognizes an epitope of the bacterial elongation factor Tu (Zipfel *et al.*, 2006). The LYS M motif proteins CERK1 and LYM1 and LYM3 perceive bacterial peptidoglycan, PGN. CERK1 is also required for perception of chitin by LYK5 and LYK4 in Arabidopsis and CEBiP in rice (Cao *et al.*, 2014a). EIX2 from tomato perceives xylanase, from fungal pathogens. The LRR-RKs PEPR1 and PEPR2 perceive danger peptides actively transcribed to amplify defense responses (Krol *et al.*, 2010). The Legume-type LecRK DORN1 perceives ATP as a danger molecule to signal defense responses (Cao *et al.*, 2014b).

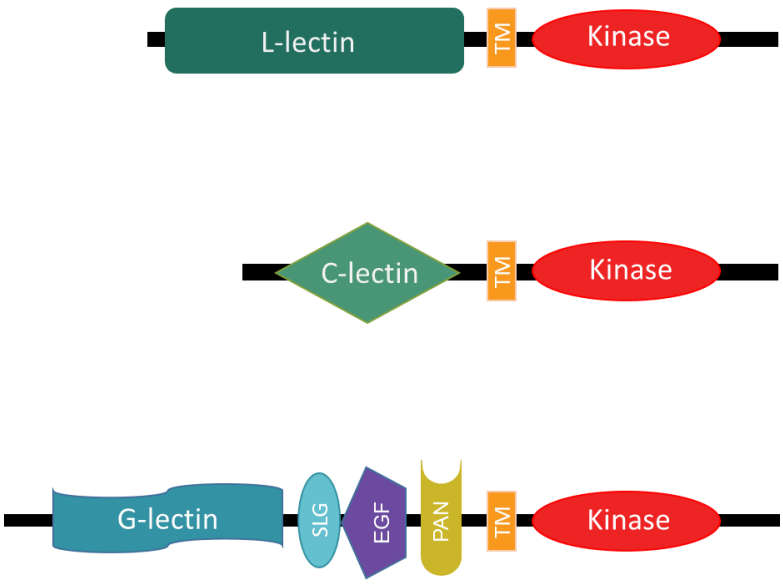

Figure 3.2. Lectin receptor kinases (LecRKs) domains and organization. G-lectin, C-lectin and L-lectin are the motifs localized in the ectodomains of G-type, C-type, and L-type LecRKs, respectively.

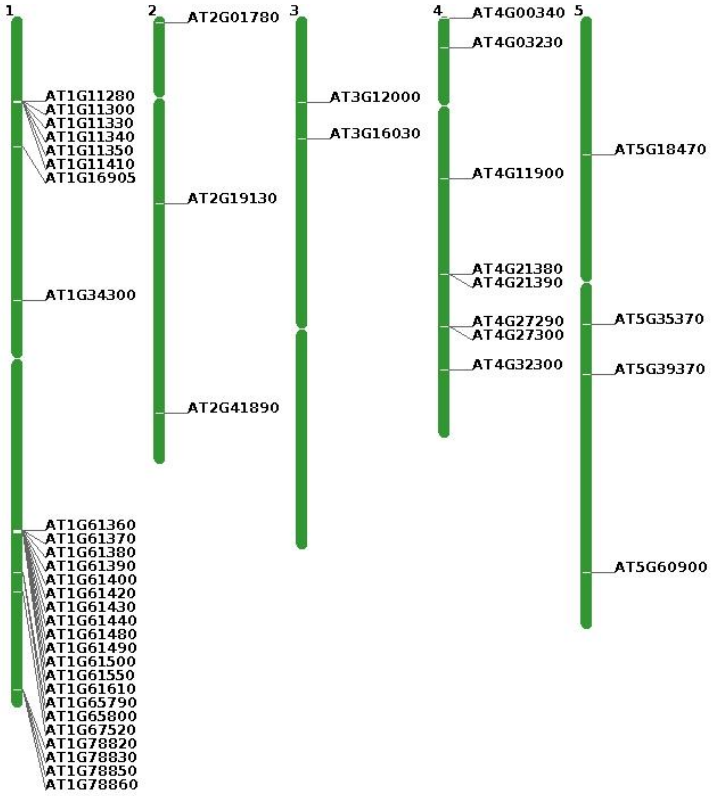

Figure 3.3. Genome organization of G-LecRKs in Arabidopsis. Figure presents arrangement of G-LecRKs on the five Arabidopsis chromosomes. This figure was prepared using Chromosome Map Tool from The Arabidopsis Information Resource (TAIR).

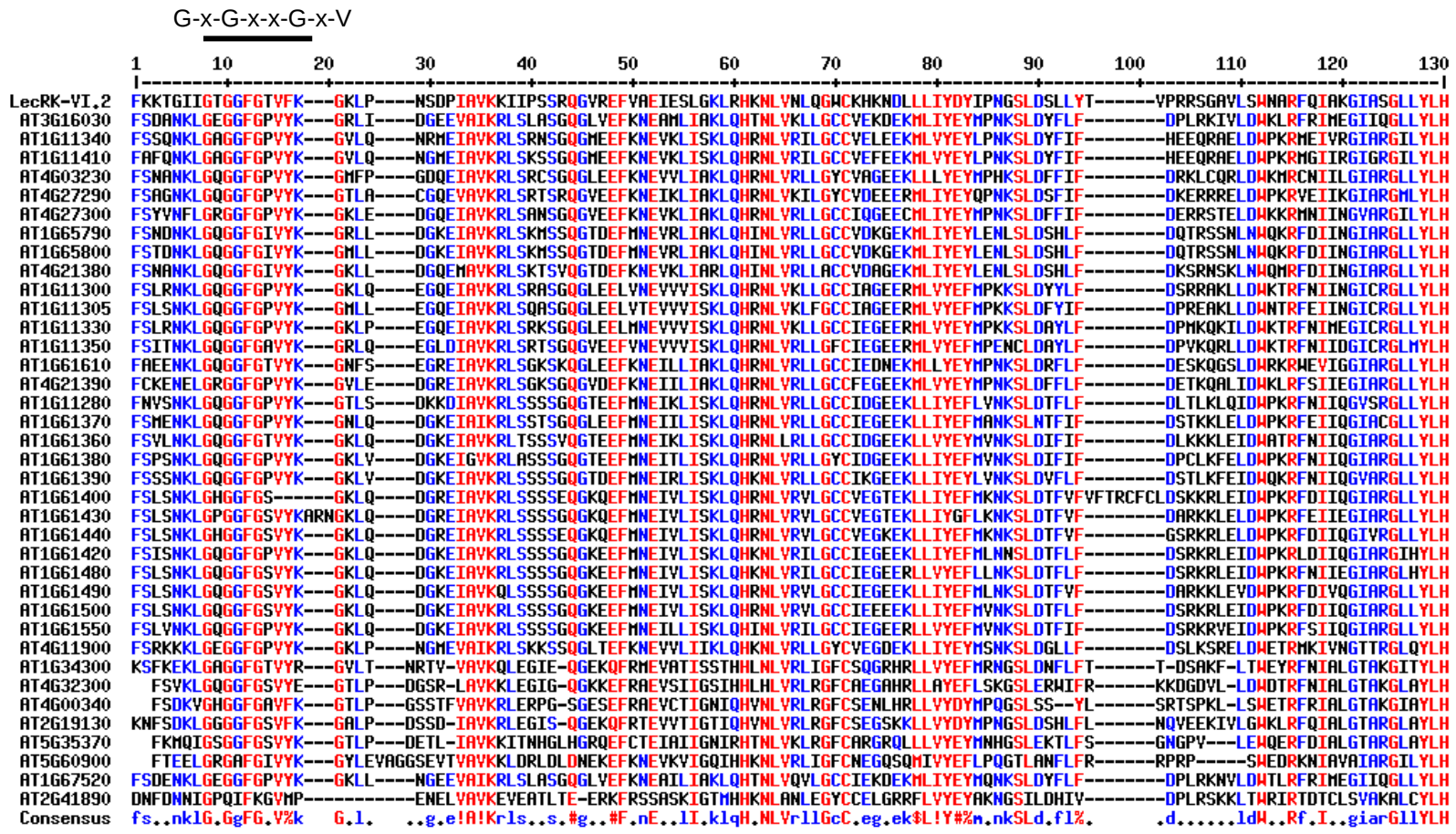
G-x-G-x-x-G-x-V
1 10 20 30 40 50 60 70 80 90 100 110 120 130
LecRK-VI.2
AT3G16030
AT1G11340
AT1G11410
AT4G03230
AT4G27290
AT4G27300
AT1G65790
AT1G65800
AT4G21380
AT1G11300
AT1G11305
AT1G11330
AT1G11350
AT1G61610
AT4G21390
AT1G11280
AT1G61370
AT1G61360
AT1G61380
AT1G61390
AT1G61400
AT1G61430
AT1G61440
AT1G61420
AT1G61480
AT1G61490
AT1G61500
AT1G61550
AT4G11900
AT1G34300
AT4G32300
AT4G00340
AT2G19130
AT5G35370
AT5G60900
AT1G67520
AT2G41890
Consensus

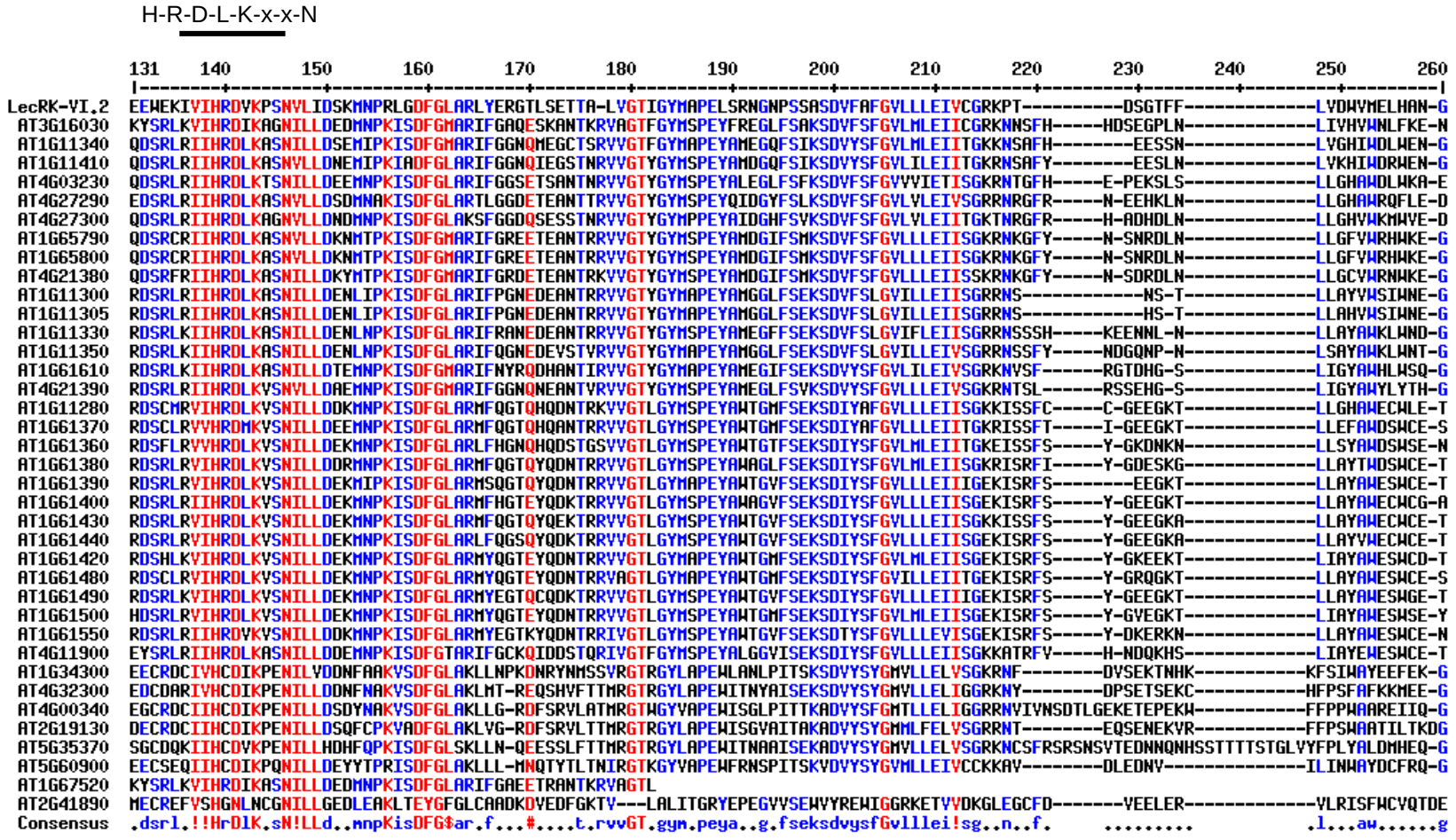
H-R-D-L-K-x-x-N
131 140 150 160 170 180 190 200 210 220 230 240 250 260
LecRK-VI.2
AT3G16030
AT1G11340
AT1G11410
AT4G03230
AT4G27290
AT4G27300
AT1G65790
AT1G65800
AT4G21380
AT1G11300
AT1G11305
AT1G11330
AT1G11350
AT1G61610
AT4G21390
AT1G11280
AT1G61370
AT1G61360
AT1G61380
AT1G61390
AT1G61400
AT1G61430
AT1G61440
AT1G61420
AT1G61480
AT1G61490
AT1G61500
AT1G61550
AT4G11900
AT1G34300
AT4G32300
AT4G00340
AT2G19130
AT5G35370
AT5G60900
AT1G67520
AT2G41890
Consensus

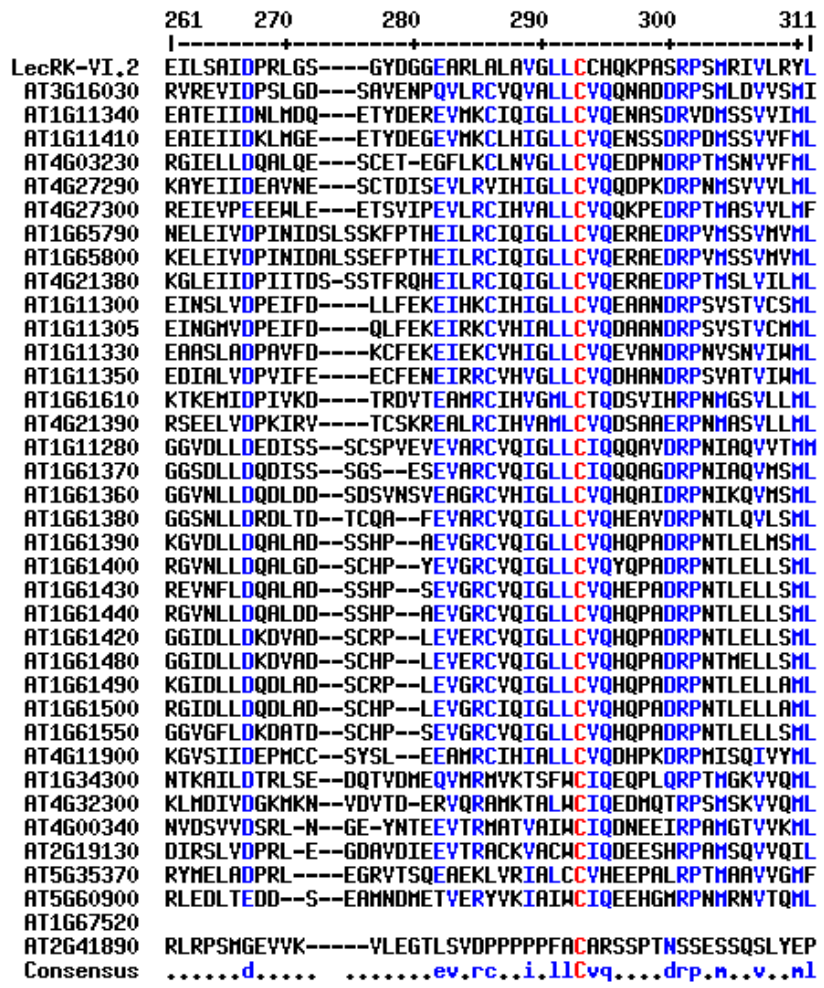

Figure 3.4. Alignment of predicted amino acid sequences of Arabidopsis G-LecRKs kinase domains with the L-LecRK-VI.2. Lines on top of alignment show subdomains I and II, ATP binding site (GxGxxGxV) and subdomain VI, the serine/threonine kinase active site (HRDLKxxN).

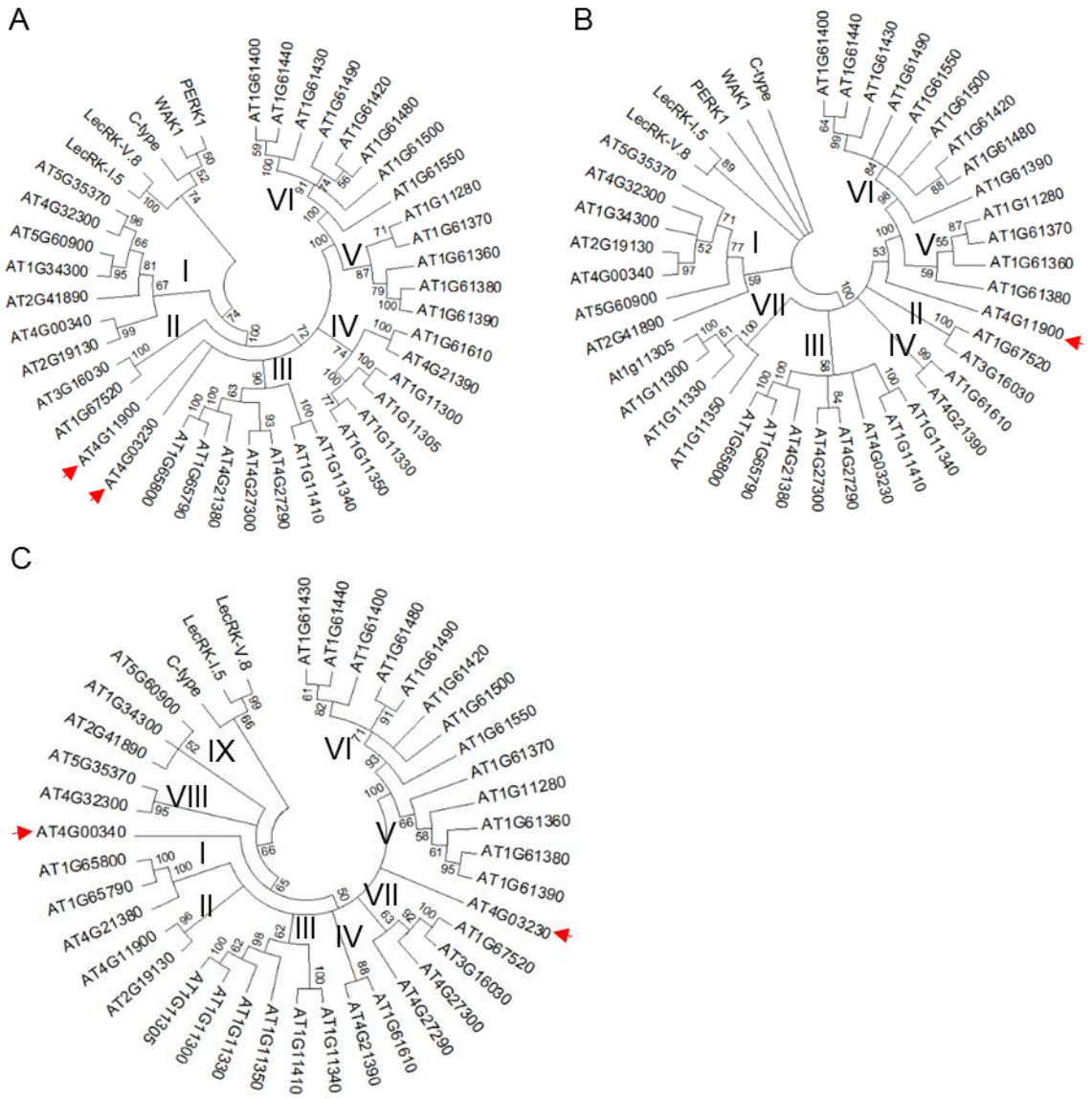

Figure 3.5. Phylogenetic analysis and classification of Arabidopsis G-LecRK proteins. The evolutionary history was inferred using the Neighbor-Joining method with 1000 replicates (Saitou & Nei, 1987). Branches corresponding to partitions reproduced in less than 50% bootstrap replicates are collapsed. The evolutionary distances were computed using the Poisson correction method (Zuckerkandl & Pauling, 1965) and are in the units of the number of amino acid substitutions per site. The analysis involved 42 amino acid sequences. All ambiguous positions were removed for each sequence pair. Evolutionary analyses were conducted in MEGA7 (Kumar *et al.*, 2016). Trees were generated from alignment of (A) full-length protein sequences; (B) kinase domains; (C) lectin domains. Red arrows indicate singletons according to phylogenetic analysis.

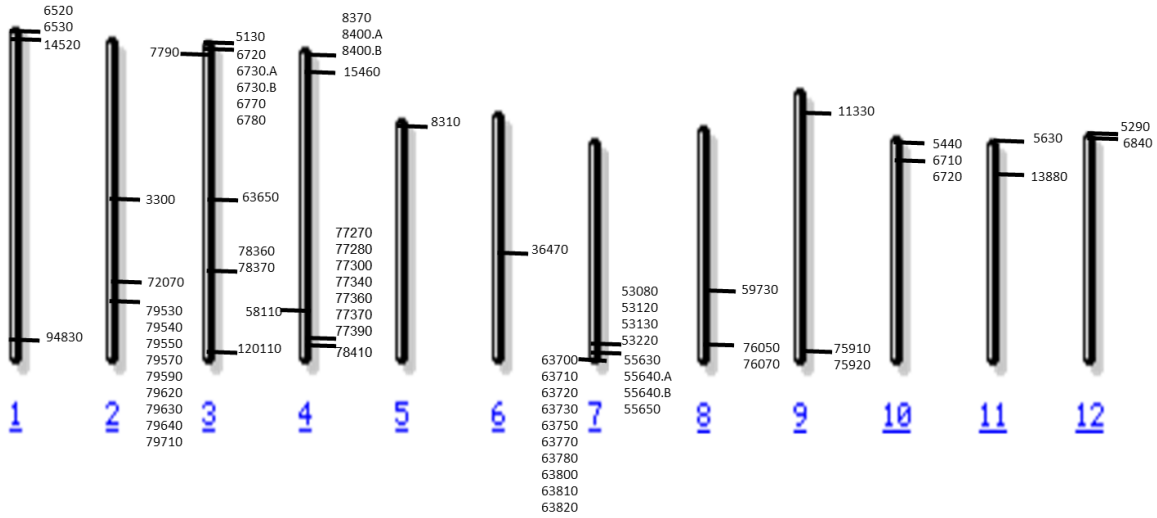

Figure 3.6. Genome organization of G-LecRKs in tomato. Figure presents arrangement of G-LecRKs on the 12 tomato chromosomes. This figure was prepared using NCBI map viewer from NCBI.

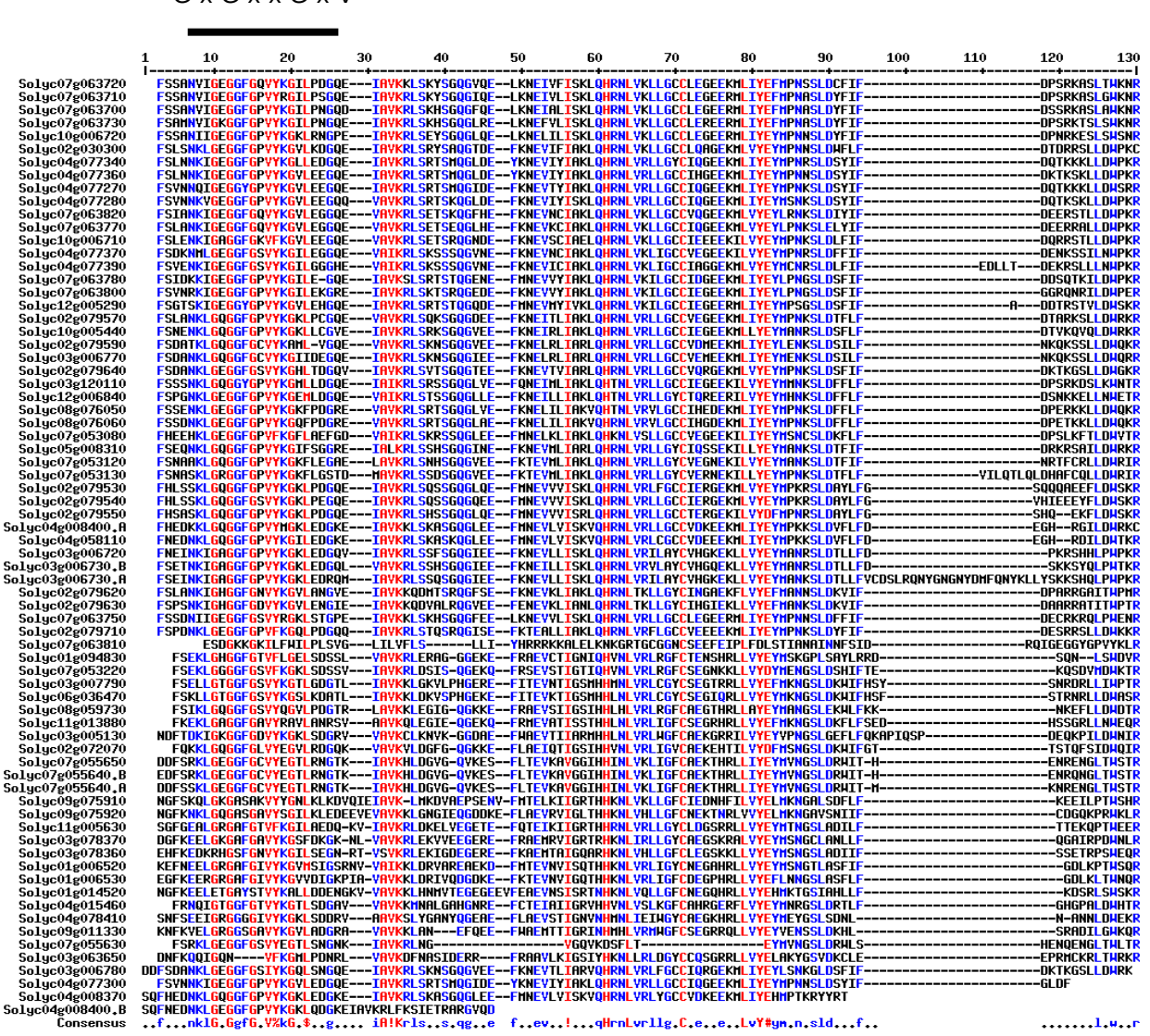
G-x-G-x-x-G-x-V

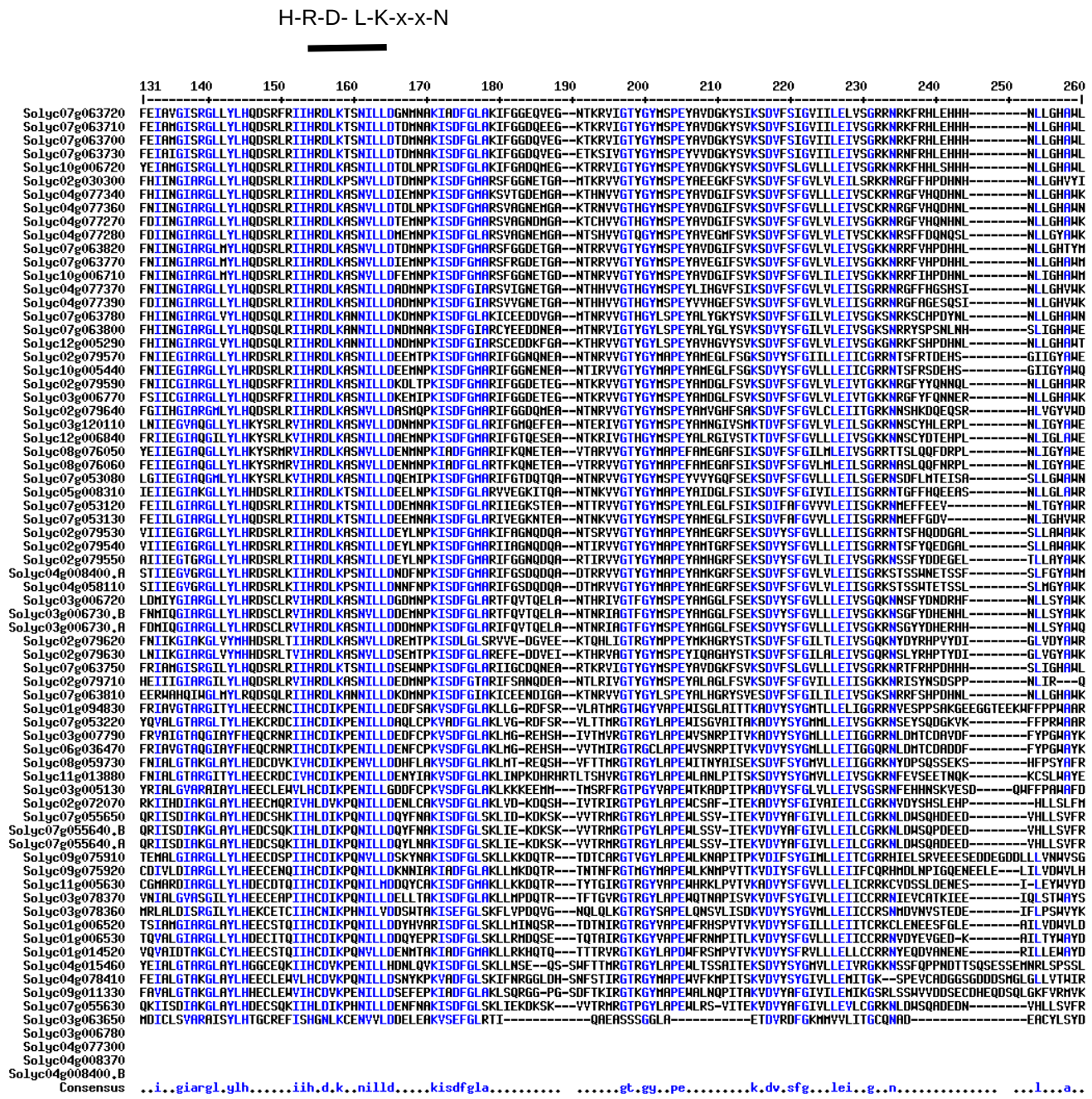
H-R-D- L-K-x-x-N
131 140 150 160 170 180 190 200 210 220 230 240 250 260
Solyc07g063720
Solyc07g063710
Solyc07g063700
Solyc07g063730
Solyc10g006720
Solyc02g030300
Solyc04g077340
Solyc04g077360
Solyc04g077270
Solyc04g077280
Solyc07g063820
Solyc07g063770
Solyc10g006710
Solyc04g077370
Solyc04g077390
Solyc07g063780
Solyc07g063800
Solyc12g005290
Solyc02g079570
Solyc10g005440
Solyc02g079590
Solyc03g006770
Solyc02g079640
Solyc03g120110
Solyc12g006840
Solyc08g076050
Solyc08g076060
Solyc07g053080
Solyc05g008310
Solyc07g053120
Solyc07g053130
Solyc02g079530
Solyc02g079540
Solyc02g079550
Solyc04g008400.A
Solyc04g058110
Solyc03g006720
Solyc03g006730.B
Solyc03g006730.A
Solyc02g079620
Solyc02g079630
Solyc07g063750
Solyc02g079710
Solyc07g063810
Solyc01g094830
Solyc07g053220
Solyc03g007790
Solyc06g036470
Solyc08g059730
Solyc11g013880
Solyc03g005130
Solyc02g072070
Solyc07g055650
Solyc07g055640.B
Solyc07g055640.A
Solyc09g075910
Solyc09g075920
Solyc11g005630
Solyc03g078370
Solyc03g078360
Solyc01g006520
Solyc01g006530
Solyc01g014520
Solyc04g015460
Solyc04g078410
Solyc09g011330
Solyc07g055630
Solyc03g063650
Solyc03g006780
Solyc04g077300
Solyc04g008370
Solyc04g008400.B
Consensus

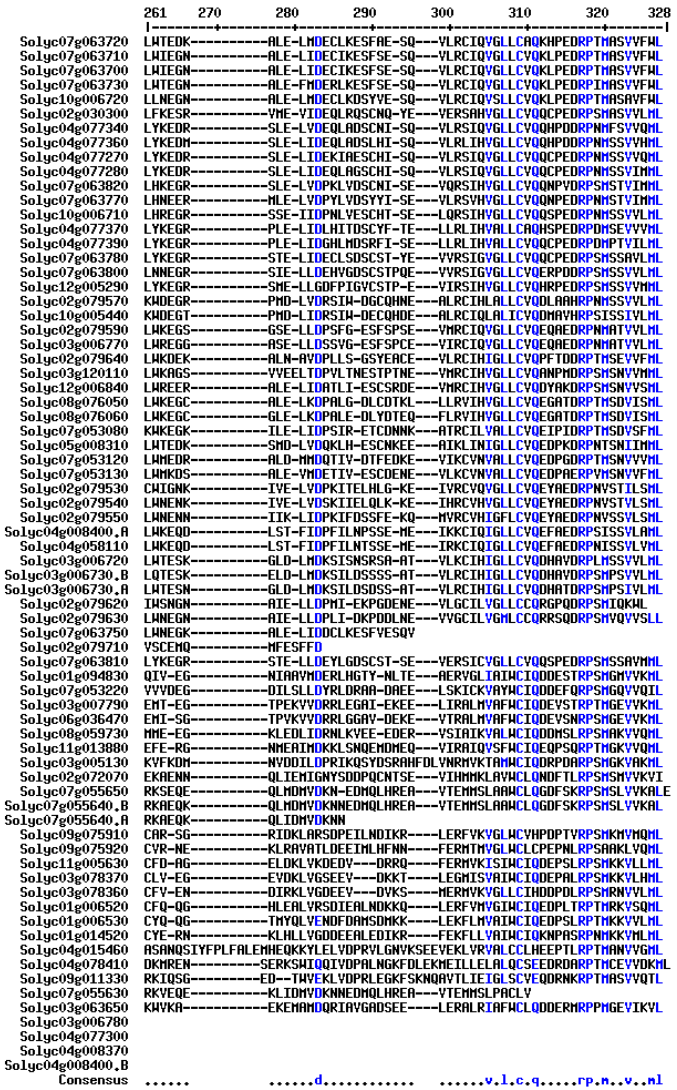

Figure 3.7. Alignment of predicted amino acid sequences of tomato G-LecRKs kinase domains with the L-LecRK-VI.2. Lines on top of alignment show subdomains I and II, ATP binding site (GxGxxGxV) and subdomain VI, the serine/threonine kinase active site (HRDLKxxN).

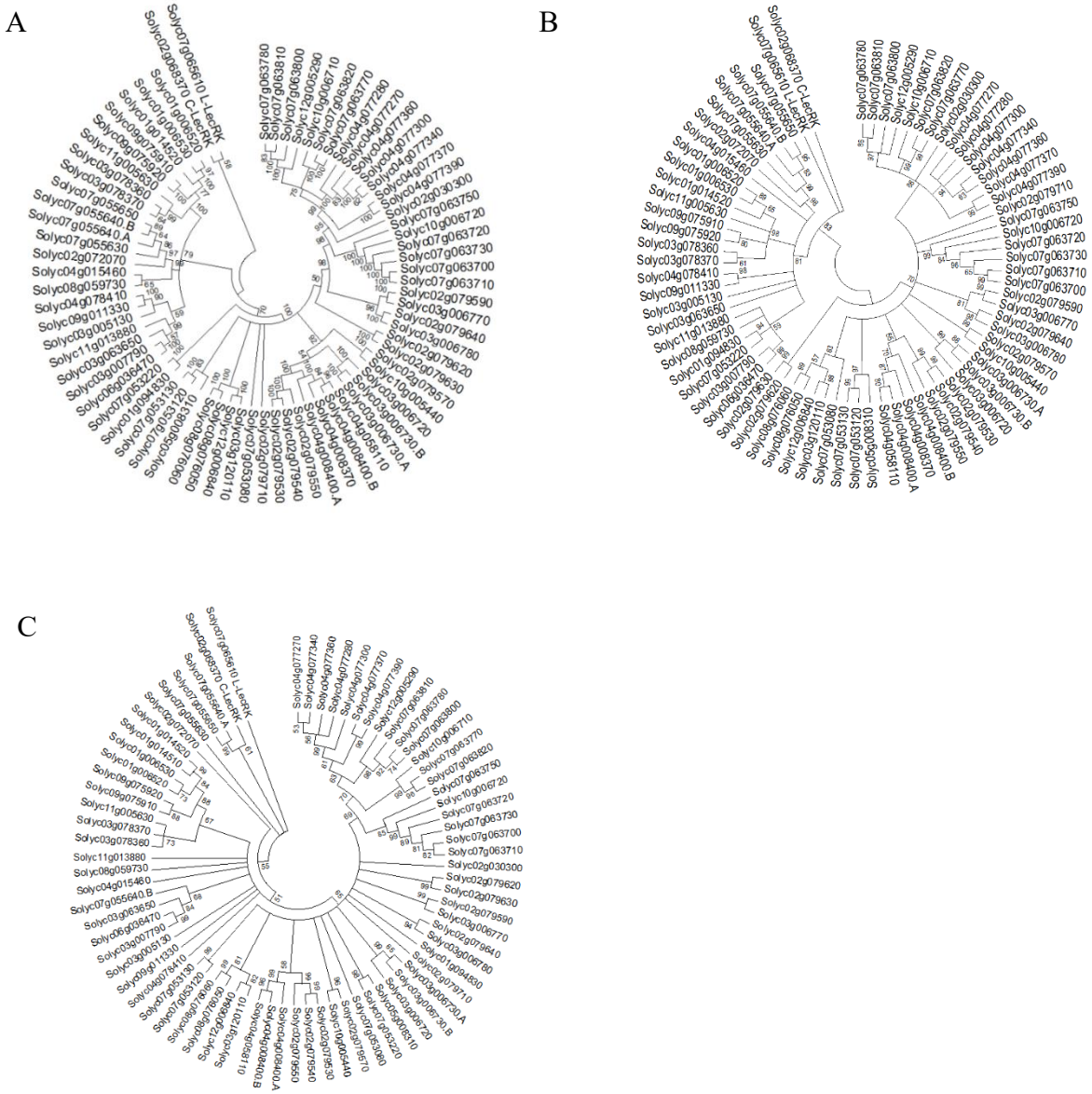

Figure 3.8. Phylogenetic analysis and classification of tomato G-LecRK proteins. The evolutionary history was inferred using the Neighbor-Joining method with 1000 replicates (Saitou & Nei, 1987). Branches corresponding to partitions reproduced in less than 50% bootstrap replicates are collapsed. The evolutionary distances were computed using the Poisson correction method (Zuckerkandl & Pauling, 1965) and are in the units of the number of amino acid substitutions per site. The analysis involved 75 amino acid sequences. All ambiguous positions were removed for each sequence pair. Evolutionary analyses were conducted in MEGA7 (Kumar *et al.*, 2016). Trees were generated from alignment of (A) full-length protein sequences; (B) kinase domains; (C) lectin domains.

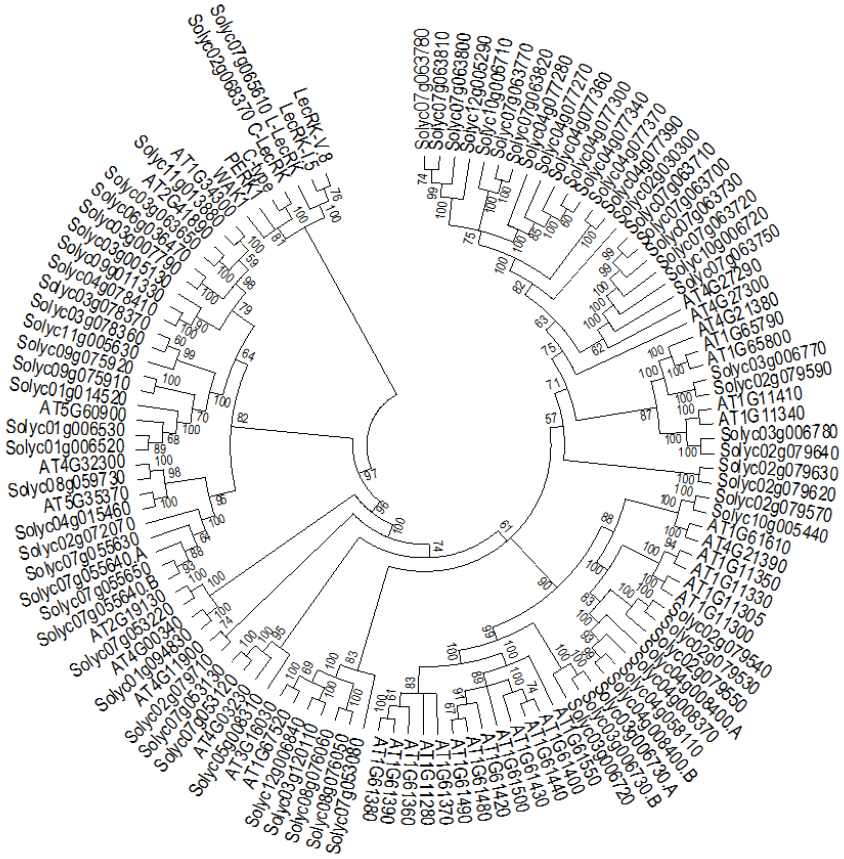

Figure 3.9. Phylogenetic analysis of Arabidopsis (AT) and tomato (Solyc) G-LecRK proteins. The evolutionary history was inferred using the Neighbor-Joining method with 1000 replicates (Saitou & Nei, 1987). Branches corresponding to partitions reproduced in less than 50% bootstrap replicates are collapsed. The evolutionary distances were computed using the Poisson correction method (Zuckerkandl & Pauling, 1965) and are in the units of the number of amino acid substitutions per site. The analysis involved 119 amino acid sequences. All ambiguous positions were removed for each sequence pair. Evolutionary analyses were conducted in MEGA7 (Kumar *et al.*, 2016).

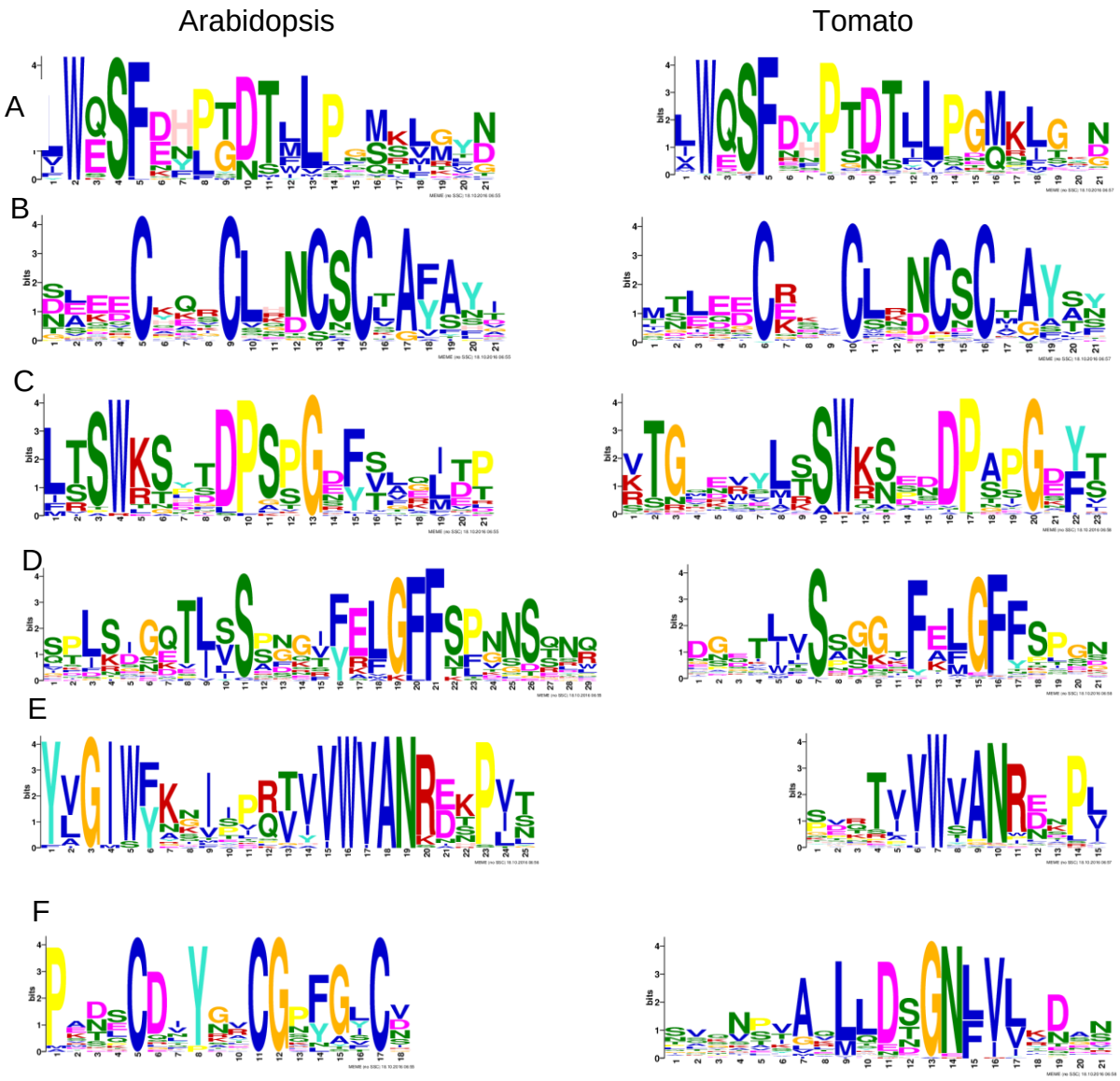

Figure 3.10. Conserved motifs in extracellular domains of Arabidopsis and tomato G-LecRKs. Motifs presented as identified using MEME.

Table 3.1. Genes encoding a G-type and additional predicted domains ("x" denotes presence of domain and "–" denotes absence). Domains were predicted using Interpro, from The European Bioinformatic Institute, which consolidates predictions from distinct databases. EGF, epidermal growth factor; PAN, plasminogen apple nematode; TM, transmembrane.

	Locus	G-Lectin	S-locus glycoprotein	EGF	PAN	TM	Kinase
1	AT1G11340	x	x	x	x	x	x
2	AT1G11410	x	x	x	x	x	x
3	AT1G61360	x	x	x	x	x	x
4	AT1G61380	x	x	x	x	x	x
5	AT1G61390	x	x	x	x	x	x
6	AT1G61550	x	x	x	x	x	x
7	AT1G61610	x	x	x	x	x	x
8	AT2G19130	x	x	x	x	x	x
9	AT4G27290	x	x	x	x	x	x
10	AT4G03230	x	x	x	x	x	x
11	AT1G11280	x	x	-	x	x	x
12	AT1G11300	x	x	-	x	x	x
13	AT1G11305	x	x	-	x	x	x
14	AT1G11330	x	x	-	x	x	x
15	AT1G11350	x	x	-	x	x	x
16	AT1G61370	x	x	-	x	x	x
17	AT1G61400	x	x	-	x	x	x
18	AT1G61420	x	x	-	x	x	x
19	AT1G61430	x	x	-	x	x	x
20	AT1G61440	x	x	-	x	x	x
21	AT1G61480	x	x	-	x	x	x
22	AT1G61490	x	x	-	x	x	x
23	AT1G61500	x	x	-	x	x	x
24	AT1G65790	x	x	-	x	x	x
25	AT1G65800	x	x	-	x	x	x
26	AT2G41890	x	x	-	x	x	x
27	AT4G11900	x	x	-	x	x	x
28	AT4G21380	x	x	-	x	x	x
29	AT4G21390	x	x	-	x	x	x
30	AT4G27300	x	x	-	x	x	x
31	AT1G34300	x	x	-	-	x	x
32	AT4G00340	x	x	-	-	x	x
33	AT3G16030	x	-	-	x	x	x
34	AT4G32300	x	-	-	-	x	x
35	AT5G35370	x	-	-	-	x	x
36	AT1G67520	x	-	-	x	-	x*
37	AT5G60900	x	-	-	x	-	x
38	AT1G16905	x	-	-	-	x	-
39	AT1G78830	x	-	-	x	x	-
40	AT3G12000	x	x	-	x	x	-
41	AT5G18470	x	-	-	-	x	-
42	AT1G78820	x	-	-	x	-	-
43	AT1G78850	x	-	-	x	-	-
44	AT1G78860	x	-	-	x	-	-
45	AT2G01780	x	-	-	-	-	-
46	AT5G39370	x	-	-	-	-	-

Table 3.2. Arabidopsis G-LecRKs classification and nomenclature.

Proposed Clade name	Proposed gene name	Cluster	Locus
G-LecRK-I	*G-LecRK-I.1*	1A	AT1G11340
	G-LecRK-I.2	1A	AT1G11410
G-LecRK-II	*G-LecRK-II.1*	1A	AT1G11300
	G-LecRK-II.2	1A	AT1G11305
	G-LecRK-II.3	1A	AT1G11330
	G-LecRK-II.4	1A	AT1G11350
G-LecRK-III	*G-LecRK-III.1*	-	AT1G67520
	G-LecRK-III.2	-	AT3G16030
G-LecRK-IV	*G-LecRK-IV.1*	1C	AT1G65790
	G-LecRK-IV.2	1C	AT1G65800
	G-LecRK-IV.3	4A	AT4G21380
	G-LecRK-IV.4	4B	AT4G27290
G-LecRK-V	*G-LecRK-V.1*	1B	AT1G61610
	G-LecRK-V.2	4A	AT4G21390
G-LecRK-VI	*G-LecRK-VI.1*	1A	AT1G11280
	G-LecRK-VI.2	-	AT1G61360
	G-LecRK-VI.3	1B	AT1G61370
	G-LecRK-VI.4	1B	AT1G61380
	G-LecRK-VI.5	1B	AT1G61390
	G-LecRK-VI.6	1B	AT1G61400
	G-LecRK-VI.7	1B	AT1G61420
	G-LecRK-VI.8	1B	AT1G61430
	G-LecRK-VI.9	1B	AT1G61440
	G-LecRK-VI.10	1B	AT1G61480
	G-LecRK-VI.11	1B	AT1G61490
	G-LecRK-VI.12	1B	AT1G61500
	G-LecRK-VI.13	1B	AT1G61550
Singletons	*G-LecRK-S.1*	-	AT1G34300
	G-LecRK-S.2	-	AT2G19130
	G-LecRK-S.3	-	AT2G41890
	G-LecRK-S.4	-	AT4G00340
	G-LecRK-S.5	-	AT4G03230
	G-LecRK-S.6	-	AT4G11900
	G-LecRK-S.7	4B	AT4G27300
	G-LecRK-S.8	-	AT4G32300
	G-LecRK-S.9	-	AT5G35370
	G-LecRK-S.10	-	AT5G60900

Table 3.3. Arabidopsis G-LecRKs localization prediction. Localization was predicted using SUBA, TargetP and CELLO. PM, plasma membrane; SP, secretion pathway; MT, mitochondria, C, cytoplasm; N, nucleus. "-" denotes no prediction.

	Locus	SUBA	TargetP	CELLO
1	AT1G11280	PM	-	PM
2	AT1G11300	PM	SP	PM
3	AT1G11305	-	SP	PM
4	AT1G11330	PM	SP	PM
5	AT1G11340	PM	SP	PM
6	AT1G11350	PM	SP	PM
7	AT1G11410	PM	SP	PM
8	AT1G34300	PM	SP	PM
9	AT1G61360	PM	SP	PM
10	AT1G61370	PM	SP	PM
11	AT1G61380	PM	SP	PM
12	AT1G61390	PM	MT	PM
13	AT1G61400	PM	MT	PM
14	AT1G61420	PM	SP	PM
15	AT1G61430	PM	SP	PM
16	AT1G61440	PM	SP	PM
17	AT1G61480	PM	SP	PM
18	AT1G61490	PM	SP	PM
19	AT1G61500	PM	SP	PM
20	AT1G61550	PM	SP	PM
21	AT1G61610	PM	SP	PM
22	AT1G65790	PM	SP	PM
23	AT1G65800	PM	SP	PM
24	AT1G67520	PM	SP	PM
25	AT2G19130	PM	SP	PM
26	AT2G41890	PM	SP	PM
27	AT3G16030	PM	SP	PM
28	AT4G00340	PM	SP	PM
29	AT4G03230	PM	SP	PM
30	AT4G11900	PM	SP	PM
31	AT4G21380	PM	SP	PM
32	AT4G21390	PM	SP	PM
33	AT4G27290	PM	SP	N / PM
34	AT4G27300	PM	SP	PM
35	AT4G32300	PM	SP	PM
36	AT5G35370	PM	SP	PM
37	AT5G60900	PM	SP	C / N / PM

Table 3.4. Genes encoding a G-type lectin and additional predicted domains ("x" denotes presence of domain and "–" denotes absence). Domains were predicted using Interpro, from The European Bioinformatic Institute, which consolidates predictions from distinct tools. Numbers under Transmembrane domain indicate number of transmembrane domains predicted.

	Gene	G-Lectin	S-locus glycoprotein	EGF	PAN	TM	Kinase
1	Solyc02g079640	x	x	x	x	x	x
2	Solyc04g008400.A	x	x	x	x	x	x
3	Solyc04g058110	x	x	x	x	x	x
4	Solyc07g063770	x	x	x	x	x	x
5	Solyc10g006710	x	x	x	x	x	x
6	Solyc11g005630	x	x	x	x	x	x
7	Solyc02g030300	x	x	-	x	x	x
8	Solyc02g079530	x	x	-	x	x	x
9	Solyc02g079540	x	x	-	x	x	x
10	Solyc02g079550	x	x	-	x	x	x
11	Solyc02g079570	x	x	-	x	x	x
12	Solyc02g079590	x	x	-	x	x	x
13	Solyc02g079620	x	x	-	x	x	x
14	Solyc02g079630	x	x	-	x	x	x
15	Solyc02g079710	x	x	-	x	x	x
16	Solyc03g006720	x	x	-	x	x	x
17	Solyc03g006730.A	x	x	-	x	x	x
18	Solyc03g006730.B	x	x	-	x	x	x
19	Solyc03g006770	x	x	-	x	x	x
20	Solyc03g006780	x	x	-	x	x	x
21	Solyc03g063650	x	x	-	x	x	x
22	Solyc04g008370	x	x	-	x	x	x
23	Solyc04g077270	x	x	-	x	x	x
24	Solyc04g077280	x	x	-	x	x	x
25	Solyc04g077300	x	x	-	x	x	x
26	Solyc04g077340	x	x	-	x	x	x
27	Solyc04g077360	x	x	-	x	x	x
28	Solyc04g077370	x	x	-	x	x	x
29	Solyc04g077390	x	x	-	x	x	x
30	Solyc04g078410	x	x	-	x	x	x
31	Solyc05g008310	x	x	-	x	x	x
32	Solyc07g053080	x	x	-	x	x	x

33	Solyc07g053120	x	x	-	x	x	x
34	Solyc07g053130	x	x	-	x	x	x
35	Solyc07g063700	x	x	-	x	x	x
36	Solyc07g063710	x	x	-	x	x	x
37	Solyc07g063720	x	x	-	x	x	x
38	Solyc07g063730	x	x	-	x	x	x
39	Solyc07g063750	x	x	-	x	x	x
40	Solyc07g063780	x	x	-	x	x	x
41	Solyc07g063800	x	x	-	x	x	x
42	Solyc09g011330	x	x	-	x	x	x
43	Solyc10g005440	x	x	-	x	x	x
44	Solyc10g006720	x	x	-	x	x	x
45	Solyc12g005290	x	x	-	x	x	x
46	Solyc01g094830	x	x	-	x	x	x
47	Solyc04g008400.B	x	x	x	x	x	x
48	Solyc07g053220	x	x	-	x	x	x
49	Solyc02g072070	x	-	-	x	x	x
50	Solyc03g120110	x	-	-	x	x	x
51	Solyc08g076050	x	-	-	x	x	x
52	Solyc08g076060	x	-	-	x	x	x
53	Solyc12g006840	x	-	-	x	x	x
54	Solyc01g006520	x	x	-	-	x	x
55	Solyc03g005130	x	x	-	-	x	x
56	Solyc03g007790	x	x	-	-	x	x
57	Solyc03g078360	x	x	-	-	x	x
58	Solyc03g078370	x	x	-	-	x	x
59	Solyc06g036470	x	x	-	-	x	x
60	Solyc09g075910	x	x	-	-	x	x
61	Solyc09g075920	x	x	-	-	x	x
62	Solyc11g013880	x	x	-	-	x	x
63	Solyc01g006530	x	-	-	-	x	x
64	Solyc01g014520	x	-	-	-	x	x
65	Solyc04g015460	x	-	-	-	x	x
66	Solyc07g055650	x	-	-	-	x	x
67	Solyc08g059730	x	-	-	-	x	x
68	Solyc07g063820	x	x	-	x	-	x
69	Solyc07g063810	x	-	-	x	-	x
70	Solyc07g055630	x	-	-	-	-	x
71	Solyc07g055640.A	x	-	-	-	-	x

72	Solyc07g055640.B	x	-	-	-	-	x
73	Solyc07g009410	x	-	-	x	-	-
74	Solyc07g053090	x	x	-	x	x	-
75	Solyc04g077310	x	x	-	-	x	-
76	Solyc10g006690	x	x	-	x	-	-
77	Solyc04g077320	x	x	-	-	-	-
78	Solyc07g009440	x	x	-	-	-	-
79	Solyc07g055690	x	x	-	-	-	-
80	Solyc01g014510	x	-	-	-	-	-

Table 3.5. Tomato G-LecRKs with truncated kinase subdomains. Tomato G-LecRK kinase domain amino acid sequences were aligned and searched for the presence of the known 11 kinase subdomains (I-XI) (Hanks & Hunter, 1995).

Tomato G-LecRK	Present kinase subdomains
Solyc04g008400.B	I and II
Solyc03g006780	I to V
Solyc04g008370	I to V
Solyc04g077300	I to V
Solyc07g055630	I, II, VI-X
Solyc07g055640.A	I-X
Solyc02g079710	I-X
Solyc07g063750	I-X

Table 3.6. Tomato G-LecRKs classification and nomenclature.

Proposed Clade name	Proposed gene name	Cluster	Locus
I	G-LecRK-I.1	1A	Solyc01g006520
	G-LecRK-I.2	1A	Solyc01g006530
II	G-LecRK-II.1	-	Solyc02g030300
	G-LecRK-II.2	4B	Solyc04g077270
	G-LecRK-II.3	4B	Solyc04g077280
	G-LecRK-II.4	4B	Solyc04g077340
	G-LecRK-II.5	4B	Solyc04g077360
	G-LecRK-II.6	4B	Solyc04g077370
	G-LecRK-II.7	4B	Solyc04g077390
	G-LecRK-II.8	7C	Solyc07g063770
	G-LecRK-II.9	7C	Solyc07g063780
	G-LecRK-II.10	7C	Solyc07g063800
	G-LecRK-II.11	7C	Solyc07g063820
	G-LecRK-II.12	10A	Solyc10g006710
	G-LecRK-II.13	10A	Solyc10g006720
	G-LecRK-II.14	-	Solyc12g005290
III	G-LecRK-III.1	-	Solyc02g072070
	G-LecRK-III.2	7B	Solyc07g055630
	G-LecRK-III.3	7B	Solyc07g055640.A
	G-LecRK-III.4	7B	Solyc07g055640.B
IV	G-LecRK-IV.1	2A	Solyc02g079540
	G-LecRK-IV.2	2A	Solyc02g079550
V	G-LecRK-V.1	2A	Solyc02g079570
	G-LecRK-V.2	-	Solyc10g005440
VI	G-LecRK-VI.1	2A	Solyc02g079590
	G-LecRK-VI.2	3A	Solyc03g006770
VII	G-LecRK-VII.1	2A	Solyc02g079620
	G-LecRK-VII.2	2A	Solyc02g079630
VIII	G-LecRK-VIII.1	2A	Solyc02g079640
	G-LecRK-VIII.2	3A	Solyc03g006780
IX	G-LecRK-IX.1	3A	Solyc03g006720
	G-LecRK-IX.2	3A	Solyc03g006730.A
	G-LecRK-IX.3	3A	Solyc03g006730.B
X	G-LecRK-X.1	-	Solyc03g007790
	G-LecRK-X.2	-	Solyc06g036470

XI	G-LecRK-XI.1	-	Solyc03g120110
	G-LecRK-XI.2	-	Solyc12g006840
XII	G-LecRK-XII.1	4A	Solyc04g008400.A
	G-LecRK-XII.2	-	Solyc04g058110
XIII	G-LecRK-XIII.1	7A	Solyc07g053120
	G-LecRK-XIII.2	7A	Solyc07g053130
XIV	G-LecRK-XIV.1	7C	Solyc07g063700
	G-LecRK-XIV.2	7C	Solyc07g063710
	G-LecRK-XIV.3	7C	Solyc07g063720
	G-LecRK-XIV.4	7C	Solyc07g063730
XV	G-LecRK-XV.1	8A	Solyc08g076050
	G-LecRK-XV.2	8A	Solyc08g076060
Singletons	G-LecRK-S.1	-	Solyc01g014520
	G-LecRK-S.2	-	Solyc01g094830
	G-LecRK-S.3	2A	Solyc02g079530
	G-LecRK-S.4	-	Solyc02g079710
	G-LecRK-S.5	-	Solyc03g005130
	G-LecRK-S.6	-	Solyc03g063650
	G-LecRK-S.7	3B	Solyc03g078360
	G-LecRK-S.8	3B	Solyc03g078370
	G-LecRK-S.9	4A	Solyc04g008370
	G-LecRK-S.10	4A	Solyc04g008400.B
	G-LecRK-S.11	-	Solyc04g015460
	G-LecRK-S.12	4B	Solyc04g077300
	G-LecRK-S.13	-	Solyc04g078410
	G-LecRK-S.14	-	Solyc05g008310
	G-LecRK-S.15	7A	Solyc07g053080
	G-LecRK-S.16	7A	Solyc07g053220
	G-LecRK-S.17	7B	Solyc07g055650
	G-LecRK-S.18	7C	Solyc07g063750
	G-LecRK-S.19	7C	Solyc07g063810
	G-LecRK-S.20	-	Solyc08g059730
	G-LecRK-S.21	-	Solyc09g011330
	G-LecRK-S.22	9A	Solyc09g075910
	G-LecRK-S.23	9A	Solyc09g075920
	G-LecRK-S.24	-	Solyc11g005630
	G-LecRK-S.25	-	Solyc11g013880

Table 3.7. Tomato G-LecRKs localization prediction. Localization was predicted using TargetP and CELLO. PM, plasma membrane; SP, secretion pathway; MT, mitochondria, C, cytoplasm; N, nucleus; CH, chloroplast; EX, extracellular. "-" denotes no prediction.

	Gene	TargetP	CELLO
1	Solyc01g006520	SP	PM
2	Solyc01g006530	SP	PM / N
3	Solyc01g014520	SP	N
4	Solyc01g094830	SP	PM
5	Solyc02g030300	-	PM
6	Solyc02g072070	SP	PM
7	Solyc02g079530	SP	PM
8	Solyc02g079540	SP	PM
9	Solyc02g079550	SP	PM
10	Solyc02g079570	SP	PM
11	Solyc02g079590	SP	PM
12	Solyc02g079620	SP	PM
13	Solyc02g079630	CH	EX / PM
14	Solyc02g079640	SP	PM
15	Solyc02g079710	SP	PM
16	Solyc03g005130	SP	PM
17	Solyc03g006720	SP	PM
18	Solyc03g006730.A	SP	PM
19	Solyc03g006730.B	MT	PM
20	Solyc03g006770	SP	PM
21	Solyc03g006780	SP	PM
22	Solyc03g007790	SP	PM
23	Solyc03g063650	SP	PM
24	Solyc03g078360	SP	PM
25	Solyc03g078370	SP	PM
26	Solyc03g120110	SP	PM
27	Solyc04g008370	SP	PM / N
28	Solyc04g008400.A	SP	PM
29	Solyc04g008400.B	-	PM / N
30	Solyc04g015460	SP	PM
31	Solyc04g058110	SP	PM
32	Solyc04g077270	SP	PM
33	Solyc04g077280	SP	PM
34	Solyc04g077300	SP	PM

35	Solyc04g077340	SP	PM
36	Solyc04g077360	SP	PM
37	Solyc04g077370	SP	PM
38	Solyc04g077390	SP	PM
39	Solyc04g078410	SP	PM
40	Solyc05g008310	SP	PM
41	Solyc06g036470	SP	EX / PM
42	Solyc07g053080	SP	PM
43	Solyc07g053120	SP	PM
44	Solyc07g053130	SP	PM
45	Solyc07g053220	SP	PM
46	Solyc07g055630	-	N / C / MT
47	Solyc07g055640.A	MT	MT
48	Solyc07g055640.B	-	C / N
49	Solyc07g055650	-	PM / MT
50	Solyc07g063700	SP	PM
51	Solyc07g063710	SP	PM
52	Solyc07g063720	SP	PM
53	Solyc07g063730	SP	PM
54	Solyc07g063750	SP	PM
55	Solyc07g063770	SP	PM
56	Solyc07g063780	SP	PM
57	Solyc07g063800	SP	PM
58	Solyc07g063810	MT	PM
59	Solyc07g063820	SP	PM
60	Solyc08g059730	SP	PM
61	Solyc08g076050	SP	PM
62	Solyc08g076060	-	PM
63	Solyc09g011330	SP	PM
64	Solyc09g075910	SP	PM
65	Solyc09g075920	SP	PM
66	Solyc10g005440	SP	PM
67	Solyc10g006710	SP	PM
68	Solyc10g006720	SP	PM
69	Solyc11g005630	MT	PM
70	Solyc11g013880	SP	PM
71	Solyc12g005290	SP	PM
72	Solyc12g006840	SP	PM

General Conclusions

Plant parasitic nematodes can cause great crop losses of approximately US$80 billion per year worldwide (Nicol *et al.*, 2011; Jones *et al.*, 2013). Interestingly, despite the large number of plant parasitic nematodes currently identified, the biggest damage is caused by a few species, among which are *Meloidogyne* spp, the most important group of plant parasitic nematodes according to a recent classification (Jones *et al.*, 2013). These nematodes are also known by the common name “root-knot nematodes” (RKNs) because of the symptoms they cause on the roots of most plant species. Regardless of the large number of species described in this genus, four species *M. arenaria*, *M. hapla*, *M. incognita* and *M. javanica* are known to be widespread and cause most of the crop damage around the world.

Once the RKN infective stage, the second stage juveniles (J2s) localize the host, they penetrate at the root elongation zone and migrate between plant cells towards the vascular cylinder, where they establish their feeding sites, the giant cells, which are surrounded by asymmetrically dividing neighboring cells, forming the galls (de Almeida Engler *et al.*, 2010; Rodiuc *et al.*, 2014). When they establish the feeding site, RKNs become sedentary and manipulate cell machinery to their benefit. As a result, these giant cells become nutrient sinks from which the nematodes feed throughout their life cycle. Because of the central importance on the maintenance of parasitism, giant cells formation and their modulation by RKN

effectors has been extensively studied (Goto *et al.*, 2013; Hewezi & Baum, 2013; Goverse & Smant, 2014; Rodiuc *et al.*, 2014).

Additionally, vast research has focused on the characterization of the transcriptome of nematode-infected roots to understand the interaction between plants and nematodes (Ithal *et al.*, 2007; Barcala *et al.*, 2010; Kyndt *et al.*, 2012; Ji *et al.*, 2013; Portillo *et al.*, 2013). Although first studies relied on collection of root galls, which includes the feeding site and surrounding cells, later studies tried to precisely define the differences taking place at distinct cells during interaction, performing microdissection of feeding sites and comparing transcriptome in giant cells and gall cells (Klink *et al.*, 2007; Barcala *et al.*, 2010).

When my research begun, little was known about the first hours of interaction between plants and nematodes and defense responses taking place at this early stage. The existing work was mainly on the detection of ROS after RKN inoculation of Arabidopsis and tomato roots (Huang *et al.*, 1971; Zacheo *et al.*, 1982; Melillo *et al.*, 2006). In the last 2 years, the first nematode-associated molecular pattern was characterized and the early stages of interaction between the cyst nematode *Heterodera schachtii* and Arabidopsis was also investigated (Siddique *et al.*, 2014; Kammerhofer *et al.*, 2015; Manosalva *et al.*, 2015).

The results of my dissertation research also focused on the early interaction between RKN and plants and allowed characterization of plant responses to nematode migration inside root tissue. Consequently, the results presented in the first chapter of my dissertation showed for the first time the conservation of PTI

signaling partners for nematode perception, as it has been shown for microbial pathogens (Zipfel, 2014; Bigeard *et al.*, 2015; Choi & Klessig, 2016). Despite the knowledge that RKNs migrate inside plant tissues without causing great damage, this was the first work that demonstrated nematode perception in the complete absence of root penetration, using reporter lines and nematode extracts. The results presented in the first chapter are in accordance with current literature on the perception of microbial pathogens that RKN are also perceived by cell surface localized plant receptors that require the co-receptor BAK1.

The second chapter of my dissertation describes the investigation of transcriptome changes in the mutant *bak1-5* as compared to wild type plants and reveals enrichment for terms related to extracellular localization, which might show a role for BAK1 in controlling transcription of extracellular-localized proteins. Interestingly, *bak1-5* mutants have enrichment for terms related to phosphorus starvation, which could be an additional signaling pathway in which BAK1 is involved besides development and defense. Although a role for BAK1 in phosphorus starvation has not been established, the BAK1 associated protein BIK1 was previously shown to be a negative regulator of phosphate homeostasis in Arabidopsis and to be responsive to phosphorus starvation (Zhang *et al.*, 2016). Considering BAK1 and BIK1 are parts of the same protein complex at the plasma membrane, it is possible that BAK1 is also involved in phosphate homeostasis.

This RNAseq is the first whole genome transcriptome assessment of plant response to RKN migration. To our knowledge there is one additional investigation

of transcriptome response to RKN infection at an early time point, but due to technology limitation only 8 transcripts were evaluated (Lambert *et al.*, 1999). The RNAseq analysis proved to be a useful tool once again for identification of candidate genes for functional analysis. Furthermore, it allowed the identification of a negative regulator of immunity against RKN which may have broad implications for crop protection. The proposal of candidate homologs in tomato and the possibility to use current genome editing tools opens the way to breed for new resistant cultivars and provide growers with alternative plant genotypes for RKN control. It is important to emphasize the relevance of developing alternative controls for RKN, considering the restriction on the use of chemical nematicides, the development of virulent RKN strains on traditional resistant crop varieties, the widespread detection of the four main RKN species and the considerable number of crops they infect.

Root inhibition, ROS assay and quantification of transcript differential expression using RT-PCR are tools commonly used in plant pathology research in the past decades and have proven reliable to characterize plant responses to pathogens or elicitors. Using these well-established tools, I was able to demonstrate that mutations in the G-LecRK-VI.13 gene results in enhanced resistance to RKN likely as a result of increased basal levels of jasmonic acid biosynthesis or signaling in roots of these mutants. It will be interesting to characterize the other RLK encoding genes from the RNAseq analysis to identify

additional players of the PTI response to RKN and potentially identify a nematode recognition receptor.

The unbiased investigation allowed by RNAseq led to the characterization of a gene family that has not been extensively investigated, the G-type lectin receptor kinases (G-LecRKs), a family of proteins predicted to interact with carbohydrates. My investigation resulted in an update of the characterization of this family in Arabidopsis and the first description of the members of this family in tomato. Additionally, to harmonize the nomenclature of these genes in both Arabidopsis and tomato, I proposed a nomenclature system based on the one already established for another LecRK gene family in Arabidopsis, that takes into consideration not only the physical localization of the gene, but also the amino acid identity level between members of the family. Morevover, I identified motifs largely conserved among members of G-LecRKs across a single plant species as well as those conserved between tomato and Arabidopsis G-LecRKs, revealing potential essential sites for protein activity and, therefore, shedding light on understanding the function and activity of these proteins.

References

Barcala M, Garcia A, Cabrera J, Casson S, Lindsey K, Favery B, Garcia-Casado G, Solano R, Fenoll C, Escobar C. 2010. Early transcriptomic events in microdissected Arabidopsis nematode-induced giant cells. *Plant Journal* **61**(4): 698-712.

Bigeard J, Colcombet J, Hirt H. 2015. Signaling mechanisms in pattern-triggered immunity (PTI). *Molecular Plant* **8**(4): 521-539.

Choi HW, Klessig DF. 2016. DAMPs, MAMPs, and NAMPs in plant innate immunity. *BMC Plant Biology* **16**(1): 232.

de Almeida Engler J, Rodiuc N, Smertenko A, Abad P. 2010. Plant actin cytoskeleton remodeling by plant parasitic nematodes. *Plant Signaling & Behavior* **5**(3): 213-217.

Goto DB, Miyazawa H, Mar JC, Sato M. 2013. Not to be suppressed? Rethinking the host response at a root-parasite interface. *Plant Science* **213**: 9-17.

Goverse A, Smant G. 2014. The activation and suppression of plant innate immunity by parasitic nematodes. *Annual Review of Phytopathology* **52**: 243-265.

Hewezi T, Baum TJ. 2013. Manipulation of plant cells by cyst and root-knot nematode effectors. *Molecular Plant-Microbe Interactions* **26**(1): 9-16.

Huang CS, Lin LH, Huang SP. 1971. Changes in peroxidase isoenzymes in tomato galls induced by *Meloidogyne incognita*. *Nematologica* **17**: 460-466.

Ithal N, Recknor J, Nettleton D, Hearne L, Maier T, Baum TJ, Mitchum MG. 2007. Parallel genome-wide expression profiling of host and pathogen during soybean cyst nematode infection of soybean. *Molecular Plant-Microbe Interactions* **20**(3): 293-305.

Ji H, Gheysen G, Denil S, Lindsey K, Topping JF, Nahar K, Haegeman A, De Vos WH, Trooskens G, Van Criekinge W, et al. 2013. Transcriptional analysis through RNA sequencing of giant cells induced by *Meloidogyne graminicola* in rice roots. *Journal of Experimental Botany* **64**(12): 3885-3898.

Jones JT, Haegeman A, Danchin EGJ, Gaur HS, Helder J, Jones MGK, Kikuchi T, Manzanilla-López R, Palomares-Rius JE, Wesemael WML,

et al. 2013. Top 10 plant-parasitic nematodes in molecular plant pathology. *Molecular Plant Pathology* **14**(9): 946-961.

Kammerhofer N, Radakovic Z, Regis JMA, Dobrev P, Vankova R, Grundler FMW, Siddique S, Hofmann J, Wieczorek K. 2015. Role of stress-related hormones in plant defence during early infection of the cyst nematode *Heterodera schachtii* in Arabidopsis. *New Phytologist* **207**: 778-789.

Klink VP, Overall CC, Alkharouf NW, MacDonald MH, Matthews BF. 2007. Laser capture microdissection (LCM) and comparative microarray expression analysis of syncytial cells isolated from incompatible and compatible soybean (*Glycine max*) roots infected by the soybean cyst nematode (*Heterodera glycines*). *Planta* **226**(6): 1389-1409.

Kyndt T, Denil S, Haegeman A, Trooskens G, Bauters L, Van Criekinge W, De Meyer T, Gheysen G. 2012. Transcriptional reprogramming by root knot and migratory nematode infection in rice. *New Phytologist* **196**: 887-900.

Lambert KN, Ferrie BJ, Nombela G, Brenner ED, Williamson VM. 1999. Identification of genes whose transcripts accumulate rapidly in tomato after root-knot nematode infection. *Physiological and Molecular Plant Pathology* **55**: 341-348.

Manosalva P, Manohar M, von Reuss SH, Chen S, Koch A, Kaplan F, Choe A, Micikas RJ, Wang X, Kogel K-H, et al. 2015. Conserved nematode signalling molecules elicit plant defenses and pathogen resistance. *Nature Communications* **6**: 7795.

Melillo MT, Leonetti P, Bongiovanni M, Castagnone-Sereno P, Bleve-Zacheo T. 2006. Modulation of reactive oxygen species activities and H2O2 accumulation during compatible and incompatible tomato-root-knot nematode interactions. *New Phytologist* **170**: 501-512.

Nicol JM, Turner SJ, Coyne DL, den Nijs L, Hockland S, Maafi ZT 2011. Current nematode threats to world agriculture. In: Jones JT, Gheysen G, Fenoll C eds. *Genomics and molecular genetics of plant–nematode interactions*. Heidelberg: Springer, 21–44.

Portillo M, Cabrera J, Lindsey K, Topping J, Andres MF, Emiliozzi M, Oliveros JC, Garcia-Casado G, Solano R, Koltai H, et al. 2013. Distinct and conserved transcriptomic changes during nematode-induced giant cell development in tomato compared with Arabidopsis: a functional role for gene repression. *New Phytologist* **197**: 1276-1290.

Rodiuc N, Vieira P, Banora MY, de Almeida Engler J. 2014. On the track of transfer cell formation by specialized plant-parasitic nematodes. *Frontiers in Plant Science* **5**: 160.

Siddique S, Matera C, Radakovic ZS, Shamim Hasan M, Gutbrod P, Rozanska E, Sobczak M, Angel Torres M, Grundler FM. 2014. Parasitic worms stimulate host NADPH oxidases to produce reactive oxygen species that limit plant cell death and promote infection. *Science signaling* **7**(320): ra33.

Zacheo G, Bleve-Zacheo T, Lamberti F. 1982. Involvement of superoxide dismutases and superoxide radicals in the susceptibility and resistance of tomato plants to infestation by *Meloidogyne incognita*. *Nematologia Mediterranea* **10**: 75-80.

Zhang H, Huang L, Hong Y, Song F. 2016. BOTRYTIS-INDUCED KINASE1, a plasma membrane-localized receptor-like protein kinase, is a negative regulator of phosphate homeostasis in *Arabidopsis thaliana*. *BMC Plant Biology* **16**(1): 152.

Zipfel C. 2014. Plant pattern-recognition receptors. *Trends in Immunology* **35**: 345-351.

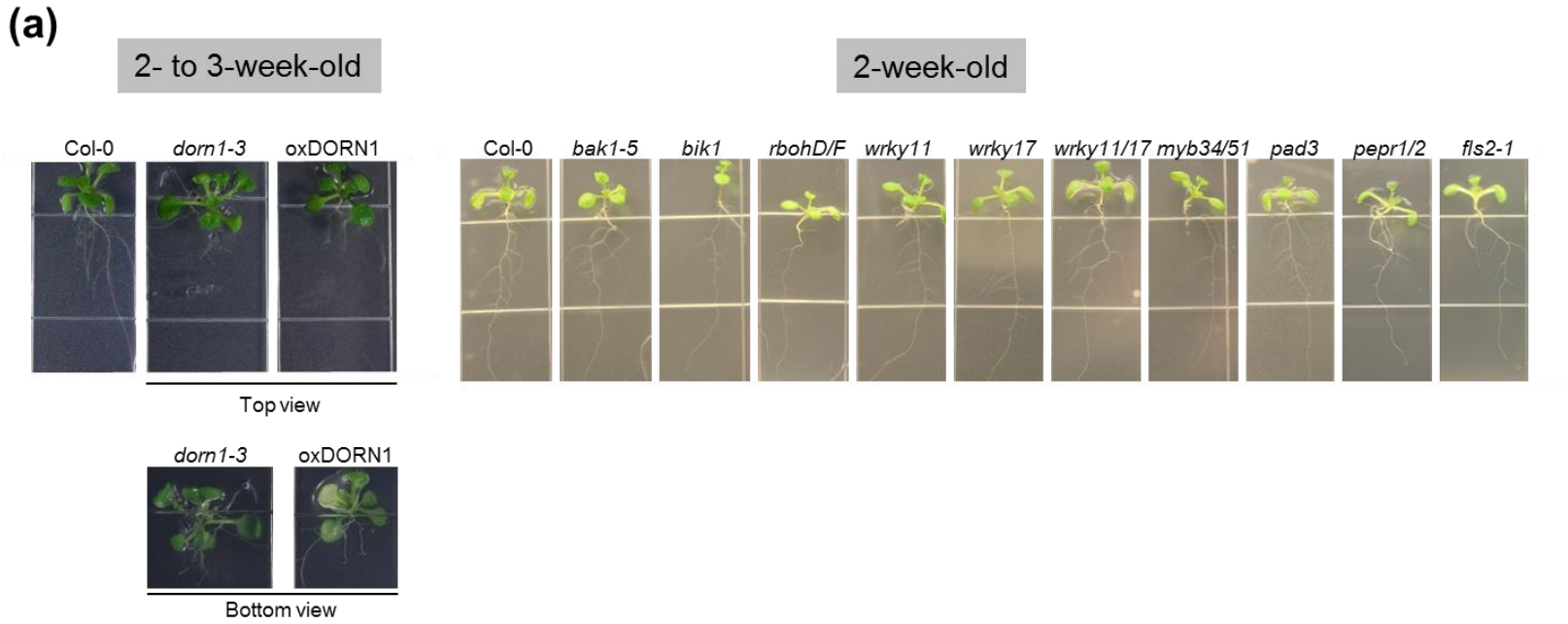

Appendix A. Root phenotypes of 2- to 3-week-old (a) and 1-week-old (b) seedlings of *A. thaliana* wild type Col-0 and mutants. Seedlings were germinated on Gamborg media supplemented with 3% sucrose and 0.6% daishin agar and maintained in plant growth rooms with 12 h light photoperiod at 24˚C.

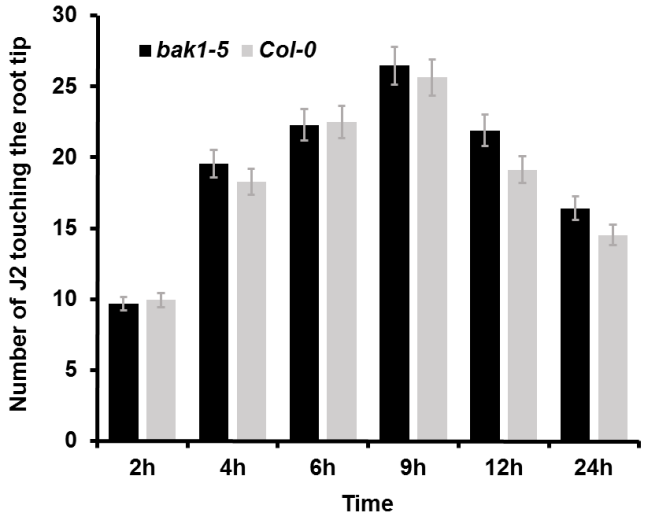

Appendix B. RKNs are equally attracted to the roots of *A. thaliana* wild type Col-0 and *bak1-5* mutant. Number of J2s touching the root tip of 8-day-old *A. thaliana* seedlings ± SE, n=48, at the indicated time after exposure to nematodes. This experiment was repeated twice with similar results. No significant difference was observed between the two genotypes.

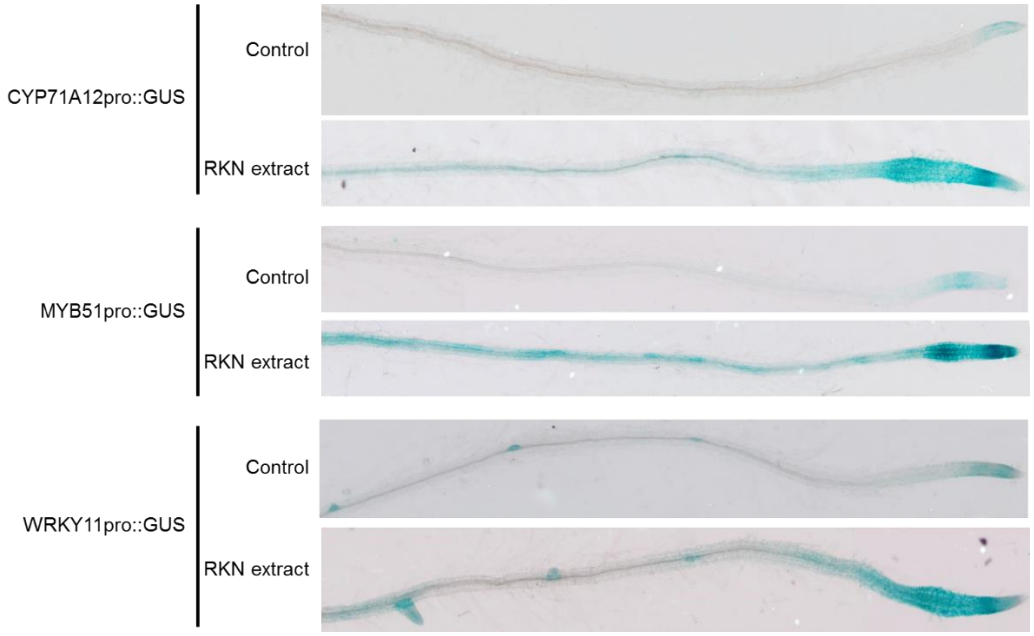

Appendix C. RKN crude extracts do not elicit GUS activity in the root maturation zone of *A. thaliana* GUS reporter lines. GUS activity was evaluated 24 h post treatment with crude RKN extracts. This experiment was performed six times with similar results

Appendix D . List of differentially expressed genes in naïve *bak1-5* roots as compared to naïve Col-0 roots with FDR<0.01 and 1<FC<1.

Accession number	Description	logFC
AT1G53480	mto 1 responding down 1	6.37
AT4G12490	Bifunctional inhibitor/lipid-transfer protein/seed storage 2S albumin superfamily	3.25
AT5G35777	transposable element gene	2.62
AT4G12500	Bifunctional inhibitor/lipid-transfer protein/seed storage 2S albumin superfamily	2.34
AT3G27940	Lob domain-containing protein 26	2.29
AT2G16190	Hydroxyproline-rich glycoprotein	2.20
AT3G06545	Unknown protein	1.93
AT2G16180	transposable element gene	1.88
AT4G01390	TRAF-like family protein	1.84
AT4G22214	Defensin-like (DEFL) family protein	1.81
AT4G11190	Disease resistance-responsive (dirigent-like protein) family protein	1.80
AT1G71920	HISTIDINE BIOSYNTHESIS 6B	1.76
AT5G50700	hydroxysteroid dehydrogenase 1	1.71
AT5G06905	cytochrome P450, family 712, subfamily A, polypeptide 2	1.71
AT2G28860	cytochrome P450, family 710, subfamily A, polypeptide 4	1.68
AT2G26560	phospholipase A 2A	1.68
AT3G16530	Lectin like protein	1.65
AT5G53190	Nodulin MtN3 family protein	1.65
AT5G09570	Cox19-like CHCH family protein	1.63
AT1G19960	Transmembrane receptor	1.60
AT5G06900	cytochrome P450, family 93, subfamily D, polypeptide 1	1.59
AT1G52130	Mannose-binding lectin superfamily protein	1.59
AT1G15540	2-oxoglutarate (2OG) and Fe(II)-dependent oxygenase superfamily protein	1.59
AT3G52970	cytochrome P450, family 76, subfamily G, polypeptide 1	1.59
AT5G63580	flavonol synthase 2	1.54

AT1G51840	protein kinase-related	1.54
AT1G51830	Leucine-rich repeat protein kinase family protein	1.53
AT4G14250	structural constituent of ribosome	1.53
AT5G36140	cytochrome P450, family 716, subfamily A, polypeptide 2	1.53
AT1G52790	2-oxoglutarate (2OG) and Fe(II)-dependent oxygenase superfamily protein	1.52
AT2G18470	proline-rich extensin-like receptor kinase 4	1.48
AT2G27535	ribosomal protein L10A family protein	1.47
AT5G47600	HSP20-like chaperones superfamily protein	1.47
AT4G24890	purple acid phosphatase 24	1.43
AT4G22610	Bifunctional inhibitor/lipid-transfer protein/seed storage 2S albumin superfamily	1.43
AT5G24780	vegetative storage protein 1	1.43
AT5G50600	hydroxysteroid dehydrogenase 1	1.40
AT4G38970	fructose-bisphosphate aldolase 2	1.38
AT1G77110	Auxin efflux carrier family protein	1.36
AT3G13950	Unknown protein	1.36
AT5G42600	marneral synthase	1.36
AT5G17700	MATE efflux family protein	1.34
AT5G57785	Unknown protein	1.33
AT5G37990	S-adenosyl-L-methionine-dependent methyltransferases superfamily protein	1.33
AT5G47990	cytochrome P450, family 705, subfamily A, polypeptide 5	1.33
AT5G48485	Bifunctional inhibitor/lipid-transfer protein/seed storage 2S albumin superfamily	1.32
AT3G59710	NAD(P)-binding Rossmann-fold superfamily protein	1.32
AT5G22890	C2H2 and C2HC zinc fingers superfamily protein	1.31
AT5G48010	thalianol synthase 1	1.31
AT5G38020	S-adenosyl-L-methionine-dependent methyltransferases superfamily protein	1.27
AT4G22217	Arabidopsis defensin-like protein	1.27
AT5G20710	beta-galactosidase 7	1.26
AT5G50760	SAUR-like auxin-responsive protein family	1.25

AT1G69880	thioredoxin H-type 8	1.25
AT5G38100	S-adenosyl-L-methionine-dependent methyltransferases superfamily protein	1.25
AT5G48000	cytochrome P450, family 708, subfamily A, polypeptide 2	1.25
AT5G42580	cytochrome P450, family 705, subfamily A, polypeptide 12	1.22
AT2G05400	Ubiquitin-specific protease family C19-related protein	1.22
AT4G00780	TRAF-like family protein	1.21
AT4G39770	Haloacid dehalogenase-like hydrolase (HAD) superfamily protein	1.20
AT2G02990	ribonuclease 1	1.20
AT5G28145	transposable element gene	1.20
AT1G14960	Polyketide cyclase/dehydrase and lipid transport superfamily protein	1.19
AT5G52390	PAR1 protein	1.19
AT4G12480	Bifunctional inhibitor/lipid-transfer protein/seed storage 2S albumin superfamily	1.19
AT5G62330	Plant invertase/pectin methylesterase inhibitor superfamily protein	1.18
AT1G08430	aluminum-activated malate transporter 1	1.18
AT2G30750	cytochrome P450, family 71, subfamily A, polypeptide 12	1.18
AT5G24770	vegetative storage protein 2	1.18
AT3G08860	Pyrimidine 4	1.17
AT2G26370	MD-2-related lipid recognition domain-containing protein	1.17
AT3G28300	AT14A	1.16
AT5G44400	FAD-binding Berberine family protein	1.16
AT2G39310	JAL22 - jacalin related lectin	1.15
AT3G57160	Unknown protein	1.14
AT5G10330	histidinol phosphate aminotransferase 1	1.13
AT1G67110	cytochrome P450, family 735, subfamily A, polypeptide 2	1.12
AT2G34490	cytochrome P450, family 710, subfamily A, polypeptide 2	1.12
AT4G12550	Auxin-Induced in Root cultures 1	1.11
AT1G65970	thioredoxin-dependent peroxidase 2	1.10
AT2G43510	TI1 - trypsin inhibitor protein 1	1.10

AT1G73120	Unknown protein	1.09
AT1G55670	photosystem I subunit G	1.08
AT5G26270	Unknown protein	1.05
AT2G01610	Plant invertase/pectin methylesterase inhibitor superfamily protein	1.03
AT1G78460	SOUL heme-binding family protein	1.02
AT1G10640	Pectin lyase-like superfamily protein	1.00
AT4G37050	PATATIN-like protein 4	-1.00
AT1G08310	alpha/beta-Hydrolases superfamily protein	-1.01
AT2G40750	WRKY54	-1.01
AT3G53830	Regulator of chromosome condensation (RCC1) family protein	-1.02
AT5G63130	Octicosapeptide/Phox/Bem1p family protein	-1.02
AT4G27280	Calcium-binding EF-hand family protein	-1.03
AT4G29780	Unknown protein	-1.03
AT1G64670	alpha/beta-Hydrolases superfamily protein	-1.03
AT1G08090	nitrate transporter 2:1	-1.04
AT1G49450	Transducin/WD40 repeat-like superfamily protein	-1.05
AT1G73010	phosphate starvation-induced gene 2	-1.05
AT4G28150	Protein of unknown function (DUF789)	-1.06
AT3G45960	expansin-like A3	-1.06
ATMG00980	Ribosomal protein S12/S23 family protein	-1.06
AT3G03530	NPC4	-1.07
AT3G56970	basic helix-loop-helix (bHLH) DNA-binding superfamily protein	-1.07
AT5G15960	stress-responsive protein (KIN1) / stress-induced protein (KIN1)	-1.10
AT5G05410	DRE-binding protein 2A	-1.11
AT3G47950	H(+)-ATPase 4	-1.12
AT1G66400	calmodulin like 23	-1.12
AT1G29740	Leucine-rich repeat transmembrane protein kinase	-1.13
AT2G07751	NADH:ubiquinone/plastoquinone oxidoreductase, chain 3 protein	-1.13

AT2G19200	Unknown protein	-1.13
AT1G01580	ferric reduction oxidase 2	-1.14
AT2G11810	monogalactosyldiacylglycerol synthase type C	-1.15
AT2G07675	Ribosomal protein S12/S23 family protein	-1.16
AT1G49030	PLAC8 family protein	-1.17
AT1G07135	glycine-rich protein	-1.17
AT1G29670	GDSL-like Lipase/Acylhydrolase superfamily protein	-1.17
AT5G54790	VUP4 – Vascular-related unknown protein 4	-1.18
AT1G08100	nitrate transporter 2.2	-1.18
AT3G47380	Plant invertase/pectin methylesterase inhibitor superfamily protein	-1.18
AT4G14630	germin-like protein 9	-1.18
AT4G35190	Putative lysine decarboxylase family protein	-1.19
AT3G22910	ATPase E1-E2 type family protein	-1.20
AT1G26200	TRAM, LAG1 and CLN8 (TLC) lipid-sensing domain containing protein	-1.21
AT1G08440	Aluminium activated malate transporter family protein	-1.21
AT4G17680	SBP (S-ribonuclease binding protein) family protein	-1.23
AT5G39720	avirulence induced gene 2 like protein	-1.23
AT3G17790	PAP17 - purple acid phosphatase 17	-1.24
AT3G52820	purple acid phosphatase 22	-1.24
AT5G20410	monogalactosyldiacylglycerol synthase 2	-1.24
AT3G58060	Cation efflux family protein	-1.25
AT3G29000	Calcium-binding EF-hand family protein	-1.28
AT5G51190	Integrase-type DNA-binding superfamily protein	-1.29
AT5G57560	Xyloglucan endotransglucosylase/hydrolase family protein	-1.29
AT3G54450	Major facilitator superfamily protein	-1.30
AT5G33355	Defensin-like (DEFL) family protein	-1.31
AT2G18550	homeobox protein 21	-1.31
AT3G30210	myb domain protein 121	-1.31

AT1G18300	nudix hydrolase homolog 4	-1.33
AT5G52310	low-temperature-responsive 78 (LTI78) / desiccation-responsive 29A (RD29A)	-1.34
AT1G14540	Peroxidase superfamily protein	-1.36
AT1G58420	Uncharacterised conserved protein UCP031279	-1.37
AT1G27730	salt tolerance zinc finger	-1.37
AT1G13480	Protein of unknown function (DUF1262)	-1.37
AT4G22120	ERD (early-responsive to dehydration stress) family protein	-1.37
AT4G24170	ATP binding microtubule motor family protein	-1.38
AT5G39670	Calcium-binding EF-hand family protein	-1.38
AT1G05650	Pectin lyase-like superfamily protein	-1.40
AT5G24860	flowering promoting factor 1	-1.40
AT1G23110	Unknown protein	-1.42
AT1G73220	organic cation/carnitine transporter1	-1.42
AT3G44260	Polynucleotidyl transferase, ribonuclease H-like superfamily protein	-1.42
ATMG00990	NADH dehydrogenase 3	-1.43
AT5G08250	Cytochrome P450 superfamily protein	-1.44
AT2G17660	RPM1-interacting protein 4 (RIN4) family protein	-1.44
AT3G46400	Leucine-rich repeat protein kinase family protein	-1.44
AT1G47603	purine permease 19	-1.44
AT5G28520	Mannose-binding lectin superfamily protein	-1.48
AT4G25470	C-repeat/DRE binding factor 2	-1.55
AT4G13395	ROTUNDIFOLIA like 12	-1.55
AT4G09110	RING/U-box superfamily protein	-1.56
AT2G41810	Unknown protein	-1.57
AT3G47420	phosphate starvation-induced gene 3	-1.59
AT5G17350	Unknown protein	-1.59
AT2G23400	Undecaprenyl pyrophosphate synthetase family protein	-1.61
AT5G42380	calmodulin like 37	-1.67

AT4G24570	dicarboxylate carrier 2	-1.70
AT3G09922	IPS1 - induced by phosphate starvation 1	-1.71
AT1G34047	Defensin-like (DEFL) family protein	-1.71
AT3G23250	MYB15	-1.71
AT4G27657	Unknown protein	-1.74
AT5G20150	SPX domain gene 1	-1.76
AT4G26050	plant intracellular ras group-related LRR 8	-1.81
AT2G43890	Pectin lyase-like superfamily protein	-1.81
AT1G56600	galactinol synthase 2	-1.84
AT5G60770	nitrate transporter 2.4	-1.87
AT1G73000	PYR1-like 3	-1.96
AT3G20360	TRAF-like family protein	-2.21
AT1G50050	CAP (Cysteine-rich secretory, Antigen 5,Pathogenesis-related 1) superfamily	-2.22
AT1G66930	Protein kinase superfamily protein	-2.32
AT4G25490	C-repeat/DRE binding factor 1	-2.33
AT5G20790	Unknown protein	-2.35
AT2G02010	glutamate decarboxylase 4	-2.53
AT4G32950	Protein phosphatase 2C family protein	-2.76
AT2G36255	Defensin-like (DEFL) family protein	-2.86
AT5G54700	Ankyrin repeat family protein	-2.92
AT3G45060	high affinity nitrate transporter 2.6	-2.96
AT5G43360	phosphate transporter 1;3	-2.97
AT1G20860	phosphate transporter 1;8	-3.01
AT2G04460	transposable element gene	-3.70
AT3G25240	Protein of unknown function	-4.18

Appendix E . List of differentially expressed genes in response to root-knot nematode penetration/migration in Col-0 roots with FDR<0.01 and 1<FC<1.

Accession number	Description	FC
AT3G44860	farnesoic acid carboxyl-O-methyltransferase	9.89
AT2G24850	tyrosine aminotransferase 3	7.85
AT2G26380	Leucine-rich repeat (LRR) family protein	6.78
AT5G05340	Peroxidase superfamily protein	6.62
AT4G37710	VQ motif-containing protein	6.04
AT5G12020	17.6 kDa class II heat shock protein	5.42
AT1G64160	Disease resistance-responsive (dirigent-like protein) family protein	5.30
AT3G44870	S-adenosyl-L-methionine-dependent methyltransferases superfamily protein	5.15
AT3G60120	beta glucosidase 27	4.98
AT4G21380	receptor kinase 3	4.89
AT3G49620	2-oxoglutarate (2OG) and Fe(II)-dependent oxygenase superfamily protein	4.75
AT5G61890	Integrase-type DNA-binding superfamily protein	4.46
AT3G60420	Phosphoglycerate mutase family protein	4.31
AT1G56250	phloem protein 2-B14	4.13
AT5G13220	jasmonate-zim-domain protein 10	4.13
AT5G20230	blue-copper-binding protein	4.09
AT1G70130	Concanavalin A-like lectin protein kinase family protein	4.02
AT5G12030	heat shock protein 17.6A	3.91
AT1G56240	phloem protein 2-B13	3.64
AT4G22470	protease inhibitor/seed storage/lipid transfer protein (LTP) family protein	3.50
AT3G47480	Calcium-binding EF-hand family protein	3.44
AT5G39580	Peroxidase superfamily protein	3.42
AT3G16530	Lectin like protein induced by chitin	3.36
AT5G07310	Integrase-type DNA-binding superfamily protein	3.29
AT2G30750	CYP71A12	3.19

AT5G36925	Aracin1	3.16
AT5G39100	germin-like protein 6	3.14
AT5G06720	peroxidase 2	3.05
AT5G64870	SPFH/Band 7/PHB domain-containing membrane-associated protein family	2.96
AT1G49570	Peroxidase superfamily protein	2.95
AT1G32970	Subtilisin-like serine endopeptidase family protein	2.92
AT2G29460	glutathione S-transferase tau 4	2.87
AT5G52670	Copper transport protein family	2.86
AT4G22610	Bifunctional inhibitor/lipid-transfer protein/seed storage 2S albumin superfamily	2.86
AT1G69920	glutathione S-transferase TAU 12	2.79
AT2G41100	Calmodulin like 12 / Touch 3	2.73
AT4G24340	Phosphorylase superfamily protein	2.72
AT5G22300	nitrilase 4	2.71
AT1G69930	glutathione S-transferase TAU 11	2.70
AT5G40000	P-loop containing nucleoside triphosphate hydrolases superfamily protein	2.69
AT1G76640	Calcium-binding EF-hand family protein	2.55
AT4G22710	cytochrome P450, family 706, subfamily A, polypeptide 2	2.55
AT4G12490	Bifunctional inhibitor/lipid-transfer protein/seed storage 2S albumin superfamily	2.54
AT1G53540	HSP20-like chaperones superfamily protein	2.53
AT3G59710	NAD(P)-binding Rossmann-fold superfamily protein	2.49
AT1G66090	Disease resistance protein (TIR-NBS class)	2.47
AT1G02930	glutathione S-transferase 6	2.43
AT5G19110	Eukaryotic aspartyl protease family protein	2.42
AT1G35140	Phosphate-responsive 1 family protein	2.41
AT5G52390	PAR1 protein	2.40
AT2G44578	RING/U-box superfamily protein	2.36
AT2G02010	glutamate decarboxylase 4	2.34
AT1G33030	O-methyltransferase family protein	2.33

AT2G28500	LOB domain-containing protein 11	2.33
AT1G14550	Peroxidase superfamily protein	2.33
AT2G02990	ribonuclease 1	2.31
AT5G40590	Cysteine/Histidine-rich C1 domain family protein	2.28
AT4G22690	cytochrome P450, family 706, subfamily A, polypeptide 1	2.28
AT1G62280	SLAC1 homologue 1	2.24
AT3G47340	glutamine-dependent asparagine synthase 1	2.21
AT3G26830	PAD3	2.18
AT2G17330	CYP51A1	2.17
AT1G72930	toll/interleukin-1 receptor-like	2.16
AT5G64120	Peroxidase superfamily protein	2.15
AT5G52720	Copper transport protein family	2.14
AT3G54150	S-adenosyl-L-methionine-dependent methyltransferases superfamily protein	2.13
AT4G38420	SKU5 similar 9	2.10
AT2G19800	myo-inositol oxygenase 2	2.09
AT4G18170	WRKY DNA-binding protein 28	2.09
AT2G41380	S-adenosyl-L-methionine-dependent methyltransferases superfamily protein	2.07
AT2G43530	Defensin-like (DEFL) family protein	2.07
AT5G38940	RmlC-like cupins superfamily protein	2.06
AT5G19880	Peroxidase superfamily protein	2.06
AT4G36430	Peroxidase superfamily protein	2.05
AT1G05700	Leucine-rich repeat transmembrane protein kinase protein	2.02
AT4G01390	TRAF-like family protein	2.02
AT4G22020	pseudogene glycine rich protein	2.01
AT5G54710	Ankyrin repeat family protein	1.99
AT2G46750	ATGULLO2	1.99
AT1G02920	glutathione S-transferase 7	1.95
AT1G08830	copper/zinc superoxide dismutase 1	1.94

AT2G26370	MD-2-related lipid recognition domain-containing protein	1.93
AT5G22580	Stress responsive A/B Barrel Domain	1.92
AT1G36622	Unknown	1.92
AT4G04760	Major facilitator superfamily protein	1.92
AT2G43510	Defensin-like (DEFL) family protein - Trypsin inhibitor	1.91
AT4G12480	Bifunctional inhibitor/lipid-transfer protein/seed storage 2S albumin superfamily	1.90
AT5G39110	RmlC-like cupins superfamily protein	1.89
AT2G24600	Ankyrin repeat family protein	1.89
AT1G26380	FAD-binding Berberine family protein	1.87
AT3G28600	P-loop containing nucleoside triphosphate hydrolases superfamily protein	1.86
AT4G21680	NITRATE TRANSPORTER 1.8	1.86
AT1G14540	Peroxidase superfamily protein	1.85
AT3G23250	MYB 15	1.83
AT4G00910	Aluminium activated malate transporter family protein	1.80
AT2G26740	soluble epoxide hydrolase	1.79
AT1G65500	Unknown	1.77
AT2G40330	PY1-like 6	1.76
AT3G17690	ATCNGC19	1.76
AT1G51830	Leucine-rich repeat protein kinase family protein	1.75
AT2G18150	Peroxidase superfamily protein	1.75
AT4G22214	Defensin-like (DEFL) family protein	1.75
AT5G06860	polygalacturonase inhibiting protein 1	1.74
AT3G48850	phosphate transporter 3;2	1.74
AT5G57220	cytochrome P450, family 81, subfamily F, polypeptide 2	1.72
AT1G21520	unknown	1.72
AT5G35940	Mannose-binding lectin superfamily protein	1.72
AT3G46230	heat shock protein 17.4	1.71
AT3G20395	NA	1.71

AT2G36800	DGOT-1	1.71
AT5G46590	NAC domain containing protein 96	1.69
AT4G08040	1-aminocyclopropane-1-carboxylate synthase 11	1.69
AT4G08770	Peroxidase superfamily protein	1.68
AT1G47510	inositol polyphosphate 5-phosphatase 11	1.68
AT5G12340	Unknown	1.67
AT5G37490	ARM repeat superfamily protein	1.66
AT1G23730	beta carbonic anhydrase 3	1.66
AT5G01380	Homeodomain-like superfamily protein	1.65
AT2G31081	CLE4	1.65
AT1G19380	Protein of unknown function (DUF1195)	1.64
AT2G43140	basic helix-loop-helix (bHLH) DNA-binding superfamily protein	1.62
AT3G22910	ATPase family	1.62
AT2G47550	Plant invertase/pectin methylesterase inhibitor superfamily	1.61
AT2G04040	MATE efflux family protein	1.61
AT3G28580	P-loop containing nucleoside triphosphate hydrolases superfamily protein	1.60
AT3G23240	ERF1	1.58
AT4G13300	terpenoid synthase 13	1.58
AT4G06746	related to AP2 9	1.58
AT2G44840	ERF13	1.57
AT3G16150	ASPGB1	1.57
AT1G66280	Glycosyl hydrolase superfamily protein	1.56
AT4G10500	2-oxoglutarate (2OG) and Fe(II)-dependent oxygenase superfamily protein	1.56
AT1G51840	protein kinase-related	1.56
AT3G09940	ATMDAR3	1.55
AT5G38100	S-adenosyl-L-methionine-dependent methyltransferases superfamily protein	1.55
AT2G28860	cytochrome P450, family 710, subfamily A, polypeptide 4	1.54
AT5G46330	Leucine-rich receptor-like protein kinase family protein	1.53

AT2G18140	Peroxidase superfamily protein	1.53
AT1G61560	Seven transmembrane MLO family protein	1.52
AT1G15040	Class I glutamine amidotransferase-like superfamily protein	1.52
AT4G31500	cytochrome P450, family 83, subfamily B, polypeptide 1	1.52
AT5G02170	Transmembrane amino acid transporter family protein	1.51
AT3G27950	GDSL motif	1.51
AT3G30775	Methylenetetrahydrofolate reductase family protein	1.51
AT3G46110	Domain of unknown function (DUF966)	1.51
AT3G61280	Arabidopsis thaliana protein of unknown function (DUF821)	1.51
AT5G03390	Protein of unknown function (DUF295)	1.50
AT4G13310	cytochrome P450, family 71, subfamily A, polypeptide 20	1.50
AT2G28190	copper/zinc superoxide dismutase 2	1.49
AT3G59750	Concanavalin A-like lectin protein kinase family protein	1.48
AT4G16260	Glycosyl hydrolase superfamily protein	1.48
AT5G38710	Methylenetetrahydrofolate reductase family protein	1.48
AT5G26920	Cam-binding protein 60-like G	1.47
AT5G39050	HXXXD-type acyl-transferase family protein	1.47
AT1G08430	aluminum-activated malate transporter 1	1.47
AT4G35770	Rhodanese/Cell cycle control phosphatase superfamily protein	1.47
AT2G32190	unknown	1.46
AT5G24140	squalene monooxygenase 2	1.46
AT4G02330	Plant invertase/pectin methylesterase inhibitor superfamily	1.46
AT5G36220	cytochrome p450 81d1	1.46
AT4G08950	Phosphate-responsive 1 family protein	1.45
AT5G38200	Class I glutamine amidotransferase-like superfamily protein	1.45
AT5G64750	Integrase-type DNA-binding superfamily protein	1.43
AT4G02520	glutathione S-transferase PHI 2	1.43
AT1G06540	unknown	1.43

AT1G66160	CYS, MET, PRO, and GLY protein 1	1.42
AT5G22890	C2H2 and C2HC zinc fingers superfamily protein	1.41
AT3G29670	HXXXD-type acyl-transferase family protein	1.41
AT3G48580	xyloglucan endotransglucosylase/hydrolase 11	1.41
AT1G13480	Protein of unknown function (DUF1262)	1.41
AT5G20820	SAUR-like auxin-responsive protein family	1.41
AT5G46050	peptide transporter 3	1.40
AT1G69880	thioredoxin H-type 8	1.40
AT2G38870	PR-6 proteinase inhibitor group	1.40
AT2G43000	ANAC042	1.40
AT1G31290	ARGONAUTE 3	1.40
AT2G02930	glutathione S-transferase F3	1.39
AT3G25730	Ethylene response DNA binding factor 3	1.38
AT5G53990	UDP-Glycosyltransferase superfamily protein	1.38
AT1G55200	Protein kinase protein with adenine nucleotide alpha hydrolases-like domain	1.37
AT4G08780	Peroxidase superfamily protein	1.37
AT1G30530	UDP-glucosyl transferase 78D1	1.36
AT5G19890	Peroxidase superfamily protein	1.36
AT5G23820	MD-2-related lipid recognition domain-containing protein	1.36
AT2G34350	Major facilitator superfamily protein	1.36
AT1G06520	glycerol-3-phosphate acyltransferase 1	1.36
AT3G25760	AOC1	1.34
AT4G11170	Disease resistance protein (TIR-NBS-LRR class) family	1.33
AT3G14620	CYP72A8	1.32
AT4G14365	XB3 ortholog 4 in Arabidopsis thaliana	1.32
AT5G57560	Xyloglucan endotransglucosylase/hydrolase family protein	1.32
AT3G50930	cytochrome BC1 synthesis	1.32
AT5G41280	Receptor-like protein kinase-related family protein	1.31

AT5G50760	SAUR-like auxin-responsive protein family	1.31
AT4G34510	3-ketoacyl-CoA synthase 17	1.31
AT2G32660	receptor like protein 22	1.30
AT5G18470	Curculin-like (mannose-binding) lectin family protein	1.30
AT1G53980	Ubiquitin-like superfamily protein	1.30
AT3G15356	legume lectin family protein - fungus resistance	1.30
AT5G26220	ChaC-like family protein	1.30
AT4G12470	azelaic acid induced 1	1.29
AT4G21830	methionine sulfoxide reductase B7	1.29
AT3G01970	WRKY45	1.28
AT2G38860	DJ-1E	1.28
AT4G21840	methionine sulfoxide reductase B8	1.28
AT3G04420	ANAC048	1.27
AT2G34930	LRR cell wall response to fungus	1.27
AT1G73805	Calmodulin binding protein-like	1.26
AT2G36110	polynucleotydil	1.26
AT4G30270	xyloglucan endotransglucosylase/hydrolase 24	1.25
AT1G17380	jasmonate-zim-domain protein 5	1.25
AT1G35910	Haloacid dehalogenase-like hydrolase (HAD) superfamily protein	1.25
AT1G72920	Toll-Interleukin-Resistance (TIR) domain family protein	1.24
AT4G26200	1-amino-cyclopropane-1-carboxylate synthase 7	1.24
AT3G18250	putative membrane liproprotein	1.24
AT3G13610	2-oxoglutarate (2OG) and Fe(II)-dependent oxygenase superfamily protein	1.23
AT1G56430	nicotianamine synthase 4	1.23
AT2G04050	MATE efflux family protein	1.23
AT3G13950	unknown	1.22
AT1G60730	NAD(P)-linked oxidoreductase superfamily protein	1.22
AT2G43620	Chitinase family protein	1.21

AT5G52320	cytochrome P450, family 96, subfamily A, polypeptide 4	1.21
AT1G76930	extensin 4	1.21
AT1G66600	ABA overly sensitive mutant 3	1.20
AT5G47220	ethylene responsive element binding factor 2	1.19
AT3G23550	MATE efflux family protein	1.19
AT5G06730	Peroxidase superfamily protein	1.18
AT1G18970	germin-like protein 4	1.18
AT4G25810	xyloglucan endotransglycosylase 6	1.18
AT4G01700	Chitinase family protein	1.18
AT2G05380	glycine-rich protein 3 short isoform	1.18
AT5G05730	anthranilate synthase alpha subunit 1	1.17
AT5G24600	Protein of unknown function, DUF599	1.17
AT2G27389	unknown endomembrane	1.16
AT1G72450	jasmonate-zim-domain protein 6	1.16
AT2G36690	2-oxoglutarate (2OG) and Fe(II)-dependent oxygenase superfamily protein	1.16
AT5G64810	WRKY DNA-binding protein 51	1.16
AT3G25770	AOC2	1.16
AT2G22880	VQ motif-containing protein	1.16
AT2G34390	Aquaporin NIP2	1.15
AT1G61550	S-locus lectin protein kinase family protein	1.15
AT1G07400	HSP20-like chaperones superfamily protein	1.15
AT3G04720	PR-4	1.15
AT2G19190	FLG22-induced receptor-like kinase 1	1.15
AT1G26250	Proline-rich extensin-like family protein	1.15
AT5G28646	TPX2 (targeting protein for Xklp2) protein family	1.14
AT2G26530	Protein of unknown function (DUF1645)	1.14
AT5G52750	Heavy metal transport/detoxification superfamily protein	1.14
AT3G51450	Calcium-dependent phosphotriesterase superfamily protein	1.12

AT4G18250	receptor serine/threonine kinase, putative	1.11
AT3G04220	TIR-NB-LRR - membrane	1.11
AT5G37820	NOD26-like intrinsic protein 4;2	1.10
AT5G05390	laccase 12	1.10
AT5G23830	MD-2-related lipid recognition domain-containing protein	1.10
AT4G29690	Alkaline-phosphatase-like family protein	1.09
AT1G09932	Phosphoglycerate mutase family protein	1.09
AT1G76520	Auxin efflux carrier family protein	1.09
AT1G79160	unknown	1.09
AT2G44290	seed storage 2S	1.09
AT5G05600	2-oxoglutarate (2OG) and Fe(II)-dependent oxygenase superfamily protein	1.09
AT5G47980	HXXXD-type acyl-transferase family protein	1.09
AT3G07000	cystein histidine rich	1.07
AT4G22212	Arabidopsis defensin-like protein	1.07
AT5G25250	SPFH/Band 7/PHB domain-containing membrane-associated protein family	1.07
AT1G66700	S-adenosyl-L-methionine-dependent methyltransferases superfamily protein	1.07
AT4G15350	cytochrome P450, family 705, subfamily A, polypeptide 2	1.06
AT1G60750	NAD(P)-linked oxidoreductase superfamily protein	1.05
AT5G48010	thalianol synthase 1	1.05
AT5G47990	cytochrome P450, family 705, subfamily A, polypeptide 5	1.04
AT2G42720	F-box skip2-like	1.04
AT2G29440	glutathione S-transferase tau 6	1.04
AT5G39120	RmlC-like cupins superfamily protein	1.04
AT1G19250	flavin-dependent monooxygenase 1	1.04
AT2G28210	alpha carbonic anhydrase 2	1.03
AT5G09980	elicitor peptide 4 precursor	1.03
AT4G15530	pyruvate orthophosphate dikinase	1.03
AT5G05365	Heavy metal transport/detoxification superfamily protein	1.03

AT5G26260	TRAF-like family protein	1.02
AT1G25083	Glutamine amidotransferase type 1 family protein	1.02
AT5G39150	RmlC-like cupins superfamily protein	1.01
AT5G58610	PHD finger transcription factor, putative	1.01
AT1G11330	S-locus lectin protein kinase family protein	1.01
AT1G80840	WRKY DNA-binding protein 40	1.01
AT1G53708	ROTUNDIFOLIA like 9	1.01
AT5G14730	unknown	1.00
AT1G25155	Glutamine amidotransferase type 1 family protein	1.00
AT1G03980	phytochelatin synthase 2	1.00
AT1G09950	RESPONSE TO ABA AND SALT 1	1.00
AT3G48510	NA	-1.00
AT1G80340	gibberellin 3-oxidase 2	-1.00
AT2G25680	molybdate transporter 1	-1.00
AT2G38790	NA	-1.00
AT5G45310	NA	-1.01
AT1G28610	GDSL-like Lipase/Acylhydrolase superfamily protein	-1.01
AT2G24400	SAUR-like auxin-responsive protein family	-1.01
AT5G55250	IAA carboxylmethyltransferase 1	-1.01
AT1G70890	MLP-like protein 43	-1.01
AT4G13550	triglyceride lipases;triglyceride lipases	-1.01
AT3G15050	NA	-1.02
AT1G70830	MLP-like protein 28	-1.02
AT4G08290	nodulin MtN21 /EamA-like transporter family protein	-1.03
AT1G13600	basic leucine-zipper 58	-1.03
AT4G23870	NA	-1.03
AT5G45650	subtilase family protein	-1.03
AT5G51760	Protein phosphatase 2C family protein	-1.03

AT4G11310	Papain family cysteine protease	-1.04
AT4G15290	Cellulose synthase family protein	-1.04
AT4G23496	SPIRAL1-like5	-1.04
AT5G25240	NA	-1.04
AT2G31560	NA	-1.07
AT3G29410	NA	-1.07
AT5G09210	GC-rich sequence DNA-binding factor-like protein	-1.07
AT3G56275	NA	-1.07
AT1G78390	nine-cis-epoxycarotenoid dioxygenase 9	-1.08
AT1G31750	proline-rich family protein	-1.08
AT5G41590	Protein of unknown function (DUF567)	-1.09
AT1G22160	Protein of unknown function (DUF581)	-1.10
AT4G27657	NA	-1.11
AT3G45680	Major facilitator superfamily protein	-1.11
AT5G06530	ABC-2 type transporter family protein	-1.12
AT4G36740	homeobox protein 40	-1.13
AT4G25100	Fe superoxide dismutase 1	-1.13
AT3G48740	Nodulin MtN3 family protein	-1.14
AT5G06760	Late Embryogenesis Abundant 4-5	-1.15
AT5G58780	Undecaprenyl pyrophosphate synthetase family protein	-1.15
AT1G52690	Late embryogenesis abundant protein (LEA) family protein	-1.17
AT1G02205	Fatty acid hydroxylase superfamily	-1.18
AT1G23160	Auxin-responsive GH3 family protein	-1.19
AT4G38690	PLC-like phosphodiesterases superfamily protein	-1.20
AT1G68040	S-adenosyl-L-methionine-dependent methyltransferases superfamily protein	-1.20
AT4G28790	basic helix-loop-helix (bHLH) DNA-binding superfamily protein	-1.21
AT2G47010	NA	-1.21
AT5G15180	Peroxidase superfamily protein	-1.21

AT1G14700	purple acid phosphatase 3	-1.22
AT5G65340	Protein of unknown function, DUF617	-1.22
AT1G55410	NA	-1.22
AT4G16980	arabinogalactan-protein family	-1.22
AT3G21670	NA	-1.23
AT3G05936	NA	-1.24
AT5G59220	highly ABA-induced PP2C gene 1	-1.24
AT3G02515	NA	-1.25
AT3G27250	NA	-1.27
AT3G22830	NA	-1.28
AT2G20880	Integrase-type DNA-binding superfamily protein	-1.29
AT4G25470	C-repeat/DRE binding factor 2	-1.30
AT2G47020	NA	-1.30
AT2G43010	NA	-1.31
AT1G05650	Pectin lyase-like superfamily protein	-1.32
AT1G08440	Aluminium activated malate transporter family protein	-1.33
AT1G71200	basic helix-loop-helix (bHLH) DNA-binding superfamily protein	-1.33
AT2G43050	NA	-1.33
AT5G06900	cytochrome P450, family 93, subfamily D, polypeptide 1	-1.34
AT5G51990	C-repeat-binding factor 4	-1.35
AT2G17660	RPM1-interacting protein 4 (RIN4) family protein	-1.37
AT5G47450	tonoplast intrinsic protein 2;3	-1.38
AT1G47603	purine permease 19	-1.39
AT4G18650	transcription factor-related	-1.39
AT1G24130	Transducin/WD40 repeat-like superfamily protein	-1.40
AT4G15320	cellulose synthase-like B6	-1.41
AT2G47770	ATTSPO	-1.42
AT2G18550	homeobox protein 21	-1.42

AT4G33550	Bifunctional inhibitor/lipid-transfer protein/seed storage 2S albumin superfamily	-1.43
AT1G71050	Heavy metal transport/detoxification superfamily protein	-1.43
AT2G21820	unknown	-1.52
AT5G26730	Fasciclin-like arabinogalactan family protein	-1.53
AT1G79130	SAUR-like auxin-responsive protein family	-1.55
AT4G17680	SBP (S-ribonuclease binding protein) family protein	-1.58
AT1G76800	Vacuolar iron transporter (VIT) family protein	-1.58
AT3G25620	ATP-binding cassete 21	-1.59
AT2G43890	pectin-lyase like	-1.61
AT4G25480	dehydration response element B1A	-1.61
AT2G31550	SGNH-hydrolase	-1.69
AT1G21890	nodulin MtN21 /EamA-like transporter family protein	-1.78
AT5G52300	CAP160 protein	-1.82
AT5G66400	Dehydrin family protein	-1.89
AT1G62420	Protein of unknown function (DUF506)	-1.89
AT4G06477	transposable element gene	-1.97
AT5G23990	ferric reduction oxidase 5	-2.03
AT2G35300	LEA4-2	-2.20
AT4G39000	glycosyl hydrolase 9B17	-2.22
AT4G25490	C-repeat/DRE binding factor 1	-2.34
AT5G14570	high affinity nitrate transporter 2.7	-2.72
AT2G25625	chloroplast vesiculation CV	-3.10

Appendix F. List of differentially expressed genes in response to root-knot nematode penetration/migration in *bak1-5* roots with FDR<0.01 and 1<FC<1.

Accession number	Description	Log FC
AT5G05340	Peroxidase superfamily protein	8.36
AT4G37710	VQ motif-containing protein	7.72
AT5G61890	Integrase-type DNA-binding superfamily protein	6.27
AT5G12020	17.6 kDa class II heat shock protein	6.13
AT1G64160	Disease resistance-responsive (dirigent-like protein) family protein	6.12
AT2G24850	tyrosine aminotransferase 3	5.77
AT3G12900	2-oxoglutarate (2OG) and Fe(II)-dependent oxygenase superfamily protein	5.50
AT3G44860	farnesoic acid carboxyl-O-methyltransferase	4.72
AT1G56240	phloem protein 2-B13	4.68
AT5G12030	heat shock protein 17.6A	4.64
AT3G60120	beta glucosidase 27	4.31
AT3G44870	S-adenosyl-L-methionine-dependent methyltransferases superfamily protein	4.23
AT5G20230	blue-copper-binding protein	4.19
AT3G47480	Calcium-binding EF-hand family protein	3.90
AT2G02010	glutamate decarboxylase 4	3.76
AT5G64870	SPFH/Band 7/PHB domain-containing membrane-associated protein family	3.68
AT5G13220	jasmonate-zim-domain protein 10	3.57
AT5G52670	Copper transport protein family	3.42
AT1G69930	glutathione S-transferase TAU 11	3.41
AT1G32970	Subtilisin-like serine endopeptidase family protein	3.35
AT5G43360	phosphate transporter 1;3	3.28
AT2G04460	transposable element gene	3.25
AT5G39580	Peroxidase superfamily protein	3.19
AT4G23600	Tyrosine transaminase family protein	3.14
AT5G54710	Ankyrin repeat family protein	3.00

AT2G41100	Calmodulin-like 12	2.95
AT3G23250	myb domain protein 15	2.91
AT1G53540	HSP20-like chaperones superfamily protein	2.86
AT1G70720	Plant invertase/pectin methylesterase inhibitor superfamily protein	2.81
AT2G36110	NA	2.75
AT3G45060	high affinity nitrate transporter 2.6	2.74
AT1G26390	FAD-binding Berberine family protein	2.71
AT1G66930	Protein kinase superfamily protein	2.69
AT5G06720	peroxidase 2	2.68
AT2G32487	NA	2.66
AT3G02840	NA	2.66
AT4G22210	low-molecular-weight cysteine-rich 85	2.62
AT2G44840	NA	2.61
AT1G69920	glutathione S-transferase TAU 12	2.59
AT1G49570	Peroxidase superfamily protein	2.57
AT5G40590	Cysteine/Histidine-rich C1 domain family protein	2.55
AT4G22470	protease inhibitor/seed storage/lipid transfer protein (LTP) family protein	2.53
AT4G08040	1-aminocyclopropane-1-carboxylate synthase 11	2.47
AT2G19800	myo-inositol oxygenase 2	2.42
AT3G22910	NA	2.42
AT4G02330	Plant invertase/pectin methylesterase inhibitor superfamily	2.41
AT4G33720	CAP(Cysteine-rich secretory, Antigen 5, Pathogenesis-related 1) superfamily	2.39
AT3G46230	heat shock protein 17.4	2.39
AT5G40000	P-loop containing nucleoside triphosphate hydrolases superfamily protein	2.37
AT2G30750	CYP71A12	2.36
AT2G24600	Ankyrin repeat family protein	2.34
AT1G65481	NA	2.32
AT1G09950	RESPONSE TO ABA AND SALT 1	2.30

AT4G14630	germin-like protein 9	2.25
AT5G26920	Cam-binding protein 60-like G	2.22
AT4G01360	NA	2.19
AT1G35140	Phosphate-responsive 1 family protein	2.18
AT5G59990	CCT motif family protein	2.18
AT1G67000	Protein kinase superfamily protein	2.17
AT5G57560	Xyloglucan endotransglucosylase/hydrolase family protein	2.16
AT3G47340	glutamine-dependent asparagine synthase 1	2.16
AT2G46400	NA	2.11
AT5G19110	Eukaryotic aspartyl protease family protein	2.10
AT3G27950	NA	2.10
AT5G20790	NA	2.08
AT2G41240	NA	2.07
AT2G43620	NA	2.06
AT2G43140	NA	2.05
AT3G17690	NA	2.02
AT2G17330	NA	2.01
AT2G19210	Leucine-rich repeat transmembrane protein kinase protein	2.01
AT1G65500	NA	2.00
AT2G47550	NA	1.99
AT4G32950	Protein phosphatase 2C family protein	1.99
AT1G76640	Calcium-binding EF-hand family protein	1.99
AT1G73220	organic cation/carnitine transporter1	1.98
AT4G26050	plant intracellular ras group-related LRR 8	1.97
AT1G56160	myb domain protein 72	1.97
AT1G31290	ARGONAUTE 3	1.97
AT2G44578	NA	1.96
AT3G59710	NAD(P)-binding Rossmann-fold superfamily protein	1.95

AT4G24340	Phosphorylase superfamily	1.95
AT1G50090	D-aminoacid aminotransferase-like PLP-dependent enzymes superfamily	1.93
AT1G19380	Protein of unknown function (DUF1195)	1.93
AT1G01580	ferric reduction oxidase 2	1.92
AT2G28850	cytochrome P450, family 710, subfamily A, polypeptide 3	1.92
AT1G55200	Protein kinase protein with adenine nucleotide alpha hydrolases-like domain	1.92
AT3G15370	NA	1.92
AT2G28210	alpha carbonic anhydrase 2	1.90
AT1G58420	Uncharacterised conserved protein UCP031279	1.90
AT5G47220	ethylene responsive element binding factor 2	1.88
AT5G35940	Mannose-binding lectin superfamily protein	1.85
AT2G28860	cytochrome P450, family 710, subfamily A, polypeptide 4	1.85
AT5G19890	Peroxidase superfamily protein	1.84
AT3G45960	expansin-like A3	1.84
AT5G52720	Copper transport protein family	1.83
AT5G39670	Calcium-binding EF-hand family protein	1.82
AT5G39120	RmlC-like cupins superfamily protein	1.82
AT3G09922	NA	1.82
AT2G44220	NA	1.80
AT3G29252	NA	1.79
AT1G50050	CAP(Cysteine-rich secretory, Antigen 5, Pathogenesis-related 1) superfamily	1.79
AT2G41810	NA	1.77
AT4G18250	receptor serine/threonine kinase, putative	1.77
AT4G08770	Peroxidase superfamily protein	1.77
AT3G47720	similar to RCD one 4	1.77
AT4G10265	Wound-responsive family protein	1.76
AT3G29970	B12D protein	1.75
AT4G36430	Peroxidase superfamily protein	1.73

AT5G20150	SPX domain gene 1	1.73
AT4G18170	WRKY DNA-binding protein 28	1.72
AT4G22710	cytochrome P450, family 706, subfamily A, polypeptide 2	1.72
AT5G42380	calmodulin like 37	1.70
AT4G00390	DNA-binding storekeeper protein-related transcriptional regulator	1.70
AT1G23730	beta carbonic anhydrase 3	1.69
AT1G80840	WRKY DNA-binding protein 40	1.69
AT5G24600	Protein of unknown function, DUF599	1.68
AT3G21720	NA	1.68
AT1G18970	germin-like protein 4	1.67
AT3G58060	Cation efflux family protein	1.64
AT1G76210	Arabidopsis protein of unknown function (DUF241)	1.62
AT2G17850	Rhodanese/Cell cycle control phosphatase superfamily protein	1.62
AT1G76650	calmodulin-like 38	1.57
AT2G32140	NA	1.57
AT4G21650	Subtilase family protein	1.57
AT5G60770	nitrate transporter 2.4	1.57
AT5G39180	RmlC-like cupins superfamily protein	1.56
AT2G44080	NA	1.54
AT5G38940	RmlC-like cupins superfamily protein	1.54
AT1G65860	flavin-monooxygenase glucosinolate S-oxygenase 1	1.53
AT5G52750	Heavy metal transport/detoxification superfamily protein	1.53
AT5G39150	RmlC-like cupins superfamily protein	1.53
AT3G30775	Methylenetetrahydrofolate reductase family protein	1.53
AT3G12220	NA	1.51
AT3G26830	PAD3	1.51
AT1G08165	NA	1.50
AT5G41290	Receptor-like protein kinase-related family protein	1.49

AT5G64750	Integrase-type DNA-binding superfamily protein	1.49
AT4G36110	SAUR-like auxin-responsive protein family	1.48
AT1G08100	nitrate transporter 2.2	1.47
AT4G16260	Glycosyl hydrolase superfamily protein	1.47
AT5G10040	NA	1.46
AT4G26200	1-amino-cyclopropane-1-carboxylate synthase 7	1.46
AT5G18470	Curculin-like (mannose-binding) lectin family protein	1.46
AT5G28960	NA	1.45
AT3G04220	NA	1.45
AT2G34390	NA	1.43
AT1G08440	Aluminium activated malate transporter family protein	1.43
AT1G08830	copper/zinc superoxide dismutase 1	1.43
AT1G14540	Peroxidase superfamily protein	1.42
AT3G50440	methyl esterase 10	1.42
AT1G77120	alcohol dehydrogenase 1	1.41
AT5G48430	Eukaryotic aspartyl protease family protein	1.41
AT1G35625	RING/U-box superfamily protein	1.41
AT3G50930	cytochrome BC1 synthesis	1.41
AT1G08090	nitrate transporter 2:1	1.40
AT4G19690	iron-regulated transporter 1	1.40
AT1G07135	glycine-rich protein	1.40
AT4G13310	cytochrome P450, family 71, subfamily A, polypeptide 20	1.39
AT2G17845	NAD(P)-binding Rossmann-fold superfamily protein	1.39
AT1G54890	Late embryogenesis abundant (LEA) protein-related	1.38
AT1G55440	Cysteine/Histidine-rich C1 domain family protein	1.38
AT1G21520	NA	1.37
AT2G29460	glutathione S-transferase tau 4	1.37
AT2G26400	acireductone dioxygenase 3	1.37

AT3G56970	basic helix-loop-helix (bHLH) DNA-binding superfamily protein	1.37
AT4G08780	Peroxidase superfamily	1.36
AT4G22610	Bifunctional inhibitor/lipid-transfer protein/seed storage 2S albumin superfamily	1.36
AT2G38870	NA	1.36
AT3G20110	NA	1.35
AT2G22880	VQ motif-containing protein	1.35
AT1G29740	Leucine-rich repeat transmembrane protein kinase	1.34
AT4G15370	baruol synthase 1	1.34
AT5G62520	similar to RCD one 5	1.34
AT1G72940	Toll-Interleukin-Resistance (TIR) domain-containing protein	1.34
AT2G20142	Toll-Interleukin-Resistance (TIR) domain family protein	1.34
AT5G46050	peptide transporter 3	1.33
AT5G25260	SPFH/Band 7/PHB domain-containing membrane-associated protein family	1.33
AT1G73120	NA	1.33
AT3G43190	sucrose synthase 4	1.32
AT4G22690	cytochrome P450, family 706, subfamily A, polypeptide 1	1.32
AT5G65140	Haloacid dehalogenase-like hydrolase (HAD) superfamily protein	1.32
AT1G56600	galactinol synthase 2	1.32
AT4G14365	XB3 ortholog 4 in Arabidopsis thaliana	1.31
AT5G19097	transposable element gene	1.30
AT2G32190	NA	1.30
AT3G47420	phosphate starvation-induced gene 3	1.30
AT5G41300	Receptor-like protein kinase-related family protein	1.30
AT3G20395	NA	1.29
AT1G07400	HSP20-like chaperones superfamily protein	1.29
AT1G27730	salt tolerance zinc finger	1.28
AT5G22580	Stress responsive A/B Barrel Domain	1.27

AT1G26250	Proline-rich extensin-like family protein	1.27
AT1G28370	ERF domain protein 11	1.27
AT2G40330	NA	1.27
AT2G14247	Expressed protein	1.27
AT5G39160	RmlC-like cupins superfamily protein	1.27
AT4G38420	SKU5 similar 9	1.26
AT3G27070	NA	1.26
AT4G27730	oligopeptide transporter 1	1.26
AT4G19980	NA	1.26
AT1G73010	phosphate starvation-induced gene 2	1.25
AT4G24570	dicarboxylate carrier 2	1.25
AT4G15150	glycine-rich protein	1.25
AT4G13395	ROTUNDIFOLIA like 12	1.25
AT1G10400	UDP-Glycosyltransferase superfamily protein	1.24
AT3G01900	NA	1.24
AT5G57920	early nodulin-like protein 10	1.24
AT1G02930	glutathione S-transferase 6	1.24
AT2G26440	Plant invertase/pectin methylesterase inhibitor superfamily	1.23
AT5G38820	Transmembrane amino acid transporter family protein	1.23
AT5G67080	mitogen-activated protein kinase kinase kinase 19	1.23
AT1G61340	F-box family protein	1.22
AT5G06730	Peroxidase superfamily protein	1.22
AT4G01700	Chitinase family protein	1.22
AT3G05858	NA	1.22
AT5G50610	NA	1.21
AT4G38410	Dehydrin family protein	1.21
AT4G25810	xyloglucan endotransglycosylase 6	1.21
AT1G49100	Leucine-rich repeat protein kinase family protein	1.21

AT2G34180	NA	1.21
AT5G41080	PLC-like phosphodiesterases superfamily protein	1.21
AT1G21210	wall associated kinase 4	1.21
AT2G18620	Terpenoid synthases superfamily protein	1.21
AT2G19590	ACC oxidase 1	1.21
AT4G22212	Arabidopsis defensin-like protein	1.20
AT4G24410	NA	1.20
AT5G57220	cytochrome P450, family 81, subfamily F, polypeptide 2	1.20
AT4G33070	Thiamine pyrophosphate dependent pyruvate decarboxylase family protein	1.20
AT3G04420	NA	1.19
AT3G44260	Polynucleotidyl transferase, ribonuclease H-like superfamily protein	1.19
AT1G16370	organic cation/carnitine transporter 6	1.19
AT1G35910	Haloacid dehalogenase-like hydrolase (HAD) superfamily protein	1.19
AT1G53860	Remorin family protein	1.19
AT4G21680	NITRATE TRANSPORTER 1.8	1.19
AT1G13480	Protein of unknown function (DUF1262)	1.19
AT4G25310	2-oxoglutarate (2OG) and Fe(II)-dependent oxygenase superfamily protein	1.18
AT5G64120	Peroxidase superfamily protein	1.18
AT5G04730	Ankyrin-repeat containing protein	1.18
AT4G17030	expansin-like B1	1.17
AT5G46590	NAC domain containing protein 96	1.17
AT2G26530	Protein of unknown function (DUF1645)	1.17
AT5G17350	NA	1.17
AT1G26200	TRAM, LAG1 and CLN8 (TLC) lipid-sensing domain containing protein	1.17
AT1G72920	Toll-Interleukin-Resistance (TIR) domain family protein	1.17
AT3G61190	BON association protein 1	1.17
AT3G48460	GDSL-like Lipase/Acylhydrolase superfamily protein	1.16
AT1G28480	Thioredoxin superfamily protein	1.16

AT5G60350	NA	1.16
AT3G10930	NA	1.16
AT2G43890	NA	1.15
AT2G16660	Major facilitator superfamily protein	1.15
AT3G29000	NA	1.15
AT4G19720	Glycosyl hydrolase family protein with chitinase insertion domain	1.14
AT1G21525	NA	1.14
AT3G03660	NA	1.14
AT4G08950	Phosphate-responsive 1 family protein	1.13
AT5G28520	Mannose-binding lectin superfamily protein	1.13
AT1G17380	jasmonate-zim-domain protein 5	1.13
AT1G12805	nucleotide binding	1.13
AT4G34060	demeter-like protein 3	1.12
AT5G66640	DA1-related protein 3	1.12
AT2G19200	NA	1.11
AT5G64810	WRKY DNA-binding protein 51	1.11
AT4G02170	NA	1.11
AT2G11810	monogalactosyldiacylglycerol synthase type C	1.11
AT5G39130	RmlC-like cupins superfamily protein	1.11
AT1G52700	alpha/beta-Hydrolases superfamily protein	1.10
AT5G39720	avirulence induced gene 2 like protein	1.10
AT4G11140	cytokinin response factor 1	1.09
AT3G21560	NA	1.09
AT5G54165	NA	1.09
AT1G74650	myb domain protein 31	1.09
AT4G07960	Cellulose-synthase-like C12	1.08
AT3G55700	UDP-Glycosyltransferase superfamily protein	1.08
AT3G09940	NA	1.08

AT3G03530	NA	1.08
AT1G74000	strictosidine synthase 3	1.08
AT4G37850	basic helix-loop-helix (bHLH) DNA-binding superfamily protein	1.08
AT5G51750	subtilase 1.3	1.08
AT1G79160	NA	1.07
AT2G28190	copper/zinc superoxide dismutase 2	1.06
AT4G12545	Bifunctional inhibitor/lipid-transfer protein/seed storage 2S albumin superfamily protein	1.06
AT5G28510	beta glucosidase 24	1.06
AT5G54490	pinoid-binding protein 1	1.06
AT1G58936	Inositol-pentakisphosphate 2-kinase family protein	1.06
AT2G18140	Peroxidase superfamily protein	1.06
AT2G34350	NA	1.05
AT5G43590	Acyl transferase/acyl hydrolase/lysophospholipase superfamily protein	1.05
AT5G45220	Disease resistance protein (TIR-NBS-LRR class) family	1.05
AT3G04370	NA	1.04
AT1G64910	UDP-Glycosyltransferase superfamily protein	1.04
AT5G51760	Protein phosphatase 2C family protein	1.04
AT2G45080	NA	1.04
AT3G02620	NA	1.04
AT5G19100	Eukaryotic aspartyl protease family protein	1.04
AT2G16630	Pollen Ole e 1 allergen and extensin family protein	1.04
AT4G36220	ferulic acid 5-hydroxylase 1	1.04
AT2G18150	Peroxidase superfamily protein	1.03
AT1G19180	jasmonate-zim-domain protein 1	1.03
AT1G26730	EXS (ERD1/XPR1/SYG1) family protein	1.03
AT2G46130	NA	1.03
AT5G47980	HXXXD-type acyl-transferase family protein	1.03

AT4G10270	Wound-responsive family protein	1.03
AT4G23810	WRKY family transcription factor	1.03
AT2G45560	NA	1.02
AT4G18280	glycine-rich cell wall protein-related	1.02
AT3G59900	auxin-regulated gene involved in organ size	1.02
AT5G15960	stress-responsive protein (KIN1) / stress-induced protein (KIN1)	1.02
AT1G66400	calmodulin like 23	1.02
AT4G10310	high-affinity K+ transporter 1	1.02
AT1G09932	Phosphoglycerate mutase family protein	1.02
AT5G25250	SPFH/Band 7/PHB domain-containing membrane-associated protein family	1.01
AT2G34930	NA	1.01
AT3G28580	NA	1.01
AT4G39830	Cupredoxin superfamily protein	1.01
AT3G26840	NA	1.01
AT3G61930	NA	1.01
AT5G26220	ChaC-like family protein	1.01
AT5G02780	glutathione transferase lambda 1	1.00
AT5G05390	laccase 12	1.00
AT3G55310	NAD(P)-binding Rossmann-fold superfamily protein	1.00
AT2G26370	MD-2-related lipid recognition domain-containing protein	1.00
AT4G24110	NA	1.00
AT4G10500	2-oxoglutarate (2OG) and Fe(II)-dependent oxygenase superfamily protein	1.00
AT5G09570	Cox19-like CHCH family protein	-1.00
AT4G29905	NA	-1.00
AT4G36230	NA	-1.00
AT2G29010	NA	-1.01
AT4G16270	Peroxidase superfamily protein	-1.01
AT4G35480	RING-H2 finger A3B	-1.02

AT3G28740	NA	-1.03
AT1G30760	FAD-binding Berberine family protein	-1.03
AT1G05560	UDP-glucosyltransferase 75B1	-1.03
AT1G15540	2-oxoglutarate (2OG) and Fe(II)-dependent oxygenase superfamily protein	-1.04
AT3G54530	NA	-1.04
AT5G37990	S-adenosyl-L-methionine-dependent methyltransferases superfamily protein	-1.04
AT4G02280	sucrose synthase 3	-1.04
AT1G13600	basic leucine-zipper 58	-1.04
AT5G45310	NA	-1.04
AT4G14060	Polyketide cyclase/dehydrase and lipid transport superfamily protein	-1.05
AT5G63580	flavonol synthase 2	-1.05
AT5G04370	S-adenosyl-L-methionine-dependent methyltransferases superfamily protein	-1.05
AT1G70890	MLP-like protein 43	-1.06
AT5G24770	vegetative storage protein 2	-1.07
AT5G14070	Thioredoxin superfamily protein	-1.07
AT3G09390	NA	-1.08
AT1G01670	RING/U-box superfamily protein	-1.09
AT3G56260	NA	-1.09
AT2G40100	NA	-1.09
AT4G08290	nodulin MtN21 /EamA-like transporter family protein	-1.09
AT5G48485	Bifunctional inhibitor/lipid-transfer protein/seed storage 2S albumin superfamily protein	-1.09
AT4G08555	NA	-1.10
AT2G21640	NA	-1.10
AT1G61840	Cysteine/Histidine-rich C1 domain family protein	-1.10
AT5G25130	cytochrome P450, family 71, subfamily B, polypeptide 12	-1.10
AT3G26040	NA	-1.11
AT3G59480	pfkB-like carbohydrate kinase family protein	-1.11

AT1G60750	NAD(P)-linked oxidoreductase superfamily protein	-1.11
AT3G44300	nitrilase 2	-1.12
AT3G05650	NA	-1.13
AT1G71200	basic helix-loop-helix (bHLH) DNA-binding superfamily protein	-1.13
AT5G66780	NA	-1.13
AT4G28040	nodulin MtN21 /EamA-like transporter family protein	-1.13
AT5G52790	CBS domain-containing protein with a domain of unknown function (DUF21)	-1.13
AT4G24890	purple acid phosphatase 24	-1.13
AT1G14700	purple acid phosphatase 3	-1.13
AT1G65970	thioredoxin-dependent peroxidase 2	-1.13
AT2G43050	NA	-1.13
AT5G57785	NA	-1.14
AT3G08860	NA	-1.14
AT5G52300	CAP160 protein	-1.15
AT1G52130	Mannose-binding lectin superfamily protein	-1.15
AT4G12490	Bifunctional inhibitor/lipid-transfer protein/seed storage 2S albumin superfamily protein	-1.19
AT4G16008	NA	-1.20
AT4G08360	KOW domain-containing protein	-1.21
AT4G25780	CAP (Cysteine-rich secretory proteins, Antigen 5, and Pathogenesis-related 1 protein) superfamily protein	-1.21
AT3G54830	Transmembrane amino acid transporter family protein	-1.22
AT3G09220	NA	-1.23
AT2G22990	sinapoylglucose 1	-1.25
AT1G19960	NA	-1.26
AT3G26740	NA	-1.28
AT5G50690	hydroxysteroid dehydrogenase 7	-1.31
AT1G07985	Expressed protein	-1.31
AT5G43450	2-oxoglutarate (2OG) and Fe(II)-dependent oxygenase superfamily protein	-1.32

AT5G50760	SAUR-like auxin-responsive protein family	-1.33
AT4G23670	Polyketide cyclase/dehydrase and lipid transport superfamily protein	-1.36
AT5G50590	hydroxysteroid dehydrogenase 4	-1.36
AT5G66400	Dehydrin family protein	-1.37
AT3G13840	NA	-1.38
AT1G52790	2-oxoglutarate (2OG) and Fe(II)-dependent oxygenase superfamily protein	-1.41
AT5G17700	MATE efflux family protein	-1.42
AT5G22890	C2H2 and C2HC zinc fingers superfamily protein	-1.42
AT2G13810	AGD2-like defense response protein 1	-1.43
AT3G46900	copper transporter 2	-1.44
AT2G34490	NA	-1.45
AT1G67110	cytochrome P450, family 735, subfamily A, polypeptide 2	-1.47
AT5G50600	hydroxysteroid dehydrogenase 1	-1.49
AT5G59080	NA	-1.53
AT2G42250	NA	-1.54
AT2G47770	NA	-1.55
AT2G05380	glycine-rich protein 3 short isoform	-1.56
AT5G62330	NA	-1.59
AT4G38970	fructose-bisphosphate aldolase 2	-1.60
AT5G53190	Nodulin MtN3 family protein	-1.62
AT2G05400	Ubiquitin-specific protease family C19-related protein	-1.70
AT4G01390	TRAF-like family protein	-1.71
AT4G18650	transcription factor-related	-1.73
AT1G78390	nine-cis-epoxycarotenoid dioxygenase 9	-1.76
AT5G23980	ferric reduction oxidase 4	-1.77
AT1G08430	aluminum-activated malate transporter 1	-1.78
AT5G50700	hydroxysteroid dehydrogenase 1	-1.78
AT2G25625	NA	-1.80

AT3G13950	NA	-1.88
AT4G14250	structural constituent of ribosome	-1.90
AT4G12500	Bifunctional inhibitor/lipid-transfer protein/seed storage 2S albumin superfamily protein	-1.90
AT3G28345	NA	-1.97
AT5G47600	HSP20-like chaperones superfamily protein	-1.97
AT5G20710	beta-galactosidase 7	-2.04
AT1G52820	2-oxoglutarate (2OG) and Fe(II)-dependent oxygenase superfamily protein	-2.13
AT1G51840	protein kinase-related	-2.24
AT5G28145	transposable element gene	-2.29
AT1G51830	Leucine-rich repeat protein kinase family protein	-2.30
AT1G52800	2-oxoglutarate (2OG) and Fe(II)-dependent oxygenase superfamily protein	-2.63
AT5G35777	transposable element gene	-2.89
AT3G06545	NA	-3.06
AT5G06900	cytochrome P450, family 93, subfamily D, polypeptide 1	-3.26
AT2G16190	NA	-3.34
AT3G52970	cytochrome P450, family 76, subfamily G, polypeptide 1	-3.81
AT2G16180	transposable element gene	-4.13
AT5G06905	cytochrome P450, family 712, subfamily A, polypeptide 2	-4.58